

**INVESTIGATING BASAL GANGLIA FUNCTION USING
ULTRA-HIGH FIELD MRI**

Turki S Sabrah Abualait, MSc.

**Thesis submitted to the University of Nottingham
for the degree of Doctor of Philosophy**

November 2012

Dedication

To my parents, for their love, endless support and encouragement; and for devoting their lives to teach me.

And to my grandfather, who spurred on my wonder at this life.

Acknowledgements

First and foremost I would like to thank my supervisors, Stephen Jackson and Susan Francis, for their continued support and guidance. This thesis would never have taken shape without their invaluable advices. I would also like to thank Rosa Sanchez for her assistance with the fMRI work.

I would like to thank the former and current members of the lab for their support and friendships: Catherine, Amy, Elena, Se-Ho, Laura, Lisa, Amelia, Jane, Martin Schürmann and Roger Newport. I would also like to thank all the people with whom I have worked over the past three years without whom none of this work could have been done, and particularly those who participated in my experiments. Further thanks go to all people in the MR centre for being helpful.

I am deeply indebted to my family for their continuous support and help throughout my PhD period. Special thanks must go to my brothers and sisters for their support and encouragement. Many thanks must go to all my relatives for being supportive and helpful.

Last, but by no means least, I want to express my gratitude to Aisha, Khalid and Effat for being patient with me.

Abstract

The basal ganglia (BG) are a group of highly interconnected nuclei that are located deep at the base of the cerebral cortex. They participate in multiple neural circuits or 'loops' with cognitive and motor areas of the cerebral cortex. The basal ganglia has primarily been thought to be involved in motor control and learning, but more recently a number of brain imaging studies have shown that the basal ganglia are involved also in cognitive function. The aim of this work is to investigate the role of the basal ganglia in cognitive control and motor learning by examining its involvement in GO/WAIT and GO/NO-GO tasks, and Motor Prediction task, respectively. Ultra-high field (7 Tesla) fMRI is used to provide higher BOLD contrast and thus higher achievable spatial resolution. A dual echo gradient echo EPI method is used to obtain high quality images from both cortical and sub-cortical regions. A common neural basis across different forms of response inhibition using GO/WAIT and GO/NO-GO cognitive paradigms is observed in the experiments of Chapter 4, as well as distinct brain regions involved in withholding and cancelling of motor responses. Using the GO/WAIT cognitive paradigm in Chapter 5 individuals with Tourette syndrome (TS) are compared to age and gender-matched control healthy subjects (CS), and it is shown that TS subjects are unable to recruit critical cortical and sub-cortical nodes that are typically involved in mediating behavioural inhibition. Furthermore, in Chapter 6, the role of the basal ganglia in motor learning is investigated using the Motor Prediction task. The findings show that the basal ganglia and midbrain regions (i.e., habenula) are involved in motor prediction and enhancing the reinforcement learning process.

This thesis aims to investigate the basal ganglia function in cognitive and motor tasks, and concludes with suggested further studies to advance our understanding of the role of the basal ganglia nuclei in cognitive function.

Table of Contents

| | |
|--|-----------|
| CHAPTER 1 | 1 |
| 1.1 Introduction | 1 |
| 1.2 Anatomical structures of the Basal Ganglia | 1 |
| 1.3 Internal architecture | 6 |
| 1.3.1 Direct and Indirect Pathways | 6 |
| 1.3.2 The Subthalamic “hyperdirect” Pathway | 8 |
| 1.3.3 Multiple Parallel Loops | 10 |
| 1.4 The Basal Ganglia: Beyond the Motor System | 12 |
| 1.5 Overview of the Thesis | 16 |
| CHAPTER 2 | 20 |
| 2.1 Introduction | 20 |
| 2.2 Functional Magnetic Resonance Imaging | 21 |
| 2.3 The principle physics of MRI | 21 |
| 2.4 BOLD fMRI | 24 |
| 2.5 Experimental Design | 27 |
| 2.6 Pre-processing steps | 31 |
| 2.6.1 Slice Timing | 32 |
| 2.6.2 Realignment or (Motion correction) | 33 |
| 2.6.3 Spatial Co-registration | 34 |
| 2.6.4 Spatial Normalization | 35 |
| 2.6.5 Spatial Smoothing | 36 |
| 2.7 Statistical Analysis | 37 |
| CHAPTER 3 | 41 |
| 3.1 Introduction | 41 |
| 3.2 Use of fMRI data at Ultra-high magnetic field | 42 |
| 3.2.1 Theory of optimal echo time | 44 |
| 3.2.2 Multi-echo acquisition | 47 |
| 3.2.3 Analysis of multi-echo data (Echo weighting) | 48 |

| | |
|--|------------|
| 3.3 Experiment 1 | 50 |
| 3.3.1 Material and Methods | 50 |
| 3.3.2 Data Analysis | 52 |
| 3.3.4 Results | 56 |
| 3.3.4 Discussion | 67 |
| | |
| CHAPTER 4 | 69 |
| | |
| 4.1 Introduction: Executive functions | 69 |
| | |
| 4.2 Inhibition: A Definition, Concepts and their Relations | 70 |
| | |
| 4.3 Response Inhibition as a Measure of Executive Functions | 74 |
| | |
| 4.4 Experiment 1 | 76 |
| 4.4.1 Material and Methods | 76 |
| 4.4.2 Data Analysis | 80 |
| 4.4.3 Results | 83 |
| 4.4.4 Summary | 88 |
| | |
| 4.5 Experiment 2 | 92 |
| 4.5.1 Material and Methods | 93 |
| 4.5.2 Data Analysis | 94 |
| 4.5.3 Results | 95 |
| 4.5.4 Summary | 99 |
| | |
| 4.6 Experiment 3 | 103 |
| 4.6.1 Material and Methods | 104 |
| 4.6.2 Data Analysis | 105 |
| 4.6.3 Results | 106 |
| 4.6.4 Summary | 109 |
| | |
| 4.7 Direct comparison between experiments | 111 |
| | |
| 4.8 General discussion | 120 |
| 4.8.1 Behavioural results | 120 |
| 4.8.2 Imaging results | 121 |
| | |
| CHAPTER 5 | 128 |
| | |
| 5.1 Introduction | 128 |
| | |
| 5.2 Tourette syndrome (TS) | 128 |
| | |
| 5.3 The neural basis of TS | 129 |
| | |
| 5.4 Morphometric neuroimaging of Tourette syndrome | 130 |
| | |
| 5.5 Functional Neurimaging studies of Tourette syndrome | 132 |

| | |
|--|------------|
| 5.6 Experiment 4 | 136 |
| 5.6.1 Material and Methods | 136 |
| 5.6.2 Data Analysis | 139 |
| 5.6.3 Results | 142 |
| 5.6.4 Discussion | 155 |
| | |
| CHAPTER 6 | 162 |
| | |
| 6.1. Introduction: Motor learning | 162 |
| | |
| 6.2 Experiment 5 | 165 |
| 6.2.1 Material and Methods | 165 |
| 6.2.2 Data Analysis | 169 |
| 6.2.3 Results | 173 |
| 6.2.4 Discussion | 187 |
| | |
| CHAPTER 7 | 197 |
| | |
| 7.1 General discussion | 197 |
| | |
| 7.2 Using fMRI to measure neural inhibition | 204 |
| | |
| 7.3 Future directions | 205 |
| | |
| 7.4 Conclusion | 206 |
| | |
| REFERENCES | 208 |

Chapter 1

1.1 Introduction

The basal ganglia are a group of highly interconnected nuclei located deep within the cerebral cortex. The basal ganglia have been implicated in many aspects of brain function including motor learning (Levy et al., 1997), memory (Pasupathy and Miller, 2005), planning (Kim et al., 1994; Weder et al., 1999), action selection (Alexander and Crutcher, 1990; Allen et al., 1997), task-switching and the processing of rewards (Robbins and Everitt, 1999).

This chapter has three main purposes. The first is to present an overview of the principle anatomical components of the basal ganglia, including their important subdivisions. Second, I will discuss the internal architecture of the basal ganglia including the intrinsic and extrinsic connections and will explain the pathways of the basal ganglia. Third, the functions of the basal ganglia will be illustrated by reviewing studies ranging from lesion experiments in animals, to clinical population-based and functional imaging studies in humans.

1.2 Anatomical Structures of the Basal Ganglia

The basal ganglia (BG) are a group of grey matter nuclei, these are subcortical structures which are located deep at the base of the cerebral cortex. The basal ganglia is a functional unit composed of four major structures; the striatum (putamen and caudate nucleus), the globus pallidus or pallidum (GP), the substantia nigra (SN), and the subthalamic nucleus (STN), as shown in Figure 1. Three of these structures (the striatum, the pallidum, and the substantia nigra) have important subdivisions that will be explained in the following sections. All of the nuclei of the basal ganglia are

classified into three main types of structure; the input, intermediate, and output structures.

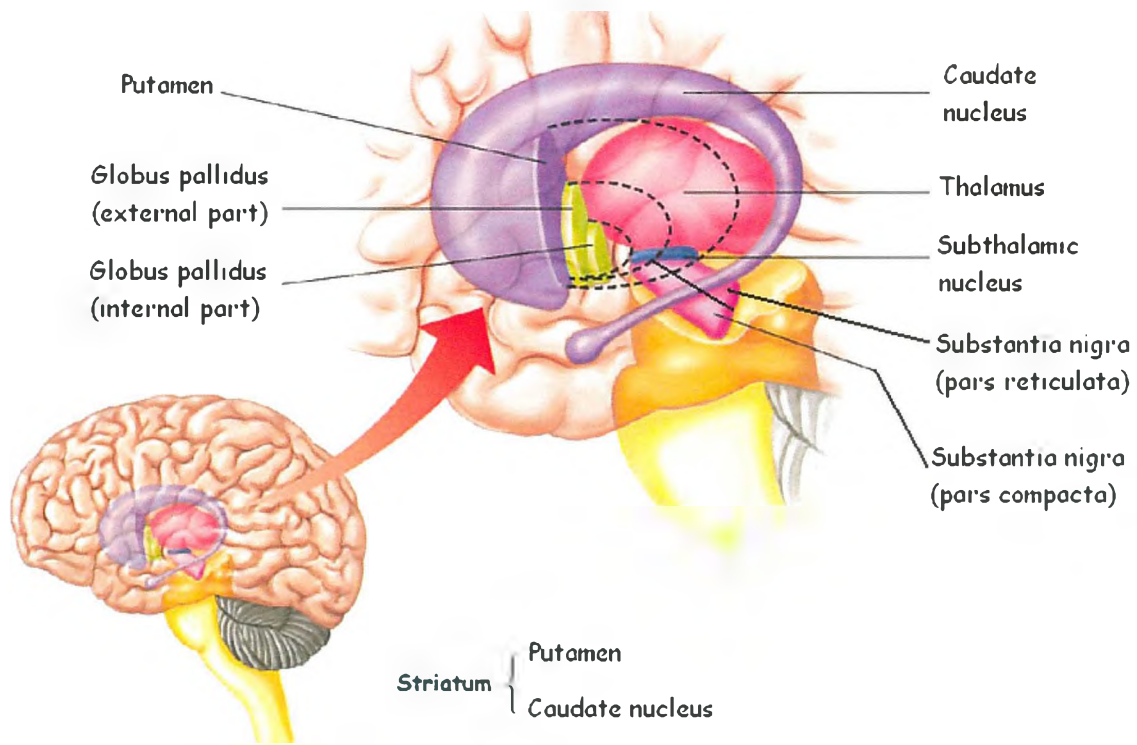


Figure 1.1. The principle components of the basal ganglia. Figure obtained and modified from (<http://cti.itc.virginia.edu>).

The striatum (putamen and caudate nucleus) is the main input structure that receives direct projections from nearly the entire cerebral cortex. The striatum is the primary recipient of information and input from outside of the basal ganglia, in this sense it is a “doorway” from the cerebral cortex. Most of the afferent inputs are glutaminergic (excitatory) projections which arise from the cerebral cortex areas. The striatum also receives excitatory inputs from thalamic nuclei and the midbrain nuclei. The striatum is further divided into two main nuclei, the *caudate nucleus* (CD) and *putamen* (PUT). The caudate nucleus receives input from the prefrontal cortex, with the internal BG loop involving the caudate nucleus being associated with the processing of motor planning and cognitive function. The putamen is highly

connected with motor areas of the cerebral cortex; it receives input from the motor, premotor, supplementary motor and somatosensory cortex. The putamen connections within the internal BG circuit and cerebral cortex are strongly implicated in the process of motor execution.

All intermediate structures of the basal ganglia, which include the subthalamic nucleus (STN), globus pallidus pars externa (GPe) and the substantia nigra pars compacta (SNc) (as will be outlined in the sections below), project most heavily to other nuclei within the basal ganglia, modulating their function or output, as shown in Figure 1.2.

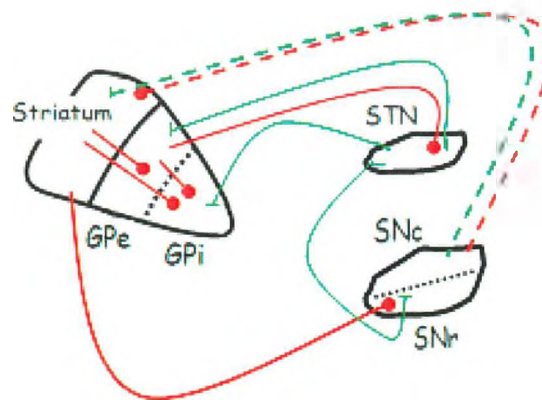


Figure 1.2. Internal architecture of the basal ganglia. Intrinsic circuit. Red lines indicate inhibitory (GABAergic) projections; green lines indicate excitatory (glutamatergic) projections. Key nuclei: GPe, external segment of globus pallidus; STN, subthalamic nucleus; GPi, internal segment of the globus pallidus; SNr, substantia nigra pars reticulata; SNc, substantia nigra pars compacta.

The globus pallidus (GP) is subdivided into internal and external segments; globus pallidus pars interna (GPi) and globus pallidus pars externa (GPe). The GPi is an extrinsic structure that mainly consists of large neurons that project outside of the basal ganglia. About 70% of the GPi neurons send collateral projections to both the thalamus and the brainstem, and the other GPi neurons (20%) project to the lateral habenular nucleus (Parent and De Bellefeuille, 1982). The GPi neurons are inhibitory

and use GABA as a neurotransmitter (Penney and Young, 1981). The GPi receives information from the striatum, through inhibitory projections, and the STN, through excitatory projections, and sends output to the thalamus, STN, and SNr nuclei.

The *substantia nigra* (SN) is divided into two portions, the substantia nigra pars compacta (SNc) and the substantia nigra pars reticulata (SNr). The SNr consists of large neurons that receive similar patterns of input as those of the GPi. Moreover, similar to the GPi, the SNr is a BG output structure, and sends GABAergic projections to various thalamic nuclei (ventroanterior (VA)/ventrolateral (VL)/dorsomedial (DM)) which project back upon cerebral cortex. Moreover, the SNr project, through inhibitory axons, to brainstem, specifically midbrain nuclei, as shown in Figure 1.3. However, there are no direct projections from the basal ganglia to the spinal cord, and no direct inputs to basal ganglia structures from the spinal cord or brainstem nuclei.

The SNc is a cellularly dense black pigmented region which is an important source of dopamine synthesis. It receives GABAergic and inhibitory input from the striatum. The SNc projects back to striatum and other basal ganglia nuclei such as GPe and STN, supplying the basal ganglia with the neurotransmitter dopamine, as shown in Figure 1.2. This dopamine pathway and the reciprocal connection between the SNc and the striatum are thought to play a critical role in reinforcement learning and the process of reward that is carried out by the basal ganglia (DeLgado et al., 2005; Jones et al., 2011).

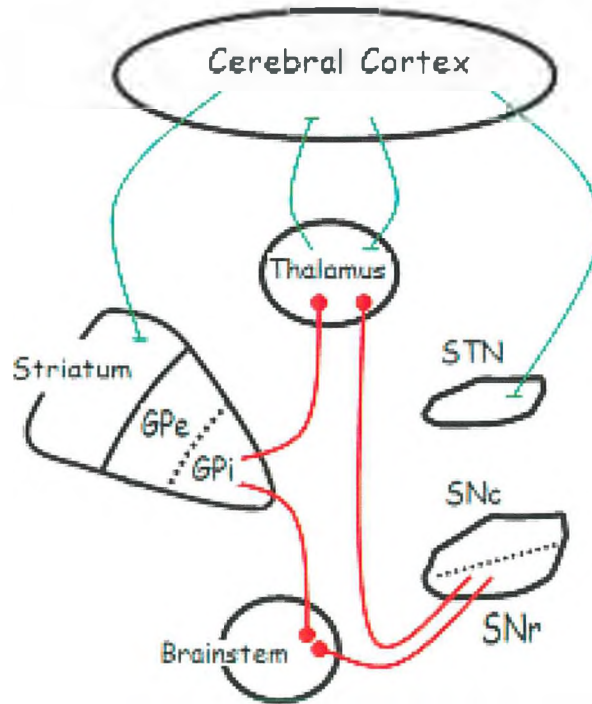


Figure 1.3. Internal architecture of the basal ganglia. Extrinsic circuit. Red lines indicate inhibitory (GABAergic) projections; green lines indicate excitatory (glutamatergic) projections.

The *subthalamic nucleus* (STN) is viewed as an intermediate structure because it projects to another basal ganglia structure. However, the STN is also considered as an input structure, since it receives direct projections from areas of the frontal lobes (Monakow et al., 1978; Nambu et al., 1996; Mink, 2003). The STN receives an inhibitory GABAergic projection from the GPi, and an excitatory glutaminergic projection from the motor areas of the cerebral cortex. The STN sends an excitatory glutaminergic output to the GPi, GPe and SNr. The connections between the STN and the GPi are highly divergent in which each axon from the STN ensheathes many GPi neurons (Parent and Hazrati, 1993). Although the STN receives input from the cerebral cortex and projects to both segments of GPi and SNr, it is different from the striatum in several ways. Firstly, unlike striatum, the cortical input to the STN is from the frontal lobe areas only. Secondly, the output from STN is excitatory, whereas the output from striatum is inhibitory (Nambu et al., 2002).

1.3 Internal architecture

1.3.1 Direct and Indirect Pathways

The output structures of BG are thought to be modulated by two parallel pathways, as shown in Figure 4: the direct pathway and indirect pathway (Alexander et al., 1990; DeLong, 2000; Mink, 1996). The direct (feed) pathway projects from the striatum to the internal segment of the globus pallidus (GPi) and the substantia nigra pars reticulata (SNr). This pathway is the main output pathway of the basal ganglia that projects, through inhibitory GABAergic fibres, to the ventral anterior (VA) and ventral lateral (VL) thalamic nuclei, which themselves project primarily to the supplementary and pre-motor cortices, prefrontal areas, and limbic cortex. In recurrent connections, cortical inputs into this pathway inhibit the spontaneous activity of the GPi/SNr nuclei, release the thalamic nuclei from their tonic inhibitory influence, and thus activate the cerebral cortex. Therefore, the direct pathway has an *enhancement* effect, which disinhibits the thalamic activity and enhances thalamocortical activities. Specifically for motor control, activation of the direct pathway facilitates movement.

In contrast, the indirect pathway originates from the striatum with GABAergic projections to the GPe, from there it projects to the GPi/SNr or from the GPe to the subthalamic nucleus (STN), and finally projects to the GPi/SNr as shown in Figure 4. Activity in the GPe promotes thalamic activity, by inhibiting the STN. The STN excites the GPi/SNr, through glutamatergic connections, in order to suppress thalamic activity, thereby decreasing thalamocortical activity. Therefore, the indirect pathway has an *inhibitory* effect. In terms of motor control, activation of the indirect pathway inhibits movement.

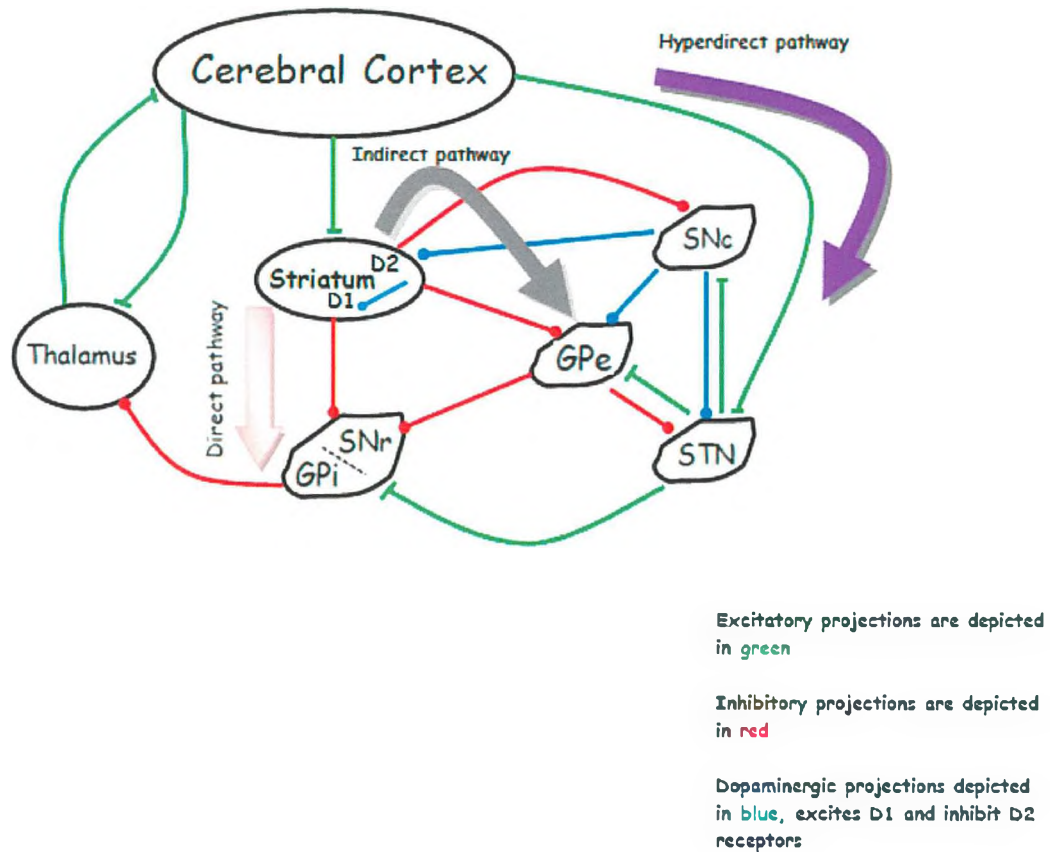


Figure 1.4. A schematic of the main pathways (models) of the basal ganglia. Simplified illustration of the direct, indirect and hyperdirect pathways of the basal ganglia. Red lines indicate inhibitory (GABAergic) projections; green lines indicate excitatory (glutamatergic) projections. Blue lines indicate modulatory (dopaminergic) projections. (D1), dopamine receptor type one; (D2), dopamine receptor type two. Key nuclei: GPe, external segment of globus pallidus; STN, subthalamic nucleus; GPi, internal segment of the globus pallidus; SNr, substantia nigra pars reticulata; SNc, substantia nigra pars compacta.

It is possible that the direct and indirect pathways converge on the same pathway in the GPi, and thus work competitively to facilitate and inhibit a particular response. This competitive process occurs in parallel for multiple responses which allows for “selective” control of different responses (Beiser & Houk, 1998; Mink, 1996). Therefore, one response might involve a Go signal to particular area of thalamus, in conjunction with a No-Go signal sent to another thalamic nucleus that involved in competing responses. The balance between the direct and indirect pathways is regulated by the differential actions of dopamine on striatal neurons that

are released from the terminals of neurons in the SNc. Special dopamine receptor type one (D1) in the striatum are excited by dopamine, acting on the direct pathway and has a facilitation effect, whilst dopamine receptor type two (D2) is acting on the indirect pathway and has an inhibition effect (DeLong, 2000). Since these two types of receptors have different functions when dopamine is released, the direct and the indirect pathways are affected differently by the dopaminergic projections from the SNc. However, the dopaminergic inputs to these pathways lead to the same effect which facilitates movements by reducing inhibition of the thalamocortical neurons (Albin et al., 1989).

It has been suggested that there is an antagonistic balance relationship between the direct and indirect pathways. The direct pathway is thought to facilitate and promote movements while the indirect pathway is thought to suppress and inhibit movements (Albin et al, 1989; DeLong, 1990). Therefore, reduced conduction through the indirect pathway leads to large and fast movements as in hemiballismus and dystonia disorders. On the other hand, facilitated conduction through the indirect pathway leads to slow movements as in Parkinson's disease (Alexander, 1994).

1.3.2 The Subthalamic “hyperdirect” Pathway

Over the past two decades, the 'direct and indirect pathways model' has revolutionarily changed the understanding of structural and functional aspects of the basal ganglia. This model was successful in explaining particular aspects of motor control and movement disorders (Nambu et al., 2004; Obeso et al., 2008). However, much evidence and results have shown the limitations of this classical model in explaining the underlying mechanisms of some motor and cognitive functions.

Recently, a pathway called 'cortico-subthalamo-pallidal hyperdirect pathway', also termed simply the 'hyperdirect' pathway here, has been introduced and become a focus of attention (Nambu et al., 2009), this is also illustrated in Figure 1.4. Unlike the direct and indirect pathways, the hyperdirect pathway is a direct cortico-subthalamic projection that bypasses the striatum. In this updated model, the STN joins the striatum as an input structure receiving direct excitatory projections from most of the cortical regions (Mink et al., 2003). The STN sends excitatory projections to the GPi nucleus and from there projects to the thalamic nuclei. This pathway stimulates the STN which leads to increased activity in the GPi. The global excitation of the GPi increases the tonic inhibition on the thalamus, which reduces the thalamo-cortical excitability and thus suppresses behaviour. This pathway acts faster than the direct and indirect pathways because this hyperdirect route has fewer synapses than the other pathways (Nambu et al., 2000; Mink et al., 2003).

Nambu et al., (2004) emphasized the functional significance of this 'hyperdirect' pathway and presented it as a new dynamic model of the basal ganglia. This pathway contributes to the filtering mechanism of direct and indirect pathways, allowing facilitating desired actions and suppressing competing motor programs. When an intended action is about to be initiated, a signal from the cerebral cortex is conveyed through the 'hyperdirect' pathway (cortex-STN-GPi) to activate the STN, which leads to increased activation of the GPi and therefore inhibition of the thalamic nuclei and cortical areas that are related to both the selected motor program and other competing programs. Second, a few milliseconds later, another signal is sent through the 'direct pathway' (cortico-striato-pallidal pathway) (cortex-striatum-GPi) to inhibit the GPi neurons encoding the desired action, and therefore activates only the selected

and desired motor program through disinhibition of selected thalamic nuclei. Finally, a signal through the ‘indirect pathway’ (cortico-striato-external pallido-subthalamo-internal pallidal pathway) (cortex-striatum- GPe-STN-GPi) terminates the motor command and stops the movement at the appropriate time. This model of information processing has a temporal evolution in order to ensure that only the desired motor programme is initiated, executed and terminated at the appropriate times, whilst other competing motor programs are canceled and prevented (Nambu et al., 2000, 2004). Thus, the hyperdirect pathway plays a crucial role in stopping responses that have already begun execution. This is an important mechanism in discontinuing one task and switching to another task or participating in stimulus-driven suppression of motor responses (Aron et al., 2006). Moreover, this pathway has been linked with inhibiting irrelevant motor programs and/or changing motor plans (Nambu, 2008). Since this route applies a ‘brake’ to responses, it is implicated in executive control, allowing cognitive operations to take place before responding (Winstanley et al., 2005).

1.3.3 Multiple Parallel Loops

As mentioned previously, the striatum receives excitatory inputs from nearly all the cerebral cortex regions. The projection from the cerebral cortex to the striatum has a roughly topographical organization. This means that specific areas of the cerebral cortex map to specific parts of the striatum (Alexander et al., 1986; Lawrence et al., 1998; Nambu et al., 2002). These associations are maintained in projections throughout the basal ganglia. For instance, the motor cortex and somatosensory areas project to the posterior putamen and the prefrontal cortex projects to the anterior part of the caudate nucleus. It has been suggested that the topographical relationship between the cerebral cortex and the striatum provides a basis for the segregation of

functionally multiple circuits- often called ‘loops’- in the basal ganglia (Alexander et al., 1986). These circuits or ‘loops’ are believed to be spatially segregated, based on the findings of some experiments in nonhuman primates (Middleton and Strick, 1997). These loops include motor, cognitive, oculomotor or visual, and affective connections, as illustrated in Figure 1.5.

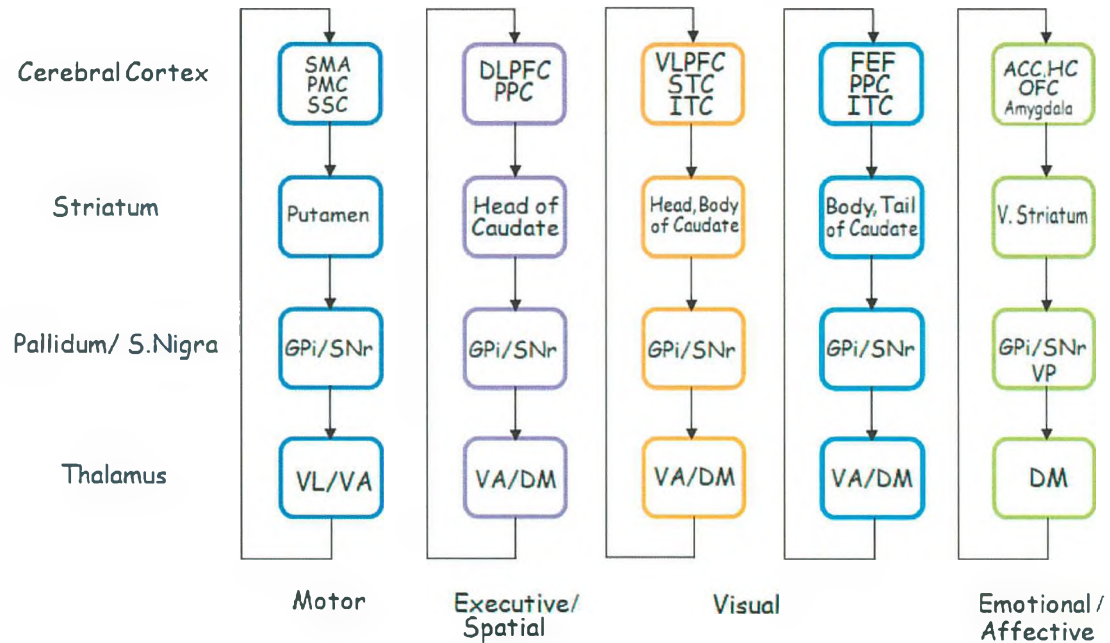


Figure 1.5. Cortical– sub-cortical (basal ganglia) loops, modified from the scheme of (Alexander et al., 1986). Five parallel loops are shown, with plausible functions labelled at the bottom. In the top row of rounded rectangles, the cortical areas that receive the thalamic projections are indicated. The second row represents the striatum, the third row the pallidum, and the bottom row the thalamus. SMA, supplementary motor area; PMC, premotor cortex; SSC, somatosensory cortex; DLPFC, dorsolateral prefrontal cortex; PPC, posterior parietal cortex; VLPFC, ventrolateral prefrontal cortex; OFC, orbitofrontal cortex; FEF, frontal eye field; ITC, STC, superior temporal cortex; inferior temporal cortex; ACC, anterior cingulate cortex; HC, hippocampal cortex; V striatum, ventral striatum; ; VP, ventral pallidum; GPe, external segment of globus pallidus; STN, subthalamic nucleus; GPi, internal segment of the globus pallidus; SNr, substantia nigra pars reticulata; SNc, substantia nigra pars compacta; VL, ventrolateral thalamic nucleus; VA, ventral anterior nucleus of the thalamus; DM, dorsomedial nucleus of the thalamus. Reproduced from Alexander GE, DeLong MR, Strick PL (1986) Parallel Organization of Functionally Segregated Circuits Linking Basal Ganglia and Cortex. *Annu Rev Neurosci* 9:357–381.

Within each circuit/loop there appear to be subcircuits such that the primary motor cortex and premotor cortex have non-identical connections with basal ganglia structures. Similarly, dorsolateral and orbitofrontal circuits have distinct connectivity

patterns. Each of these loops, which involve cortex, striatum, pallidum, and thalamic nuclei, carry different types of information. Since these segregated re-entrant loops gather different information from widespread cortical areas, they enable the basal ganglia nuclei to influence a broad range of functions, far more than simply motor function. Looking at the connections of these loops, it's clear that many inputs and outputs of the basal ganglia nuclei involve cortical areas that have little direct motor or sensory function. In addition to that, the outputs of the basal ganglia do not only target motor areas of the cerebral cortex but also target multiple regions of cortex, including prefrontal cortical regions that play an important role in executive functions. It has been postulated that the basal ganglia might act to link the functions of these segregated loops together (Wichmann and DeLong, 1999).

1.4 The Basal Ganglia: Beyond the Motor System

Historically, the basal ganglia have been known to be involved in motor functions. This is predominantly due to damage to the basal ganglia nuclei in a broad range of neurological disorders producing marked motor deficits, ranging from bradykinesia (the slowness of movement) to involuntary movements. The relationship between basal ganglia and the motor control has been suggested by clinical neurological observations on patients with movement disorders such as Parkinson disease, Huntington disease, Tourette syndrome, hemiballismus and dystonia disorders (Bevan et al., 2006; DeLong and Wichmann, 2007). These motor disorders reveal motor and postural control impairments associated with dysfunction in the basal ganglia (Utter and Basso, 2008).

Recently, the classical view that the basal ganglia are simply and solely the ‘generator’ of movement has been challenged. Multiple lines of evidence indicate that the basal ganglia are also involved in ‘non-motor’ functions. First, from the multiple reciprocal projections and loops with cerebral cortex, as mentioned previously, it is clear that the basal ganglia is involved in higher order cognitive aspects of motor control due to its interaction with higher order cortical areas. Second, the activation of some neurons in some basal ganglia structures is more related to cognitive function than to motor function. It has been found that “non-motor” neurons appear to be located within regions of the GPi and SNr that target prefrontal and inferior temporal regions of the cortex (Beiser et al., 1998). Finally, in some cases, damage to the basal ganglia cause mainly cognitive disturbances without gross motor impairments. The basal ganglia have been implicated in a wide array of ‘non motor’ cognitive functions. These include functions such as planning, switching, inhibition, sequencing, learning, timing, and the processing of reward.

The BG have been implicated in cognitive flexibility. There is abundant evidence from functional imaging data that indicates that the basal ganglia are activated during the performance of attentional set-shifting, reversal learning, and task-switching paradigms (Rogers et al., 2000; Cools et al., 2002, 2004; Leber et al., 2008). Van Schouwenburg and colleagues (2010) combined the use of an attention-switching paradigm with fMRI and dynamic casual modality (DCM) to investigate the mechanism by which the BG may control attentional flexibility. It was found that the BOLD signal in the BG was significantly greater during novel switch trials than during repeat trials. This higher activation was specifically found in the ventral striatum. Existing evidence from clinical studies on patients with Parkinson’s disease

indicates impairment in the ability to flexibly switch attention in response to the environmental changes (Rogers et al., 2000; Cools et al., 2002, 2004; Leber et al., 2008).

Recent studies of functional brain imaging have shown the involvement of the basal ganglia in the processes of planning and execution of actions. Some studies using event-related fMRI designs have investigated the neural substrates involved in motor planning (Boecker et al., 2008; Elsinger et al., 2006). It was found that the striatum, specifically the caudate nucleus, is involved in the active planning of a novel action. These studies also provided further evidence that the putamen is involved in the execution of non-routine actions. Interestingly, these results demonstrate that planning-related activity is not exclusively observed in motor regions of the cerebral cortex such as the Pre-/SMA and cingulate motor cortex (Arnold and Trojanowski, 1996), but also in the basal ganglia nuclei. In line with the previous studies a positron emission tomography (PET) (Owen et al., 1996) showed significant increased activity in the caudate nucleus in conditions when multiple actions had to be planned in advance during the performance of a planning task (for example, the Tower of London task).

A vast array of research has linked the basal ganglia, particularly the striatum, to various aspects of learning such as habit formation (Jog. et al., 1999), skill learning (Poldrack et al., 1999) and reward-based learning (O'Doherty et al., 2004; Delgado et al., 2005). Several theoretical models of learning have suggested that the basal ganglia plays a critical role in reinforcement learning based on the reward signal encoded in the dopaminergic neurons from the substantia nigra pars compacta (SNc) (Cromwell

and Schultz, 2003). Kenji Doya (1999) hypothesized three learning modules that can be assembled in visually-guided behaviour. One of these postulated modules was that the basal ganglia are specialized in reinforcement learning, which can be used to evaluate the current state and to select an action based on the evaluation.

In non-human primate experiments, by recording the activity of midbrain dopaminergic (DA) neurons during the performance of behavioral tasks, Schultz (2000) found that DA neurons in SNc show phasic increase in firing in response to an unpredicted reward or a sensory cue that indicates the delivery of a reward in the near future. These findings give strong evidence that the basal ganglia code a prediction error of reward delivery. Results from functional neuroimaging studies in humans support the same hypothesis, with the ventral striatum being activated by reward unpredictability (Berns et al., 2001). Moreover, other neuroimaging studies using learning paradigms involving feedback have shown increased activation in the striatum differentiating between positive and negative feedback (Poldrack et al., 1999, 2001; Seger and Cincotta, 2005). In neuropsychological studies, patients with Parkinson's disease, compared with control subjects, are impaired at a feedback-based learning task whilst good in learning during a non-feedback version of the same task (Shohamy et al. 2004; Poldrack et al., 2001). This accumulating evidence suggests that the striatum, the primary input structure of the basal ganglia, is part of a circuit responsible for mediating reward processing during learning.

Encoding time is crucial for motor learning and cognitive actions. Many lines of evidence, including functional imaging studies in humans, and lesion studies in humans and animals, suggest that the basal ganglia are important for temporal

processing (Meck et al., 2008). Ivry (1996) has suggested that the basal ganglia are crucial to the effective running of an “internal clock” and are involved in the timing of long intervals (seconds range). Numerous imaging studies in humans using different timing tasks, such as the repetitive tapping paradigm (Rao et al., 1997; Rubia et al., 1998), duration discrimination and reproduction (Rao et al., 2001; Fernandez-Ruiz et al., 2003; Harrington et al., 2004; Lewis and Miall 2006) have provided evidence that the basal ganglia play a key role in temporal processing. For example, Jahanshahi and colleagues (2006), using (PET) technique, have shown that the substantia nigra is significantly more activated in a time reproduction task than the control reaction time task. It was also found that the putamen was highly activated in the long interval timing rather than the short interval. In clinical studies, patients with Parkinson’s disease (PD) also show significant deficits in performing timing tasks, deficits that are improved with dopaminergic medication (Pastor et al., 1992; Malapani et al., 1998).

From anatomical point of view, it is noteworthy that the basal ganglia circuits related to ‘non-motor’ functions share the same intrinsic neuronal circuits with those related to motor control. Therefore, it is not surprising to find that there are similarities between the basic cognitive functions and motor functions of the basal ganglia. For example, the basal ganglia have been viewed as a ‘centralized selection device’ for both cognitive and motor activities and this device is specialized to resolve conflicts between competitors (Gurney et al., 1998).

1.5 Overview of the Thesis

Over the past decade, the functional contribution of the basal ganglia has been extensively investigated. Traditionally, the basal ganglia have been considered to be a

part of the motor circuit, however extensive evidence now indicates a role for the basal ganglia in learning and cognition (Doya, 2000; Krebs et al., 2001; Sommer et al., 1999).

The main aim of this work is to study basal ganglia function using fMRI at ultra-high magnetic field (7Tesla). The role of the basal ganglia is investigated first in healthy subjects and then in subjects with neurological syndromes specifically studying Tourette syndrome. Two processes are investigated, that of cognition (including the neural processes of inhibition of competing motor programs using the 'GO/WAIT task' and 'GO/NO-GO task' and modification of this paradigm). Second, motor learning, including motor prediction and reward mechanism using the 'Motor Prediction task' are investigated.

A schematic overview of this thesis is shown in Figure 1.6. This flowchart shows parallel lines of basal ganglia function with the relevant experimental paradigms. A brief overview of the experimental chapters follows.

Chapter 2 introduces the aspects that are involved in conducting a functional MR experiment, ranging from the fundamental principles of MRI to the acquisition, statistical analysis and interpretation of the fMRI results. Chapter 3 outlines the imaging methodology used in this thesis experiments. Chapter 4 describes the concept and mechanism of inhibition in cognition. This chapter includes the first three empirical experiments that were carried out using the 'GO/WAIT' paradigm. Experiment (1), a 'GO/WAIT' paradigm with fixed interval timing was used in order to elucidate the neural substrates of the inhibitory process.

Experiment (2), a ‘GO/NO-GO’ paradigm is performed to look at the underlying mechanism of cancelling an ongoing intended response, and the results are compared with that of Experiment (1). Experiment (3), a ‘GO/WAIT’ paradigm with variable interval timing was used rather than fixed interval timing as in Experiment (1). The aim of setting variable timing was to attenuate the effect of learning to predict the offset time of the stimulus that was seen in the results of Experiment (1).

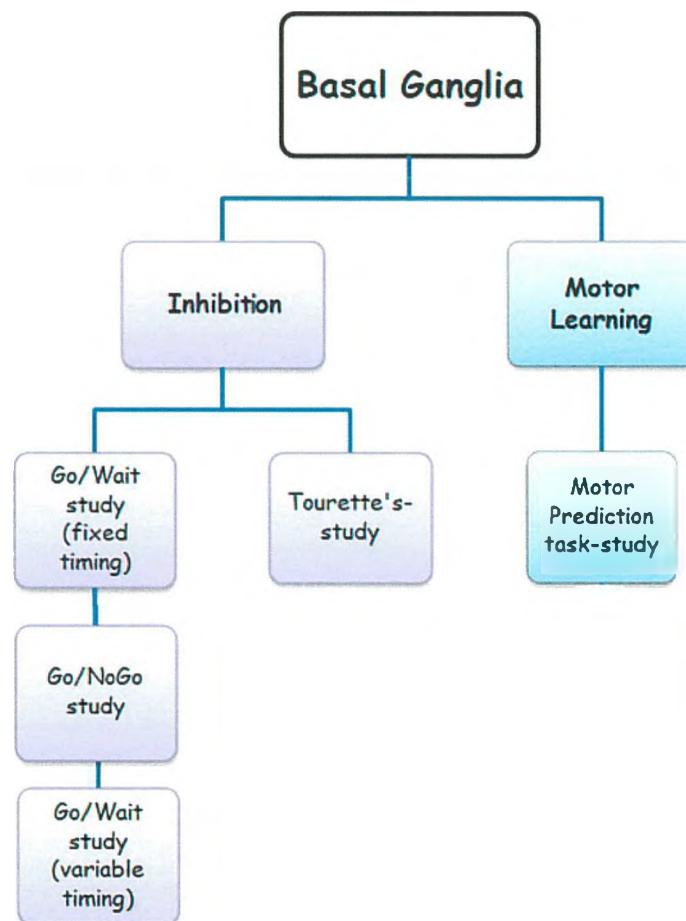


Figure 1.6. A schematic overview shows the experimental pathways of this thesis.

A clinical overview of Tourette syndrome with its diagnosis and symptoms are introduced in Chapter 5. In addition, a group with Tourette syndrome and age-matched control group (Experiment 4) were tested using the same ‘GO/WAIT’

paradigm of Chapter 1 in order to investigate the role of the basal ganglia in this disorder.

A broad introduction to motor learning, with a discussion of involvement of the basal ganglia in mediating the learning process is described in Chapter 6. In this chapter, Experiment (5) was conducted using the Motor Prediction task to investigate the basal ganglia function in encoding the immediate reward, and the prediction of future reward. Finally, a summary of findings and concluding remarks of the experimental results obtained, with the future directions of this work, are outlined in Chapter 7.

Chapter 2

2.1 Introduction

Neuroimaging techniques provide a powerful tool for localizing brain areas that are active whilst performing certain tasks. These techniques can be utilized to investigate the neural substrates of human motor control and cognitive functions, areas of interest in this thesis. There are many techniques to measure brain function, including functional Magnetic Resonance Imaging (fMRI), positron emission tomography (PET), single positron emission computerized tomography (SPECT), magnetoencephalography (MEG) (Hämäläinen et al., 1993), and electroencephalography (EEG) with the analysis of event-related potentials (ERP's) techniques (Fabiani et al., 2007) and oscillatory activity (Pizzagalli, 2007).

This chapter mainly focuses on fMRI method as it is a widely used technique and as all of the experiments in this thesis are performed using fMRI. This chapter provides a general overview of the various stages and aspects involved in conducting a functional MR experiment, ranging from the basic principles of MRI physics to fMRI methodology and the statistical analysis and interpretation of the results. The first section of this chapter covers the principles of MRI physics and how imaging data are acquired. The second section explains the underlying mechanisms of the Blood Oxygenation Level-Dependent (BOLD) contrast. In the third section, attention is paid to how to select and design an optimal fMRI experiment that can maximize the probability of finding reliable results. Finally, the fourth section will be dedicated to the pre-processing steps and statistical analysis of fMRI data.

2.2 Functional Magnetic Resonance Imaging (fMRI)

Functional Magnetic Resonance Imaging (fMRI) has established itself as a standard tool for mapping activation patterns in the brain, both in normal healthy subjects and in disease. fMRI is a technique that can be used to provide activation maps demonstrating which areas of the brain are involved in a particular task or function.

fMRI has several significant advantages over other neuroimaging techniques: it is a non-invasive tool, and does not involve radiation, and also does not need contrast agent to be administered, making it safe for the subject and repeatable. It has excellent spatial and good temporal resolution compared, for example, to PET. The interdisciplinary nature of this method, make it an appealing technique which crosses the borders of neuroscience, psychology, psychiatry and physics. fMRI measures the haemodynamic response associated with neural activity in the brain, and produces images of activated areas in the brain by detecting the indirect effect of neural activity on regional blood volume, blood flow and oxygen consumption (Ogawa et al., 1992).

2.3 The principle physics of MRI

As the fMRI technique depends on subtle properties of the MRI signal, it is necessary to understand in some detail how magnetic resonance imaging works.

Many atomic nuclei have intrinsic magnetic moments. When they are placed in an external magnetic field, the magnetic moments precess about the direction of the main magnetic field (B_0), at a particular frequency, which is dependent on their electromagnetic environment, the frequency of this precession is known as the Larmor

frequency, as shown in Figure 2.1. In theory, all nuclei with magnetic moment can spin around their axis and can be used to obtain magnetic signals. However, hydrogen nuclei (protons) are the most commonly used in MRI (Buxton, 2002; Hashemi et al., 2004; Horowitz, 1995; Jezzard et al., 2001) due to their relative abundance in the brain tissues and their high sensitivity for producing a magnetic resonance signal (Bushong, 1996).

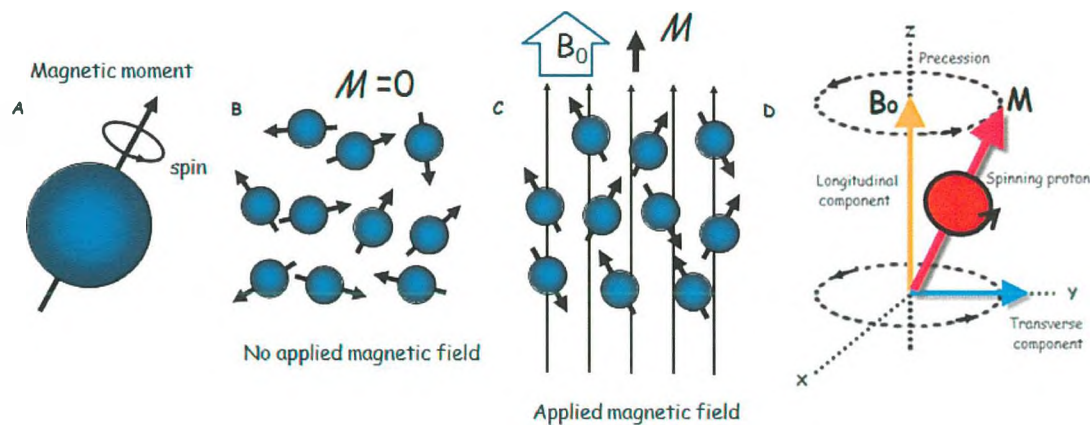


Figure 2.1. (A) Intrinsic magnetic moment. (B) In the absence of a strong magnetic field, the spins are oriented randomly. Thus, there is no net magnetization (M). (C) In an applied magnetic field, B_0 , the spins align with the applied field in their equilibrium state. This results in net magnetization (M). (D) Spin (protons) precess about the applied magnetic field, B_0 , which is along z axis. The frequency of this precession is proportional to the applied field.

In the presence of a static magnetic field the hydrogen atoms align themselves with this field and reach an equilibrium state (a net magnetisation state, M) in which \sim 1ppm of spins are aligned with the main magnetic field, B_0 . In addition to aligning with the field, the spins precess at the Larmor frequency, $\omega = \gamma B_0$, where γ is the gyromagnetic ratio of the nuclei and B_0 is the main static magnetic field. For protons at 3 Tesla this corresponds to 128MHz. When a radio frequency pulse (RF), B_1 , is applied to the tissues at a similar frequency to the Larmor frequency, the hydrogen atoms absorb energy (excitation) and their equilibrium state is perturbed, resulting in more spins in the higher energy state and the spins being brought into phase. Once the

radio frequency (RF) pulse is turned off, the spins emit energy at the same radio frequency until the nuclei return to their equilibrium state and dephase. This return to the equilibrium state and dephasing is termed relaxation and can be considered in terms of either the *longitudinal relaxation time* (T_1) (where net magnetization in z axis return to equilibrium) or *transverse relaxation time* (T_2 or T_2^* contrast) (as the spins tend to move out of phase).

As the nuclei return to equilibrium they produce an oscillating magnetic field which induces a small current in the receiver coil. This signal is called the free induction decay (FID). By Fourier transforming, this signal is converted into a nuclear magnetic resonance (NMR) frequency, converting the signal from the time domain into the frequency domain.

3D spatial information can be obtained from the NMR signal by applying a magnetic gradient field (in each direction x , y , z) in addition to the main static magnetic field, B_0 . Strong magnetic field gradients cause nuclei at different locations to precess at different rates due to the Larmor frequencies being different at distinct spatial locations. A process called slice selection is used to select a slice, this is then encoded in 2D using frequency and phase encoding gradients.

As explained in the previous section, the amount of energy released by the hydrogen molecules after the termination of the RF-pulse gradually decays over time. The rate of this decay (T_1 or T_2/T_2^*) differs for different tissues and this allows the distinction between different types of tissue possible in MRI. For example, distinguishing between white matter (WM), grey matter (GM), and cerebral spinal

fluid (CSF) in the brain anatomical images. In order to investigate the brain at work, T_2^* must be applied to locate functionally active areas.

The imaging timing parameters of echo time (TE) (the time between RF pulse and measurement) and repetition time (TR) (the time between successive RF pulses) need to be set carefully in order to achieve the required image contrast, such as T_1 weighted, T_2 weighted and proton density (PD) weighted image contrast. The image contrast can be manipulated by altering the TR and TE. For instance, if the TE is short, and the TR is also kept short, this result in sensitivity to the difference in T_1 between different tissues, and the obtained image is called a T_1 weighted. A T_1 weighted image is typically used for a structural or anatomical scan, as it shows good contrast between white and grey matter.

Alternatively, if the TE is long and the TR is also long, the sensitivity to the difference in T_2 for the different tissues is increased, and the acquired image is called a T_2 weighted image. T_2 weighted images are often collected for pathological scans, because lesions appear very bright (Horowitz, 1995; Jezzard et al., 2001). If TE is short and TR is long, the signal will depend little on the T_1 and T_2 values of the tissue and will depend mainly on proton density on the tissues. Thus, the resulting image is called a proton density (PD) weighted image.

2.4 BOLD fMRI

fMRI is sensitive to the haemodynamic changes that are associated with neural activity. The BOLD (Blood Oxygenation Level-Dependent) effect is the most common source of contrast in fMRI images. When neurons are activated, there is an

increase in blood flow, blood volume and oxygen consumption local to that region of the brain. The brain over compensates and as a result, the cerebral venous oxyhaemoglobin (the oxygen-carrying protein within the red blood cells) concentration increases and the deoxyhaemoglobin concentration decreases. Deoxyhaemoglobin is paramagnetic, whilst oxyhaemoglobin is diamagnetic. As the deoxyhaemoglobin has paramagnetic properties it will cause an inhomogeneity in the magnetic field surrounding it. Therefore, a high level of deoxyhaemoglobin in the blood will lead to an increase in the magnetic field inhomogeneity, increased dephasing of spins, resulting in a decrease in the fMRI signal (Detre and Wang, 2002; Heeger and Ress, 2002; Ogawa et al., 1990a, 1990b; Ogawa et al., 1992;). Thus, on activation the resulting increase in oxyhaemoglobin, causes a change in the local magnetic properties of surrounding tissue in the brain, leading to an increase in image intensity on the fMRI scan in those active brain areas.

The resulting change in fMRI signal as a function of time in response to a temporary increase in neuronal activity (an event) is known as the haemodynamic response function (HRF) (Heeger et al., 2002). The shape of the HRF in response to an event is shown in Figure 2.2, it starts with an initial dip due to the increase in deoxyhaemoglobin level before the blood flow increases, this is followed by a large increase of ~ 1-2 % at high field (3T) of the BOLD fMRI signal that reaches its peak at about 5-6 seconds after the onset of the stimulus (Hoge and Pike, 2001). This increase is a result of increasing oxyhaemoglobin level and the relative decrease in deoxyhaemoglobin level, which in turn leads to an increase in the BOLD fMRI signal. This signal then decays back to the resting level (baseline level), and then undershoots, between 15-25 seconds, termed the post stimulus undershoot. This signal

is cumulative however, so if the brain area under investigation is kept activated the HRF stays at its peak value. In this way active voxels (volume elements of the functional image) can be distinguished from voxels that are not active.

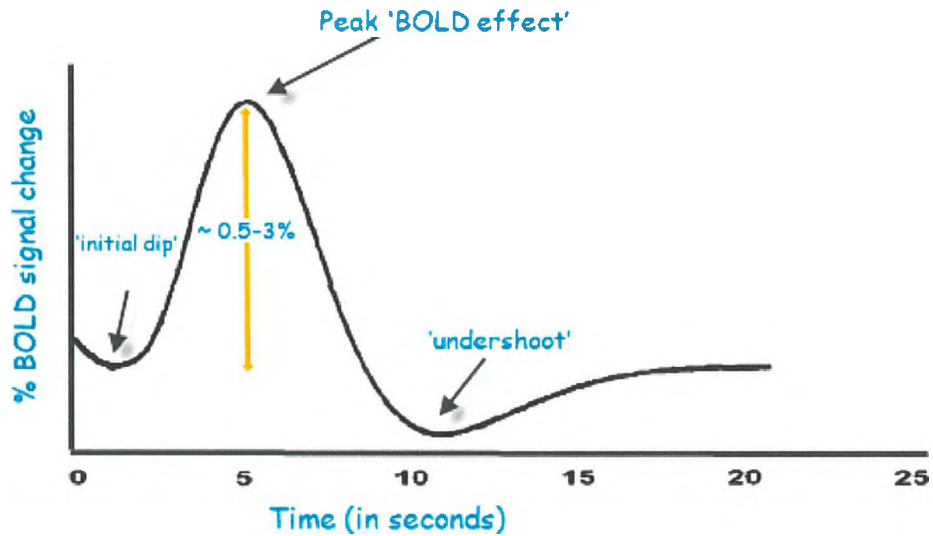


Figure 2.2. Typical (canonical) hemodynamic response function (HRF)

The type of scanning sequence that is most commonly used to obtain functional images is an echo planar imaging (EPI) sequence. Echo planar imaging (EPI) is one of the rapid MRI techniques which was proposed by Peter Mansfield (Mansfield et al., 1977). EPI is a rapid and efficient MRI method that can acquire an image, from a single free induction decay signal (FID), in about 40 to 100 ms. In the EPI sequence, all the signal information required to form the image is acquired in a ‘single shot’. The imaging speed in EPI arises from the use of higher gradient amplitudes and faster sampling. Such a rapid imaging acquisition technique has many advantages in MRI. For example, the motion-related artifacts in the images can be reduced by the rapid scan. Moreover, the imaging speed can provide an outstanding insight into dynamic processes such as the neural activity of the brain. In fMRI, the strength of the BOLD signal measured depends critically on the imaging timing parameters of echo time (TE). The optimal TE for BOLD contrast is that which

matches the T_2^* of the tissue of interest. The T_2^* is defined as a time constant describing the exponential decay of signal, due to transverse relaxation.

2.5 Experimental Design

The ultimate success of any fMRI experiment depends fundamentally on three main stages; the design of the experiment and the stimulus paradigm, the scanning sequence used to acquire images, and the data is pre-processed and statistical analysis, as shown in Figure 2.3. This section contains a description of the optimal experimental design, and of different types of experimental design used in fMRI research with their advantages and limitations regarding their ability to answer particular scientific questions.

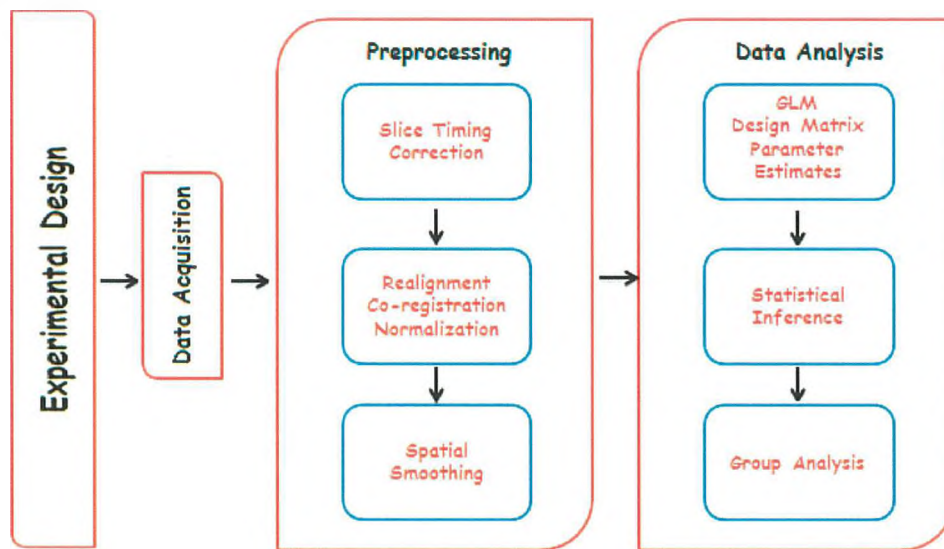


Figure 2.3. The fMRI data processing pipeline illustrates the key stages in the fMRI experiment. The pipeline shows the path from 1) experimental design, to 2) data acquisition, and 3) pre-processing and analysis stages.

Experimental design is the key component of the fMRI studies and critical to allow good interpretation of the results. Developing a proper experimental paradigm requires careful consideration regarding the study objectives, research question, and

statistical models. Taking into account these issues, the optimal design can increase the probability of finding reliable results and maximizes the statistical significance in order to draw solid inferences. The choice of task and the timing parameters between stimuli determine the statistical activation maps.

Functional MRI is dependent upon haemodynamic changes of the neural activity. Therefore, to investigate a specific cognitive function the fMRI experiment must be designed within the constraints of the spatiotemporal characteristics of the BOLD signal. The spatial characteristics derived from the vascular architecture and the temporal characteristics include the fact that the HRF is transient, delayed, and dispersed over time and the time constant of the HRF is longer than the sampling interval of neural events. These are the fundamental characteristics that should be considered in designing an fMRI experiment.

There are two main types of experimental designs utilized in fMRI experiments. These are block and event-related designs (Buckner et al., 1996; Dale and Buckner, 1997).

The block design, also called a 'boxcar', is the most commonly used experimental design and dominated the early years of fMRI research. In a block design, a series of sequential trials in one condition is presented during a specific length of time. In this type of design, two or more conditions can be alternated in different blocks, as shown in Figure 2.4.

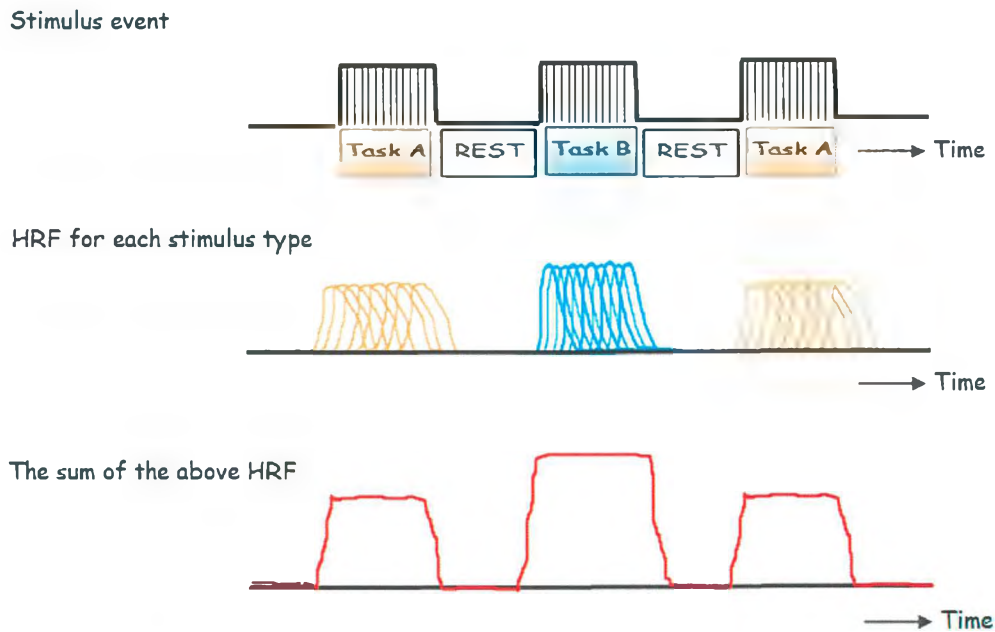


Figure 2.4. Block design. First row shows time blocks of two tasks which are interleaved with time blocks of rest. Second row shows the BOLD response which is composed from the individual HRF from each stimulus of each task block. Third row shows the sum of the HRF.

The main advantage of a block design arises from the fact that the increase in the BOLD signal in response to a series of stimuli is an additive process. This leads to an increase in the HRF during multiple presentations of stimuli in a single period of time. Therefore, a block design provides superior statistical power (Friston et al., 1999). However, in a block design, the randomization and spacing of different stimulus categories is not possible and only one task condition can be presented within each block. This makes the type of event order within each block predictable (Aguirre and D'Esposito, 2000; Donaldson and Buckner, 2001). The alternation of two conditions in different blocks allows the BOLD signal acquired during one task condition to be compared to other blocks involving different task conditions. This is called a subtraction comparison strategy (Aguirre and D'Esposito, 2000; Donaldson and Buckner, 2001). However, there are weaknesses of using such a block design to adopt a subtraction strategy (Friston et al., 1996b; Aguirre and D'Esposito, 2000). For example, the main assumption of the subtraction strategy is a principle known as pure

insertion. This implies that the two (or more) conditions can be linearly added. If this assumption fails, the difference in the fMRI signal between two cognitive conditions will reflect the interactions among the cognitive components of a task. Use of the block subtraction leads to criticism related to the cognitive and neuropsychological process, and the underlying assumptions. Although, a block design offers high statistical power, it is hard to draw strong inferences due to these problems (Aguirre and D'Esposito, 2000).

The second type of experimental design is the event-related (ER) design (Aguirre and D'Esposito, 2000; Donaldson and Buckner, 2001). In an event related design, rapid mixed trials of different task conditions are presented. The advantage of this design is that the HRF time course in response to event stimulus presentation can be estimated, as shown in Figure 2.5. However, the statistical power of event related design is lower, compared to the block design, due to the small signal change in the BOLD signal in response to a single stimulus presentation (Aguirre and D'Esposito, 2000; Donaldson et al., 2001).

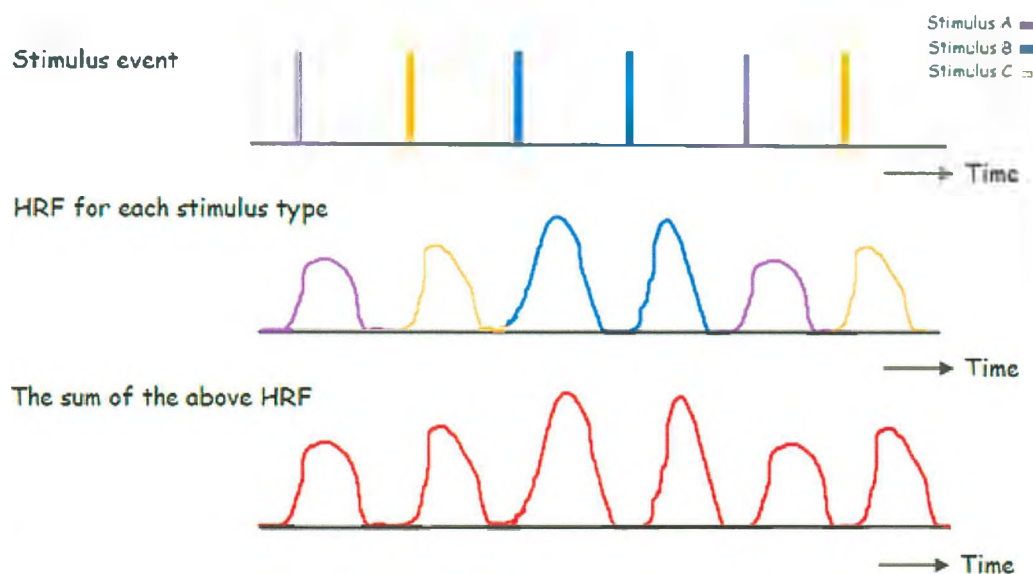


Figure 2.5. An Event-related design. First row shows different types of stimulus events. Second row shows the the BOLD response which is composed from individual HRF from each stimulus. Third row shows the sum of the HRF.

An event-related design takes the advantage of the rapid data acquisition capabilities of fMRI, which allows images to be created of the neural activity related to a particular stimulus or cognitive event within a trial. There are several important advantages of event-related designs over block designs. First, it permits randomized and intermixed events of different types to be presented far enough apart in time, as is standard in neuropsychological and electrophysiological studies. This means that the HRF in response to a stimulus or cognitive event is allowed to return to baseline before the onset of the next event. Therefore, this leads to reduced confounds arising from stimulus order predictability and HRF habituation. Second, the ability to categorize events responses post-hoc based on the subject's behaviour such as response accuracy (Carter et al., 1998), or subsequent memory (Wagner et al., 1998), is another potential advantage of this design. For some studies an experimental question cannot be answered using a block design (Donaldson and Buckner, 2001), and the event-related design becomes the only valid choice for these studies. For instance, some events cannot be blocked, such as the occurrence of "oddball" stimuli (Clark et al, 2001) as used in chapter 4 of this thesis. Taking into account these advantages of event-related designs and the research question that needs to be answered in this thesis, all experiments in this thesis used an event-related (ER) design.

2.6 Pre-processing steps

In order to carry out a successful statistical analysis, there are some assumptions related to the fMRI data that must be met. First, it is assumed that all the voxels in an image are acquired at one same point in the time series, so each voxel in a volume is assumed to represent the same point or moment in time. Second, it is

assumed that each data point in the time series from a given voxel was acquired from that same voxel, therefore, each voxel represents the same location throughout the time series. Finally, it is assumed that the residual variance after removing the effects of interest will be constant over time and have a Gaussian distribution. Moreover, when performing analyses across subjects to infer group results, it is assumed that each voxel will correspond to the same structural brain area in all subjects as all subject's brains are assumed to be aligned. After the acquisition of imaging data and before carrying out a statistical analysis it is therefore necessary to apply a number of pre-processing steps to the fMRI data to meet these assumptions (Smith et al., 2001). These include; slice timing correction, spatial realignment, spatial co-registration, spatial normalization and spatial smoothing, as illustrated in Figure 2.3. These steps aim to remove various artefacts in the data and increase the validity and sensitivity of the statistical analysis. The following sections will discuss each of these steps briefly and their consequences for data interpretation.

2.6.1 Slice Timing

Based on the assumptions of statistical analysis, all the voxels in a given image acquired at a given time point of the time series are collected at the same point. Due to the fact that most fMRI BOLD signal sequences obtain imaging data slice-by-slice, some slices are collected later during the volume acquisition than others. Therefore, there will be a temporal difference between the acquisition of the first slice and of the last slice. In order to solve this problem, all slices of a volume must be adjusted in the temporal domain. This can be achieved by applying a temporal correction for the differences in acquisition time between the slices. This is called slice timing correction (Smith et al., 2001). Before this step takes place, a 'reference

slice' must be chosen; this is the point in time that the entire volume is adjusted to. Then, an interpolation method is used to shift in time all the other slices in the image volume to the reference slice. Slice timing correction is especially important for fMRI data collected with a long TR ($> 3s$) where expected HRF amplitude may vary significantly over the volume. However, some researchers do not apply slice timing correction, as the data might be confounded by errors of temporal interpolation.

2.6.2 Realignment or (Motion correction)

The main problem in the fMRI experiments is movement of the subject's head during the acquisition of the time series. Head movements lead to the fact that the same voxel does not necessarily represent the same location in the brain throughout the time series (Ashburner and Friston, 2000, 2003a; Brammer, 2001). However, in the statistical analysis, it is assumed that the data at the same voxel in a particular individual represents the same brain region throughout the fMRI time series.

Head movements can be associated with task performance or be random in nature. If the movements occur during task performance, this can result in an increase in the BOLD fMRI signal and lead to false positive activations (Ashburner and Friston, 2000, 2003a; Brammer, 2001). On the other hand, if the movements are not related to the task performance they will add to the residual noise and reduce the sensitivity of the statistical analysis (Ashburner and Friston, 2000, 2003a; Brammer, 2001). The first step in reducing motion effects is to choose a reference volume. This is typically either the first image or the mean image of the fMRI time series. Then, the realignment process takes place, in which typically the position of the brain is changed, and not the size or the shape. This realignment, with three translations

(x,y,z) and three rotations (yaw, pitch and roll), treats the head as a rigid object and is therefore called a rigid body transformation. The realignment is done by a least square method that minimise the difference in signal intensity between each volume in the time series and the reference volume. There are some limitations to the realignment process. Firstly, the brain is not a rigid object. Heart-beat and respiration (physiological movements) cause variations in the size and the shape of the brain. Usually, this source of movement can be ignored (Brammer, 2001). Secondly, if the head movements are too excessive, the minimization algorithm may get stuck in a local minimum (Ashburner and Friston, 2000, 2003a; Brammer, 2001). However, some new approaches have been proposed to minimise the least mean square difference between the volumes in the time series and the reference volume in order to decrease this risk (Jenkinson et al., 2002). The third and main limitation is that even perfect realignment will not remove all movement related variance (Ashburner and Friston, 2000, 2003a; Brammer, 2001). The problem is that, during movement, the image not only moves, but also fundamentally changes the MR signal in a complex way.

2.6.3 Spatial Co-registration

Co-registration is also called ‘between-modality rigid registration’, and aligns scans from the same subject from different types of modalities together. For example, to align a functional low resolution EPI image to the same subject’s structural high resolution T₁-weighted anatomical image (Ashburner and Friston, 2003a; Jenkinson, 2001). This step can be performed for a number of reasons. First, it allows overlaying the statistical activation map on a high resolution anatomical scan of that same subject. Second, co-registration can help with spatial normalization of the data to a

known template space. The parameters that are used to match the anatomical image to the standard brain can then be applied to the functional images allowing these to be matched to the standard brain, therefore providing better matching and results (Ashburner and Friston, 2003a; Jenkinson, 2001). Because functional and anatomical images are collected with different types of sequences and different tissue types have different signal intensities, it is not appropriate to use a least squares intensity difference method to match these images. Instead, mutual information theory can be used to maximize mutual information among of the two images, and intensity prediction degree, where the intensity of one image can be used to predict the intensity of the other image (Cover and Thomas, 1991).

2.6.4 Spatial Normalization

Normalization refers to the process of fitting the orientation, size and shape of the brain of each subject to that of a standard brain template (i.e., the Talairach brain template or the Montreal Neurological Institute (MNI) brain templates as used in this thesis) (Ashburner and Friston, 2000, 2003b). Spatial normalization can be done by using a number of linear transformation parameters. Additionally, the images can be ‘warped’ and transformed by multiplying them by a series of nonlinear cosine basis functions, in order to give a better match to the standard template (Ashburner and Friston, 2000, 2003b). There are several important advantages to this step. First, it enables quantitative comparisons to be made across or between subjects because the same brain area of each subject represents the same anatomical location. Second, it improves the comparison with other published studies. Third, it allows generalization of the results to a larger population (Ashburner and Friston, 2000, 2003b). However, some potential confounds with normalization should be considered, such as a

reduction in spatial resolution, and decrease in the activation strength by subject averaging due to partial voluming.

2.6.5 Spatial Smoothing

Applying spatial smoothing to the functional imaging data leads to blurring of the image intensities in space. There are a number of good reasons to apply smoothing on the imaging data. First, smoothing removes the high spatial frequencies which increases the signal-to-noise ratio (SNR) in the BOLD fMRI signal. Second, smoothing removes small frequency differences, therefore, improves comparisons across subjects. Third, smoothing helps to meet the requirements for applying the Gaussian Random Field Theory, a multiple-comparisons correction method, which assumes that the variations across space are continuous and normally distributed (Smith et al., 2001).

Smoothing involves the convolution of the image voxels with an isotropic Gaussian kernel, which is a 3D normal distribution curve often described by the full width of the kernel at half its maximum height (FWHM). The width of the smoothing curve is defined in millimetres, and the amount of smoothing (FWHM) chosen is typically two or three times the voxel size. This should be considered, as the smoothing amount will influence the size of the brain region where a significant increase in the BOLD signal can be detected in the statistical analysis. For example, smoothing with a FWHM of 6mm will result in not being able to detect areas of significant increase in the BOLD signal that are smaller than 6mm (Smith et al., 2001).

In addition to smoothing in the spatial domain, smoothing in the temporal domain can also be performed to improve the signal-to-noise ratio (SNR). Temporal smoothing is the process of filtering unwanted temporal frequencies from the data (Kiebel and Holmes, 2003; Smith et al., 2001). Such low frequencies in the fMRI time series can arise from the physiological-related noise (such as heartbeat and breathing) or physical (scanner-related) noise (as the scanner heats up or due to any instability in the scanner hardware). These sources of low frequencies can be dealt with by using a high pass temporal filter. A high pass filter removes all frequencies below the specified cut-off frequency from the dataset (Smith et al., 2001). By reducing these low frequency drifts that may appear in the time series, the SNR will be improved and the power of statistical data analysis will be increased (Kiebel and Holmes, 2003; Smith et al., 2001).

2.7 Statistical Analysis

After the pre-processing steps, a statistical analysis can be performed on the imaging data. Two goals of statistical analysis include; i) detection of active brain areas that show a significant and consistent activation during task performance and ii) the estimation of the hemodynamic response function (HRF).

There are many software packages available from different laboratories (i.e., FSL at <http://www.fmrib.ox.ac.uk/fsl>; Brain Voyager at <http://www.brainvoyager.de>; SPM at <http://www.Wl.ion.usl.ac.uk/spm>; and AFNI at <http://afni.nimh.nih.gov/afni>). However, this section will focus on the statistical parametric mapping (SPM) software (Friston et al., 1995) since this is the software that is used in analysing all experiments in this thesis.

The General Linear Model (GLM) and theory of Gaussian random fields are the most commonly methods that are used in statistical analysis of fMRI data (Friston et al., 1995, 1996a; Kiebel et al., 2003; Lange et al., 1999; Worsley, 2001). The GLM is used to specify the experimental conditions in the form of a design matrix, which defines the experimental design and the nature of the hypothesis testing to be implemented. The linear regression is the commonly used parametric model in GLM. The GLM is an equation that associates the observations to the expected signal, by expressing the observations (response variable Y) in terms of linear combination of expected components (or explanatory variables X) and some residual error (ϵ). This equation is $Y = X\beta + \epsilon$, X is known as the design matrix that contains the explanatory variables and β is the unknown parameter to be estimated (termed the parameter estimates) and ϵ is the residual error.

The statistical parametric mapping approach is a univariate approach used to determine the parameter estimates of a general linear model (GLM) at each voxel in the brain (Kiebel and Holmes 2007; Kiebel et al., 2003; Friston et al., 1995; Lange, 2000; Worsley, 2001). This means that each voxel in each volume is estimated and analysed separately. The BOLD fMRI response is modelled and contained in the design matrix, as shown in Figure 2.6. Then, the parameters (parameter matrix) of this model are estimated. Finally, this parameter matrix is compared to the error matrix for each voxel individually, reaching its highest level in a test statistic (t-score and Z-score) for each voxel.

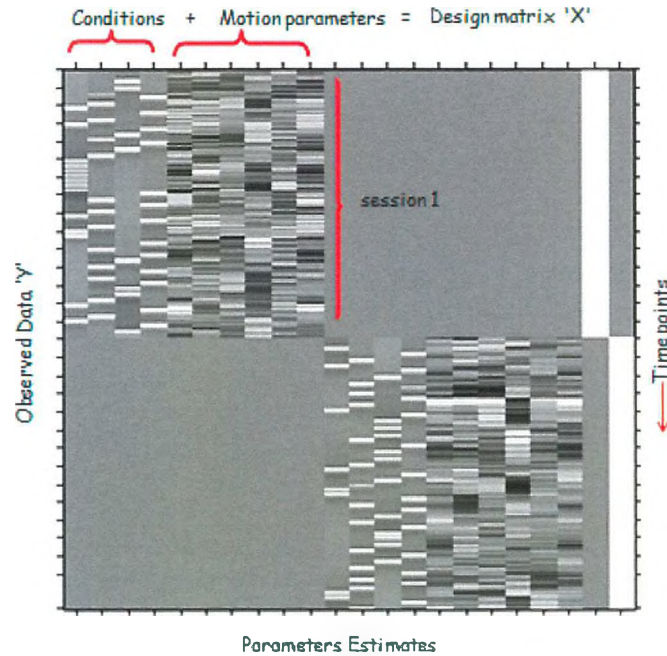


Figure 2.6. A design matrix with columns for each parameter (in this example, four conditions of interest in addition to the motion parameters).

The parameter estimates (or effect sizes) are then subjected to a statistical test (contrast), which results in a statistical parametric map (Poline et al. 2007). The inferences about these parameter estimates are made using the estimated variance. The null hypothesis that some contrast or linear combination of the estimates is zero can be tested by using the T statistic to give an $SPM\{t\}$ map. The T contrast is used to look at the difference between two conditions (each within one regressor). The T contrast is one-tailed test (directional test) which allows one to enquire the difference between the two conditions for example ($A > B$) or ($A < B$). On the other hand, the null hypothesis that all estimates are zero is tested by using the F statistic to give an $SPM\{F\}$ map (Friston et al., 1995, 2006). The F contrast is used to look at the difference of variations for each condition of each regressor. The F contrast is two-tailed test (non-directional test) which allows comparison of the variances of the residual errors of one or several conditions, regardless of directions.

Analysis of fMRI data from multiple subjects (group analysis) determines the differences of the activated regions in different groups of subjects. The main goal of the group analysis is to generalize individual findings to the population. There are two main approaches of group analysis, fixed-effects (FFX) or random-effects (RFX) analysis. The FFX approach only takes into account the intra-subject variability. This method treats the subject as a fixed variable (constant) in the GLM. The FFX approach is used to report results as case studies and cannot be used to draw inferences about population effects. FFX analysis typically takes place within the concept of the General Linear Model (GLM) as described in earlier sections. Alternatively, the RFX approach takes into account the inter-subject variability. This method treats the subject as a random variable in the model. The RFX is used to make inferences generalized to the population from which subjects are drawn (Beckmann et al., 2001). The RFX analysis can be conducted by the following steps. First, fitting a multiple-subject separable GLM (GLM for each subject) at the first level, as described in the previous sections. Second, the effect of interest for each subject should be defined to create a contrast image. Finally, entering the contrast images into a GLM at the second level that implements a one-sample t-test or any other tests (Frison and Pocock, 1992; Holmes et al., 1998). In this thesis RFX approach was used in analyzing all the experiments.

Chapter 3

3.1 Introduction

To date, most functional magnetic resonance imaging (fMRI) studies use MR scanners of magnetic field strength of 3 Tesla. However, ultra high-field (UHF) MR scanners (here defined to be 7 Tesla) are now becoming increasingly more widely used as they become available from all MR manufacturers. UHF provides increased signal-to-noise ratio (SNR) and significant advantages for fMRI due to the increase in sensitivity to Blood Oxygenation Level-Dependent (BOLD) contrast (Turner et al., 1993; Gati et al., 1997; Yacoub et al., 2001). However, moving to ultra-high field also presents several challenges.

In this thesis all the experimental fMRI studies presented are performed at 7 Tesla. This chapter introduces the use of a dual-echo gradient echo EPI acquisition scheme used to collect the fMRI data, and the methods for optimizing BOLD sensitivity across cortical and sub-cortical regions.

The primary aim of this chapter is to investigate the advantages of a dual-echo gradient echo EPI acquisition for a cognitive (GO/WAIT) task, variants of this paradigm are then performed in subsequent Chapters 4 and 5 of this thesis. The (GO/WAIT) cognitive task has been previously shown to involve neural activity in a network of cortical and sub-cortical brain regions (Jackson et al., 2001; Swainson et al., 2003). The value of performing a dual-echo image acquisition at 7 Tesla in order to gain increased SNR and BOLD contrast-to-noise ratio (CNR) to assess subtle

changes in cortical and sub-cortical responses, at higher spatial resolution than at 3 Tesla, is assessed.

This chapter begins with an outline of the advantages of 7 Tesla for fMRI and the challenges faced. The use of the dual-echo scheme is then introduced, and simulations to highlight the advantage of this scheme for the study of cortical and sub-cortical areas provided. A study of the GO/WAIT task at 7 Tesla then follows.

3.2 Use of fMRI data at Ultra-high magnetic field

Ultra-high field (greater than 3 Tesla) has several advantages for fMRI associated with the increased magnet field strength leading to an increase in signal intensity. The main benefit of imaging at ultra-high field (UHF) is the increased signal-to-noise ratio (SNR), which allows higher spatial resolution imaging voxels to be collected. Another significant advantage of carrying out fMRI experiments at ultra-high field is the resulting increase in BOLD contrast (Yacoub et al., 2001, 2003; van der Zwaag et al., 2009). This can allow a decrease in the number of trials required in an fMRI experiment for a significant activation, and it can be highly advantageous to the investigation of subtle cognitive processes and single events, such as when performing an fMRI experiment with oddball or rare events. Furthermore, ultra-high field offers most benefit for fMRI experiments carried out at high spatial resolution due to the increased BOLD contrast sensitivity, and reduction in relative contribution of physiological noise to signal (Triantafyllou et al., 2005).

Improved spatial sensitivity is intrinsically obtained at ultra-high field when imaging at echo times (TEs) optimised for grey matter, since the intravascular signal

is diminished due to the disproportional shortening of blood T_2/T_2^* compared to tissue T_2/T_2^* (Thulborn et al., 1982, Gati et al., 1997, Duong et al., 2003). In contrast, at field strengths of 1.5 - 3 Tesla a substantial fraction of the gradient-echo signal arises from intravascular effects (Boxerman et al., 1995, Song et al., 1996, Buxton et al., 1998). Furthermore, signal changes arising from the capillary bed increase relative to those from the macrovasculature as field strength increases (Yacoub et al., 2003). These combined factors contribute to the improved spatial specificity of BOLD fMRI at ultra-high field, which is valuable for high-resolution fMRI (Bodurka et al., 2007; Triantafyllou et al., 2005).

However, to take full advantage of the potential benefits of ultra-high field, challenges must be overcome in order to acquire high quality images, particularly in deep cortical grey matter and brain areas close to air-tissue interfaces. At UHF, it is more challenging to achieve a homogeneous magnetic field throughout the imaging volume. The main magnetic field (B_0) homogeneity suffers at interfaces between soft tissue and air, termed as the magnetic susceptibility effect, which results in greater signal 'drop-out' in various brain regions, typically those close to air-tissue interfaces such as orbitofrontal cortex and temporal lobes (Schenck, 1996). Strategies for dealing with these issues are discussed in the following section.

Most functional magnetic resonance imaging (fMRI) experiments are based on using a single gradient-echo echo-planar imaging (GE-EPI) readout scheme to detect the BOLD signal. Although GE-EPI provides excellent temporal resolution, it is highly sensitive to magnetic field inhomogeneities causing susceptibility artefacts in the form of signal loss and image distortion, particularly in sub-cortical regions where

there is an increase in the susceptibility gradient. With increasing magnetic field strength, T_2^* becomes shorter due to increased tissue magnetic susceptibility effects at macroscopic and microscopic scales (Hagberg et al., 2002). This leads to considerable variation in the T_2^* of grey matter across the brain (Peters et al., 2007) particularly between cortical and sub-cortical regions which are of interest in this thesis with inferior regions typically having shorter T_2^* . This results in a significant variation in the optimal echo time for BOLD fMRI, which should match resting T_2^* . It has been shown that this issue can be addressed by collecting GE-EPI data at multiple echo times (Posse et al., 1999; Poser et al., 2006). The following sections are dedicated to describe the theory of using a multi-echo EPI approach and the optimal echo times required for the study of cortical and sub-cortical areas involved in cognitive function.

3.1.2 Theory of optimal echo time

In fMRI, the source of BOLD contrast is the local increase in the transverse relaxation time, T_2^* , in response to task performance, which is typically detected using a GE-EPI acquisition at a single fixed echo time, TE, matched to the T_2^* of the grey matter in the brain region that is involved in the task. The optimal echo time, TE, for maximum BOLD contrast can be shown to be that equal to the local T_2^* of the tissue as follows:

The signal, S, at a given echo time (TE) is given by:

$$S = S_0 e^{-TE/T_2^*} = S_0 e^{-TE \times R_2^*}$$

where S_0 is the equilibrium magnetisation, and T_2^* is the transverse relaxation time of the tissue at rest, which can be rewritten in terms of the relaxation rate R_2^* where

$$R_2^* = 1/T_2^*.$$

The BOLD contrast, C is given by the change in signal, dS , expressed as:

$$C = \frac{dS}{dR_2^*} \Delta R_2^* = -S \times TE \times \Delta R_2^*$$

The optimal BOLD contrast can be found by differentiating the expression for contrast, C , and setting the result equal to zero.

$$\frac{dC}{dTE} = -S \times \Delta R_2^* + S \times TE \times R_2^* \times \Delta R_2^* = 0 \text{ at maximum}$$

Rearranging this then gives the optimal echo time of:

$$TE = \frac{1}{R_2^*} = T_2^*$$

for maximum BOLD contrast. Thus, the maximum BOLD contrast occurs when the echo time (TE) is equal to the T_2^* of the tissue of interest at rest. However, in this thesis, activation in both cortical and sub-cortical regions are of interest to the cognitive experiments. Tissue T_2^* strongly varies across cortical and sub-cortical grey matter brain regions (Hagberg et al., 2002; Peters et al., 2007), with cortical regions generally having a much longer T_2^* than sub-cortical areas, (Stocker and Simoncelli, 2006). For example, the increased presence of iron in the sub-cortical substructures leads to increased susceptibility artefacts. Figure 3.1 illustrates an example transverse signal decay curve ($S = S_0 e^{-TE/T_2^*}$) for cortical and sub-cortical regions, assuming a T_2^* value of (35 ms for cortical regions) and (15 ms for sub-cortical regions (such as the basal ganglia, BG)) at 7T.

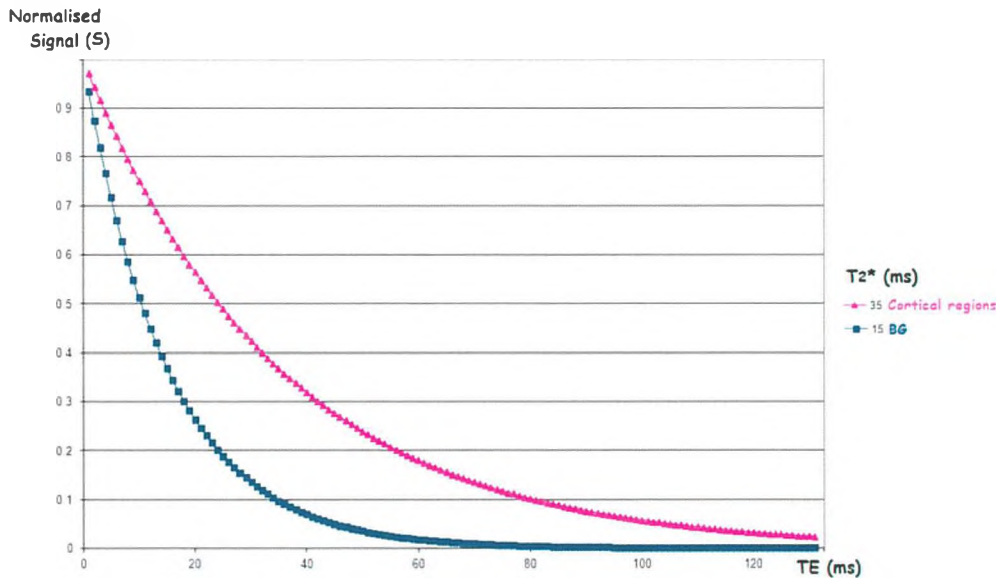


Figure 3.1. Transverse signal(s) decay curves for cortical and sub-cortical regions such as the basal ganglia (BG).

The corresponding plot of percentage BOLD signal change versus echo time, assuming a change in T_2^* of 5 ms on activation is shown in Figure 3.2 for both cortical and sub-cortical (BG) regions.

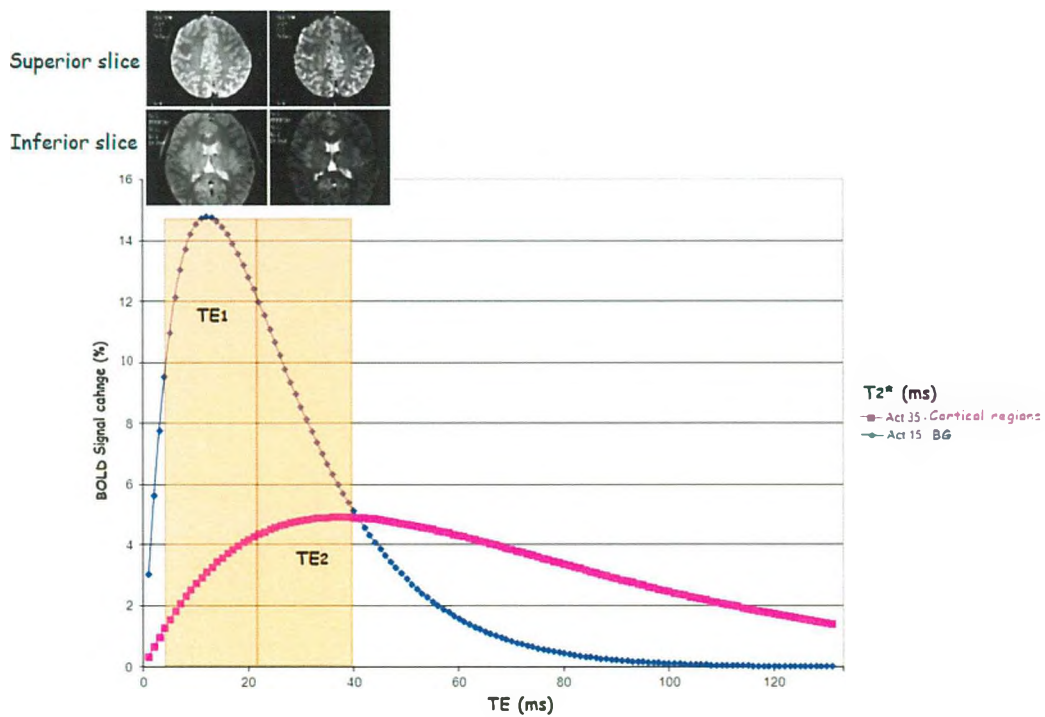


Figure 3.2. BOLD signal change (%) versus echo time (TE in ms) for both cortical and sub-cortical (Basal Ganglia, BG) regions assuming a change in T_2^* of 5 ms on activation. Inset: Example EPI image for a superior and inferior slice acquired using a dual-echo acquisition at echo times of ($TE_1 = 10.3$ ms) and ($TE_2 = 29.3$ ms).

Figure 3.2 shows that the optimal echo time for the basal ganglia (BG) is $\sim < 20\text{ms}$ while that for cortical regions is of $\sim 35\text{ ms}$. It can be seen that if only a single echo time is chosen, this can limit the detectability of the BOLD signal change when studying both cortical and sub-cortical areas. An elegant way to overcome this issue is to introduce a multi-echo image acquisition scheme, where GE-EPI data can be collected at more than one echo time following a single RF excitation pulse.

3.1.3 Multi-echo acquisition

A multiple-echo image acquisition is a method which can be used to acquire a series of gradient echo images at a number of echo times following a single excitation pulse. Since each echo time data is collected to sample a single FID, the repetition time (TR) is not increased. This method has the advantage of allowing the detection of neural activity across different regions of the brain which have different T_2^* values. This sequence is shown schematically in Figure 3.3 for the acquisition of four GE-EPI images from a single FID.

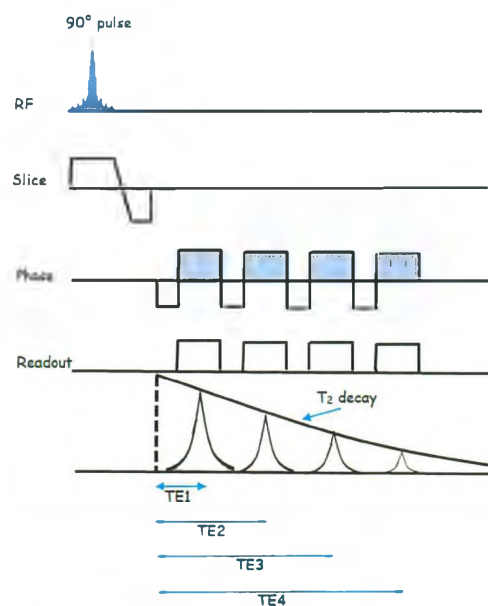


Figure 3.3. Schematic showing a multi-echo gradient echo image with the acquisition of four GE-EPI images from a single FID.

Previous studies have shown that the sensitivity of BOLD signal can be increased by combining data from multi-echo EPI sequences compared to a conventional single-echo time acquisition (Posse et al., 1999, Poser et al., 2006), with a multi-echo acquisition significantly increasing the CNR (Poser et al., 2006). However, the increased multi-echo EPI readout time and gradient cycle may slightly limit the number of slices that can be obtained in a reasonable repetition time, TR (Gowland and Bowtell, 2007). Here we used a dual-echo EPI readout scheme to limit this. Furthermore, the multi-echo readout is limited in the actual echo times that can be achieved, as the shortest separation between echo 1 and echo 2 is given by the readout duration of the EPI acquisition (as illustrated in Figure 3.3), in the case of the data acquisition in this chapter the readout duration was 19 ms. However, despite this compromise, the potential increase in CNR and the higher BOLD sensitivity make this multi-echo imaging approach promising and widely applicable (Poser et al., 2006; Li et al., 2002; Posse et al., 2003).

3.1.4 Analysis of multi-echo data (Echo weighting)

The analysis of the multi-echo fMRI data can be conducted in several ways, and these different methods will now be explored for the dual-echo acquisition (TE_1 and TE_2) used in this chapter.

Method (1): Following pre-processing a standard statistical analysis such as the general linear model (GLM) can be performed on each of the individual echo time data sets, then a single statistical activation map formed for each echo time (TE_1 and TE_2) or the two data sets (Posse et al., 1999) combined in a single GLM design matrix and a single statistical activation map formed. However, this way of combining the

data will not afford an overall CNR gain and therefore sub-optimal results, are likely to be obtained.

Method (2): The multi-echo time courses can be combined prior to statistical pre-processing potentially maximize the CNR gain. There are two main types of summation of the individual echo time (TE_1 and TE_2) data: (a) simple summation and (b) weighted summation.

(a) Simple summation takes the average of the multi-echo time courses. This type of summation leads to an increase in the SNR of the data, and also CNR increase, however by simple averaging the CNR is not optimally improved (Posse et al., 1999).

(b) Weighted summation is the optimum method of combining multi-echo data to maximize the sensitivity to the BOLD contrast. This makes a weighted summation of the time courses acquired at each echo time based on the T_2^* of the tissue. In this type of summation, the measured signal-to-noise at each echo time is used as a weighting function (Poser et al., 2006). In analysing multi-echo time courses, the weighted averaging of the individual echo images is theoretically the ideal approach to optimize the BOLD CNR. This method does however require an estimate of the T_2^* of the tissue from T_2^* maps (Posse et al., 1999; Weiskopf et al., 2005; Poser et al., 2006).

In this study, these different methods of combining dual-echo EPI data are assessed in the application to the study of a cognitive task.

3.2 Experiment

3.2.1 Material and methods

3.2.1.1 Participants

Eleven right-handed healthy participants (8 female; age range: 21–30 years with mean age of 22.8 ± 2.7 years) with no history of neurological disorders were scanned. Participants were informed of the experimental procedure before giving written consent, and were compensated for their time and inconvenience. The study was approved by the University of Nottingham Medical School Research Ethics Committee.

3.2.1.2 Experimental Task

Stimuli were presented to the subjects by a computer controlled projection system that delivered a visual stimulus to a projection screen located at the foot of the magnet bore. The participant viewed this screen using prism glasses through a system of mirrors located inside the magnet room.

Before scanning, subjects received training on the task outside of the scanner and performed a minimum of 5 trials of each type of task condition (GO/WAIT) to verify they understood the task. The study consisted of two runs of the task, each of approximately 8 minutes. A schematic of the GO/WAIT paradigm is shown in Figure 3.4. The paradigm comprised an arrow-shaped stimulus that was displayed in the centre of the screen in either green or red. Subjects were instructed to respond to each arrow by pressing a right or left button-box, depending on the arrow's direction. If the arrow was green (**GO**) subjects were asked to respond as quickly as possible, whilst subjects were asked to respond at the stimulus offset of the red (**WAIT**) arrow. Each

trial started with the presentation of a blank screen for 1500 ms, followed by a white square for fixation presented on the centre of the screen for 100 ms. Following this, a single white arrow appeared which pointed either to the right or left for a period of 250 ms, this then changed in colour to green or red. All arrows were presented for a period of 2500 ms at a rate of approximately one every 9 s, a white square for fixation was shown during the inter-stimulus-interval (ISI). Throughout the task all button presses were recorded.

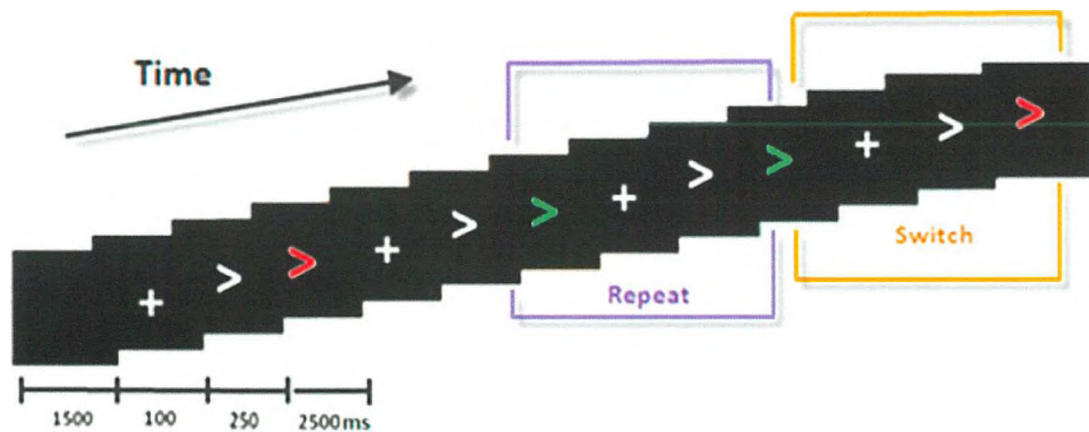


Figure 3.4. Stimuli types and timing for the GO/WAIT paradigm. Participants respond to visually presented arrows by pressing response buttons with their right or left hand, depending on the arrow's direction. Subjects switch between two arrow-discrimination tasks depending upon the colour of the arrow. If the arrow was green, participants were instructed to GO and respond as quickly as possible. If the arrow was red, participants were instructed to WAIT and respond at the stimulus offset. A switch trial involves a rule switch relative to the prior trial. A repeat trial has the same rule as on the previous trial. Arrows can point to the left (<) or right (>). In the example shown, arrows are pointing right (>) for illustration.

3.2.1.3 MRI data acquisition

MRI data were acquired on a 7 Tesla Philips Achieva System equipped with a head transmit coil and 16 channel SENSE receive coil. The subject's head was immobilized using foam cushions to reduce head movement.

To correct for field inhomogeneities and minimize geometric distortions in the EPI images, an image-based shimming technique (Poole and Bowtell, 2008) was used

prior to fMRI data acquisition to minimise the magnetic field inhomogeneity over a cuboid region within the field map data over the slices of interest. Field maps were generated using a standard B_0 -mapping sequence, which acquired two gradient echo images at echo times $TE_1 / TE_2 = 6 / 6.5$ ms.

fMRI data were collected using a dual-echo gradient echo-planar imaging (EPI) sequence (echo times: $TE_1/TE_2 = 10.3 / 29.3$ ms, 2 mm isotropic resolution with no slice gap, 32 slices, FOV = $192 \times 160 \times 164$ mm, flip angle = 90° , repetition time TR = 3 s). Two runs were performed, for each run, a total of 160 EPI volume images were acquired. Following the fMRI data acquisition, anatomical MR images were acquired using a Magnetic Prepared Rapid Acquisition Gradient Echo (MPRAGE) sequence ($TE/TR = 4.4/16$ ms, 1.5 mm isotropic resolution, flip angle = 8° , FOV = $192 \times 169 \times 164$ mm).

3.4 Data Analysis

3.4.1 Behavioural Data

The first two trials of each fMRI run and trials associated with an incorrect response were excluded from the behavioural and fMRI analyses. Mean reaction times for correct responses were entered in a two-way repeated measure ANOVA with the two factors “task” and “trial”. A paired-samples t-test was performed to compare reaction time between task and trial types. The mean of the switch cost for GO trials was calculated.

3.4.2 fMRI Data

3.4.2.1 Pre-processing steps

All fMRI data sets were processed using SPM5 (Statistical Parametric Mapping, Wellcome Department of Imaging Neuroscience; www.fil.ion.ucl.ac.uk/spm). Slice timing correction was applied. The first echo images were then realigned to the first volume data space and the realignment parameters were subsequently applied to the second echo images. Individual realignment parameters were visually inspected and any subject who moved more than one voxel during the fMRI paradigm was excluded from the study.

The dual-echo fMRI data were then combined and analyzed using two methods.

Method (1): Combining the dual echo data following the statistical processing steps; pre-processing steps were first applied to the first (echo1_*) and second echo (echo2_*) data sets, the first echo images and the second echo images were then combined in a single design matrix (combined GLM) by adding each echo time as a separate session.

Method (2): Combining the dual echo data prior to statistical processing steps.

First, T_2^* maps were formed from the dual-echo data, by averaging each of the echo 1 and echo 2 data sets over the entire fMRI paradigm, and then performing a voxel-by-voxel, linear weighted least squares fit of the two echo time data sets to $(S = S_0 e^{-TE/T_2^*})$ to fit for T_2^* . Two types of summation were then performed: (a) simple summation and (b) weighted summation which relies on the use of the T_2^* maps.

Simple summation simply takes the average of the echo data sets:

$$S(t) = \sum_{n=1}^N S(t, TE_n)$$

where $S(t, TE_n)$ is the signal at a given time point (t) and echo time (TE), and n is the echo time number and N the total number of echo times. Here, when using a dual-echo EPI acquisition $N = 2$.

Alternatively, theoretically more optimal BOLD sensitivity can be obtained by a weighted combination of the two echo data sets based on the T_2^* of the underlying tissue, measured from a T_2^* map (Posse et al., 1999; Poser et al., 2006).

$$S(t) = \sum_{n=1}^N S(t, TE_n) w(TE_n)$$

$$w(TE_n) = \frac{TE_n}{T_2^*} \exp\left(-\frac{TE_n}{T_2^*}\right)$$

where $w(TE_n)$ is the weighting factor of the individual echoes, and the other terms as described above.

Data sets were formed for both simple summation (ss_*) and weighted summation (ws_*) using a matlab script (written by Dr. Susan Francis). Pre-processing steps were then performed on these data sets, and a design matrix formed for each of the simple and weighted summation methods.

Following this, each of these combinations were spatially normalised to the MNI (Montreal Neurological Institute) space. Two independent levels of smoothing were then applied to the raw data, a 5 mm full width at half maximum (FWHM) isotropic Gaussian kernel to perform region of interest (ROI) analysis; and an 8 mm isotropic Gaussian kernel to form random effects (RFX) statistical maps. Global scaling and temporal filtering with 80 s high pass filter cut-off were then applied.

Each data set (echo1_*, echo2_* and combined GLM, ss_* and ws_*) was then analysed individually at the first level analysis using the general linear model (GLM) including contrasts for GO–Repeat, GO–Switch, WAIT–Repeat, and WAIT–Switch. The following were then assessed (a) the main effect of each task type (i) GO and (ii) WAIT, and (b) the differential contrasts of (i) GO > WAIT and (ii) WAIT > GO (for both trial types combined (Switch and Repeat)).

To contrast analysis approaches an ROI analysis was then performed to assess the parametric estimates for each model with ROIs chosen in putamen, thalamus, SMA and MFC in order to assess the difference between the cortical and sub-cortical areas across different methods. These ROI were identified anatomically, from the Automated Anatomical Labelling (ALL) Atlas (Tzourio-Mazoyer et al., 2002), based on the voxel-wise statistical map of the (WAIT > GO) contrast thresholded at ($P_{\text{FDR}} < 0.05$, corrected for multiple comparisons).

3.5 Results

3.5.1 Behavioural Data

Figure 3.5 shows the behavioural data for the (GO/WAIT) task.

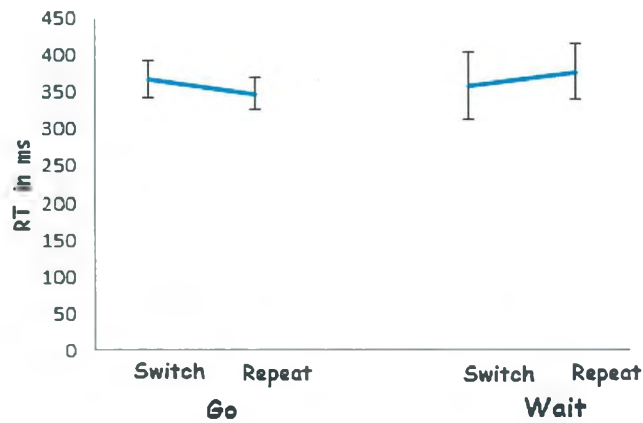


Figure 3.5. Mean reaction times (RT in ms) for all conditions; GO–Switch, GO–Repeat, WAIT–Switch and WAIT–Repeat

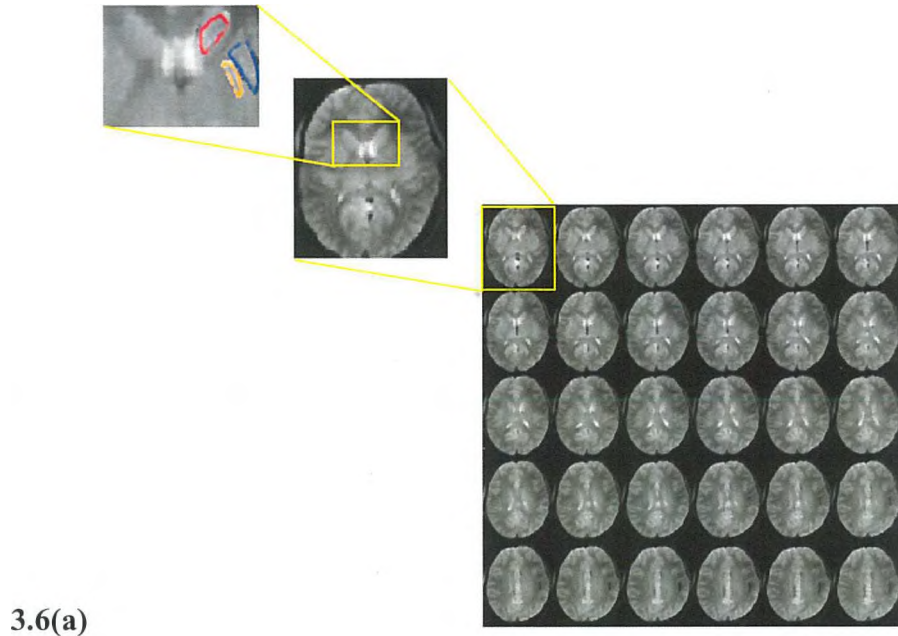
A two-way repeated measures ANOVA was conducted, with two levels of task (GO and WAIT) and two levels of trial (Switch and Repeat) within subjects. There was no significant main effect of task [$F(1, 10) = 0.077, p = 0.787$] and no significant main effect of trial [$F(1, 10) = 0.286, p = 0.604$]. However, a significant interaction between task and trial was observed [$F(1, 10) = 6.936, p < 0.025$]. The average rate of errors in WAIT events (indicating an early response) was ($5 \pm 1\%$; Mean \pm SD) across subjects, with a total of 62 errors across all 11 subjects.

A paired-samples t-test was conducted to compare the GO–Switch and GO–Repeat conditions, and the WAIT–Switch and WAIT–Repeat conditions. There was only a significant difference in the RT between the GO–Switch (367 ± 25 ms; Mean \pm SEM) and GO–Repeat conditions (348 ± 20 ms; Mean \pm SEM); ($t = 2.61, p < 0.05$) with a switch cost of (19 ± 2.5 ms; Mean \pm SD). There was no significant difference in the RT between the WAIT–Switch (359 ± 45 ms; Mean \pm SEM) and WAIT–Repeat conditions (377 ± 37 ms; Mean \pm SEM); ($t = -1.143, p = 0.28$).

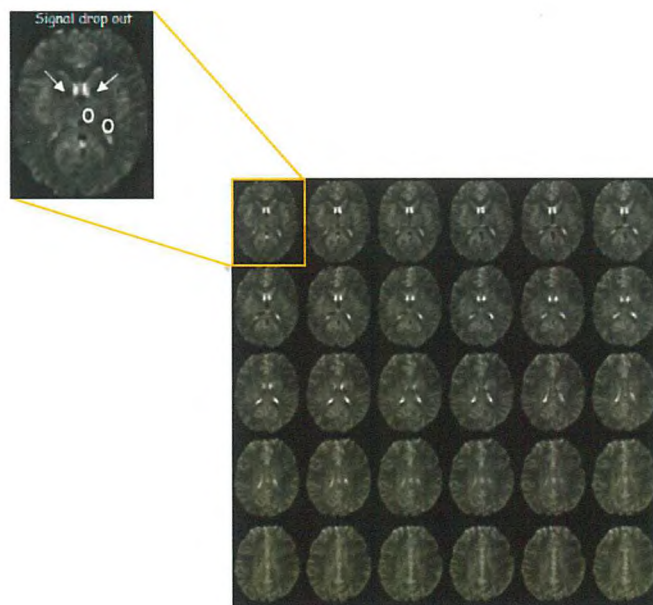
3.5.2 fMRI data

3.5.2.1 Effect of TE on image quality

Figure 3.6 shows example of dual-echo fMRI data collected at echo times $TE_1 = 10.3$ ms and $TE_2 = 29.3$ ms.



3.6(a)



3.6(b)

Figure 3.6a. Raw fMRI data acquired at short echo time ($TE_1=10.3$ ms). Images show high sensitivity to the sub-cortical (i.e., Basal Ganglia) areas. Basal ganglia nuclei can be detected easily at this short TE. Red indicates caudate, blue indicates putamen, and orange indicates globus pallidus. **3.6b.** Raw fMRI data acquired at longer echo time ($TE_2 =29.3$ ms). Images show high sensitivity to the cortical brain regions. By zooming into the image (inset) signal drop-out can be seen in the sub-cortical structures.

Clear signal dropout is seen in sub-cortical regions in Figure 3.6(b) at the longer echo time typically used for fMRI data acquisition at 7 Tesla. Figure 3.7(a) shows an example T_2^* map and Figure 3.7(b) shows the T_2^* measured in sub-cortical and cortical regions of interest. T_2^* ROI values can be seen to be significantly reduced for sub-cortical regions of caudate, putamen and globus pallidus (GP) with echo times of 20-25 ms, compared to longer T_2^* values in cortical regions, of 30-40 ms

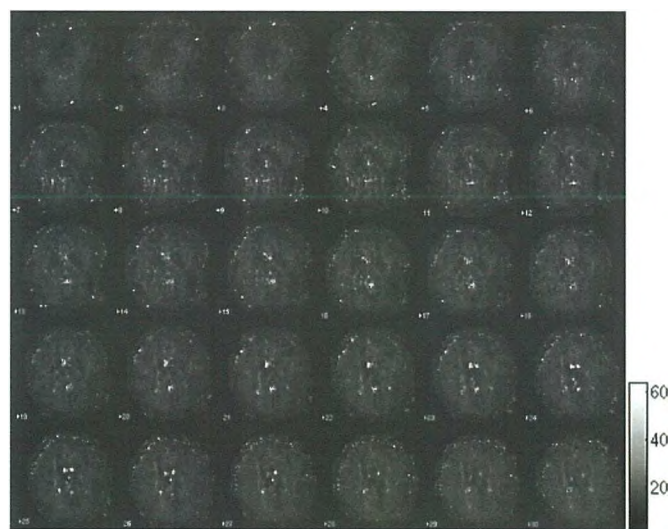


Figure 3.7a. Example T_2^* map from inferior slices to superior slices showing cortical and sub-cortical areas.

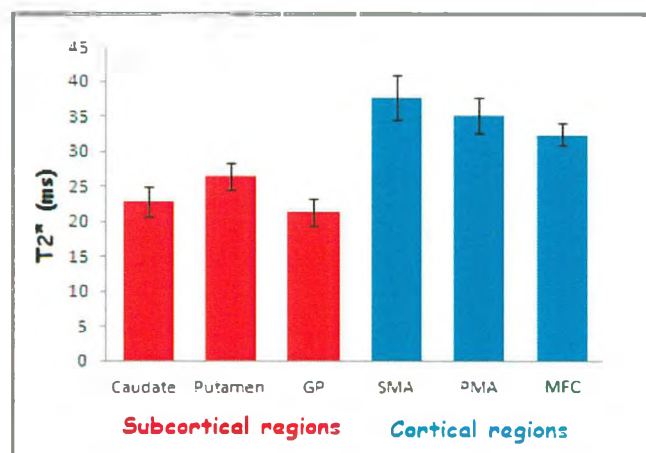


Figure 3.7b. Bar chart to illustrate the T_2^* measured in sub-cortical and cortical regions of interest. Abbreviation: GP, globus pallidus; SMA, supplementary motor cortex; PMA, premotor area; MFC, middle frontal cortex.

3.5.2.2 Assessing methods of combining dual-echo fMRI data

Figure 3.8 illustrates the random effects group maps for the (WAIT > GO) contrast and shows that more activation is found in sub-cortical areas at the shorter echo time (Echo1: Figure 3.8a), whilst in contrast increased activation was found in the cortical areas at longer echo time (Echo2: Figure 3.8b). This pattern of activity was true for all conditions of (WAIT > baseline), (GO > baseline) and (WAIT > GO). The (WAIT > GO) contrast will be used here to illustrate the effect of echo time and image summation because it is the contrast that will be used to assess motor response inhibition in investigating the role of the basal ganglia in cognitive function in the following chapter of this thesis. Table (3.1a & b) summarizes the active areas found for Echo1 and Echo2 at $P_{FDR} < 0.05$ corrected for multiple comparisons. Sub-cortical regions such as the thalamus and bilateral midbrain regions have a high T-score for Echo1.

Moreover, the BOLD signal was observed highly increased in the cortical areas such as pre-supplementary motor area (Pre-SMA), middle frontal cortex, and inferior frontal cortex using Echo2 compared to that in Echo1, as shown in Figure (3.8b) and summarized in Table (3.1b).

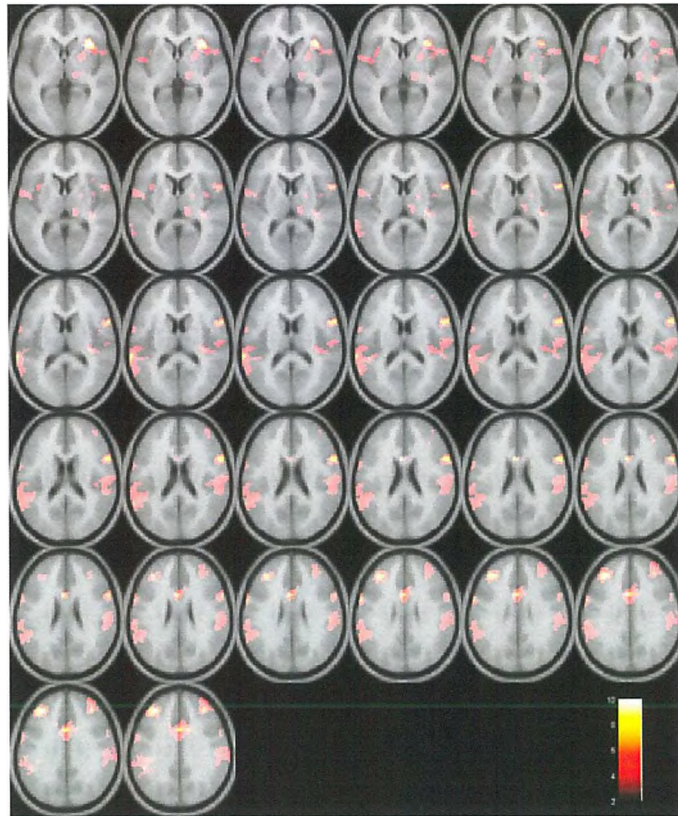


Figure 3.8a. fMRI data collected at Echo1 shows the brain regions associated with (WAIT > GO) contrast. $P_{FDR} < 0.05$ corrected for multiple comparisons.

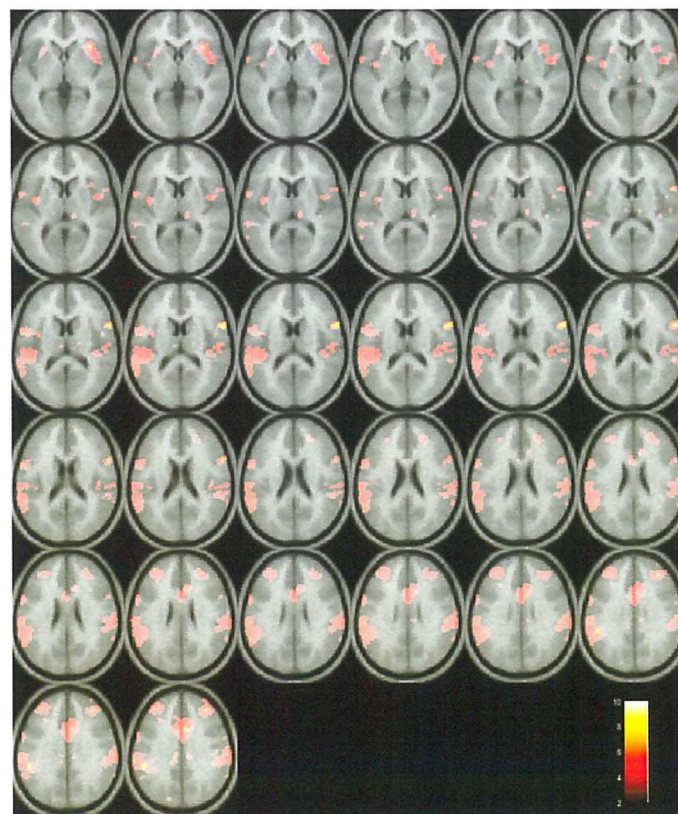


Figure 3.8b. fMRI data collected at Echo2 shows the brain regions associated with (WAIT > GO) contrast. $P_{FDR} < 0.05$ corrected for multiple comparisons.

a) Echo1

| Brain Region | Side | MNI Coordinates | | | Z-score | T value |
|-----------------------------|------|-----------------|-----|-----|---------|---------|
| | | x | y | z | | |
| (Pre)-SMA | R | 2 | 0 | 50 | 4.74 | 9.59 |
| | L | -6 | -2 | 52 | 5.01 | 11.21 |
| Middle frontal cortex | R | 40 | 46 | 18 | 3.5 | 5.09 |
| | L | -36 | 38 | 32 | 4.88 | 10.46 |
| IFC (P.Opercularis; BA 44) | R | 62 | 12 | 14 | 4.72 | 9.55 |
| Precentral gyrus (BA 6) | L | -62 | 2 | 28 | 3.96 | 6.42 |
| Postcentral gyrus (BA 2, 3) | R | 52 | -24 | 48 | 4.23 | 7.39 |
| | L | -26 | -38 | 48 | 4.71 | 9.54 |
| IPL (Precunes) | L | -26 | -50 | 52 | 4.38 | 7.98 |
| ACC | L | 0 | 10 | 30 | 4.01 | 6.60 |
| MCC | R | 12 | 10 | 36 | 4.12 | 6.81 |
| | L | -8 | -10 | 48 | 4.7 | 9.45 |
| Insula Lobe | R | 36 | 20 | 2 | 5.24 | 12.8 |
| | L | -36 | 10 | 6 | 3.17 | 4.32 |
| Rolandic operculum (OP 4) | L | -62 | 2 | 10 | 3.56 | 5.25 |
| Inferior occipital cortex | L | -30 | -90 | -12 | 3.34 | 4.7 |
| Cerebellum (Lob. VIIa Crus) | L | -38 | -72 | -20 | 3.71 | 5.66 |
| Thalamus (Pulvinar) | R | 14 | -28 | 6 | 3.51 | 5.13 |
| Brainstem (midbrain) | R | 6 | -18 | -14 | 4.48 | 8.27 |
| | L | -4 | -22 | -16 | 3.41 | 4.89 |

b) Echo2

| Brain Region | Side | MNI Coordinates | | | Z-score | T value |
|----------------------------|------|-----------------|-----|-----|---------|---------|
| | | x | y | z | | |
| (Pre)-SMA | L | 0 | -6 | 54 | 5.03 | 11.34 |
| Middle frontal cortex | R | 36 | 40 | 32 | 3.99 | 6.54 |
| | L | -34 | 42 | 36 | 3.92 | 6.3 |
| IFC (P.Opercularis; BA 44) | R | 56 | 10 | 16 | 4.43 | 8.22 |
| Postcentral gyrus (BA 3) | R | 32 | -24 | 48 | 4.47 | 8.25 |
| | L | -26 | -38 | 52 | 4.75 | 9.83 |
| IPL | L | -56 | -24 | 44 | 4.41 | 8.19 |
| IPL (Angular gyrus, BA 39) | L | -54 | -68 | 36 | 3.25 | 3.9 |
| MCC | R | 12 | 8 | 36 | 4.55 | 9.16 |
| | L | -4 | 8 | 40 | 4.64 | 9.35 |
| MTC (BA 37) | L | -50 | -62 | -4 | 3.63 | 5.51 |
| ITC (BA 19) | L | -52 | -60 | -8 | 3.29 | 4.72 |
| Insula Lobe | R | 34 | 24 | 0 | 4.43 | 8.22 |
| Rolandic operculum | R | 54 | 4 | 6 | 3.41 | 4.85 |
| Lingual gyrus | R | 24 | -96 | -18 | 2.98 | 3.39 |
| Superior occipital cortex | L | -18 | -86 | 36 | 3.12 | 3.5 |
| Inferior occipital cortex | L | -30 | -88 | -8 | 3.05 | 3.53 |
| Thalamus (Pulvinar) | R | 12 | -26 | 8 | 4.01 | 6.59 |
| Thalamus (MD nucleus) | L | -8 | -20 | 12 | 3.3 | 4.6 |

Table (3.1a & b). Significant brain areas associated with (WAIT > GO) contrast collected at Echo1 and Echo2, respectively.

Figure 3.9 shows the random effects group maps to highlight the difference in T-scores between different methods of combining the echoes; a) combined GLM, b) simple summation (ss), and c) weighted summation (ws) across cortical and sub-cortical brain regions for the (WAIT > GO) condition. Table 3.2 summarizes the T-statistics for active regions for each of the methods. The BOLD signal was observed to be increased in the cortical and sub-cortical areas using combined GLM and simple summation methods compared to that in Echo1 and Echo2. However, activation in the deep sub-cortical structures (Table 3.2c) was detected more strongly using the weighted summation method compared to that of the combined GLM and simple summation methods.

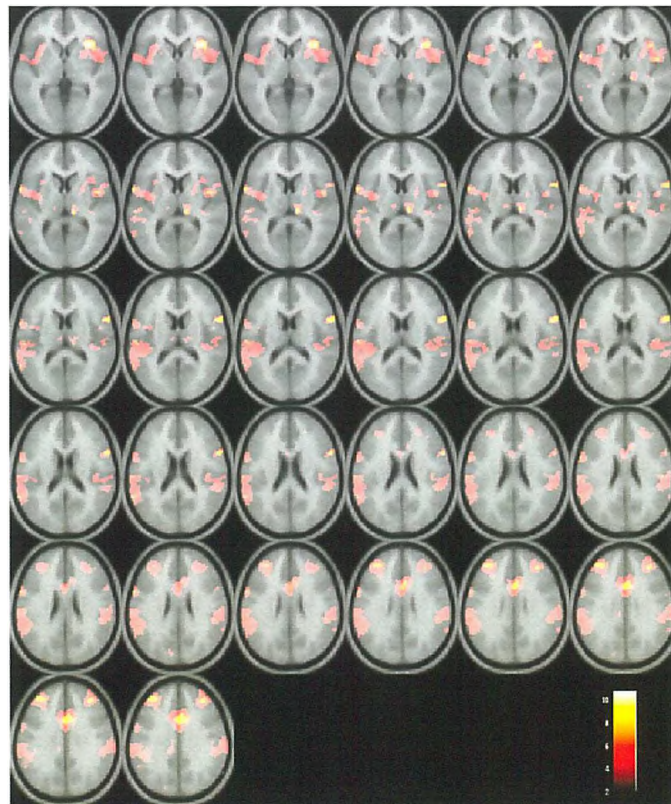


Figure 3.9a. Combining echoes in a single GLM data to show the brain regions associated with (WAIT > GO) contrast. $P_{FDR} < 0.05$ corrected for multiple comparisons.

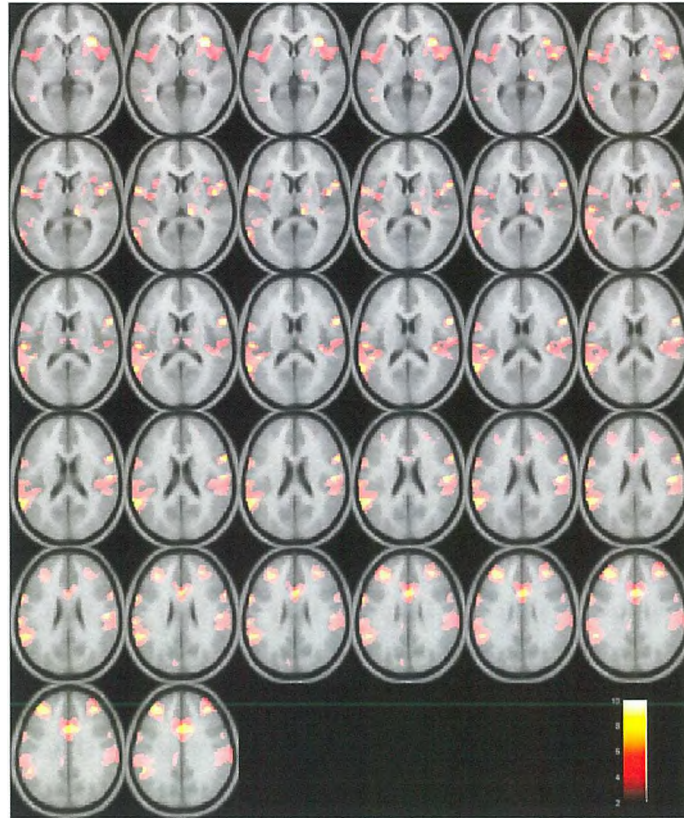


Figure 3.9b. Simple summation (ss) data shows the brain regions associated with (WAIT > GO) contrast. $P_{FDR} < 0.05$ corrected for multiple comparisons.

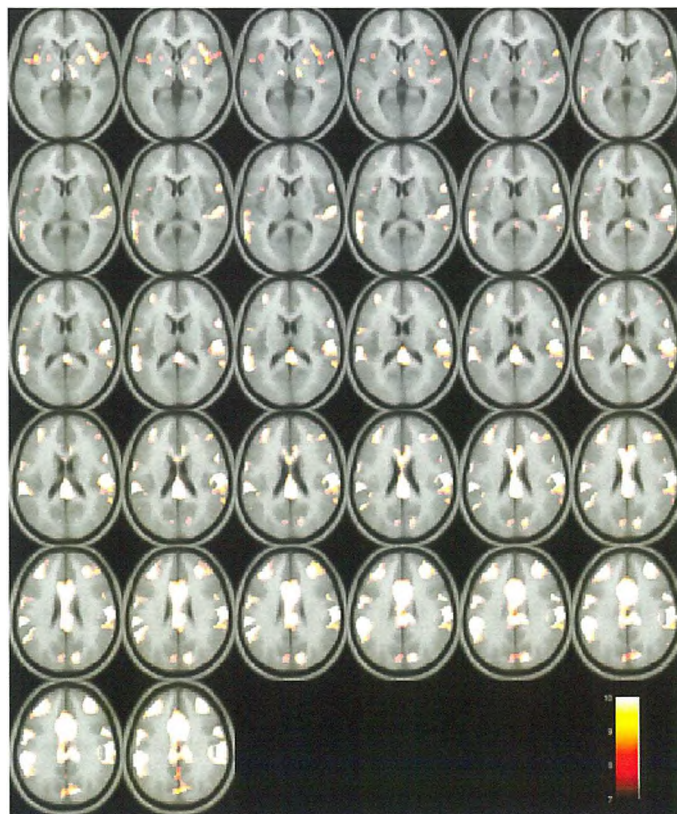


Figure 3.9c. Weighted summation (ws) data shows the brain regions associated with (WAIT > GO) contrast. $P_{FDR} < 0.05$ corrected for multiple comparisons.

a) Combined Echoes

| Brain Region | Side | MNI Coordinates | | | Z-score | T value |
|----------------------------|------|-----------------|-----|----|---------|---------|
| | | x | y | z | | |
| (Pre)-SMA | R | 6 | -4 | 54 | 4.82 | 10.12 |
| | L | -4 | 2 | 52 | 4.93 | 10.71 |
| Middle frontal gyrus | R | 34 | 38 | 32 | 4.5 | 8.54 |
| | L | -36 | 42 | 32 | 4.28 | 7.6 |
| IFC (P.Opercularis; BA 44) | R | 60 | 12 | 14 | 4.61 | 9.04 |
| Precentral gyrus (BA 6) | R | 36 | 10 | 48 | 4.06 | 6.76 |
| Postcentral gyrus (BA 2) | R | 52 | -22 | 46 | 4.3 | 7.67 |
| | L | -26 | -38 | 52 | 4.72 | 9.58 |
| IPL (Supramarginal gyrus) | R | 64 | -28 | 42 | 3.89 | 6.28 |
| IPL (Angular gyrus) | L | -52 | -68 | 40 | 3.07 | 4.11 |
| MCC (BA 24) | R | 6 | 2 | 44 | 4.72 | 9.55 |
| MTC (BA 22) | R | 52 | 10 | -6 | 3.21 | 4.41 |
| Cuneus | L | -10 | -82 | 26 | 2.97 | 3.39 |
| Insula Lobe | R | 30 | 20 | 2 | 4.93 | 10.76 |
| Rolandic operculum | R | 54 | 4 | 6 | 3.41 | 4.86 |
| Superior occipital cortex | L | -18 | -86 | 36 | 3.01 | 3.52 |
| Inferior occipital cortex | L | -30 | -86 | -8 | 3.21 | 4.4 |
| Thalamus (Pulvinar) | R | 12 | -26 | 8 | 4.42 | 8.16 |
| Thalamus (DM nucleus) | L | -8 | -18 | 12 | 3.39 | 4.81 |
| BG (Putamen) | R | 26 | 8 | 6 | 3.15 | 4.21 |

b) Simple summation (ss)

| Brain Region | Side | MNI Coordinates | | | Z-score | T value |
|----------------------------|------|-----------------|-----|-----|---------|---------|
| | | x | y | z | | |
| (Pre)-SMA | R | 4 | 2 | 46 | 4.84 | 10.21 |
| | L | -2 | 10 | 44 | 4.42 | 8.15 |
| Middle frontal gyrus | R | 36 | 40 | 32 | 4.74 | 9.66 |
| | L | -32 | 34 | 40 | 5.54 | 15.23 |
| IFC (P.Opercularis; BA 44) | R | 60 | 12 | 14 | 4.86 | 9.71 |
| Precentral gyrus (BA 6) | R | 40 | -12 | 54 | 4.3 | 7.73 |
| | L | -62 | 4 | 28 | 4.31 | 7.7 |
| Postcentral gyrus (BA 2,1) | L | -26 | -38 | 52 | 4.87 | 10.37 |
| IPL | L | -40 | -28 | 42 | 4.39 | 8.12 |
| IPL (Supramarginal gyrus) | L | -60 | -32 | 40 | 4.58 | 8.9 |
| MCC | R | 4 | 14 | 32 | 4.54 | 8.55 |
| | L | -8 | -6 | 50 | 4.78 | 9.88 |
| STC | L | -60 | -50 | 20 | 4.42 | 8.16 |
| MTC | L | -56 | -48 | 22 | 4.62 | 9.05 |
| Cuneus | L | -8 | 84 | 26 | 2.86 | 3.68 |
| Insula Lobe | R | 36 | 20 | 2 | 4.98 | 11.05 |
| Rolandic operculum | R | 48 | 0 | 10 | 4.58 | 8.59 |
| Thalamus | R | 14 | -30 | 6 | 4.5 | 8.52 |
| Thalamus (MD nucleus) | L | -6 | -16 | 12 | 3.12 | 4.22 |
| Brainstem (Midbrain) | R | 8 | -18 | -12 | 4.45 | 8.49 |
| | L | -4 | -22 | -14 | 3.76 | 5.99 |

c) Weighted summation (ws)

| Brain Region | Side | MNI Coordinates | | | Z-score | T value |
|------------------------------|------|-----------------|-----|-----|---------|---------|
| | | x | y | z | | |
| (Pre)-SMA | R | 6 | -4 | 46 | 4.51 | 8.76 |
| | L | -6 | -4 | 52 | 5.29 | 13.12 |
| Middle frontal cortex | R | 34 | 40 | 30 | 4.78 | 9.9 |
| | L | -42 | 36 | 32 | 4.46 | 8.33 |
| IFC (P.Orbitalis; BA 47) | R | 32 | 26 | -8 | 4.46 | 8.33 |
| IFC (P.Opercularis; BA 44) | R | 50 | 10 | 8 | 3.75 | 6.12 |
| Precentral gyrus (BA 6) | R | 38 | -16 | 50 | 4.67 | 9.3 |
| | L | -30 | -10 | 54 | 2.96 | 3.87 |
| Postcentral gyrus (BA 1,2,3) | R | 52 | -26 | 42 | 4.46 | 8.32 |
| | L | -52 | -24 | 52 | 4.59 | 8.91 |
| IPL (Supramarginal gyrus) | R | 58 | -30 | 36 | 4.02 | 6.64 |
| | L | -50 | -46 | 30 | 4.82 | 10.13 |
| MCC | R | 4 | 2 | 42 | 4.82 | 10.11 |
| STC | R | 54 | -32 | 16 | 3.71 | 5.75 |
| ITC | L | -46 | -62 | -8 | 4.09 | 6.88 |
| Precuneus | L | -10 | -60 | 42 | 2.88 | 3.69 |
| Cuneus | R | 14 | -84 | 24 | 3.57 | 5.28 |
| Insula Lobe | R | 44 | 4 | -6 | 3.8 | 5.88 |
| | L | -38 | 2 | -2 | 3.03 | 4.01 |
| Rolandic operculum | R | 58 | -16 | 18 | 3.87 | 5.96 |
| Inferior occipital cortex | L | -34 | -88 | -10 | 2.7 | 3.41 |
| Cerebellum (Lob. VIIa Crus) | L | -32 | -82 | -32 | 2.72 | 3.43 |
| Thalamus (VL nucleus) | R | 14 | -16 | 2 | 2.92 | 3.8 |
| BG (Putamen) | R | 22 | 6 | -6 | 2.9 | 3.7 |
| | L | -22 | 6 | 0 | 2.76 | 3.48 |
| BG (External GP) | R | 22 | -14 | 0 | 2.85 | 3.6 |
| Brainstem(Midbrain) | R | 8 | -12 | -16 | 3.42 | 4.86 |

Table (3.2a, b & c). Significant brain areas associated with (WAIT > GO) contrast using different methods of combining data; combined GLM, simple summation and weighted summation, respectively. Abbreviation: L, Left; R, right; BA, Brodmann area; Pre-SMA, pre-supplementary motor cortex; DM, dorsomedial; VL, ventrolateral; IFC, inferior frontal cortex; IPL, inferior parietal lobule; MCC, middle cingulate cortex; MTC, middle temporal cortex; ITC, inferior temporal cortex; BG, basal ganglia; GP, globus pallidus.

The results demonstrate that Echo1 is optimal to yield activity from sub-cortical regions such as basal ganglia structures. In contrast, signal drop-out was observed in sub-cortical regions using Echo2 method but was found to be optimal to detect activity from cortical regions. The results of combining echoes in a single GLM improved the BOLD sensitivity across sub-cortical and cortical areas, but not optimally. On the other hand, combining the data in a simple summation (ss) increases the SNR and CNR, however CNR was not optimally improved across all

regions. Combining the data in a weighted summation (ws) was found to be the optimal approach to optimize the sensitivity to BOLD contrast across cortical and sub-cortical areas and increase the SNR thus achieving the optimal CNR. This was further supported by the ROI analysis. Figure 3.10 shows the ROI analysis to assess the parameter estimates for each method of combining the data for the (WAIT > GO) contrast across subjects. ROIs in the putamen, thalamus, SMA and MFC are assessed and it can be seen that the weighted summation (ws) provides the optimal method of combining the fMRI data when showing cortical and sub-cortical regions.

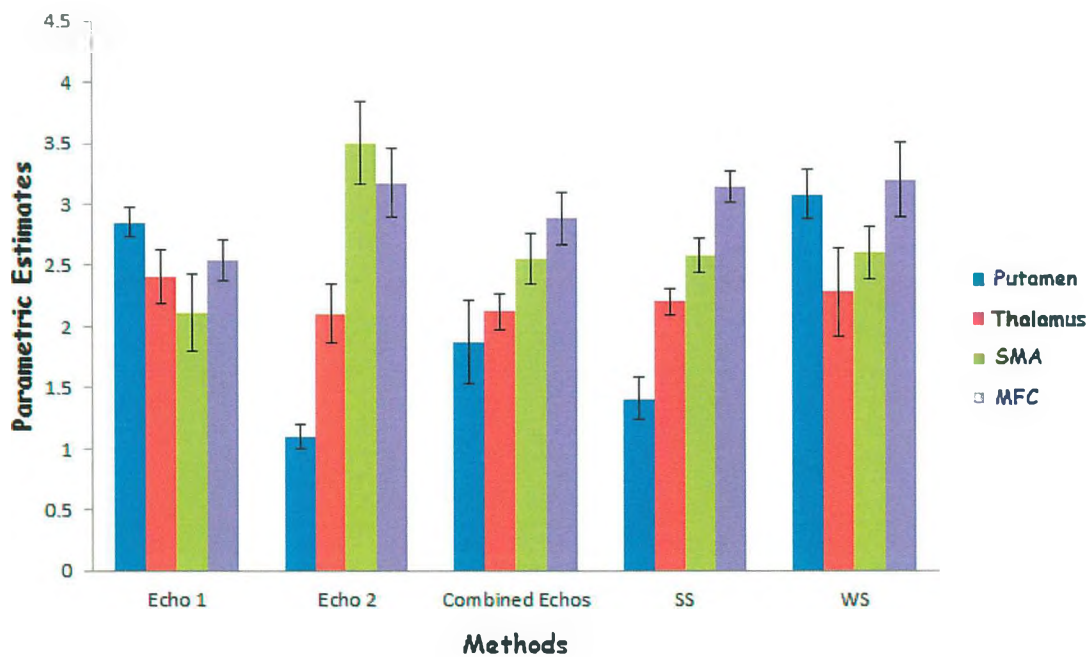


Figure 3.10. Bar chart to illustrate the mean BOLD parameter estimates for the (WAIT > GO) contrast across subjects in a priori ROIs for the different methods of combining the fMRI data. These ROI were selected as an example with putamen and thalamus regions chosen to interrogate sub-cortical regions, and SMA and MFC for cortical regions.

3.6 Discussion

The work presented in this chapter investigates the benefits of using a dual-echo gradient echo EPI acquisition scheme for the acquisition of fMRI data at 7T with sensitivity to both cortical and sub-cortical regions. The optimal method to allow the detection of neural activity across different regions of the brain with optimal sensitivity was assessed.

The shorter echo time ($TE_1=10.3$ ms) was found to be optimal to detect activity from sub-cortical regions such as basal ganglia structures (i.e., caudate and putamen) from both the optimal T-score and cluster size seen in the sub-cortical regions. In contrast, the longer echo time ($TE_2 = 29.3$ ms) was found to be optimal to detect activity from cortical regions. The analysis of the dual-echo fMRI data was conducted in a number of ways (combining single GLM, simple summation and weighted summation) to assess activity to each method. The results of the fMRI analysis of the dual-echo data demonstrate that standard statistical analysis of Echo1 showed optimal sensitivity to sub-cortical regions (Figure 3.10) and Echo2 had a significant loss in signal in sub-cortical areas. Combining echoes in a single GLM aided the sensitivity distribution across sub-cortical and cortical areas. Combining the data prior to statistical pre-processing steps in simple summation (ss) increases the SNR and CNR, however CNR was not optimally improved across all regions. Combining the data in weighted summation (ws) was found to be the optimal approach to optimize the sensitivity to BOLD contrast across cortical and sub-cortical areas and increase the SNR thus achieving the optimal CNR. This can be clearly seen by the highly significant activation that was observed in both cortical and sub-cortical brain regions in Figure 3.10. The results are in agreement with previous studies that

have demonstrated this approach (Posse et al., 1999; Weiskopf et al., 2005; Poser et al., 2006).

The finding of this chapter has shown that the sensitivity of fMRI BOLD signal can be increased by combining data from a dual-echo scheme compared to conventional single-echo time acquisition methods for improved sensitivity to cortical and sub-cortical areas (Posse et al., 1999, Poser et al., 2006). In conclusion, the results presented here suggest that combining data, from dual-echo acquisition, in weighted summation can lead to substantial gains in BOLD contrast sensitivity. Thus, due to the advantages of this approach, a dual-echo GE-EPI acquisition and the weighted summation of data are used in all experiments in this thesis to study cognitive function for which cortical and sub-cortical brain regions are of interest.

Chapter 4

4.1 Introduction: Executive functions

In everyday life, executive function is necessary for flexible interaction with and adaptation to constantly changing environments (Logan, 1985; Mesulam et al., 1986; Miller and Cohen, 2001). Executive functions can be conceptualized as a unique set of mental functions that involve numerous subdomains of thought and action. They enable a person to develop goals and create plans; remember these goals; control and orchestrate actions in accordance with internal goals; and regulate and adjust behaviour in order to achieve an ultimate goal (Lezak, 1995; Foster et al., 1997; Aron, 2009).

Executive function (sometimes referred to as “cognitive control”) can be defined as a set of high-order functions that regulate low-level processes involved in the performance of complex tasks with many cognitive or behavioural elements and demands (Band and van Boxtel, 1999; Logan, 1994). These high level functions, which require large-scale or global processes in the brain (Lawrence et al., 1998), are responsible for cognitive skills and flexibility. Executive function can be divided into a variety of cognitive constructs such as initiating goal-directed behaviour, action selection, sustained attention, motor planning and sequencing, rule acquisition and maintenance, task switching, shifting attention, inhibiting and monitoring of behaviour (Malloy et al., 1998; Royall et al., 2002; Troyer et al., 1994; Aron, 2009).

In this thesis the executive function of “inhibition” was chosen as the construct to be studied, with the role of the basal ganglia in the domain of motor response inhibition being investigated. This chapter is intended as a broad introduction to the concept of inhibition in cognition and consequently to the empirical experiments of this thesis to study the role of the basal ganglia in cognitive function.

4.2 Inhibition: A Definition, Concepts and their Relations

Inhibition is a crucial aspect of executive function that is essential for successful living (Garavan et al., 1999). The concept of inhibition is used to explain a wide range of phenomena across the domains of neuroscience, psychology, experimental psychology, cognitive psychology and neuropsychology (Figure 4.1). The term “inhibition” has a long and diverse history in neuroscience since the 19th century (Smith, 1992; Macmillan, 1996) with a diversity of meaning, varying from the underlying mechanisms of motor control, to connectivity between brain regions, and cell firing. One of the most common examples of inhibition in neuroscience is a simple reflex which was demonstrated by early neurophysiological experiments. A simple reflex is an entirely automatic and involuntary movement in response to a stimulus. Examples of such reflexes include the sudden withdrawal of a hand in response to a painful stimulus. Other meanings of the inhibition concept at the cellular level imply that within the brain there are some neurons that are inhibitory in nature, these neurons might for example use the GABAergic neurotransmitter to induce inhibition on the target neuron in the form of an inhibitory postsynaptic potential. This type of inhibition at the cellular level has an impact at the circuit and systematic level. Within the sub-cortical structures there is an intrinsic inhibitory circuit between the

basal ganglia nuclei, such as the globus pallidus internal segment (GPi) which receives information, through inhibitory projections, from the striatum. At the systematic level, the inhibition can be clearly seen in the cortico-thalamo-striatal connections, where the GPi nucleus projects, through inhibitory GABAergic neurons, to the thalamic nuclei, which eventually project to the prefrontal cortical areas which control movement initiation. In the neuroscience domain, there are also many other types and meanings of inhibition, such as “reciprocal inhibition,” “pre-pulse inhibition,” “recurrent inhibition,” and “lateral inhibition,” (Aron, 2007a) which will not be explained here as it is out of this thesis scope. Although the concept of “inhibition” in neuroscience has a wide range of phenomena (Figure 4.1), each one has a clear meaning which can be determined and observed neurophysiologically or in terms of behaviour (Aron, 2007a).

In psychology, the inhibition concept can be classified into two main streams: folk psychology and experimental psychology. In folk psychology, the concept of inhibition has many meanings (Hutto, 2008), such as a specific set of developing cognitive capacities that have functional roles in self-regulation, planning, and behaviour organization. For instance, a three year old child has difficulty in overriding their pre-potent behavioural tendency as their inhibitory control mechanism has not been yet developed and sufficiently matured (Carlson and Moses, 2001). Another example of inhibition in folk psychology is the idea of psychological repression which refers to unacceptable behaviours being repelled from the conscious mind and held or subdued in the unconscious mind by an active mechanism of inhibition (Rofé, 2008).

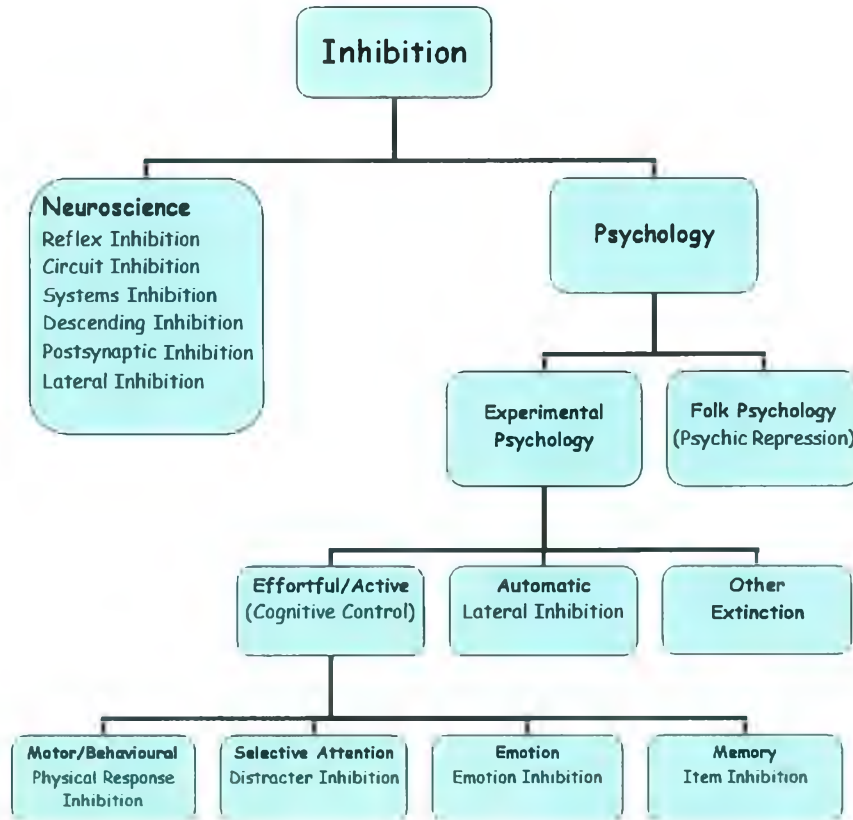


Figure 4.1. Types of inhibition in neuroscience and psychology. Figure reproduced and modified from Aron (2007a). The neural basis of inhibition in cognitive control. *Neuroscientist*, 13, 214-228.

In experimental psychology, the concept of inhibition is used to explain different forms of inhibition mechanism (Dagenbach and Carr, 1994; Dempster and Brainerd, 1995; Harnishfeger, 1995; MacLeod et al., 2003) (Fig. 4.1). The main difference is between those forms of inhibition that are automatic and those that are effortful/active (Friedman and Miyake, 2004; Nigg, 2000, Aron et al., 2006; 2007a). An example of automatic inhibition is “lateral or sensory inhibition” that develops since birth (Richards, 2003). In a sense, ‘inhibition’ is related here to the net activation of neurons and how these neurons inhibit each other by means of spreading lateral signals to neighbours in order to increase the contrast and sharpness of response representation. An example of effortful/active inhibition is the ability to resist irrelevant or interfering stimuli, and to suppress performing unwanted

movements. The experiments outlined in this thesis are uniquely concerned with this effortful/active form of inhibition and its underlying mechanism.

Research of the inhibition concept has been extended to involve the role of inhibition in cognitive psychological functions such as controlling sensory, visual, auditory distracters, unwanted memories, and motor responses. Dempster (1993) and Nigg (2000) have suggested that the concept of inhibition is a set of functions rather than a unitary or single construct. This means that inhibition can be considered as multiple functions that have common and distinct mechanisms. This led to different arguments and views about inhibition. One argument is that inhibition is used to inhibit the irrelevant information that flows into the conscious mind or awareness (cognition), whether this information is visual or auditory (Tipper, 2001). Another argument is that resisting inappropriate desires and impulses is impossible without inhibition. An alternative perspective is that resolving competition between motor commands or stopping an on-going behavioural action would not be possible without inhibition. These arguments yield a distinction between cognitive inhibition and behavioural inhibition. Nigg (2000) defines *cognitive inhibition* in terms of keeping irrelevant distracting information and undesired thoughts out of mind, and suppressing non-pertinent ideation to protect working memory. Nigg (2000) also defines *behavioural inhibition* in terms of the deliberate control of pre-potent behaviour, including suppressing a pre-potent response or cancelling a prepared response, or resisting an irrelevant response and response withholding. However, the distinction between the *cognitive* and *behavioural* inhibition is difficult without a clear description of the mechanism through which inhibition occurs.

In line with the above forms of inhibition, in this thesis, ‘inhibition’ refers to the concept of intentionally cancelling/stopping a prepared (physical) motor response or a response withholding (restrain) mechanism (Andres, 2003; Aron et al., 2004a; Boucher et al., 2007; Logan, 1994; Logan and Cowan, 1984; MacLeod et al., 2003; Miyake et al., 2000; Nigg, 2000; Ridderinkhof et al., 2004; Rubia et al., 2001; Stuphorn and Schall, 2006; Verbruggen et al., 2004; Friedman and Miyake, 2004).

4.3 Response Inhibition as a Measure of Executive Functions

Executive functions are higher-order cognitive capacities associated with the ability to engage in independent, initiating and optimizing goal-directed behaviour (Lezak et al., 1995; Royall et al., 2002). There are several behavioural tasks that have most often been used to assess how these high-level functions optimize and monitor the lower-level functions. These include task-switching (Barnes et al., 2003), Digit Symbol test (Bigler et al., 2003), Trail making test (Verghese et al., 2003) or suppressing pre-potent motor response (Verbruggen and Logan, 2009).

The requirement to suppress a pre-potent response exists in several task contexts, such as GO/NO-GO, stop signal, Wisconsin card sort, Stroop colour word, antisaccade, Eriksen flanker task, and many others (Aron et al., 2004a; Friedman and Miyake, 2004; Logan et al. 1984). Of these, the two main paradigms that are often used to study response inhibition are the GO/NO-GO paradigm (Donders, 1868/1969) and the stop-signal paradigm (Lappin and Eriksen, 1966; Logan and Cowan, 1984; Vince, 1948; Verbruggen and Logan, 2009).

Motor response inhibition can act in different ways depending on the changing environmental context. There are two main components involved in successful motor response inhibition; the ability to withhold a pre-potent response tendency (refrain/restraint) and the ability to cancel an on-going action (cancellation).

These sub-components of response suppression might have distinct and common underlying mechanisms and neural basis. In this thesis, GO/WAIT (Jackson et al., 1999, 2001; Swainson et al., 2003, Cornish et al., 2004) and GO/NO-GO paradigms (Donders, 1868/1969; Lappin and Eriksen, 1966; Logan and Cowan, 1984) are used to study the role of the basal ganglia in these sub-components of motor response inhibition; response withholding (Experiment (1)) and cancelling an on-going response (Experiment (2)), respectively. In Experiment (3) the same GO/WAIT cognitive paradigm with *variable* inter-stimulus interval (ISI) is used instead of the *fixed* (ISI) used in Experiment (1) in order to attenuate the effect of learning to predict the offset time of the stimulus. Thus, comparison of the results of Experiment (1) and Experiment (3) can draw the difference between response inhibition in predicted and unpredicted contexts.

The methods are common across the three experiments therefore here a complete description is given for the GO/WAIT paradigm, in subsequent method sections for the GO/NO-GO and GO/WAIT (variable timing) studies only key differences in the paradigm and subjects are described.

The GO/WAIT paradigm is a modified version of the GO/NO-GO task that involves response withholding. The ability to withhold a pre-potent response tendency (restraint) is one component of motor response inhibition. The GO/WAIT paradigm

used in the current study allows investigation of the neural substrates that are associated with withholding a motor response compared to immediately responding. As such, the paradigm design comprises alternating event types; a number of GO trials follow a WAIT trial (and vice versa), the switching of the motor set is inherent within such a task that includes mixed responses. The unpredictable sequence of trial ordering, and the task instruction emphasizing the need to respond quickly on the GO trials are crucial characteristics that promote immediate response. Therefore responding to, rather than inhibiting a response is made pre-potent.

In Experiment (1), in the GO/WAIT paradigm, subjects either responded promptly (GO trials) or withhold a response (WAIT trials) until stimulus offset. These events were intermixed with each other, making them unpredictable. The essence of this paradigm is that it represents an experimental model in the context of how people respond with restraint in the real-world to changing control. In the current study, an event-related fMRI design (Blamire et al., 1992; Friston et al., 1994; Buckner et al., 1996) was utilized in order to identify those of brain areas evoked by the inhibitory process in the sense of response withholding (restraint). It is noteworthy that the data in this study is the same data used in chapter 3 with only weighted summation (ws) data being further analysed in this Chapter.

4.4 Experiment 1

4.4.1 Material and methods

4.4.1.1 Participants

Eleven right-handed healthy participants (8 female; age range: 21–30 years with mean age of 22.8 ± 2.7 years) with no history of neurological disorders were scanned. Participants were informed of the experimental procedure before giving

written consent, and were compensated for their time and inconvenience. The study was approved by the Medical School Research Ethics Committee (University of Nottingham, UK).

4.4.1.2 Procedure (Apparatus)

Stimuli were presented to the participants by a computer controlled projection system that delivered a visual stimulus to a projection screen located at the foot of the magnet bore. The participant viewed this screen using prism glasses through a system of mirrors located inside the magnet room. The scanning room was darkened to allow easy visualization of the task stimuli. Participants were asked to keep their thumbs of each hand on left and right micro-switches mounted on a single (MR-compatible) response box positioned on the lower abdomen in the midline of the body.

The task was programmed and delivered using the MATLAB software package (Mathworks TM) and digital IO (input/output) routines implemented within the Data Acquisition Toolbox. Scan and task onsets were synchronized using a TTL pulse delivered to the scanner timing microprocessor board from a button box microprocessor connected to the laptop outside of the scanner in order to record the precise timing of button presses together with the timing of the acquisition of every slice in each image volume from the MR scanner.

4.4.1.3 Experimental Task

Prior to the fMRI scanning, all participants were familiarized with the task whilst outside of the scanner. Participants practiced the task briefly, completing a minimum of 5 trials of each type of task event (GO/WAIT), to verify that they understood the task.

The study consisted of two fMRI scan runs of the task, each approximately 8 min in duration. The experiment task was a 2 X 2 factorial design, as shown in Figure 4.2a. The factors were: 1. *Task* (with two levels; ‘WAIT’, ‘GO’) and 2. *Trial* (with two levels; ‘Switch’, ‘Repeat’), as shown in Figure 4.2a. The switch trial involves a rule switch compared to the prior trial, whilst the repeat trial has the same rule as on the previous trial. In this paradigm, a subject switches from immediately responding at the onset of the stimulus (GO task-green arrows) to responding at stimulus offset (WAIT task-red arrows). Therefore, a mixture of trials including Switch and Repeat trial types for each of the GO and WAIT tasks were created.

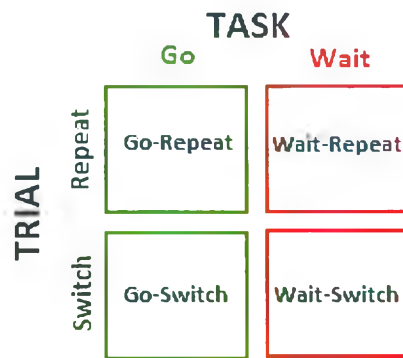
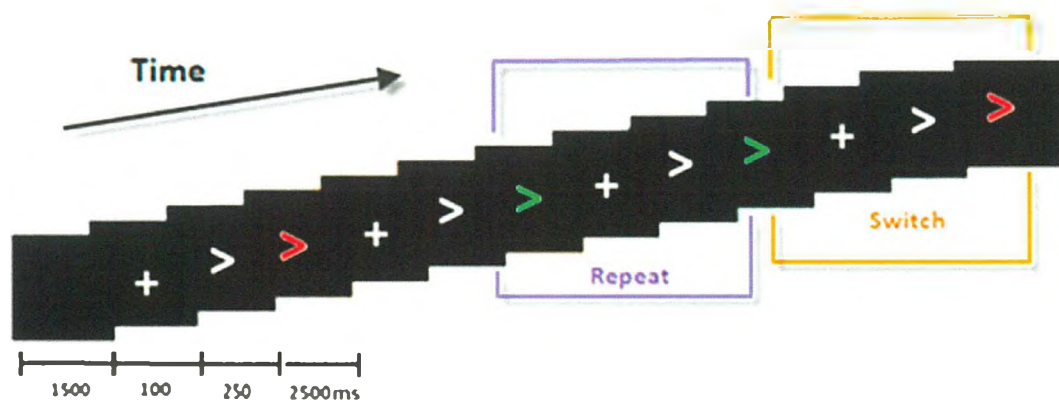


Figure 4.2. (a) Experimental paradigm with 2 X 2 factorial design of the four event types. The two factors of interest were task (GO, WAIT) and trial type (Repeat, Switch).



(b) Stimuli types and timing for the GO/WAIT paradigm. Participants respond to visually presented arrows by pressing response buttons with their right or left hand, depending on the arrow’s direction. Subjects switch between two arrow-discrimination tasks depending upon the colour of the arrow. If the arrow was green, participants were instructed to respond as quickly as possible. If the arrow was red, participants were instructed to WAIT and respond at the stimulus offset. A switch trial involves a rule switch relative to the prior trial. A repeat trial has the same rule as on the previous trial. Arrows can point to the left (<) or right (>). In the example shown, arrows are pointing right (>) for illustration.

A schematic of the GO/WAIT paradigm is shown in Figure 4.2b. The task comprised an arrow-shaped stimulus that was displayed on the centre of the screen in one of two colours (green or red). Participants were instructed to respond to each arrow by pressing a right or left button-box, depending on the arrow's direction. If the arrow was green (**GO**) participants were instructed to respond as quickly as possible. If the arrow was red (**WAIT**) participants were instructed to respond at the stimulus offset.

In this task, each trial started with the presentation of a blank screen for 1500 ms, the following set of stimulus types were then presented. A fixation cross was presented on the centre of the screen for a period of 100 ms. Following this, a single white arrow then appeared pointing to the right or left for a period of 250 ms, this then changed to green or red, as shown in Figure 4.2b. All arrows were presented for a **fixed** period of 2500 ms at a rate of one every 9 s. The white fixation cross was always represented during the inter stimulus interval. Throughout the task all button presses were recorded. A total of 98 arrows were presented during the event-related functional MRI data acquisition.

4.4.1.4 MRI data acquisition

MRI data were acquired on a 7 Tesla scanner (Philips Medical System) equipped with head only volume transmit coil and a 16 channel head SENSE receive coil. The participant's head was immobilized using foam cushions to reduce head movement, and subjects wore ear plugs to reduce the noise of the scanner. The Blood Oxygenation Level-Dependent (BOLD) fMRI signal was measured using a dual echo-planar imaging (EPI) sequence (repetition time $TR = 3$ s, echo time $TE_1 = 10.3$ ms,

$TE_2 = 29.3$ ms, flip angle = 90° , FOV = $192 \times 160 \times 164$ mm, 32 slices, slice thickness 2 mm, no slice gap, voxel size = 2 mm isotropic). For each fMRI scan, a total of 160 EPI volume images were acquired. Anatomical MR images were acquired with a magnetic prepared rapid acquisition gradient echo (MPRAGE) sequence (TR = 16 ms, TE = 4 ms, flip angle = 8° , FOV = $192 \times 169 \times 164$ mm, 169 slices per slab, slice thickness = 1 mm, no slice gap, voxel size = $1.5 \times 1.5 \times 1.5$ mm³).

4.4.2 Data Analysis

4.4.2.1 Behavioural data analysis

The first two trials of each fMRI scan and trials associated with an incorrect response were excluded from behavioural and fMRI analyses. Mean reaction times for the correct responses were entered in a two-way repeated measure ANOVA with the two factors “task” and “trial”. A paired-samples t-test was performed to compare between task and trial types.

4.4.2.2 fMRI data analysis-pre-processing

Data was analysed using Statistical Parametric Mapping SPM5 software (Wellcome Department of Cognitive Neurology, Institute of Neurology, University College London, UK, <http://www.fil.ion.ucl.ac.uk/spm>) (Friston et al., 1995) and MATLAB version 9.1 environment (MathWorks, Inc., <http://www.mathworks.com/>). Pre-processing steps included the combination of echoes, realignment to the first image of each time series using a six parameter linear transformation (a rigid-body rotation and translation correction) and reslicing of the data using sinc interpolation, as described in Chapter 3. The images for all participants were then spatially normalized into the Montreal Neurological Institute (MNI) space to remove inter-subject

anatomical variability. Data was then smoothed by convolving in space with a three-dimensional isotropic Gaussian kernel of 8 mm FWHM. This smoothing step increased the signal-to noise ratio and accounted for subtle variations in functional neuroanatomy that usually remains between subjects after spatial normalization.

4.4.2.3 fMRI data analysis-model estimation and statistics

The fMRI weighted summation (ws) data were analysed at the first and second level. At the first level analysis, each subject was modelled independently. The imaging data for each subject were analysed on a voxel-by-voxel basis using the principles of the general linear model (Friston et al., 1995) as implemented in SPM5. Prior to model estimation, all images were globally scaled and the time series filtered using a high pass filter to remove low frequency signals (below 160 s). The fMRI time series were then analysed by fitting a convolved canonical hemodynamic response function (HRF) to the onset of the stimulus for GO-Switch, GO-Repeat, WAIT-Switch and WAIT-Repeat trials. The six motion parameters (translation in and rotation about the x, y and z dimensions for each volume) were included as covariates of no interest. The incorrect trials were also included in the design matrix as a covariate of no interest. The following were then assessed (a) the main effect of each task type (i) GO and (ii) WAIT, and (b) the differential contrast of (i) (GO > WAIT) and (ii) (WAIT > GO) (for both trial types combined (switch and repeat)), chosen to study the neural basis of inhibition.

Second level analysis (group analysis) consisted of a random effects (RFX) analysis across the eleven subjects. Contrast maps from all participants were created and submitted to one sample t-test. Group maps were threshold with a height

threshold of $T = 3.01$ and extent threshold of 10 voxels, with a threshold of $P_{\text{FDR}} < 0.05$, corrected for multiple comparisons.

4.4.2.4 Region of interest (ROI) analysis

In order to further explore activity in brain areas, a region of interest (ROI) analysis was performed on those brain regions of maximal importance to the cognitive inhibition paradigm.

ROI analyses were performed on a number of brain regions that were identified both anatomically, and functionally based on the voxel-wise statistical map of the (WAIT > GO) contrast thresholded at ($P_{\text{FDR}} < 0.05$, corrected for multiple comparisons). The following ROIs were selected based on their roles in the current cognitive inhibition task (Aron, 2011). Cortical ROIs were defined functionally based on the group statistical map, using WFU_PickAtlas, by growing a sphere (10 mm radius) centred at the peak of the activation in each cluster. Functionally-defined ROIs included right SMA (6, -4, 46), left SMA (-6, -4, 52), right DLPFC (34, 40, 30), and right IFC (50, 10, 8) and anatomically-defined ROIs (MNI x, y, and z coordinates) of the right thalamus, and left putamen. The sub-cortical (basal ganglia) ROI were derived anatomically from the Automated Anatomical Labelling (ALL) Atlas (Tzourio-Mazoyer et al., 2002) implemented in the WFU_PickAtlas (<http://fmri.wfubmc.edu/cms/software#PickAtlas>) using standard MNI coordinates.

4.4.3 Results

4.4.3.1 Behavioural Data Results

Mean reaction times for the GO and WAIT conditions across subjects were calculated from the correct trials, as shown in Figure 4.3.

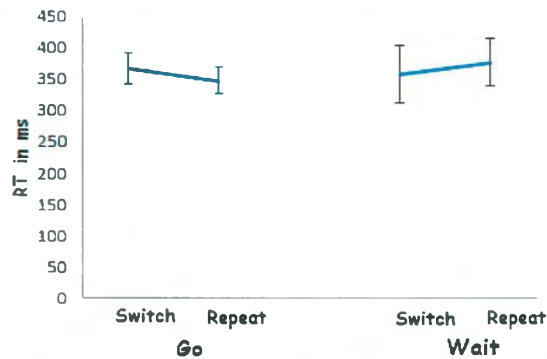


Figure 4.3. Mean reaction times for all conditions; WAIT– Switch, WAIT–Repeat, GO–Switch and GO–Repeat.

A two-way repeated measures ANOVA was conducted, with two levels of task (GO and WAIT) and two levels of trial type (Switch and Repeat) within subjects. There was no significant main effect of task [$F(1, 10) = 0.077, p = 0.787$] and no significant main effect of trial [$F(1, 10) = 0.286, p = 0.604$]. However, a significant interaction between task and trial was observed [$F(1, 10) = 6.936, p < 0.025$]. The average rate of errors in WAIT events (indicating an early response) was ($5 \pm 1\%$; $M \pm SD$) across subjects, with a total of 62 errors across all 11 subjects.

A paired-samples t-test was conducted to compare the GO–Switch and GO–Repeat conditions, and the WAIT–Switch and WAIT–Repeat conditions. There was a significant difference in the RT between the GO–Switch (367 ± 25 ms; $M \pm SEM$) and GO–Repeat conditions (348 ± 20 ms; $M \pm SEM$); ($t=2.7, p < 0.05$) and no significant difference in the scores between the WAIT–Switch (359 ± 45 ms; $M \pm SEM$) and WAIT–Repeat conditions (377 ± 37 ms; $M \pm SEM$); ($t=-1.143, p = 0.28$). The switch cost was (19 ± 2.5 ms; $M \pm SD$). These results suggest that there was a ‘switch cost’ for GO trials.

4.4.3.2 fMRI data

a) Main effect of motor execution and response withholding

The stimulus-response preparation and execution process was analysed by comparing the GO trials to baseline. For both the Repeat and Switch trials, the (GO > baseline) contrast revealed significant activation in bilateral prefrontal cortex, primary motor cortex (M1), bilateral supplementary motor area (SMA), posterior parietal cortex, insula cortex, anterior and middle cingulate cortex, ventral striatum, cerebellum, and thalamus, as shown in Figure 4.4.

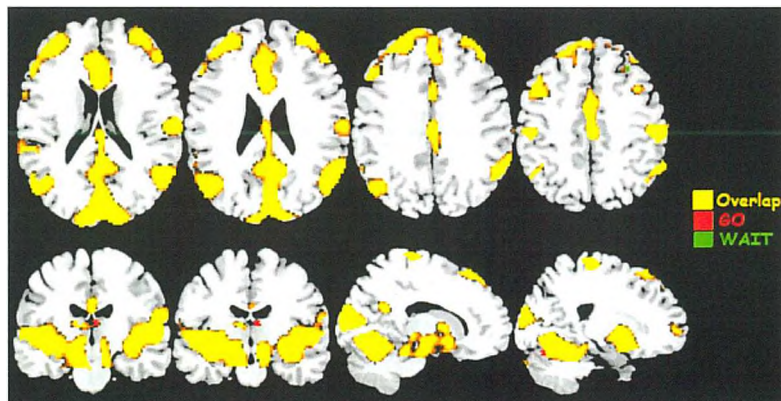


Figure 4.4. Brain regions associated with GO, WAIT conditions. ($P_{FDR} < 0.05$, corrected for multiple comparisons).

The WAIT condition involves motor selection and preparation processes though no motor execution process was engaged as the modelled period of the BOLD signal was within 500 ms and did not involve the button press. For both the Repeat and Switch trials, the (WAIT > baseline) contrast showed significant activation in bilateral prefrontal cortex, bilateral supplementary motor area (SMA), inferior parietal lobule, anterior and middle cingulate cortex, putamen, cerebellum, and thalamus (Figure 4.4).

b) (i) Motor execution compared to response withholding

The GO trials require an immediate response whilst the WAIT trials require the subjects to withhold a response until the stimulus offset, in both tasks the BOLD

signal was modelled within a period of 500 ms from the onset of the stimulus. Direct comparisons of those areas significantly more active to GO than WAIT conditions for both Repeat and Switch trials (GO > WAIT) showed no significant activation in cortical brain regions, suggesting that the GO and WAIT processes involve a similar set of cortical regions in both trial types. However, prominent activations were found in sub-cortical areas, in bilateral caudate nuclei and bilateral cerebellum (lobule VII, lobule VIIa Crus), as shown in Figure 4.5.

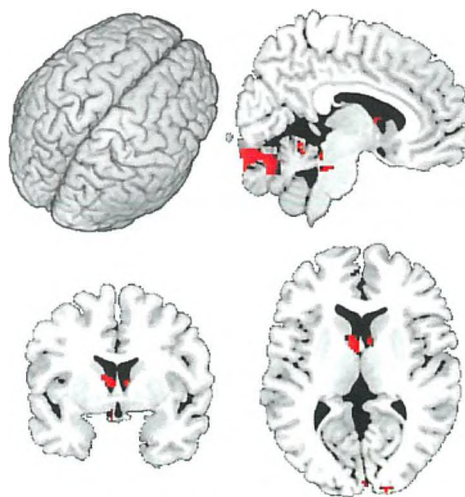


Figure 4.5. Brain regions associated with the (GO > WAIT) contrast. ($P_{FDR} < 0.05$, corrected for multiple comparisons).

(ii) Response withholding compared to motor execution

Response withholding (inhibition) process compared to immediate motor execution the (WAIT > GO) contrast, was associated with widespread cortical activation increases in bilateral supplementary motor area (SMA), bilateral dorsolateral prefrontal cortex (DLPFC), precentral gyrus, bilateral postcentral gyrus (somatosensory cortex), bilateral supramarginal gyrus, inferior frontal cortex (IFC), anterior cingulate cortex (ACC), middle temporal cortex and insula lobe, as shown in Figure 4.6 and summarised in Table 4.1. Sub-cortically, significant activation increases were identified in the thalamus and striatum.

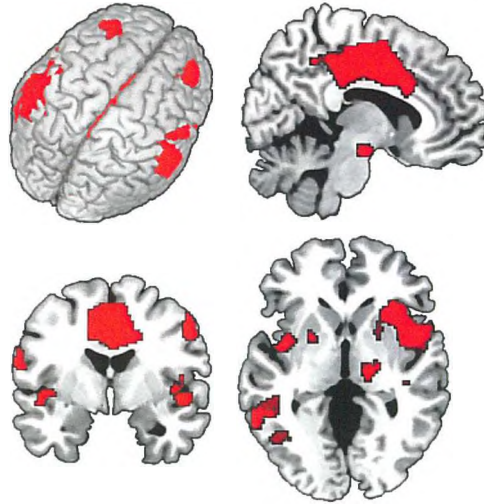


Figure 4.6. Brain regions associated with (WAIT > GO) contrast. $P_{FDR} < 0.05$ for multiple comparisons.

| Brain Region | Side | MNI Coordinates | | | Z-score | T value |
|------------------------------|------|-----------------|-----|-----|---------|---------|
| | | x | y | z | | |
| SMA | R | 6 | -4 | 46 | 4.51 | 8.76 |
| | L | -6 | -4 | 52 | 5.29 | 13.12 |
| Middle frontal cortex | R | 34 | 40 | 30 | 4.78 | 9.9 |
| | L | -42 | 36 | 32 | 4.46 | 8.33 |
| IFC (P.Orbitalis; BA 47) | R | 32 | 26 | -8 | 4.46 | 8.33 |
| IFC (P.Opercularis; BA 44) | R | 50 | 10 | 8 | 3.75 | 6.12 |
| Precentral gyrus (BA 6) | R | 38 | -16 | 50 | 4.67 | 9.3 |
| | L | -30 | -10 | 54 | 2.96 | 3.87 |
| Postcentral gyrus (BA 1,2,3) | R | 52 | -26 | 42 | 4.46 | 8.32 |
| | L | -52 | -24 | 52 | 4.59 | 8.91 |
| IPL (Supramarginal gyrus) | R | 58 | -30 | 36 | 4.02 | 6.64 |
| | L | -50 | -46 | 30 | 4.82 | 10.13 |
| MCC | R | 4 | 2 | 42 | 4.82 | 10.11 |
| STC | R | 54 | -32 | 16 | 3.71 | 5.75 |
| ITC | L | -46 | -62 | -8 | 4.09 | 6.88 |
| Precuneus | L | -10 | -60 | 42 | 2.88 | 3.69 |
| Cuneus | R | 14 | -84 | 24 | 3.57 | 5.28 |
| Insula Lobe | R | 44 | 4 | -6 | 3.8 | 5.88 |
| | L | -38 | 2 | -2 | 3.03 | 4.01 |
| Rolandic operculum | R | 58 | -16 | 18 | 3.87 | 5.96 |
| Inferior occipital cortex | L | -34 | -88 | -10 | 2.7 | 3.41 |
| Cerebellum (Lob. VIIa Crus) | L | -32 | -82 | -32 | 2.72 | 3.43 |
| (Sub)Thalamus (VL nucleus) | R | 14 | -16 | 2 | 2.92 | 3.8 |
| BG (Putamen) | R | 22 | 6 | -6 | 2.9 | 3.7 |
| | L | -22 | 6 | 0 | 2.76 | 3.48 |
| BG (External GP) | R | 22 | -14 | 0 | 2.85 | 3.6 |
| Brainstem(Midbrain) | R | 8 | -12 | -16 | 3.42 | 4.86 |

Table 4.1. Abbreviation: L, Left; R, right; BA, Brodmann area; DM, dorsomedial; VL, ventrolateral; IFC, inferior frontal cortex; IPL, inferior parietal lobule; MCC, middle cingulate cortex; MTC, middle temporal cortex; ITC, inferior temporal cortex; BG, basal ganglia; GP, globus pallidus.

The results are consistent with the results of previous studies in which GO/NO-GO and stop tasks were used to investigate the response inhibition (Konishi

et al., 1999; Garavan et al., 1999; Rubia et al., 2001; Aron and Poldrack, 2006; Zheng et al., 2008; Chikazoe et al., 2007, 2009; Coxon et al., 2009; Cai et al., 2011).

4.4.3.3 ROI and Correlation analysis results

There was a significant positive correlation between the BOLD parameter estimates of the (WAIT > GO) contrast and the mean GO-Switch RT in predefined ROIs including right thalamus and left putamen, right SMA (6, -4, 46), left SMA (-6, -4, 52), right DLPFC (34, 40, 30), and right IFC (50, 10, 8), as shown in Figure 4.7.

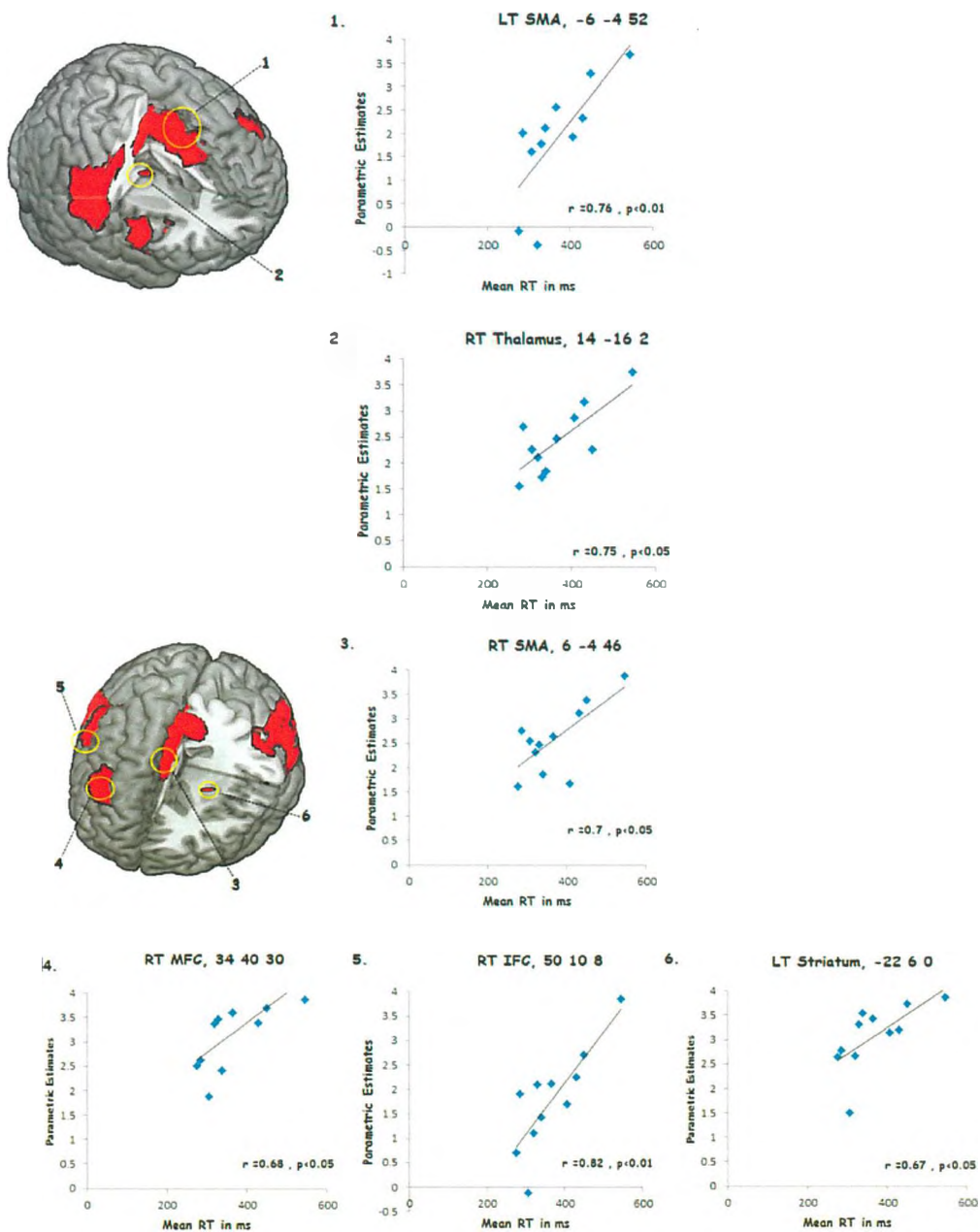


Figure 4.7. Scatter plots illustrate the correlation between the BOLD parameter estimates for the (WAIT > GO) contrast and the mean of the GO-Switch RT measures across subjects in a priori ROIs.

4.4.4 Summary

The GO/WAIT task was used to examine the role of the basal ganglia in the inhibitory process. The behavioural results revealed that reaction times (RT) on switch trials were longer than those on repeat trials for the GO task. This residual switch cost suggests that the system cannot be fully reconfigured for a task switch before stimulus onset (Rogers & Monsell 1995).

The imaging results revealed that motor preparation and execution-related activity was elicited in multiple brain regions, including bilateral prefrontal cortex, bilateral pre-supplementary motor area (pre-SMA), anterior and middle cingulate cortex, ventral striatum, cerebellum, and thalamus which is consistent with previous studies (Garavan et al., 1999; Rubia et al., 2001; Aron and Poldrack, 2006; Cai and Leung, 2009; Coxon et al., 2009), suggesting that the motor preparation and execution process engages fronto-striatal-thalamic and motor cortical nuclei. This is consistent with the so-called “direct pathway” of the basal ganglia, in which the planning regions of the prefrontal cortex send neural signals to the striatum, which then projects to the internal segment of the globus pallidus (GPi), to the thalamus, and ultimately back to the cortical motor regions; MI and SMA.

In motor preparation and execution-related activity compared to response withholding-related activity, the (GO > WAIT) contrast, no significant activation in cortical brain regions was shown suggesting that the GO and WAIT processes involve a similar set of cortical regions. However, sub-cortical activations were found in bilateral caudate nuclei and bilateral cerebellum (lobule VII, lobule VIIa Crus). Given that the BOLD signal was modelled by defining a window of interest from the onset

of the stimulus to 500ms for both tasks (GO & WAIT), this means that motor execution (button press) is included in the GO trials whilst in WAIT trials there is no motor execution within that period of time. These findings reflect that the motor preparatory process is triggered and computed before the target or stimulus is actually displayed and that advanced motor preparation is enhanced even with long preparation time prior to the offset of the stimulus that might be predictable in WAIT trials. Based on this, subjects might engage in the status of readiness and motor preparation in advance, regardless of the stimulus type.

Inhibiting an initiated response, the (WAIT > GO) contrast as a marker of response inhibition in the current study, was associated with activation in striatum and thalamus, in addition to the SMA and right IFC. This is striking as the same brain regions were found significantly active during successful stopping trials in the stop signal paradigm and GO/NO-GO studies (Konishi et al., 1998, 1999; Garavan et al., 1999; Chikazoe et al., 2010; Jahfari et al., 2009; Zandbelt and Vink, 2010; Cai et al., 2011). This putative neural network is consistent with a “hyperdirect” pathway, in which the prefrontal cortex sends direct and fast activity to the STN particularly from two main foci the pre-SMA and the rIFC (Inase et al., 1999; Aron et al., 2007b).

The rIFC activation in the present study is consistent with results of prior studies across different inhibition tasks, indicating this region is central to inhibitory control (Aron et al., 2004a; Chambers et al., 2006; Kelly et al., 2006; Cai and Leung, 2009; Cai et al., 2011; Swann et al., 2009, 2012). However, this does not necessarily imply that the rIFC (as implicated here) should be considered as the source of inhibitory cognitive control signals that operate to aid action selection by suppressing

inappropriate actions or distracting stimuli. Rather, it is likely to reflect that the IFC is the source of facilitatory signals that bias competition within action selection mechanisms in brain areas linked to motor execution. This may be accomplished by recruiting the 'hyperdirect' pathway, in which excitatory signals projects from the prefrontal cortex (including IFC) to the STN to block the execution of the Go response via the basal ganglia. However, other possibilities should be considered. For example, it might be critical for attentional detection of the stop signal stimulus (Duann et al., 2009; Hampshire et al., 2010; Sharp et al., 2010). Moreover, the rIFC has been found significantly activated for working memory monitoring, and sustained attention tasks (McNab et al., 2008; Wager and Smith, 2003).

The SMA/pre-SMA is widely considered to be of crucial importance for inhibitory control. The pre-SMA could thus implement an active mechanism of motor response inhibition, perhaps by inputting excitatory signals directly to the STN through the 'hyperdirect' pathway. This is critical in conflict resolving between competing programmes (Isoda and Hikosaka, 2007; Ridderinkhof et al., 2004). Another possibility is that the pre-SMA may be involved in the process of preparation to stop rather than stopping reactively (Jahfari et al., 2009; Chikazoe et al., 2007).

The task-demands, which involve working memory for active maintenance of task-relevant elements and online manipulation of task information, would be expected to activate mainly the dorsolateral prefrontal cortex (DLPFC), posterior parietal cortex and striatum as these regions play a critical role in mediating working memory (Petrides, 1994; Bunge et al., 2001; Muller and Knight, 2006; D'Esposito et al., 2000; Smith et al., 1999).

To relate behavioural measure to the BOLD activation, ROI analyses using predefined ROI including right thalamus, and left striatum, right and left SMA, right DLPFC and right IFC revealed significant positive correlations between the BOLD signal and the mean of the GO-Switch RT measures. This showed that increased fMRI BOLD activation is positively associated with longer reaction times (RT), suggesting that the signals arising from the cortical regions such as IFC, pre-SMA are unlikely to be inhibitory signals, but rather they are facilitatory signals influence and modulate motor output. However, an important consideration about the interpretation of the fMRI BOLD signal is that increased or decreased BOLD signal can be associated with improved cognitive process or task performance (Poldrack et al., 2006).

Although a consistent pattern of activation have been implicated in different response inhibition paradigms, including the current paradigm, different forms of inhibition might be involved in different tasks, as shown in Figure 4.8 (Aron, 2011; Chikazoe et al., 2010; Wager et al., 2005).

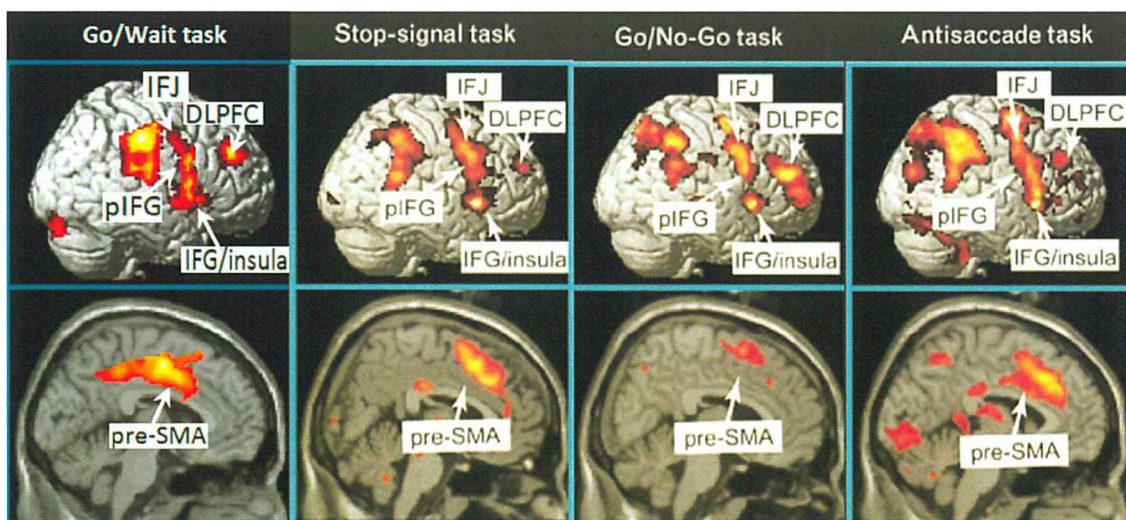


Figure 4.8. Functional magnetic resonance imaging studies of stop signal and related paradigms including the current paradigm in this thesis (1st column). Chikazoe J (2010): Localizing performance of GO/NO-GO tasks to prefrontal cortical sub-regions. *Current Opinion Psychiatry* 23, 267-272.

In the paradigm that was used in this experiment, the inter-stimulus interval was fixed (2500 ms), meaning that subjects are likely to learn to anticipate the offset time of the stimulus in WAIT trials. Thus, the question to be addressed in considering the network of activations found here is: are these activations associated with suppressing the motor response or learning to predict the offset time of the stimuli? To address this question, two further experiments follow; (1) a GO/NO-GO (Experiment 2) to investigate the sub-component of response inhibition or the cancelling of an on-going action and (2) a GO/WAIT with variable timing (Experiment 3) to attenuate the role played by the prediction of stimulus offset.

4.5 Experiment 2:

Experiment (2) of this chapter followed the same general procedure as Experiment (1) except that the GO/WAIT task was susceptible to a withholding strategy. In contrast, in this experiment, the GO/NO-GO task involves cancelling an on-going action when a NO-GO stimulus appears. The issue addressed here is: Are these inhibitory processes the same? For example, when one has to inhibit or withhold an inappropriate motor response in one status, are the same underlying mechanisms recruited as when one has to cancel or stop a response in another situation? To address this, an event-related fMRI design was utilized using the GO/NO-GO paradigm in order to identify the areas of brain activation evoked by the inhibitory process in the sense of cancelling an initiated response

In this paradigm, the subject was required to press a button in response to the green arrow (GO trials) and not to respond or cancel an on-going responding on presentation of the red arrow (a NO-GO trial).

4.5.1 Material and methods

4.5.1.1 Participants

Twelve right-handed healthy participants (7 female; age range: 20–29 years with mean age of 21.6 ± 2.4 years) with no history of neurological disorders were scanned. Participants were informed of the experimental procedure before giving written consent, and were compensated for their time and inconvenience. The study was approved by the Medical School Research Ethics Committee (University of Nottingham, UK).

4.9.2 Experimental Task and procedure

This experiment followed the same general procedure as Experiment (1) and the same paradigm was used except that subjects were instructed to cancel their responses when a NO-GO (red arrow) stimulus appeared and not respond, as shown in Figure 4.9.

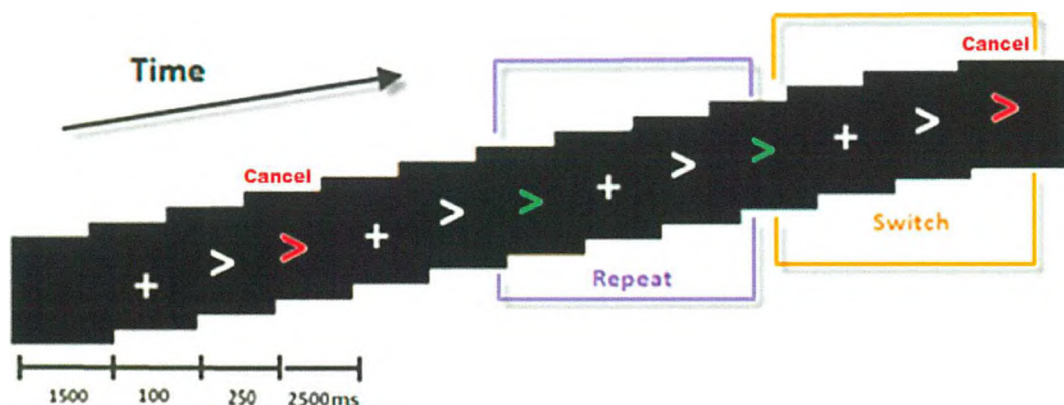


Figure 4.9. Stimuli types and timing of the GO/NO-GO paradigm; participants responded to visually presented arrows by pressing response buttons with their right or left hand, depending on the arrow's direction. Subjects had to switch between two arrow-discrimination tasks depending upon the colour of the arrow. If the arrow was green, participants were instructed to respond as quickly as possible. If the arrow was red, participants were instructed not to respond. The switch trial involves a rule switch relative to the prior trial. A repeat trial has the same rule as on the previous trial.

4.5.1.3 MRI data acquisition

fMRI data were acquired using the same scanning parameters as for Experiment (1).

4.5.2 Data Analysis

4.5.2.1 Behavioural Data

The first two trials of each run and trials associated with an incorrect response were excluded from behavioural and fMRI analyses. Mean reaction times for correct responses were entered in a separate two-way repeated measure ANOVA with the two factors being “task” and “trial”. A paired-samples t-test was performed to compare between task and trial types.

4.5.2.2 fMRI Data

fMRI data were pre-processed and analysed in the same way as described for Experiment (1).

4.5.2.3 Region of interest (ROI) analysis

The same procedure of ROI analysis was followed as for Experiment (1), with ROIs were identified both anatomically, and functionally based on the voxel-wise statistical map of the (NO-GO > GO) contrast thresholded at ($P_{\text{FDR}} < 0.05$, corrected for multiple comparisons). ROIs functionally-defined (MNI x, y, and z coordinates) included the left pre-SMA (-10, 26, 56), left SFC (-16, 30, 52), right MFC (28, 14, 42; BA 8), and right IFC (56, 20, 28; BA 9) and anatomically-defined (MNI x, y, and z coordinates) of right caudate nucleus.

4.5.2.4 Conjunction analysis

To identify common regions of activity associated with inhibition, a conjunction analyses was performed between the (WAIT > GO) contrast in Experiment (1) and the (NO-GO > GO) contrast in Experiment (2) by first thresholding the (whole-brain) statistical maps for each of the two contrasts for each subject in each experiment, then binarizing them and finally adding the images all together (Nichols et al., 2005).

4.5.3 Results

4.5.3.1 Behavioural Data

Mean reaction times of the GO task for switch and repeat trials across subjects were calculated from the correct responses, as shown in Figure 4.10.

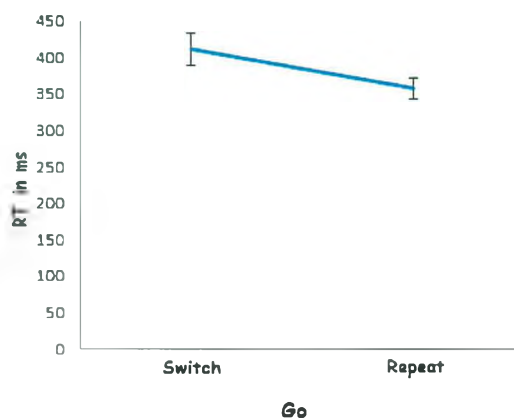


Figure 4.10. Mean reaction times for GO-Switch and GO-Repeat conditions.

A paired-samples t-test was conducted to compare between GO-Switch and GO-Repeat conditions. A significant difference in the RT for GO-Switch (410 ± 21.7 ms; $M \pm SEM$) condition and GO-Repeat (358 ± 14 ms; $M \pm SEM$); ($t=2.27$, $p < 0.05$) was found. This suggests that there was a 'switch cost' (52 ± 9 ms; $M \pm SD$) between the GO-switch and GO-repeat trials.

4.5.3.2 fMRI data

a) *Main effect of motor execution and cancelling*

The stimulus-response preparation and execution process was analyzed by comparing the GO trials to baseline, (GO > baseline) contrast, this elicited prominent activations in multiple regions, including the dorsolateral prefrontal cortex (DLPFC), anterior cingulate cortex (ACC), supplementary motor area (SMA), insula, rostralateral prefrontal cortex, ventral striatum, cerebellum, and thalamus.

The NO-GO condition involves motor selection and preparation processes, though no motor execution process was engaged as the subject was required not to respond to NO-GO stimulus. For both the Repeat and Switch trials, the (NO-GO > baseline) contrast showed significant activation in multiple regions including bilateral prefrontal cortex, bilateral pre-supplementary motor area (pre-SMA), motor cortex (M1), parietal cortex, anterior and middle cingulate cortex, cerebellum, striatum and thalamus.

b) (i) *Motor execution compared to response cancelling*

The contrast of (GO > NO-GO) trials elicited no significant activation in cortical brain regions, suggesting that the GO and NO-GO processes involve a similar set of cortical regions. However, significant activations were found in sub-cortical areas, in left striatum, left pallidum, bilateral thalamus and bilateral cerebellum (lobule VI, vermis), consistent with the result of Experiment (1) when compares motor execution with withholding (GO versus WAIT).

(ii) *Response cancelling compared to motor execution*

Response *cancelling* (inhibition) compared to immediate motor execution, the (NO-GO > GO) contrast, was associated with increased activation in bilateral pre-

supplementary motor area (pre-SMA), bilateral middle frontal cortex and superior frontal cortex (DLPFC), inferior frontal cortex (IFC), anterior cingulate cortex (ACC), and superior temporal cortex, as shown in Figure 4.11 and summarised in Table 4.2. Sub-cortically, significant activation was seen in the thalamus and striatum. This pattern of activation is similar to that seen in Experiment (1) for the (WAIT > GO) contrast. However, a distinction is the increased prefrontal cortex activity for the cancelling process than response withholding in Experiment (1).

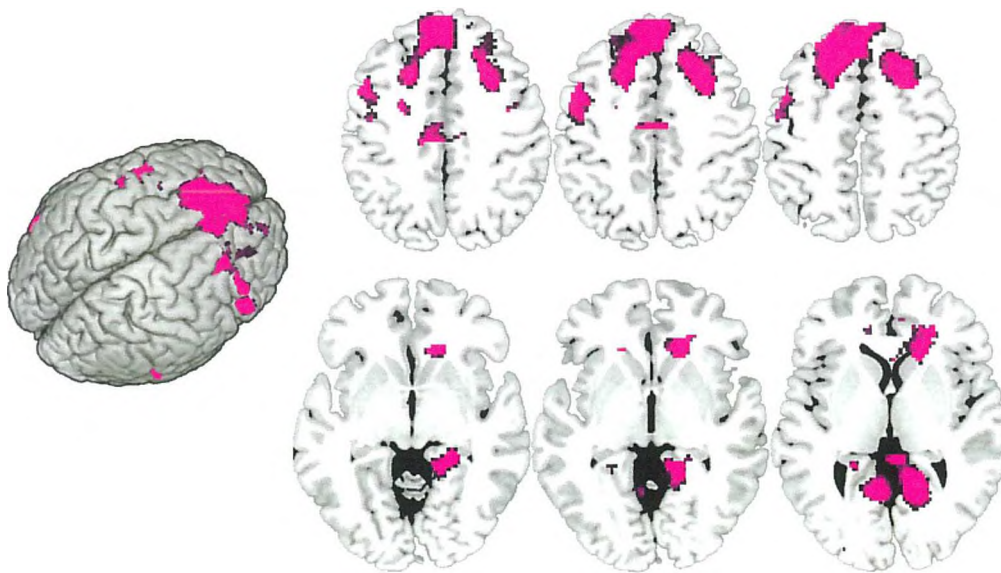


Figure 4.11. Brain regions associated with response cancelling/suppression-related activity, (NO-GO > GO) contrast. ($P_{FDR} < 0.05$ for multiple comparisons).

| Brain Region | Side | MNI Coordinates | | | Z-score | T value |
|--------------------------------|------|-----------------|-----|-----|---------|---------|
| | | x | y | z | | |
| Superior frontal cortex (BA 8) | R | 24 | 20 | 52 | 3.3 | 4.45 |
| | L | -10 | 26 | 54 | 5.29 | 13.12 |
| Middle frontal cortex | R | 28 | 14 | 42 | 3 | 3.84 |
| | L | -50 | 10 | 42 | 3.62 | 5.2 |
| Pre-SMA | L | -2 | 30 | 56 | 3.5 | 4.9 |
| IFC (BA 9) | R | 56 | 20 | 28 | 2.89 | 3.64 |
| | L | -48 | 18 | 14 | 2.75 | 3.4 |
| ACC | R | 12 | 32 | 14 | 3.04 | 4.01 |
| STC (BA 39) | L | -50 | -62 | 20 | 3.51 | 4.93 |
| Precuneus | R | 20 | -50 | 18 | 3.46 | 4.82 |
| Calcarine gyrus | R | 18 | -52 | 4 | 3.6 | 5.16 |
| | L | -16 | -56 | 12 | 3.95 | 6.1 |
| Fusiform gyrus | R | 34 | -10 | -32 | 3.33 | 4.52 |
| Hippocampus | R | 26 | -38 | -10 | 3.75 | 5.53 |
| IOC (BA 18) | L | -40 | -84 | -20 | 3.31 | 4.47 |
| Cerebellum (Lob. VIIa Crus) | R | 18 | -86 | -24 | 3.43 | 4.73 |
| BG (Caudate nucleus) | R | 18 | 26 | 0 | 3.63 | 5.23 |

Table 4.2. Significant brain areas associated with response cancelling, (NO-GO > GO) contrast.

4.5.3.3 ROI and Correlation analysis results

A significant positive correlation between the BOLD parameter estimates for the (NO-GO > GO) contrast and the mean of the GO-Switch RT was found in predefined ROI's including right caudate nucleus (18, 26, 0), left pre-SMA (-10, 26, 56), left SFC (-16, 30, 52), right MFC (28, 14, 42; BA 8), and right IFC (56, 20, 28; BA 9), as shown in Figure 4.12. These are regions that also showed significantly greater activation during response cancelling relative to motor preparation and execution.

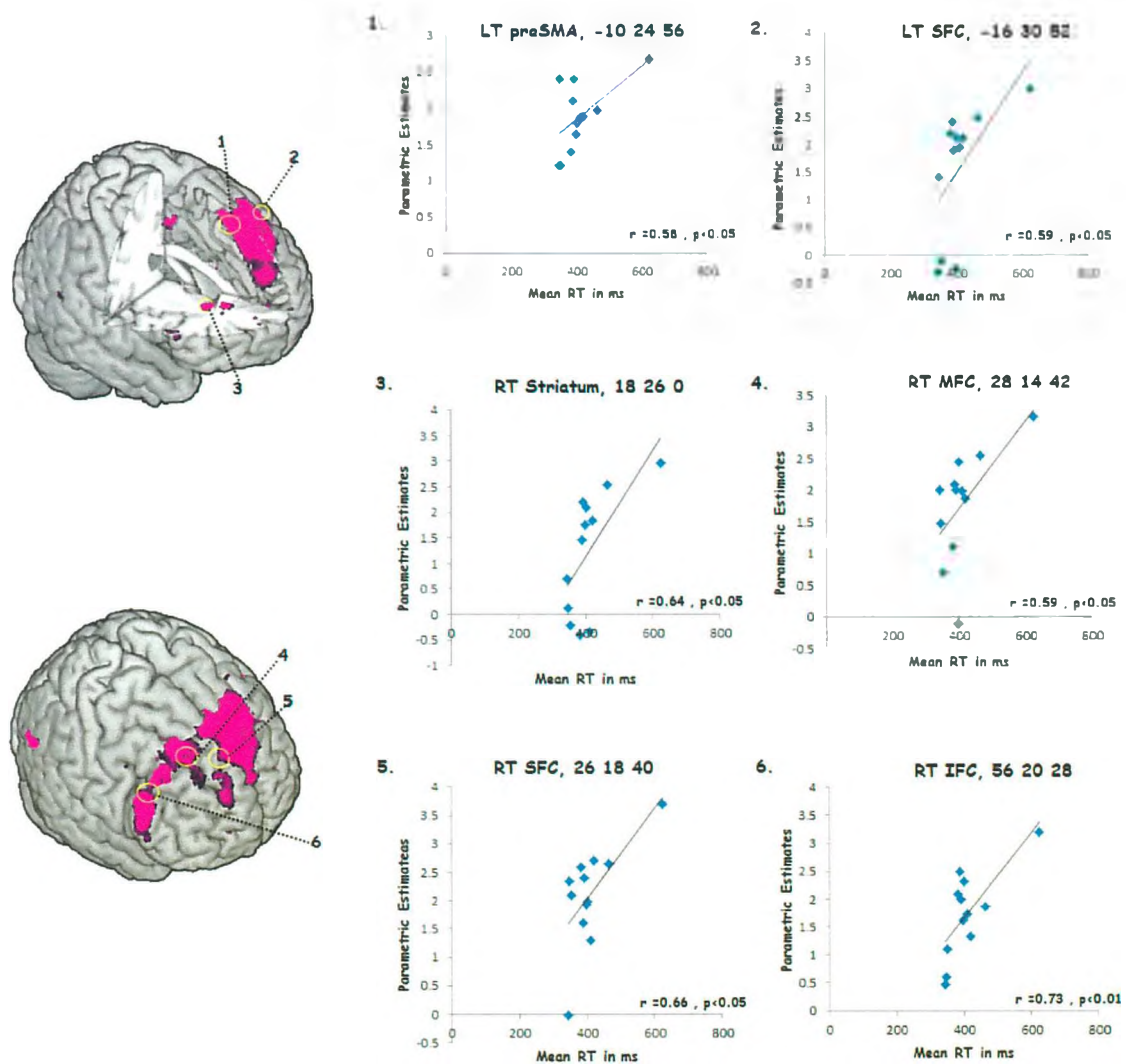


Figure 4.12. Scatter plots illustrate the correlation between the BOLD parameter estimates for the (NO-GO > GO) contrast and the mean of the GO-Switch RT measures across subjects in a priori ROIs.

4.5.3.4 Conjunction analysis results

The conjunction map shows that only one brain region, the rIFC ($x=52, y=12, z=8$), was both significantly active for restraint/withholding identified from the ((WAIT > GO contrast) in Experiment (1)) and the cancellation process identified from the ((NO-GO > GO contrast) in Experiment (2)), as shown in Figure 4.13.

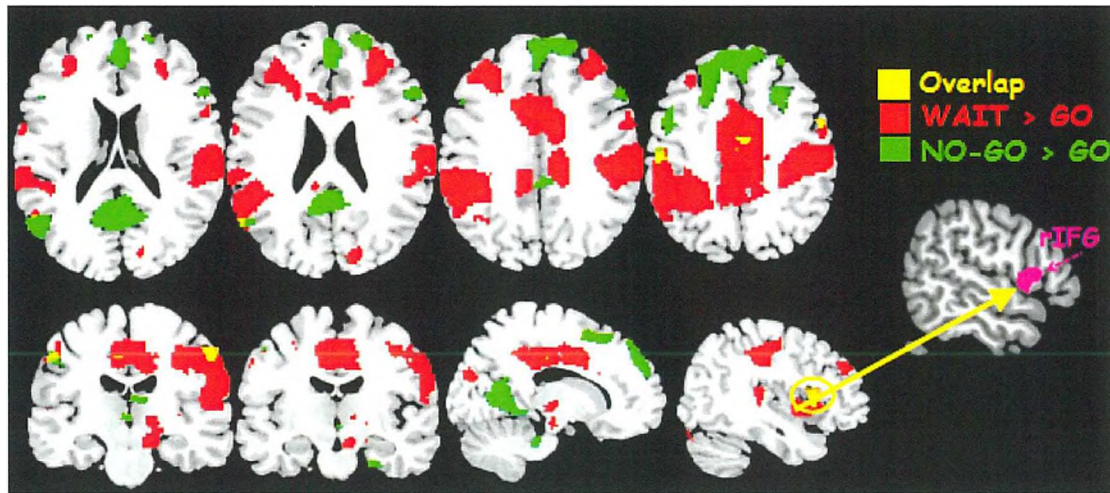


Figure 4.13. A significant conjunction effect between the (WAIT > GO) and (NO-GO > GO) contrasts, at significance of $P_{FDR} < 0.05$, corrected for multiple comparison. The only (rIFG) found to be significantly active for both tasks

4.5.4 Summary

The aim of the study was to investigate the cancellation sub-component of the inhibitory control using a GO/NO-GO paradigm and compare the result to that of task withholding in Experiment (1) for the GO/WAIT paradigm, as two sub-components of inhibitory control.

The behavioural results revealed a significant difference between the GO-Switch and GO-Repeat trials, the ‘switch cost’. This ‘residual switch cost’ remained even with long preparation intervals, suggesting that the preparation period is not enough to fully reconfigure the internal system in order to overcome the behavioural

cost (Rogers and Monsell, 1995). The behavioural result here is similar to what found in Experiment (1).

The imaging results showed that motor preparation and execution-related activity was elicited in a neural network similar to that found in Experiment (1). As previously explained, this including prefrontal cortex, bilateral pre-supplementary motor area (pre-SMA), anterior and middle cingulate cortex, ventral striatum, cerebellum, and thalamus which is consistent with the so-called “direct pathway” of the basal ganglia. Similar to Experiment (1), motor preparation and execution activity compared to response cancelling activity, the (GO > NO-GO) contrast, showed no significant activation in cortical brain regions. However, sub-cortical activations were found in bilateral caudate nuclei and bilateral cerebellum (lobule VII, lobule VIIa Crus). This result suggests the motor preparation is enhanced early even with long preparation time prior to the offset of the stimulus.

Response suppression in the context of cancelling an on-going action, (NO-GO > GO), was associated with activation in similar brain regions to that found in Experiment (1). However, for the (NO-GO > GO) contrast, the dorsolateral prefrontal cortex (DLPFC) and anterior cingulate cortex (ACC) are more involved and engaged in cancelling an initiated motor action compared to response withholding process in (Experiment 1). This may be attributed to the role of the DLPFC in the implementation of control, by organizing a representation of the relevant-task information in order to generate an appropriate motor action and actively maintain the attentional demands of the task which reflect the working memory demands and functions (Mostofsky et al., 2003; Simmonds et al., 2008). Another possibility is that

the DLPFC plays a key role in processing response suppression itself, by switching off the initiated motor set when the NO-GO stimulus appears. This is consistent with other studies that found this region to be active in response inhibition tasks (Garavan et al., 2006; Simmonds et al., 2008).

The ACC is a brain region thought to be involved in response-related processes (Paus, 1993; MacDonald and Joordens, 2000; Milham et al., 2001; Paus, 2001), such as conflict monitoring (Carter et al., 1998, 2000; MacDonald and Joorden, 2000). In this experiment, the increased activity in the ACC might reflect the conflict caused by the simultaneous activation of two competing response tendencies (GO and NO-GO stimuli) under conditions when low-frequent responses (NO-GO) are required in the context of making pre-potent responses (GO) (Braver et al., 2001). The ACC was found to be more active in the GO/NO-GO task rather than the GO/WAIT task, this may be attributed to the different task-demands as subjects need to withhold the motor response under the WAIT condition, whilst cancel the initiated motor action or switching off the motor program under the NO-GO condition. The involvement of ACC in mediating response conflict is consistent with other studies (Carter et al., 1998; Paus, 2001; Braver et al., 2001). Moreover, Nieuwenhuis and colleagues (2003) have shown that the N2 (an event-related potential (ERP) component) reflects an electrophysiological correlate of conflict between GO and NO-GO response representations that is detected in the ACC brain region. Thus, the DLPFC and ACC seem to have distinct, complementary roles in a neural network serving inhibitory control.

ROI analysis revealed significant positive correlations between the BOLD signal and the mean of the GO-Switch RT measures in right striatum, left pre-SMA, right DLPFC and right IFC (Fig. 11). This showed that increased fMRI BOLD activation is positively associated with increased reaction time (RT), supporting the idea that the cortical regions such as IFC, pre-SMA and DLPFC exert excitatory signals, rather than being the source of the inhibitory signals, to modulate motor output and aid to bias the competition between the motor responses.

Comparing inhibition contrasts, (WAIT > GO) and (NO-GO > GO), overlapping activation was found in a variety of regions including the superior and middle frontal and bilateral inferior frontal regions, inferior parietal lobule and insula cortex. Conjunction analysis was performed to investigate commonalities between the neural substrates of inhibition of withholding of a pre-potent response (WAIT > GO contrast in Experiment (1)) and cancelling an initiated motor response (NO-GO > GO contrast in Experiment (2)). The right inferior frontal cortex (rIFC) is the only region that showed robust common activation across both tasks. This result is consistent with the common activation areas was reported by Rubia et al. (2001), who also showed common activation between stop tasks and GO/NO-GO. McNab and colleagues (2008) also identified the IFC as a common activation region between the working memory task, the GO/NO-GO task and stop task.

Converging evidence has implied the right IFC (rIFC) as a key node in cognitive inhibition function. In monkey- lesion studies, damage to a homologue of IFC (the inferior prefrontal convexity in non-primate brain) impaired NO-GO performance (Mishkin et al., 1964; Iversen and Mishkin 1970; Sakagami et al., 2001;

Sasaki et al., 1989; Hasegawa et al., 2004). In human lesion studies, damage to the right IFG crucially affects and disrupts inhibition mechanism. Moreover, it has been found that the greater the damage to this region the worse the response inhibition (Aron et al., 2003). In neuroimaging studies the right-lateralized inferior frontal gyrus (rIFG) region has been observed consistently to play a critical role in response inhibition (Bunge et al., 2002; Garavan et al., 1999; Rubia et al., 2003).). Based on the conjunction analysis, it is speculated that the rIFC play a common, inhibitory function in these tasks. The rIFC exerts facilitatory projections that help in biasing the competition between motor programs (GO and NOGO/WAIT) within the striatum through the subthalamic nucleus (STN) which has abroad inhibition effects upon the striatum and palladium (Mink et al., 1996). This results in blocking the execution of the GO response. Furthermore, the correlation between the ROI and the behaviuuoral measure (RT) in both studies and the current finding of the IFC and thalamus (STN) activation strongly supports this account.

4.6 Experiment 3

Experiment (3) followed the same procedure as Experiment (1) using the same GO/WAIT cognitive paradigm except that for this study the timing of stimulus presentation was changed to be *variable* instead of the *fixed* timing used in Experiment (1). The aim of using a variable timing in this experiment was to attenuate the effect of prediction of the offset time of the stimulus. This allows the comparison of the results of Experiment (1) and Experiment (3).

4.6.1 Material and methods

4.6.1.1 Participants

Twelve right-handed healthy participants (8 female; age range: 20–30 years with mean age of 21.3 ± 1.6 years) with no history of neurological disorders were scanned. Participants were informed of the experimental procedure before giving written consent, and were compensated for their time and inconvenience. The study was approved by the Medical School Research Ethics Committee (University of Nottingham, UK).

4.6.1.2 Experimental Task and Procedure

Experiment (3) followed the same procedure as the GO/WAIT paradigm in Experiment (1) except that all arrows (green and red) were presented for a **variable** period of time from (1-3 s), rather than a **fixed** period of 2.5 s as used in Experiment (1), as shown in Figure 4.14.

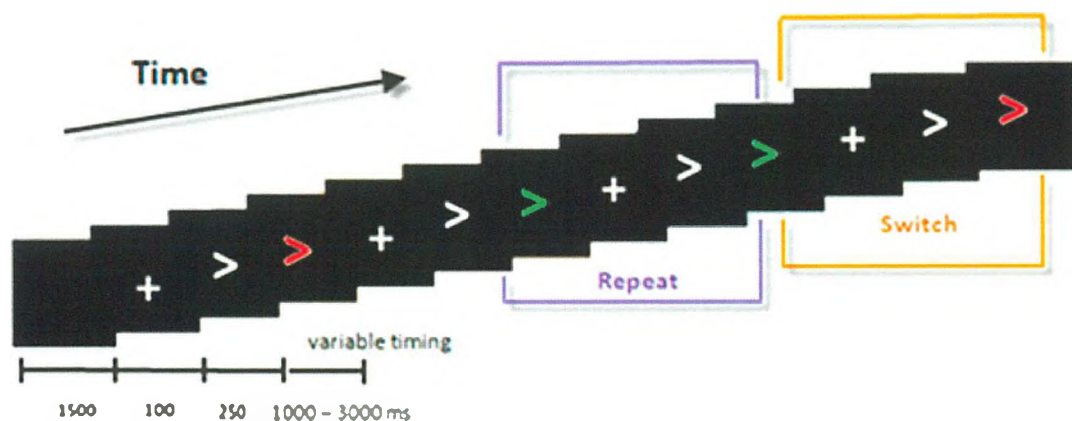


Figure 4.14. Stimuli types and timing of the GO/WAIT variable paradigm; participants responded to visually presented arrows by pressing response buttons with their right or left hand, depending on the arrow's direction. Subjects had to switch between two arrow-discrimination tasks depending upon the colour of the arrow. If the arrow was green, participants were instructed to respond as quickly as possible. If the arrow was red, participants were instructed to WAIT and respond at the stimulus offset. Red arrows were presented at variable timing from 1-3s. Switch trial involves a rule switch relative to the prior trial. Repeat trial has the same rule as on the previous trial.

4.6.1.3 MRI data acquisition

fMRI data were acquired using identical scan parameters as in previous experiments.

4.6.2 Data Analysis

4.6.2.1 Behavioral Data

The first two trials of each run and trials associated with an incorrect response were excluded from behavioural and fMRI analyses. Mean reaction times for correct responses were entered in separate two-way repeated measure ANOVA with the two factors of “task” and “trial”. A paired-samples t-test was performed to compare between task and trial types.

4.6.2.2 fMRI Data

fMRI data were pre-processed and analysed in an identical manner to Experiment (1).

4.6.2.3 Region of interest (ROI) analysis

ROIs were created as for Experiment (1) and included; anatomical –defined ROIs (MNI x, y, and z coordinates), such as the right putamen, and functionally-defined ROIs, including the left DLPFC (-36, 16, 36), right IFC (50, 10 8; P.opercularis, BA44), and right MCC (4, -32, 30).

4.6.3 Results

4.6.3.1 Behavioural Data

Figure 4.15 shows the mean reaction times of GO and WAIT conditions across subjects calculated from the correct trials.

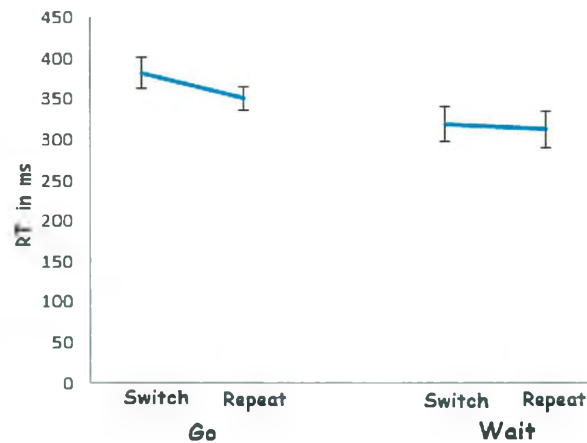


Figure 4.15. Mean reaction times for GO/WAIT variable paradigm; WAIT– Switch, WAIT–Repeat, GO–Switch and GO–Repeat.

A two-way repeated measures ANOVA was conducted, with two levels of task (GO and WAIT) and two levels of trials (Switch and Repeat) within subjects. There was a significant main effect of task [$F(1, 11) = 5.4, p < 0.05$] and a significant main effect of trial [$F(1, 11) = 6.43, p < 0.05$]. However, no significant interaction between task and trial was found [$F(1, 11) = 2.69, p = 0.129$]. The average rate of errors in WAIT events (incorrect responses) across subjects was ($6 \pm 1\%$; $M \pm SD$) and there were a total of 71 errors across 12 subjects.

A paired-samples t-test was conducted to compare the GO–Switch and GO–Repeat conditions, and the WAIT–Switch and WAIT–Repeat conditions. There was only a significant difference in RT between the GO–Switch (381 ± 18 ms; $M \pm SEM$) and GO–Repeat conditions (351 ± 14 ms; $M \pm SEM$); ($t = 2.62, p < 0.05$) and no significant difference in the scores between the WAIT–Switch (319 ± 20.6 ms; $M \pm$

SEM) and WAIT–Repeat conditions (314 ± 22 ms; $M \pm SEM$); ($t=0.58$, $p = 0.57$). The switch cost was (30 ± 8.5 ms; $M \pm SD$). These results suggest that there was a ‘switch cost’ within GO trials between GO-Switch and GO-Repeat, but no ‘switch cost’ within WAIT trials between WAIT-Switch and WAIT-Repeat.

4.6.3.2 fMRI data

a) *Main effect of motor execution and cancelling*

Motor preparation and execution processes were analysed by comparing the GO trials to baseline for both the Repeat and Switch trials (GO > baseline). A similar network of activation to Experiment (1) and (2) was found, including motor cortex, pre-supplementary motor area (pre-SMA), the dorsolateral prefrontal cortex (DLPFC), anterior cingulate cortex (ACC), insula cortex, ventral striatum, cerebellum, and thalamus. The WAIT condition involves motor selection and preparation processes. For both Repeat and Switch trials, (WAIT > baseline) led to significant activation in bilateral prefrontal cortex, bilateral supplementary motor area (SMA), motor cortex, inferior parietal lobule, anterior and middle cingulate cortex, striatum, cerebellum, and thalamus.

b) (i) *Motor execution compared to response withholding*

The contrast of (GO > WAIT) revealed no significant activation in cortical brain regions, suggesting that the GO and WAIT processes involve a similar set of cortical regions. However, significant activations were found in sub-cortical areas, in left striatum, and bilateral cerebellum (lobule VI) in line with Experiments (1) and (2).

(ii) Response withholding compared to motor execution

Response withholding (inhibition) in an unpredictable context compared to the immediate motor execution process (WAIT > GO, variable timing) contrast, was associated with increased activation in bilateral (DLPFC), inferior frontal cortex (IFC), premotor area, postcentral gyrus, supramarginal gyrus, middle cingulate cortex (MCC), superior temporal cortex (STC), and medial temporal pole. Sub-cortically, significant activation increases were identified in striatum and midbrain regions, as shown in Figure 4.16 and summarised in Table 4.3.

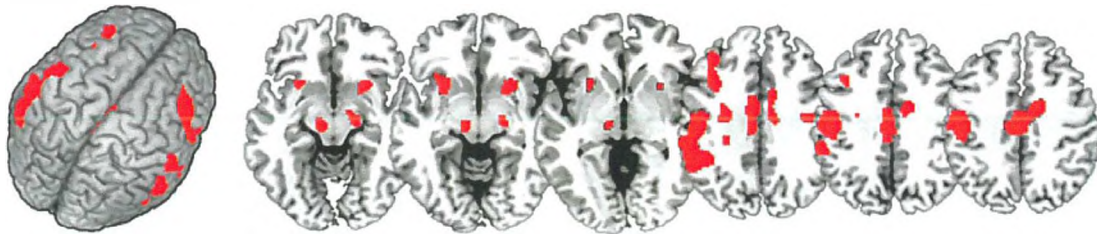


Figure 4.15. Brain regions associated with response withholding in unpredictable context. $P_{FDR} < 0.005$ corrected for multiple comparisons.

| Brain Region | Side | MNI Coordinates | | | Z-score | T value |
|------------------------------|------|-----------------|-----|-----|---------|---------|
| | | x | y | z | | |
| Middle frontal cortex (BA 9) | L | -36 | 16 | 36 | 3.34 | 4.55 |
| IFC (P.Opercularis; BA 44) | R | 60 | 14 | 8 | 3.49 | 4.88 |
| IFC (P.Triangularis) | L | -36 | 32 | 24 | 3.18 | 4.21 |
| Precentral gyrus (BA 6) | R | 38 | -12 | 34 | 3.05 | 3.94 |
| Postcentral gyrus | R | 56 | -18 | 30 | 4.09 | 6.51 |
| | L | -56 | -8 | 28 | 2.98 | 3.81 |
| IPL (Supramarginal gyrus) | R | 62 | -40 | 24 | 3 | 3.85 |
| | L | -50 | -52 | 28 | 3.98 | 6.19 |
| MCC (BA 23) | R | 4 | -32 | 30 | 3 | 3.85 |
| | L | -4 | -30 | 40 | 2.87 | 3.61 |
| STC (BA 13) | R | 64 | -18 | 6 | 3.13 | 4.09 |
| Medial Temporal pole (BA 21) | R | 52 | 4 | -16 | 3.55 | 5.04 |
| BG (Putamen) | R | 26 | 14 | -8 | 4.03 | 6.34 |
| Brainstem(Midbrain) | R | 18 | -14 | -10 | 3.03 | 3.91 |

Table 4.3. Significant brain areas associated with response withholding (inhibition) mechanism.

4.6.3.3 ROI and Correlation analysis results

A significant positive correlation between the BOLD signal and the mean of the GO-Switch RT in predefined ROIs including right putamen (26, 14, -8), left DLPFC (-36, 16, 36), right IFC (50, 10, 8; P. opercularis BA44), and right MCC (4, -32, 30) was found, as shown in Figure 4.17.

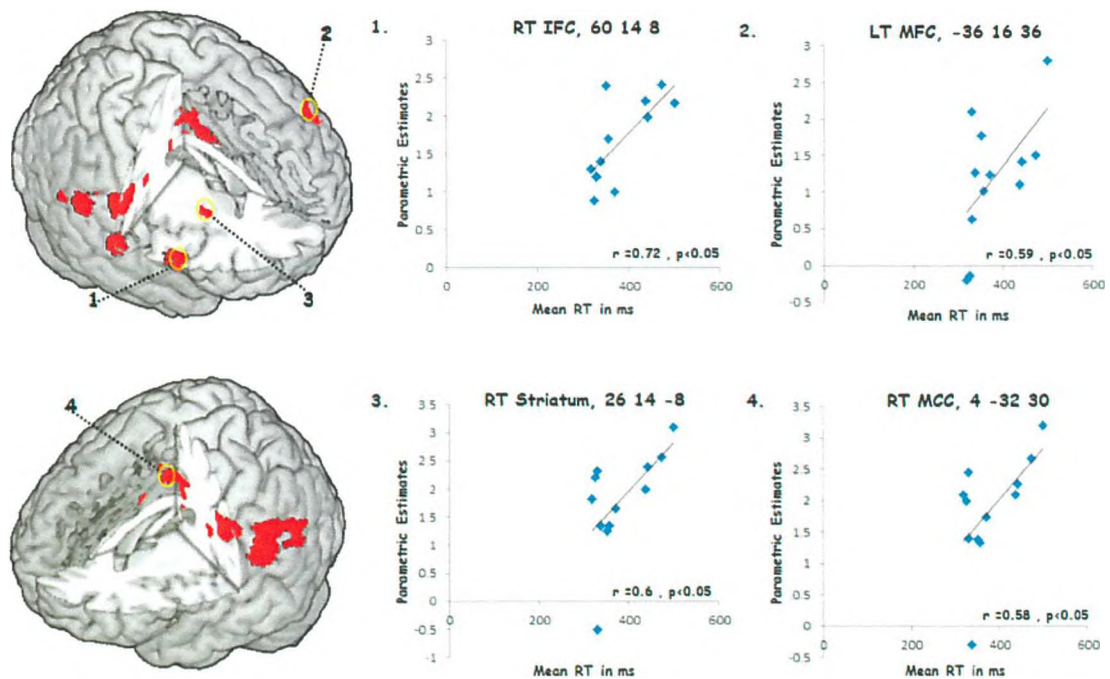


Figure 4.17. Scatter plots illustrate the correlation between the BOLD parameter estimates for the (WAIT > GO) contrast and the mean of the GO-Switch RT measures across subjects in a priori ROIs.

4.6.4 Summary

The modified GO/WAIT paradigm with variable inter-stimulus interval (ISI) was used to address the question of whether the network of activations found in Experiment (1) are associated with suppressing the motor response, or learning to predict the offset time of the stimuli. In order to attenuate the effect of learning to predict the offset time of the stimulus, the ISI in this experiment was variable (from 1-3 s), thus allowing comparison to the results of Experiment (1).

The behavioural results revealed that reaction times (RT) on switch trials were slower than repeat trials for the GO task. The residual switch cost suggests that the system cannot be fully reconfigured for a task switch before stimulus onset (Rogers & Monsell 1995).

The imaging results of motor execution activity recruited the same pattern of activation as found in Experiments (1) and (2) including bilateral prefrontal cortex, primary motor cortex (M1), bilateral pre-SMA, anterior and middle cingulate cortex, striatum, thalamus and cerebellum. These results together confirm that making a GO response engages the direct pathway of the basal ganglia.

The imaging results of the motor execution-related activity compared to response withholding-related activity, (GO > WAIT), showed no significant activation in cortical brain regions as found earlier. However, sub-cortical activations were observed in bilateral striatum and bilateral thalamus and cerebellum (lobule VIIa Crus). This supports earlier experiments and implicates that the preparatory process takes place in advance before the stimuli appear, regardless of the stimulus type and its demand.

Inhibiting an initiated response *in unpredicted context*, (WAIT > GO) contrast, yielded a similar pattern of activation that was observed in Experiment (1) including middle frontal cortex, primary motor cortex, bilateral inferior parietal lobules, middle cingulate cortex and right IFC, in addition to activation in the striatum and midbrain regions. This is a network consistent with the prediction uncertainty network observed in previous published studies (Huettel et al., 2005; Volz et al., 2003, 2004; Grinband

et al., 2006). Interestingly, the rIFC was significantly active, across the previous experiments in this chapter, which raises the importance of this node in mediating the inhibitory control (Aron et al., 2006, 2007b; Chambers et al., 2006; Cai et al., 2009, 2011; Swann et al., 2009, 2012).

ROI analyses using predefined ROI including right striatum, left DLPFC, right IFC (BA44), and right MCC (Fig. 16) revealed significant correlations between the BOLD signal and the mean of the GO-Switch RT measures. This correlation provides further support to the idea that these prefrontal cortical regions can be the source of excitatory output that projects to cortical and subcortical areas such as striatum in order to bias between the motor programs competitors and regulate motor output.

4.7 Direct comparison between experiments

Response inhibition is a crucial aspect of cognitive control that is necessary for flexible interaction with changing environmental contexts. Different forms of response inhibition are critical to the successful completion of many everyday activities and tasks. For example, one must instantly *cancel/stop* an impending response or one needs to *withhold* a pre-potent response tendency that interferes with goal-directed behaviour. These forms of inhibition were examined in Experiment (1) and (2), respectively. Many experimental paradigms treat these forms of inhibition as equivalent, based on the assumption that they share a common neural basis and a common underlying mechanism. To test whether this is true or they involve some distinct neural substrates, direct comparison between experiments (1-3) were performed.

- (a) Brain regions associated with response withholding were revealed by comparing (WAIT_{fixed} > GO) trials in Experiment (1), to (NO-GO > GO) trials in Experiment (2). Whereas brain regions associated with cancelling an impending response were revealed by comparing the (NO-GO > GO), in Experiment (2), to the (WAIT_{fixed} > GO) in Experiment (1).
- (b) Response withholding under the prediction context-associated activity were revealed by comparing the (WAIT_{fixed} > GO) trials in Experiment (1), to the (WAIT_{variable} > GO) trials in Experiment (3). Whilst brain regions associated with response withholding under the condition in which the event prediction is uncertain were revealed by comparing (WAIT_{variable} > GO) trials in Experiment (3), to the (WAIT_{fixed} > GO) trials in Experiment (1). By conducting these comparisons, the pattern of activation related to each of the inhibition sub-components was revealed and discussed in the following sections.

a) (i) Response withholding activity compared to response cancelling activity

The response withholding (inhibition) process compared to the cancellation process, (WAIT_{fixed} > NO-GO) contrast, was associated with widespread cortical activation increases in supplementary motor area (SMA), bilateral middle frontal cortex, middle cingulate cortex (MCC), superior and inferior temporal cortex, insula lobe and Rolandic operculum, as shown in Figure 4.18, and summarised in Table (4.4a). In addition, significant activation also increases were identified in the striatum. These results are consistent with previous studies of response inhibition (as reviewed in Aron, 2011; Chambers et al., 2009; Chikazoe, 2010; Levy and Wagner, 2011).

These results point to the involvement of withholding strong response tendency-associated brain regions as a subcomponent of motor response inhibition during WAIT trials. Therefore, it is important to note that increased activation in these prefrontal cortex regions (such as IFC and SMA) cannot be account for increasing inhibition. Alternatively, these regions of prefrontal cortex, rather than being involved in sending out inhibitory control signals, are involved in online task-elements maintenance and facilitation and biasing the competition between motor responses.

(ii) Response cancelling activity compared to response withholding activity

The response *cancelling* process compared to response withholding process (NO-GO > WAIT_{fixed}) contrast, was associated with increased activation in bilateral (DLPFC), ACC, rostral prefrontal cortex, paracentral lobule, cuneus and cerebellum, as shown in Figure 4.18 and summarised in Table (4.4b). In addition, significant activation was identified in ventral striatum. In line with prior studies (Aron et al., 2003, 2004, 2005; Chambers et al., 2006; Chevrier et al., 2004) similar pattern of activation was observed, particularly the involvement of the DLPFC. It is interesting to note that the neural network observed here might be dedicated to the process of cancelling an on-going action as another sub-component of the motor response inhibition.

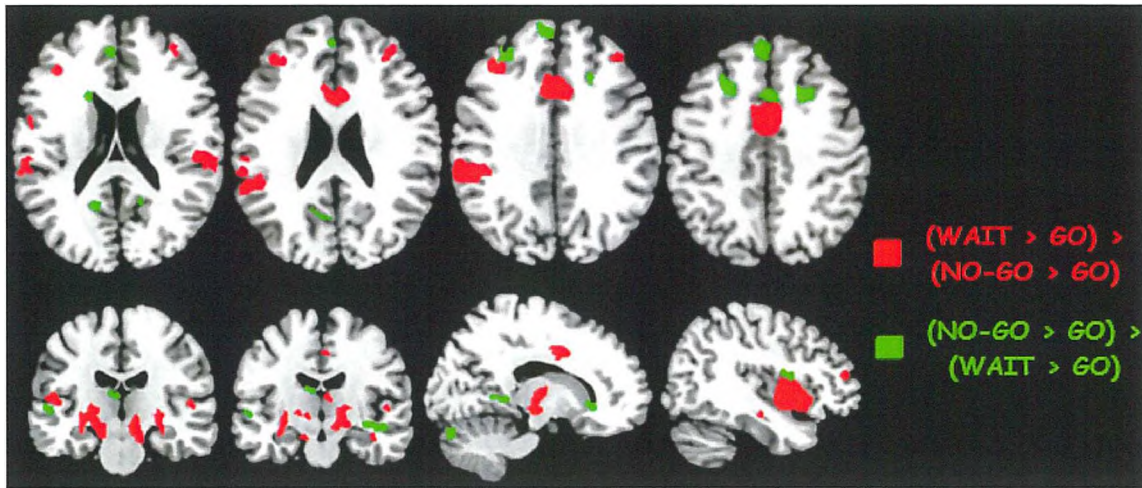


Figure 4.18. Comparison between Experiment (1) and (2) showed brain regions activity associated with $[(WAIT > GO) > (NO-GO > GO)]$ (in red) and $[(NO-GO > GO) > (WAIT > GO)]$ (in green). $P_{FDR} < 0.05$ for multiple comparisons.

| Brain Region | Side | MNI Coordinates | | | Z-score | T value |
|------------------------------|------|-----------------|-----|-----|---------|---------|
| | | x | Y | z | | |
| SMA (BA 6) | R | 4 | -2 | 48 | 5.29 | 7.81 |
| Middle frontal cortex | R | 32 | 40 | 26 | 4.12 | 5.2 |
| | L | -28 | 32 | 30 | 3.63 | 4.35 |
| MCC (BA 24) | R | 10 | 4 | 36 | 4.48 | 6.46 |
| | L | -4 | -4 | 48 | 5.78 | 9.26 |
| IPC | L | -54 | -44 | 26 | 4.68 | 5.8 |
| STC (BA 41) | L | -56 | -26 | 12 | 4.96 | 6.97 |
| ITC | R | 56 | -60 | -8 | 2.97 | 3.36 |
| | L | -42 | -62 | -8 | 3.43 | 4.02 |
| Temporal pole | R | 50 | 14 | -12 | 4.77 | 6.52 |
| Insula Lobe (BA 13) | R | 44 | 8 | -4 | 5.27 | 7.76 |
| | L | -36 | -8 | -4 | 5.12 | 7.37 |
| Rolandic operculum (BA 43) | R | 54 | -18 | 14 | 5.02 | 7.12 |
| BG (Head of Caudate nucleus) | R | 8 | 8 | 0 | 2.92 | 3.29 |

Table 4.4a. Significant brain areas associated with response withholding (inhibition) process.

| Brain Region | Side | MNI Coordinates | | | Z-score | T value |
|--------------------------------|------|-----------------|-----|-----|---------|---------|
| | | x | y | z | | |
| Superior frontal cortex (BA 8) | R | 24 | 20 | 52 | 3.42 | 3.92 |
| | L | -16 | 30 | 50 | 3.16 | 3.68 |
| Middle frontal cortex (BA 9) | L | -18 | 20 | 48 | 2.79 | 2.98 |
| ACC | L | -10 | 46 | 4 | 3.05 | 3.44 |
| Rostral PFC (BA 10) | L | -4 | 52 | 6 | 2.73 | 3.04 |
| Paracentral lobule (BA 6) | L | -2 | -32 | 58 | 3.26 | 3.77 |
| MTC (BA 39) | L | -52 | -64 | 22 | 3.01 | 3.42 |
| Precuneus | L | -16 | -56 | 14 | 3.52 | 4.17 |
| Cuneus | L | -16 | -56 | 26 | 2.85 | 3.2 |
| Calcarine gyrus | R | 16 | -58 | 18 | 2.84 | 3.18 |
| | L | -10 | -58 | 6 | 3.09 | 3.53 |
| Lingual gyrus (BA 17) | R | 16 | -52 | 4 | 3.05 | 3.51 |
| Fusiform gyrus | R | 30 | -32 | -18 | 4.42 | 5.77 |
| Parahippocampus | R | 26 | -38 | -6 | 5.36 | 8 |
| Cerebellum (VI, VIIa Crus) | R | 16 | -80 | -26 | 4.25 | 5.44 |
| BG (Caudate nucleus) | L | -6 | 6 | -12 | 3.48 | 4.11 |

Table 4.4b. Significant brain areas associated with cancellation.

Considering the interesting difference between these contrasts, it is striking to observe distinct and common brain regions. First, activation of the right SMA is observed here on response inhibition (WAIT condition), raising the possible inhibitory role of this region relative to other prefrontal cortex regions. One possibility that merits consideration is that the SMA may play a role in the process of preparation to withhold or stop rather than stopping or suppressing the response. This is in line with recent fMRI studies which suggest that this region might be more 'set-related' (Chikazoe et al., 2009; Jahfari et al., 2009). Another possibility is that the SMA may play a key role in selecting "superordinates sets of action-selection rules" which Rushworth and his colleagues (2004) referred to as an 'action set'. The 'action-set' was defined as a group of elements and rules that are necessary for selection responses. It was also suggested that the SMA is most important in the initiation and regulation of this action set depending on the stimulus-response context (Rushworth et al., 2004). However, alternative views accounts for the functional role of the pre-SMA/SMA, include conflict resolution and monitoring (Isoda and Hikosaka, 2007; Ridderinkhof et al., 2004), motivation (Scangos and Stuphorn, 2010), and modulating response thresholds (Bogacz et al., 2010).

Response suppression, in the context of cancelling an initiated response (NO-GO condition), revealed the DLPFC as a key region involved in response inhibition. One possibility is that the DLPFC has a critical role in the biasing of working memory processes rather than particularly mediating response inhibition, such as, the selection of appropriate representations for upcoming stimulus-response, on-line maintenance, and manipulation of task-relevant information is favoured over that of task-irrelevant information (Davidson and Glisky, 2002; Rowe et al., 2000, 2001; Aguirre et al.,

1999; Milham et al., 2002, Mostofsky et al., 2003; Simmonds et al., 2008). This interpretation fits with previous functional imaging studies showing persistent activation of DLPFC as it is more engaged under the conditions when there is increased working memory load in the inhibition task, (Curtis et al., 2004; Muller and Knight, 2006; Braver et al., 1997; Bung et al., 2001; Mostofsky et al., 2003) as well as recent fMRI studies (Jahfari et al., 2010; Chikazoe et al., 2010). Another possibility is that the DLPFC activity plays the predominant role in top-down attentional control (Fuster, 1997; Knight and Kaplan, 2003; D'Esposito et al., 2000; Miller and Cohen, 2001, Petrides, 2000; Smith and Jonides, 1999).

Multiple lines of evidence support that the DLPFC-particularly the middle frontal gyrus in humans is an essential region responsible for higher-order functions. First, given the fact that executive control facilitates a wide range of different sensory and motor modalities, the DLPFC is a crucial 'gateway' for integration of these modalities because of its dense neural recurrent connections to most sensory and motor cortexes and sub-cortical structures as well (Miller, 2000). Second, the DLPFC is a key region in a well-established working memory circuitry (Muller and Knight, 2006; Wager and Smith, 2003; Braver et al., 1997; Petrides, 1994). Third, tract tracing in monkey (Alexander et al., 1990) and diffusion tensor imaging (DTI) in human (Lehericy et al., 2004) have shown that the DLPFC is connected to the striatum through a so-called associative 'fronto-striatal- pallidal-thalamic' circuit. This circuit is used to cancel/stop the motor response through the indirect pathway. This is striking as the caudate nucleus was observed significantly active in the current results.

The finding of increased ACC activity in NO-GO conditions that require response inhibition or selective attention might reflect that this region is responsible for implementing attentional control. This is compatible with previous studies (Bush et al., 1998; Peterson et al., 1999; Posner and Dehaene, 1994; Posner and Digirolamo, 1998). An alternative is that the ACC might be involved in monitoring and detecting response conflict in information processing between different brain regions, which require further processing and increased cognitive control in order to resolve the conflict.

b) (i) Response withholding in predicted context compared to response withholding in unpredicted context

Response withholding in a predicted context compared to an unpredicted context, ($WAIT_{\text{fixed}} > WAIT_{\text{variable}}$) contrast, was associated with widespread cortical activation increases in right supplementary motor area (SMA), bilateral dorsolateral prefrontal cortex (DLPFC), inferior frontal cortex (IFC), precentral gyrus, postcentral gyrus, inferior parietal cortex (IPC), middle cingulate cortex (MCC), superior temporal cortex and insula lobe and inferior occipital cortex, as shown in Figure 4.19 and summarised in Table 4.5. Sub-cortically, significant activation increases were identified in putamen, thalamus and midbrain regions. The results here are consistent with the putative neural network of response inhibition found in the previous mentioned studies.

(ii) Response withholding in unpredicted context compared to response withholding in predicted context

Response withholding in an unpredicted context process compared to in a predicted manner ($WAIT_{variable} > WAIT_{fixed}$) contrast, revealed sub-cortical activation increases in bilateral caudate nuclei and bilateral thalamic nuclei, as shown in Figure 4.19 and summarized in Table (4.5a & b).

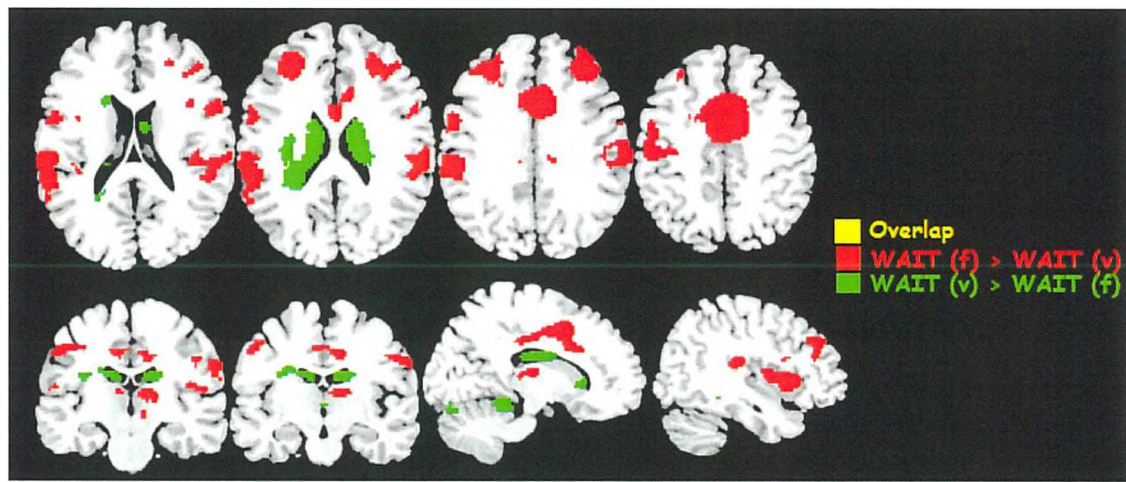


Figure 4.19. Comparison between Experiment (1) and (3) showed brain regions activity associated with ($WAIT_{fixed} > WAIT_{variable}$) (in red) and ($WAIT_{variable} > WAIT_{fixed}$) (in green). $P_{FDR} < 0.05$ for multiple comparisons.

| Brain Region | Side | MNI Coordinates | | | Z-score | T value |
|----------------------------|------|-----------------|-----|-----|---------|---------|
| | | x | y | z | | |
| SMA | R | 2 | 2 | 50 | 5.8 | 9.33 |
| Middle frontal cortex | R | 34 | 38 | 34 | 4.69 | 6.35 |
| | L | -32 | 42 | 34 | 4.6 | 6.16 |
| IFC (P.Opercularis; BA 44) | R | 60 | 10 | 14 | 4.57 | 6.08 |
| Precentral gyrus | L | -38 | 4 | 18 | 2.81 | 3.14 |
| Postcentral gyrus | R | 64 | -16 | 38 | 4.35 | 5.63 |
| IPL (BA 3) | L | -56 | -22 | 44 | 4.34 | 5.62 |
| Supramarginal gyrus | R | 52 | -20 | 24 | 4.89 | 6.79 |
| MCC | R | 10 | 12 | 32 | 4.85 | 6.71 |
| | L | -12 | -24 | 42 | 4.75 | 6.47 |
| STC | L | -52 | -24 | 12 | 4.89 | 6.79 |
| Insula Lobe | R | 32 | 22 | 2 | 4.91 | 6.84 |
| Lingual gyrus | L | -22 | -98 | -16 | 2.86 | 3.21 |
| Inferior occipital cortex | L | -28 | -90 | -8 | 3.23 | 3.73 |
| Thalamus | R | 12 | -24 | 10 | 4.14 | 5.22 |
| | L | -8 | -18 | 12 | 3.24 | 3.74 |
| BG (Putamen) | R | 24 | 6 | 6 | 3.66 | 4.39 |
| Brainstem(Midbrain) | R | 8 | -20 | -4 | 2.67 | 3.37 |
| | L | -4 | -22 | -14 | 3.87 | 4.67 |

Table 4.5a. Significant brain areas associated with response withholding in predictable context.

| Brain Region | Side | MNI Coordinates | | | Z-score | T value |
|---------------------------|------|-----------------|-----|-----|---------|---------|
| | | x | y | z | | |
| Hippocampus | R | 28 | -36 | -4 | 4.57 | 6.08 |
| Fusiform gyrus | R | 36 | -40 | -16 | 4 | 4.98 |
| Lingual gyrus | R | 18 | -42 | 2 | 2.89 | 3.25 |
| Inferior occipital cortex | L | -34 | -88 | -10 | 2.7 | 3.41 |
| Cerebellum (Lob. I-V) | R | 12 | -42 | -12 | 4.4 | 5.73 |
| (Lob. VIIa Crus) | L | -10 | -42 | -14 | 3.77 | 4.57 |
| Thalamus (VL nucleus) | R | 16 | -18 | 24 | 4.14 | 5.24 |
| | L | -14 | -22 | 24 | 4.36 | 5.64 |
| BG (Caudate nucleus) | R | 20 | 20 | 16 | 3.04 | 3.46 |
| | L | -18 | -24 | 26 | 4.64 | 6.23 |

Table 4.5b. Significant brain areas associated with response withholding in unpredictable context.

The direct comparison between studies has drawn the distinct and common neural basis across different forms of response inhibition, as summarised in Table 4.6.

| | | Direct comparison between studies | | | |
|--------------|--------------------|------------------------------------|------------------------------------|---|---|
| Brain Region | | WAIT _(fixed) > NO-GO | NO-GO > WAIT _(fixed) | WAIT _(fixed) > WAIT _(variable) | WAIT _(fixed) > WAIT _(variable) |
| Cortical | (Pre)-SMA | ✓ | | ✓ | |
| | DLPFC | ✓ | ✓ | ✓ | |
| | IFC | | | ✓ | |
| | ACC | | ✓ | | |
| | MCC | ✓ | | ✓ | |
| Subcortical | Striatum-Caudate N | ✓ | ✓ | | ✓ |
| | Striatum-Putamen | | | ✓ | |
| | GP | | | | |
| | Thalamus | | | ✓ | ✓ |
| | Midbrain | | | ✓ | |

Table 4.6. The brain regions across different forms of inhibition.

The GO/WAIT paradigm with variable interval timing (Experiment 3) was used to attenuate the prediction effect of the stimulus offset, different degrees of prediction uncertainty were induced by the variable timing of event occurrence. In contrast to predication certainty (Experiment 1) due to fixed timing of stimuli presentation, prediction uncertainty engaged bilateral thalamic nuclei and striatum.

The results here are consistent with previous reports that have shown that similar sub-cortical structures are involved in the uncertainty network (Huettel et al., 2005; Volz et al., 2003, 2004; Critchley et al., 2001; Paulus et al., 2002; Grinband et al., 2006). However, in contrast to previous studies, the results did not show uncertainty-related enhanced activations in the prefrontal regions. This may be attributed to the nature of the task used here, which investigates the response inhibition and not the prediction uncertainty.

4.8 General discussion

4.8.1 Behavioural results

In all studies (Experiment 1, 2 and 3), the behavioural results revealed that reaction times (RT) on switch trials were longer than on repeat trials for the GO task. This 'switch cost' was only of the order of ~ 30 ms because of the increasing preparation interval, which is determined by the inter-stimulus interval (ISI) (2500 ms) in the paradigm (1) and (2) and variable (ISI) (from 1-3 s) in the paradigm (3). This residual switch cost remains, even with long preparation intervals, suggesting that anticipatory preparation is not sufficient to fully overcome the behavioural cost of a switch in the GO task (Karayanidis et al., 2003; Meiran, 1996; Rogers and Monsell, 1995). The result is consistent with the existence of an endogenous 'task-set reconfiguration' (TSR) process, a set of parameters that dynamically configure perceptual and motor task-specific processes. The TSR process might include shifting attention between perceptual and conceptual attributes of the task, retrieving goals and rules, maintaining the state of readiness (activating working memory), adjusting and monitoring different responses, activation of relevant task-elements and inhibition of irrelevant task-elements (Monsell, 2003). This dynamic process must take place

before the task-specific processes can proceed in order to achieve flexible goal-directed behaviour and improve performance. Another possible theory that the switch costs are mainly attributable to conflict arising from working memory due to the recent performance of two different tasks (Allport and Wylie, 2000; Gilbert and Shallice, 2002; Yeung et al., 2003). This interference theory proposes that during the performance of a given task, the new task and its relevant representation must be facilitated and retrieved.

4.8.2 Imaging Results

Functional imaging results across Experiments 1, 2 and 3 revealed that a GO response engages brain regions of the fronto-striatal-thalamic pathway, which is consistent with the so-called 'direct pathway' of the basal ganglia, as shown in Figure 4.20. The motor plan is initiated in the motor cortical regions of the prefrontal cortex (MI, PMd), which send excitatory neural signals to the striatum, then projects to the internal segment of the globus pallidus (GPi), to the thalamus, and then ultimately back to the cortical motor regions; MI and SMA. However, this pathway does not work in isolation from others. Therefore, initial activation of the 'hyperdirect' pathway by exciting the internal segment of the globus pallidus (GPi) and the substantia nigra pars reticulata (SNr) leads to suppress all competing motor programmes.

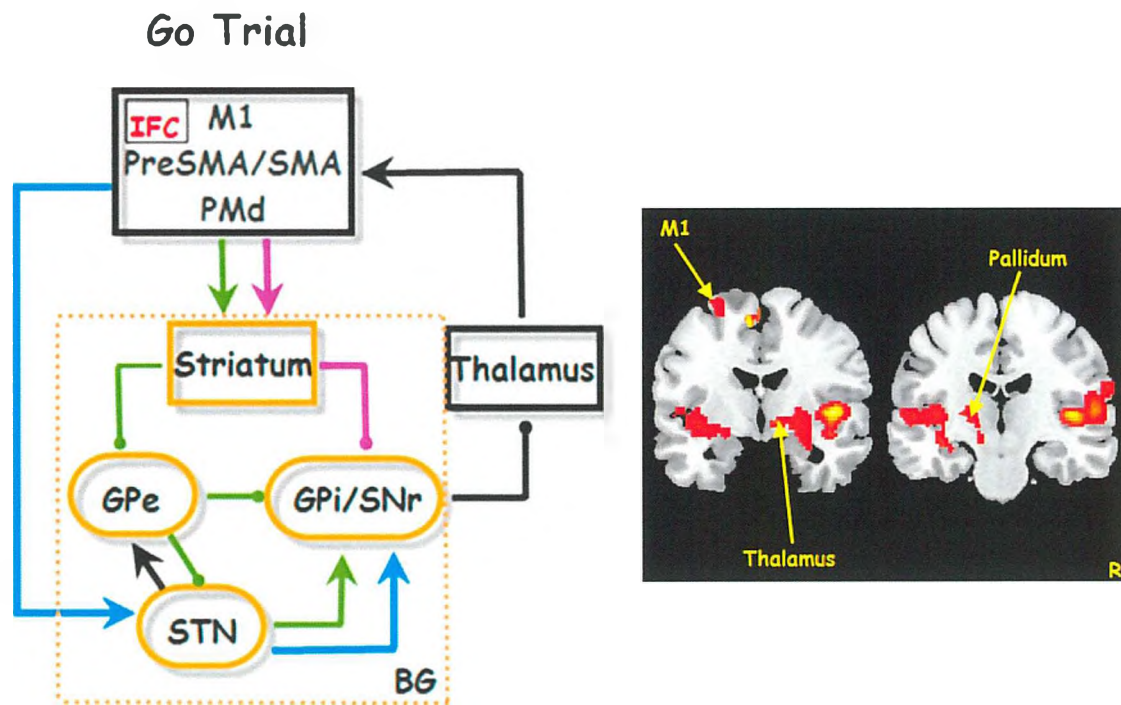


Figure 4.20. GO response engaged the direct pathway of the basal ganglia. Flow chart adapted and modified from (Nambu et al., 2002, Chambers et al., 2009). The imaging slices taken from the present study.

The imaging results across Experiments (1, 2 and 3) demonstrated that during the inhibition of an initiated response the right inferior frontal cortex (IFC) and sub-cortical regions are activated. This suggests that the ‘hyperdirect’ pathway is engaged, which projects fast and directly from the prefrontal cortex- particularly-IFC to the STN, through glutamnergic projections, that activates the GPI/ SNr and suppresses the thalamus, as shown in Figure 4.21 . This works as a ‘brake’, thus if it is triggered in time, then motor execution through the direct pathway can be cancelled.

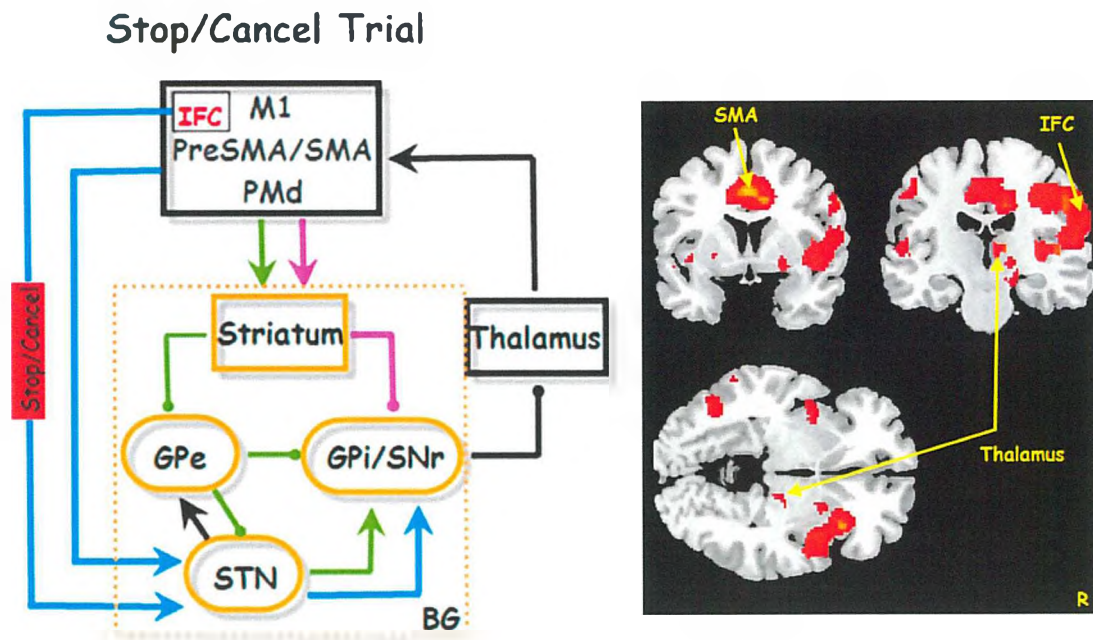


Figure 4.21. NO-GO response engaged the hyperdirect pathway of the basal ganglia. Flow chart was adapted and modified from (Nambu et al., 2002, Chambers et al., 2009). The imaging slices were taken from the present study.

It has been shown that electrical microstimulation in the motor cortex, in monkeys, produces rapid and early excitation in GPi neurons via the STN (the hyperdirect pathway) for (~8 ms), followed by a later phase of inhibition (~21 ms), and then a final period of excitation (~30 ms) (Nambu et al., 2000). This corresponds to hyperdirect pathway excitation of the GPi to inhibit thalamus, followed by inhibition via the direct pathway to activate only the selected motor program and finally excitation through the indirect pathway to complete the response or stop the movement at the appropriate time (Nambu et al., 2000, 2008).

Aron and colleagues (2007b) have shown that white matter tractography using diffusion tensor imaging (DTI) combined with fMRI using stop-signal task, reveals novel three-way connectivity between the IFC, pre-SMA, and STN in the right cerebral cortex. This indicates the importance role of the hyperdirect pathway and these critical nodes in stopping process. Interestingly, the same set of regions was

found significantly active in the current results under similar conditions when the subject needs to cancel or withhold the initiated response. Converging evidence from neuropsychological, neurophysiological, and functional neuroimaging studies, has identified the (rIFC), pre-SMA and thalamus as crucial nodes of the putative network of the response inhibition control (Aron et al., 2007b; Chambers et al., 2009; Chikazoe, 2010; Neubert et al., 2010).

In humans, neuropsychological studies have shown that damage to the rIFC impaired and disrupted the stopping process during Stop-signal task performance (Aron et al., 2003; Rieger et al., 2003). In monkey- lesion studies, damage to a homologue of IFC (the inferior prefrontal convexity in non-primate brain) impaired NO-GO performance (Mishkin, 1964; Iversen and Mishkin 1970). Microstimulation and recording studies in monkeys have indicate the role of the rIFC in successfully inhibiting motor response during performing GO/NO-GO task (Sakagami et al., 2001; Sasaki et al., 1989; Hasegawa et al., 2004).

Neurophysiological studies in humans have reported that macrostimulation of anterior SMA (pre-SMA) induces behavioural motor arrest (Fried et al., 1991; Luders et al., 1988, Swann et al., 2012). Another study has shown that the pre-SMA/SMA has a crucial role in selecting “superordinates sets of action-selection rules” (Rushworth et al., 2004). Taken together, these studies might suggest that the pre-SMA has high-order task-relevant representations rather than having a direct role in behavioural response suppressing.

The pre-SMA was found to be consistently activated in all tasks (Experiment 1, 2 and 3) in which conflict is induced by requiring subjects to represent the rules of what to do, to make selection at the initiation of switch trials, or to inhibit an already initiated response rule in favour of another response. It could play a role such as task-elements monitoring or control recruiting responses (Ridderinkhof et al., 2004; Rushworth et al., 2004).

The present results indicate the striatum as a central region in the neural network that associated with behaviour suppressing. It is striking to observe that the striatum-specifically putamen was significantly active under the situations when the subjects need to suppress their responses in the context of withholding a pre-potent response. In addition to that, the significant correlation analysis between the striatum, as an anatomical-ROI, and the behavioural RT suggest that the striatum plays a key role in response suppressing or might be involved in the preparatory process to withhold/suppress the response. The results here line up with previous mentioned studies that point to the importance of the striatum in motor response suppressing.

Interestingly, the striatum-specifically caudate nucleus was observed significantly active under the conditions in which the subjects need to suppress their responses in the context of cancelling an on-going action or response. A speculation that can be drawn from the current results is that the activation of the DLPFC was also observed under the same situation which raises the possibility that fronto-striatal indirect pathway (DLPFC-head of caudate nucleus) is engaged to selectively cancel the initiated movement. This top-down model can be engaged in selective and proactive inhibitory mechanism.

The results of the correlation analysis between predefined ROIs, including pre-SMA, IFC, thalamus, and striatum, and the behavioural measure (across all experiments in this chapter) further supported the notion that these are key regions in mediating behavioural response inhibition. The functional results combined with the correlations that were between the BOLD fMRI signals and the behavioural measure argue against the conventional direct inhibition idea that the prefrontal cortical regions (i.e, IFC, pre-SMA) send inhibitory signals. Instead, the PFC can be the source of facilitatory signals that bias competition within action selection mechanisms in brain areas linked to motor execution. The conjunction analysis between Experiments (1) and (2) revealed that rIFC is a critical region that send excitatory signals to the STN, which excites globus pallidus leading to suppress the basal-thalamo-cortical output, thus blocking the initiated GO response from being executed (Mink et al., 1996). The IFC and STN could be critical regions in either an indirect or hyperdirect pathways to control the GO and NOGO motor programs.

In conclusion, as previously mentioned, many functional imaging studies across different types of inhibition tasks (including the experiments in this chapter) point to a neural network that is critical in implementing motor response inhibition, including rIFC, pre-SMA and STN (Aron, 2011; Chambers et al., 2009; Chikazoe, 2010; Levy and Wagner, 2011). Considering these results together, it might indicate that there is top-down inhibitory control that is mediated through bypassing pathway involving the rIFC, pre-SMA and STN.

In the current results, the thalamus was significantly active under the situations when the subjects need to respond with restraint or withhold the response. Although

the thalamic coordinates found in the present experiments in this thesis come consistent with previous fMRI studies (i.e., Aron et al., 2007b), it was difficult to identify these nuclei (in definite) as the neuroimaging data underwent normalization and smoothing processes. Moreover, some midbrain regions were observed in the current results couldn't be identified because of the lack of the midbrain atlas for neuroimaging data. Further research into the putative network of response inhibition can provide bright insights into the connectivity and the effects-timing between the critical regions of this network.

Chapter 5

5.1 Introduction

Response inhibition refers to the suppression of irrelevant or inappropriate responses. It has a critical role in executive function, and has been linked to a wide range of neurological and neuropsychiatric disorders, such as attention deficit hyperactivity disorder (ADHD) (Aron and Poldrack, 2005; Nigg, 2005; Ridderinkhof et al., 2005), Tourette syndrome (TS) (Albin and Mink, 2006; Bohlhalter et al., 2006), Parkinson's disease (PD) (Gauggel et al., 2004; Wylie et al., 2009), and obsessive-compulsive disorder (OCD) (Penadès et al., 2006). In this work, Tourette syndrome (TS) was selected as an example of a clinical condition that is characterized by inhibitory deficits associated with basal ganglia dysfunction. This chapter aims to investigate the role of the basal ganglia in TS using the (GO/WAIT) cognitive inhibition paradigm described in Chapter 4. The following sections introduce Tourette syndrome, the proposed neural basis of this disorder, and the structural and functional neuroimaging studies performed to date related to this disorder.

5.2 Tourette syndrome (TS)

In the 1885, Georges Gilles de la Tourette was the first who clearly described the neurological condition of Tourettes and published his remarkable article in *Archives de Neurologie* (Tourette 1885). In this article, Tourette reported a condition (based on nine patients) that consistently exhibited various characteristics, including heritability, onset in childhood, chronic motor, stereotyped and involuntary tics, and vocal symptoms. This disorder now bears his name Tourette syndrome (TS).

Tourette syndrome (TS) is a hereditary, chronic, neurodevelopmental disorder characterized by the expression of involuntary repetitive *motor* tics, such as sudden facial grimaces or head jerks, obscene gestures or clapping and *phonic* tics, such as grunting, throat clearing or sniffing, or repeating words (e.g. echolalia, palilalia, coprolalia). Tics can be simple or complex in nature, and vary in number, frequency, and severity. The diagnostic criteria for TS requires the presence of involuntary tics defined as rapid, sudden, multiple, non-rhythmic, stereotyped motor movements and vocal tics (APA, 1994). This syndrome is often accompanied by comorbid syndromes or disorders such as obsessive compulsive disorder (OCD) and/or attention-deficit hyperactivity disorder (ADHD) (Cavanna et al., 2009).

5.3 The neural basis of TS

Although the neural basis of TS is unclear, there is an increasing body of evidence suggesting that the fronto-striato-thalamic pathway that connects specific regions of the frontal cortex to sub-cortical structures is dysfunction in this syndrome (Singer and Harris, 2003, 2006; Leckman et al., 2010; Mazzone et al., 2010). These pathways or circuits are involved not only in monitoring motor, but also cognitive processes, including voluntary motor control, action selection, facilitation of the selected movements, and inhibition of inappropriate movements. In the classical model of a movement disorder, such as PD, Huntington's disease and TS, it was proposed that the imbalance between the direct and the indirect pathways within the basal ganglia nuclei leads to hyperkinetic symptoms (Albin et al., 1989). However, this model failed to address the symptoms of TS, for example motor tics.

Another model has proposed that the basal ganglia nuclei have a key role in facilitation of selected movement and suppression of competing programs (Mink, 2003). In this model, the alteration of the local excitatory circuits in the striatum structure leads to a disinhibition of the internal segment of the globus pallidus (GPi) neurons which causes a disinhibition of cortical projections leading to symptoms, such as motor or vocal tics (Mink, 2001; Albin and Mink, 2006). Finally, it might also be that the dopaminergic nigro-striatal pathway, which arises from the SNr structure, has a role in the pathophysiology of this disorder (Krack et al., 2010).

5.4 Morphometric neuroimaging of Tourette syndrome

Several different approaches have been used to identify the neuroanatomical changes in patients with TS, including post-mortem examinations (Balthasar, 1957; Haber, 1986; Saint-Cyr et al., 1995; Yoon et al., 2007), structural MRI and DTI (Hyde et al., 1995; Bloch et al., 2005; Peterson et al., 1993, 2003; Lee et al., 2006; Singer et al., 1993; Moriarty et al., 1997, Neuner et al., 2011, Jackson et al., 2011) and functional neuroimaging studies (Baxter et al., 1990; Stoetter et al., 1992; Jeffries et al., 2002; Riddle et al., 1992; Diler et al., 2002; Klieger et al., 1997; Wolf et al., 1996; Braun et al., 1995; Eidelberg et al., 1997; Moriarty et al., 1995; Peterson et al., 1998; Kawohl et al., 2009; Marsh et al., 2007; Baym et al., 2008).

Morphometric and volumetric MRI studies have identified distinct features of neuroanatomical structures of TS, including altered sub-cortical structural volumes and asymmetry, particularly a decrease in caudate nucleus volume and an increase in the volume of the hippocampus, amygdala and thalamus (Hyde et al., 1995; Bloch et al., 2005; Peterson et al., 2003; Lee et al., 2006). In contrast, Roessner and others

(2011), using voxel-based morphometry technique (VBM), did not find any changes in the volume of the caudate nucleus. However, they did show an increased volume of the putamen nucleus bilaterally in boys with TS. Moreover, Singer and others (1993) showed significant differences in the symmetry (reduction in volume) of the striatum particularly the right putamen in TS patients compared to healthy control subjects.

Some studies have investigated the interhemispheric structural volume symmetries in individuals with TS. The corpus callosum was observed to be abnormal in individuals with TS, predominantly boys (Baumgardner et al., 1996; Peterson et al., 1994; Moriarty et al., 1997). Baumgardner and colleagues (1996) have studied children with TS and comorbid ADHD, symptom-dependent changes were involved in the corpus callosum, particularly the rostral region. It was found that the diagnosis of TS was associated with a significant increase in size and ADHD with a significant reduction in size of the rostral region of the corpus callosum. Other studies have shown that there is no difference between girls with TS and matched controls group in terms of the volume of the basal ganglia and asymmetry in the corpus callosum (Mostofsky et al., 1999; Zimmerman et al., 2000).

Many studies have investigated white-matter volume and the importance of cortical inputs to basal ganglia structures, by comparing the volume of various cortical brain regions in TS to those in controls (Felling et al., 2011; McNaught and Mink, 2011). One study showed larger dorsal prefrontal cortex (DLPFC) and parieto-occipital regions in TS (Peterson et al., 2001). Another study showed differences in the percentage of white matter in the cerebral cortex, observing that the right frontal

cortex has a larger percentage of white matter in individuals with TS (Fredericksen et al., 2002).

Other studies have revealed thinning of motor and sensory cortical regions in patients with TS (Sowell et al., 2008). Kates and colleagues (2002) showed volumetric decreases of the white matter in the left frontal cortex. Further studies have found a correlation between the location of cortical thinning and clinical symptoms in evaluating subgroups of TS patients, such as group with simple tics, complex tics, and those accompanied with OCD (Worbe et al., 2010). Jackson and colleagues (2011) have demonstrated using structural diffusion weighted imaging (DWI), diffuse abnormalities in the white matter (WM) microstructure of the TS that significantly predict tic severity in TS. Another group, using the diffusion tensor imaging (DTI), has demonstrated microstructural changes in the striatum-particularly the putamen nucleus in TS compared to healthy controls (Makki et al., 2008). Neuner and colleagues (2011), using DTI, have also shown a correlation between BG diffusivity and tic severity in TS patients.

5.5 Functional Neurimaging studies of Tourette syndrome

Functional imaging studies have also suggested that the fronto-striato-thalamic pathways are involved in the neuropathogenesis and suppression of tics in TS (Peterson et al., 1998; Stern et al., 2000; Gates et al., 2004; Kawohl et al., 2009; Serrien et al., 2005; Baym et al., 2008). Functional imaging studies of patients with TS during a finger tapping task showed increased activation in the sensorimotor cortex and supplementary motor areas (Biswal et al., 1998; Fattapposta et al., 2005).

Another study showed reduced activation of the secondary motor cortex in TS during a manipulative task (Serrien et al., 2002). In a GO/NO-GO response inhibition task it was found that TS subjects have an overactive frontomesial network including mesial frontal cortex, prefrontal and sensorimotor regions (Serrien et al., 2005). Marsh (2007) found that activation of bilateral fronto-striatal regions during the performance of a Stroop task increased with advancing age in subjects with TS. This might reflect that there is compensatory functional neuronal reorganization in TS. Similarly, an age-related immature pattern of functional connectivity was identified in the fronto-parietal and fronto-striatal networks in TS, supporting the hypothesis that TS is a developmental disorder.

Recent studies have found that tic severity is positively associated with activation of the substantia nigra and ventral tegmentum, which may suggest the involvement of the dopaminergic nigro-striatal pathway. It was also found that higher tic severity correlated with slower cognitive task performance in a 'pure' TS group (without comorbid OCD or ADHD symptoms) (Baym et al., 2008). Similarly, it was found that tic severity was significantly positively correlated with behavioral reaction time (RT) switch cost in a 'pure' TS group (without comorbid disorders) during the performance of manual task-switching (Jackson et al., 2011).

Many researches have hypothesized that the dysfunction of fronto-striato-thalamic circuits in TS leads to hyperexcitability of cortical motor regions which may be caused by dysfunctional intracortical inhibitory mechanisms (Ziemann et al., 1997; Moll, et al., 2001; Gilbert, et al., 2005; Orth, et al., 2008; Orth and Rothwell 2009; Baumer, et al., 2010; Heise, et al., 2010). Evidence from transcranial magnetic

resonance (TMS), comparing individuals with TS to healthy controls, has supported this hypothesis by examining the corticospinal excitability, short-interval intracortical inhibition and intracortical facilitation. It has been found that the duration of the cortical silent period (CSP) induced by TMS to motor cortex, and the magnitude of the short-interval intracortical inhibition (SICI) that is observed, are significantly reduced in individuals with TS compared to control subjects. Moreover, the degree of reduction in SICI observed in individuals with TS has been shown to correlate with ADHD scores in individuals with TS (Gilbert, et al., 2004, 2005) and with clinical measures of tic severity (Gilbert, et al., 2004, Orth et al., 2008).

Recent studies have shown that individuals with TS clearly exhibit reduced motor evoked potentials (MEPs) amplitudes and significant reduced short-interval intracortical inhibition (SICI) during the early phase of movement preparation (Heise et al., 2010, Jackson et al., 2012). This is consistent with recent functional neuroimaging findings in (Jackson et al. 2011), in which the BOLD signal in the motor cortex of individuals with TS was significantly decreased compared to control subjects. Importantly, all together, these findings support the view that the control over motor tics in individuals with TS might come through the active inhibition of hyperexcitable motor cortex (Muller et al., 2006, Jackson et al., 2007, Jackson et al., 2011).

Considerable evidence from the above mentioned studies suggests the involvement of fronto-striato-thalamic circuits in the pathophysiology of TS (Peterson et al., 1998; Stern et al., 2000; Gates et al., 2004; Kawohl et al., 2009; Serrien et al., 2005; Baym et al., 2008). However, many of these reported results are not in

concordance across studies. There are a number of limitations within studies of TS that affect the conclusions that can be drawn from these studies, including the small number of TS subjects involved, and the variety of confounding factors such as age, sex, and hand dominance. Moreover, factors that are related to the current status, such as the severity of Tourette syndrome symptom and medication used, can affect the findings of the studies. Finally, the presence and control of comorbidity syndromes such as ADHD and OCD in some studies can add to variability and inter-study differences. For example, it was found that the volumetric asymmetry in the globus pallidus (GP) was attributable to the effects of TS subjects with comorbid ADHD compared to subjects with only TS (Singer et al., 1993). Furthermore, neuroimaging studies of Tourette syndrome have used different behavioural paradigms with different behavioural and cognitive demands, therefore making it difficult to compare between these studies.

Tourette syndrome has been associated with a deficit in cognitive control such as the ability to suppress an inappropriate movement that might interfere with the planned meaningful goal-directed behaviour (Bornstein and Baker, 1991; Johannes et al., 2001; Watkins et al., 2005). Several studies of inhibitory functioning in TS have included the assessment of patients' ability to suppress a motor response. Channon (2006) reported impairments in motor response inhibition during the performance of a flanker task. Similarly another study, using the stop signal task, has reported a deficit in stopping a pre-potent response (Goudriaan et al., 2006). However, other studies have reported that patients with TS perform normally on the GO/NO-GO task (Roessner et al., 2008; Watkins et al., 2005). Moreover, some studies have

investigated verbal response inhibition using the Stroop task and found no evidence of impairment (Channon et al., 1992; Goudriaan et al., 2006).

In the current study patients with ‘pure’ TS (only Tourette syndrome without comorbid disorders such as ADHD and/or OCD), and an age and gender-matched control group are studied. This study aims to investigate the role of the sub-cortical structures in motor response inhibition in individuals with TS. Based on the previous findings, the main hypothesis of this study is that the fronto-striatal pathway is affected in individuals with TS, and so the TS group may recruit different brain regions for response inhibition compared to the healthy control group. To test this hypothesis, event-related fMRI was used to identify the neural network involved in response inhibition using a (GO/WAIT) cognitive task, as described in chapter 4.

5.6 Experiment 4

5.6.1 Materials and Methods

5.6.1.1 Inclusion and exclusion criteria

Children aged between 13–18 yrs with Tourette syndrome (TS) and healthy age and gender-matched controls were recruited for participation in this study. Children with serious neurological or psychiatric conditions, other than TS-without comorbid attention deficits hyperactivity disorder (ADHD) or obsessive compulsive disorder (OCD), were not included in the study. The healthy control group was also screened for ADHD using the Strengths and Difficulties Questionnaire (SDQ) (Goodman 2001; Muris et al., 2003). Exclusion criteria were set *a priori*: participants were excluded from analysis if scans had poor quality due to excessive head movement (translational displacement > 3 mm in any plane).

5.6.1.2 Participants

Eight patients with Tourette syndrome took part in the study. Of the eight TS subjects recruited, three TS participants were excluded, two due to excessive head motion during scanning (more than 3 mm, as defined above) and one TS subject withdrew from the MRI session. The resulting sample size analysed was five TS children (2 females; mean age, 15.7 ± 1.9 SD years). The healthy control subject (CS) group comprised eight age-matched controls (2 females; mean age, 16 ± 1.6 SD years) (Table 5.1).

| | Tourette Syndrome Subjects (TS) | Healthy Control Subjects (CS) |
|------------------------------|--|--|
| Number of subjects | 5 | 8 |
| Age (mean, SD) | 15.7 (1.9) | 16 (1.6) |
| Sex (percentage boys) | 60 | 75 |
| IQ (mean, SD) | 96 (24.55) | 123 (11.33) |

Abbreviations: SD, standard deviation; IQ, intelligence quotient; TS, Tourette syndrome; CS, Control subjects.

Table 5.1. Comparison of characteristics of Tourette syndrome (TS) and Healthy Control subject groups who are included in fMRI data analysis.

5.6.1.3 Recruitment and screening

Patients were recruited through the Tourette syndrome clinic in the Child and Adolescent Psychiatry Department at the Queens Medical Centre, Nottingham, UK. All participants provided informed consent according to procedures and ethics approved by the North Nottingham Healthcare Trust, Nottingham, UK. The IQ of all participants was obtained using the Wechsler Abbreviated Scale of Intelligence (WASI) vocabulary and matrix reasoning subscales (Hays et al. 2002) (Table 5.1). The control group showed a slightly higher IQ than the TS group (123 ± 11 for controls and 96 ± 25 for TS subjects). TS subjects were assessed for the current tic

severity on the day of testing using the Yale Global Tics Severity Scale which comprises motor scale (Leckman et al. 1989) (Table 5.2).

| Subject | Sex | Age | YGTSS | YMS | Phonic | Medication | Tics - description |
|---------|-----|-----|-------|-----|--------|-----------------------|--|
| 1 | M | 18 | 18 | 11 | 7 | Clonidine 75mcgs ,tds | coughing, grunting , eye blinking and head jerks |
| 2 | F | 17 | 10 | 5 | 0 | Clonidine 75mcgs ,tds | eye blinking and nose movements |
| 3 | M | 18 | 29 | 8 | 16 | Clonidine 50mcgs ,tds | facial grimace, grunting, coprolalia and repeating words |
| 4 | M | 15 | 38 | 8 | 10 | Clonidine 50mcgs ,tds | nose movements, arm gestures and throat clearing |
| 5 | M | 15 | 11 | 6 | 0 | None | eye blinking, eye movements, leg movements |

(Age, in years at the time of fMRI scanning). YGTSS, Yale Global Tic Severity Scale; YMS, Yale Motor score; Phonic, Phonic score;

Table 5.2. Clinical characteristics of the TS subjects included in the fMRI data analysis.

5.6.1.4 Experimental Task and Procedure

This task followed the same general procedure as that described for the (GO versus WAIT) paradigm in Chapter 4. The task comprised an arrow-shaped stimulus that was displayed on the centre of the screen in one of two colours (green or red). Participants were instructed to respond to each arrow by pressing a right or left button-box, depending on the arrow's direction. If the arrow was green (**GO**) participants were instructed to respond as quickly as possible. If the arrow was red (**WAIT**) participants were instructed to respond at the stimulus offset. In this paradigm, a subject switches from immediately responding at the onset of the stimulus (GO task-green arrows) to responding at stimulus offset (WAIT task-red arrows). Therefore, a mixture of trials included Switch and Repeat trial types for each of the GO and WAIT tasks were created.

5.6.1.4 MRI data acquisition

fMRI data were acquired using the same MR scanning parameters as described in Chapters 3 and 4. To summarize, the fMRI acquisition used a double echo acquisition with echo times (TEs) of 10.3 ms and 29.3 ms, and a repetition time (TR) of 3s. MR data was acquired with a 2mm³ isotropic spatial resolution with a matrix size of 192 × 160 × 164 mm.

5.6.2 Data Analysis

5.6.2.1 Behavioural data analysis

The first two trials of each run and trials associated with an incorrect response were excluded from behavioural and fMRI analyses. Data were analysed at both; within-group and between-group levels. Mean reaction times for correct responses were entered in a two-way repeated measure ANOVA with the two factors “task” and “trial” for each group, Tourette and controls (within-group effect). A 2 x 2 × 2 mixed ANOVA was performed to examine the within-subject effects of task type (GO, WAIT) and trial type (Switch and Repeat) upon performance of each group (Controls vs. Tourette syndrome) on the GO/WAIT task.

5.6.2.2 fMRI data analysis-pre-processing

fMRI data were pre-processed as described previously in Chapter 4, see Section 4.4.2.2.

5.6.2.3 *fMRI within-group analysis*

fMRI data were initially analysed at the single subject level, and then second level analyses were performed for within-group and between-group effects. The fMRI data for each subject in each group was analysed on a voxel-by-voxel basis using the principles of the general linear model (Friston et al., 1995), as implemented in SPM5. Prior to model estimation, all images were globally scaled and the time series were filtered using a high pass filter to remove low frequency signals (below 165 s). fMRI time series were analysed by fitting a convolved canonical hemodynamic response function (HRF) to the onset of the stimulus for GO switch, GO repeat, WAIT switch and WAIT repeat trials. The six motion parameters (indicating amount of translation in and rotation about the x, y and z dimensions for each volume) were included as covariates of no interest. The incorrect trials were also included in the design matrix as a covariate of no interest. The following were then assessed (a) the main effect of each task type (i) GO and (ii) WAIT, and (b) the difference contrast of WAIT > GO (for both trial types combined (switch and repeat)), this differential contrast was chosen to study the mechanism of inhibition.

A second level analysis was then performed. Firstly, a fixed effects analysis (FFX) was conducted, this type of group analysis being chosen based on several studies which have hypothesized that the neural activity involved in response inhibition is different in individuals with TS and healthy control subjects (i.e., Jackson et al., 2011). Fixed effects (FFX) analysis combines the data from multiple subjects into a single GLM design. (a) The main effects of the task, WAIT and GO, and (b) the differential contrast (WAIT>GO) were assessed for both the TS and CS. Although

FFX approach leads to high statistical power, the results are valid only for the examined group of subjects (TS or CS) and cannot be generalized.

Despite the fact the number of subjects that included within both TS and CS in this experiment is small, a significant and strong BOLD response was nevertheless predicted given that ultra-high MR field strength (7 T) is used in this study. Therefore, a RFX analysis was also performed, which takes into account both intra-subject and inter-subject variability, making it possible to draw inferences about the population from which the subjects are drawn (Beckmann et al., 2001). Contrast maps from the first level were used to compute the identical contrasts as for the FFX analysis: (a) main effects of the task, WAIT and GO, and (b) the differential contrast (WAIT > GO) for both TS and CS. Group maps were threshold with a height threshold of $T = 3.17$ and extent threshold of 10 voxels, with a threshold of $P_{\text{uncorrected}} < 0.001$ for multiple comparisons.

5.6.2.4 Region of interest (ROI) and correlation analysis within groups

The ROI procedure was performed as described in Chapter 4. Functionally-defined ROIs, by growing a sphere (10 mm radius) centred at the peak of the activation in each cluster, were derived from the FFX ((WAIT + GO) > baseline) contrast for the TS and CS subjects combined. This contrast was chosen as it would identify areas ROIs active in the current cognitive task independent of subject group. ROIs assessed included: left pre-supplementary areas (pre-SMA; -10, 24, 58), bilateral middle frontal cortex (MFC; 42/-44, 14/32, 42/28), right anterior cingulate cortex (ACC; 6, 38, 0; BA 24), right superior frontal cortex (SFC; 22, 34, 46) and left anteromedial prefrontal cortex (AMPFC; -6, 38, 52). These ROIs were then used to

interrogate the BOLD parameter estimates for the (WAIT > GO) condition and correlate these measures with the following:

- (i) *Correlation between BOLD signal and behavioural RTs in Control Subjects and Tourettes Subjects-* The correlation between the BOLD response (determined by BOLD parameter estimates) and behavioural RTs for each group (TS and CS) was estimated. The behavioural RT used in this correlation was the subject's median reaction time for the GO switch task.
- (ii) *Correlation between BOLD signal and clinical scores for Tourettes Subjects-* The correlation between the BOLD response (parameter estimates) and clinical scores in the TS subjects was estimated. The correlation to both the individual Yale Global Tic Severity Scale (YGTSS) and Yale Motor Scale (YMS) were assessed separately.

5.6.2.5 fMRI between-group analysis

Finally to compare subject groups, the comparison of (WAIT > GO) for TS and CS subjects was assessed using a FFX and RFX approach [i.e., $(\text{WAIT} > \text{GO})_{\text{TS}} > (\text{WAIT} > \text{GO})_{\text{CS}}$ and the opposite contrast of $(\text{WAIT} > \text{GO})_{\text{CS}} > (\text{WAIT} > \text{GO})_{\text{TS}}$], and maps of these conditions formed at ($P_{\text{uncorrected}} < 0.001$) for multiple comparison.

5.6.3 Results

5.6.3.1 Behavioural Results

Figure 5.1 shows the median reaction times to the task for the TS and CS groups. Within-group analyses of the reaction time data for simple main effects of task, trial and the interaction revealed a significant main effect of task [$F(1, 4) = 8.1, p$

< 0.05] in the TS subjects, whilst there was no significant main effect of task [$F(1, 7) = 3.8, p = 0.107$] within the control subjects (CS). In contrast, a significant main effect of trial [$F(1, 7) = 7.96, p < 0.05$] was found within the control subjects while there was no significant main effect of trial [$F(1, 4) = 1.62, p = 0.244$] within TS subjects.

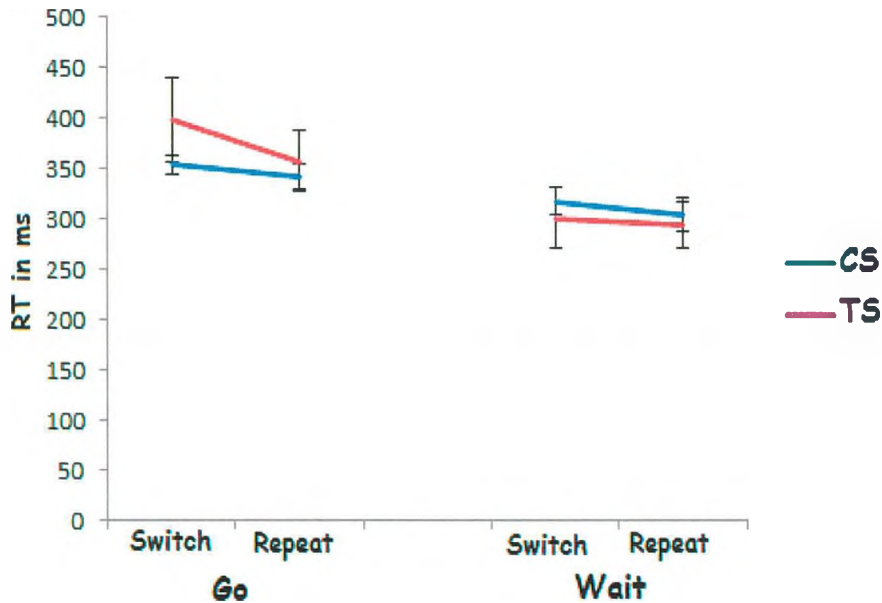


Figure 5.1. Median reaction times (RT) for all conditions; WAIT– Switch, WAIT–Repeat, GO–Switch and GO–Repeat for the TS and CS.

Importantly, a significant ‘switch cost’ for the GO–Switch (399 ± 103 ms, $M \pm SD$) versus GO–Repeat (358 ± 75 ms, $M \pm SD$) conditions was observed within TS ($t=2.8, p < 0.05$), however, there was no significant ‘switch cost’ for GO–Switch (354 ± 25 ms, $M \pm SD$) versus GO–Repeat (342 ± 35 ms, $M \pm SD$) conditions within CS ($t=1.37, p = 0.2$). Finally, no significant interaction between task and trial for both groups TS [$F(1, 4) = 0.012, p = 0.914$] and CS [$F(1, 7) = 3.67, p = 0.11$] was found. These results suggest that there was a ‘switch cost’ within GO trials in TS subjects but

no significant 'switch cost' in the CS. Moreover, the results showed no 'switch cost' within WAIT trials for both groups.

Behavioural data were analysed using a 2 X 2 X 2 mixed ANOVA with the between-subject factor of group (TS and controls) and the within-subject factors of task type (WAIT and GO) and trial type (Switch and Repeat). Significant main effects of task [$F=9.4$, $p < 0.01$] and trial [$F=6.3$, $p < 0.05$] were observed. By contrast, no significant main effect of group [$F=0.9$, $p < 0.311$] was found. There was no significant interaction effect between the (i) task and trial [$F=0.8$, $p < 0.389$], (ii) task and groups [$F=0.52$, $p < 0.485$], and (iii) trial and groups [$F=1.31$, $p < 0.275$]. Finally, no significant interaction effect between task and trial and groups [$F=1.13$, $p < 0.307$] were found.

For the control subjects, the average error rate in WAIT events (early response) across subjects was (5.5 ± 2 %; $M \pm SD$), with a total of 44 errors across all 8 subjects. No significant difference was found in the error rate for the Tourettes subjects, with an average error rate in WAIT events across subjects being (6.5 ± 1 %; $M \pm SD$), with a total of 31 errors across the 5 subjects where fMRI data were analysed.

5.6.3.2 fMRI results

Control Subject (CS) Group (Fixed Effects Analysis)

a) Main effect of task; the GO and WAIT processes

In the CS, the (GO > baseline) contrast, for both the Repeat and Switch trials, revealed motor preparation and execution processes, with within-group analysis revealing increased activation in multiple regions including bilateral prefrontal cortex, inferior frontal cortex (IFC), primary motor cortex (M1), bilateral supplementary motor area (SMA), posterior parietal cortex, insula, anterior and middle cingulate cortex, striatum, thalamus and cerebellum. The WAIT condition involved motor selection and preparation processes though no motor execution process was engaged, as the modeled period of BOLD signal was within 500 ms and did not involve the button press. For the (WAIT > baseline) contrast, for both the Repeat and Switch trials, group analysis revealed increased activation in multiple brain regions including bilateral motor cortex, IFC, left supplementary motor area (SMA), inferior parietal lobule, anterior and middle cingulate cortex, insula cortex and cerebellum. In addition, significant activation extended to sub-cortical structures including left striatum, bilateral pallidum, and thalamus.

b) Response withholding compared to motor-execution; (WAIT > GO)

In the CS group, neural activity during response withholding (inhibition) compared to the immediate motor execution process, the (WAIT > GO) contrast, yielded significant activation in bilateral supplementary motor area (SMA), left dorsolateral prefrontal cortex (DLPFC), inferior frontal cortex (IFC), precentral gyrus, bilateral postcentral gyrus (somatosensory cortex), bilateral inferior parietal cortex,

anterior cingulate cortex (ACC), middle temporal cortex, insula cortex and cerebellum, as shown in Figure 5.2. Table 5.3 provides a complete summary of these brain areas.

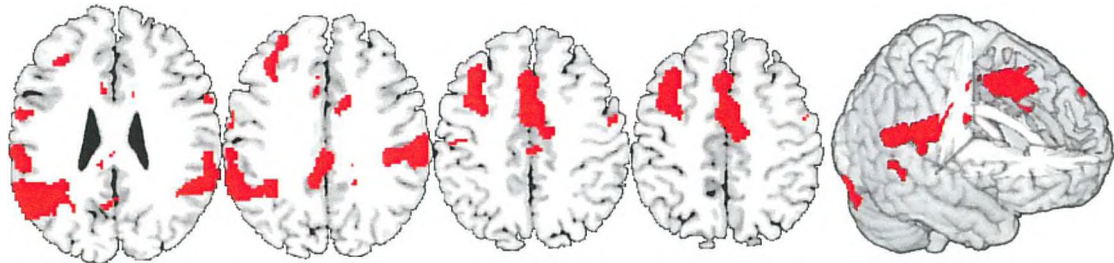


Figure 5.2. FFX analysis of brain regions associated with response withholding, the (WAIT>GO) contrast, in the CS group. ($P_{uncorrected} < 0.001$ for multiple comparisons).

| Brain Region | Side | MNI Coordinates | | | Z-score | T value |
|------------------------------|------|-----------------|-----|-----|---------|---------|
| | | x | y | Z | | |
| Pre-SMA | L | 0 | 0 | 52 | 4.94 | 4.96 |
| Middle frontal cortex | L | -36 | 18 | 50 | 4.11 | 4.12 |
| IFC (P.Opercularis; BA 44) | L | -50 | 12 | 12 | 3.89 | 3.9 |
| Precentral gyrus | L | 60 | 8 | 26 | 3.47 | 3.48 |
| Postcentral gyrus (BA 1,2,3) | R | 40 | -28 | 38 | 6.11 | 6.14 |
| IPL (Supramarginal gyrus) | L | -62 | -4 | 32 | 5.2 | 5.2 |
| | R | 60 | -28 | 36 | 5.14 | 5.15 |
| IPL (Angular gyrus) | L | -56 | -34 | 26 | 5.9 | 5.92 |
| | R | 46 | -52 | 28 | 4.67 | 4.68 |
| Corpus Callosum | L | -56 | -62 | 28 | 6.22 | 6.25 |
| | R | 0 | -22 | 22 | 3.24 | 3.24 |
| MCC | R | 12 | 6 | 36 | 3.45 | 3.45 |
| PCC | L | -8 | 0 | 40 | 3.6 | 3.61 |
| | L | -8 | -34 | 30 | 3.4 | 3.41 |
| Insula Lobe | L | -32 | 22 | 2 | 5.16 | 5.17 |
| Cerebellum (Lob. VIIa Crus) | R | 32 | -84 | -34 | 5.46 | 5.48 |
| | L | -28 | -90 | -30 | 7.31 | 7.35 |
| | R | 22 | 6 | -6 | 2.9 | 3.7 |

Table 5.3. Significant brain areas associated with response withholding, the (WAIT > GO) contrast, in the CS group.

Tourettes Subject Group (Fixed Effects Analysis)

a) Main effect of task; the GO and WAIT processes

In the TS group, the (GO>baseline) contrast, the TS FFX subject analysis showed a similar pattern of activation to that observed for the CS group, although less activation was observed in the striatum and thalamus. Again the (WAIT > baseline) contrast for the TS group showed a similar pattern of activation as observed in the CS, except strong activation in bilateral DLPFC and less activation in the pallidum sub-cortical structure.

b) Response withholding compared to motor-execution; (WAIT > GO)

For the (WAIT > GO) contrast, in contrast to the CS group, the TS group showed significant activation in bilateral DLPFC, bilateral somatosensory extending to the inferior parietal cortex, insula and the cerebellum, as shown in Figure 5.3 and summarized in Table 5.4.

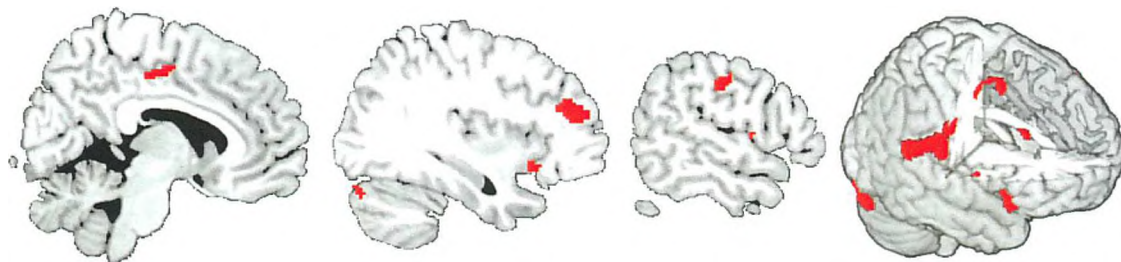


Figure 5.3. Brain regions associated with response withholding activity, the (WAIT > GO) contrast, in the TS group. ($P_{uncorrected} < 0.001$ for multiple comparisons).

| Brain Region | Side | MNI Coordinates | | | Z-score | T value |
|-----------------------------|------|-----------------|-----|-----|---------|---------|
| | | x | y | z | | |
| Middle frontal cortex | R | 32 | 44 | 18 | 4.16 | 4.17 |
| | L | -30 | 26 | 30 | 3.26 | 3.26 |
| Postcentral gyrus (BA,1,3) | R | 56 | -16 | 38 | 3.52 | 3.52 |
| | L | -60 | -4 | 18 | 3.9 | 3.93 |
| IPL (Supramarginal gyrus) | R | 68 | -18 | 24 | 4.01 | 4.02 |
| MCC | R | 10 | -18 | 46 | 3.59 | 3.59 |
| Fusiform gyrus | R | 28 | -90 | -26 | 4.89 | 4.9 |
| Insula Lobe | R | 42 | 10 | -2 | 3.32 | 3.32 |
| | L | -44 | -8 | 18 | 3.4 | 3.41 |
| Cerebellum (Lob. VIIa Crus) | R | 42 | -80 | -24 | 3.53 | 3.53 |
| | L | -26 | -90 | -32 | 3.3 | 3.3 |

Table 5.4. Significant brain areas associated with response withholding, the (WAIT > GO) contrast, in the TS group.

5.6.3.3 ROI and correlation analysis

(i) Correlation of BOLD data with Reaction Time

Figures (5.4 a-c) illustrate the correlation between the BOLD response (parameter estimates for the (WAIT > GO) contrast) and the GO-Switch RT in *a priori* ROIs for the CS and TS subjects. The BOLD response was found to be significantly positively linearly correlated with RT measures in the left pre-SMA and right ACC in the CS.

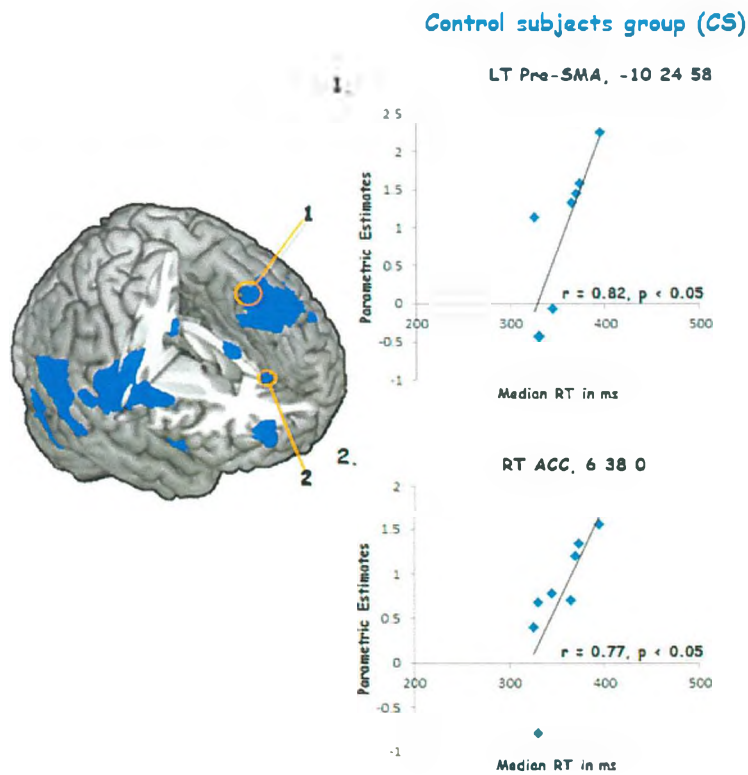


Figure 5.4a. Scatter plots to illustrate the correlation between the BOLD (WAIT > GO) parametric estimates and the median of the GO-Switch RT measures for subjects in the CS group in *a priori* ROIs.

Control subjects group (CS)

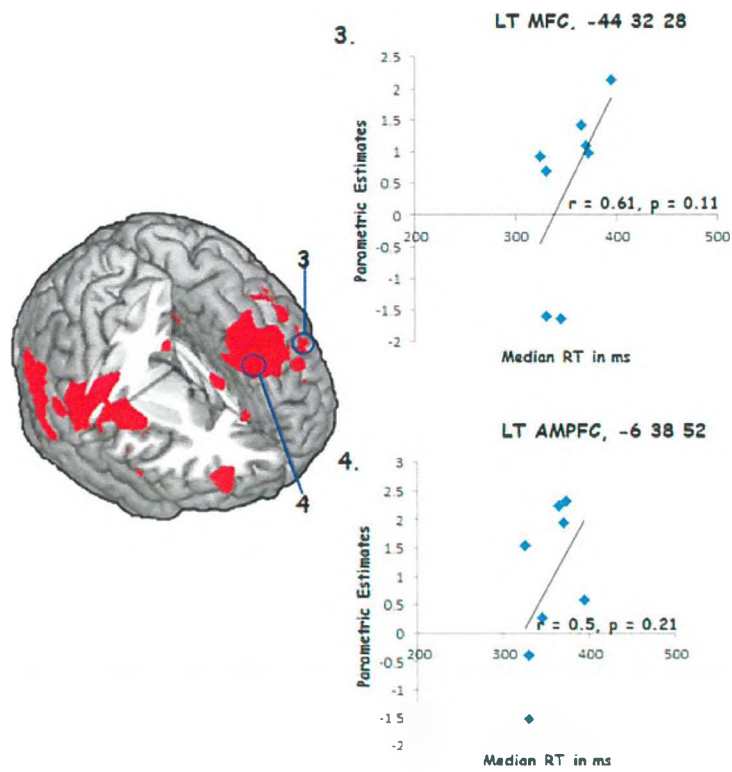


Figure 5.4b. Scatter plots to illustrate the correlation between the BOLD (WAIT > GO) parametric estimates and the median of the GO-Switch RT measures for subjects in the CS group in a priori ROIs.

Control subjects group (CS)

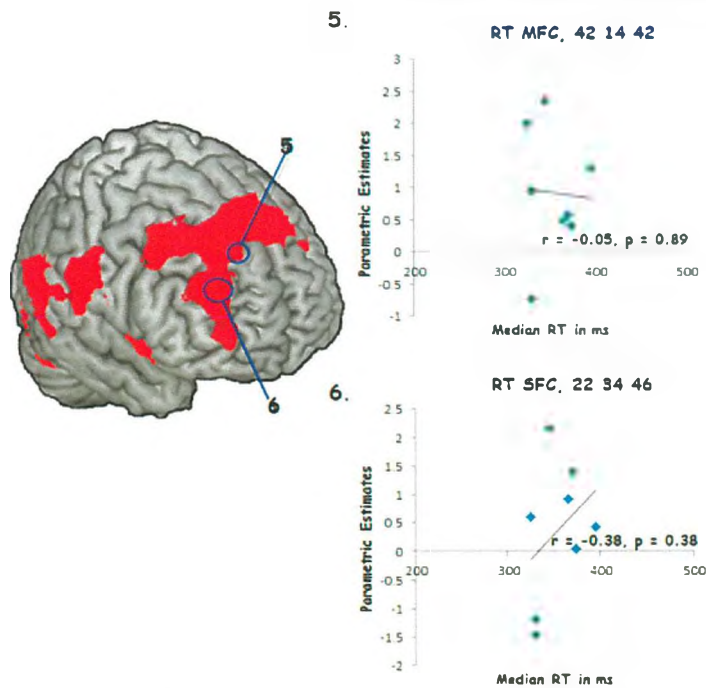


Figure 5.4c. Scatter plots to illustrate the correlation between the BOLD (WAIT > GO) parametric estimates and the median of the GO-Switch RT measures for subjects in the CS group in a priori ROIs.

(ii) Correlation of BOLD data with Clinical Score

The correlation of the BOLD parameter estimates for the (WAIT > GO) contrast with clinical score for the TS group are shown in (Figures 5.5 and 5.6). Analysis revealed that tic severity (YGTSS) score was highly positively associated with the BOLD response, as shown in Figure 5.5. However, despite there being a trend, no significant correlation was found between BOLD response and the Yale Motor Scale, as shown in Figure 5.6.

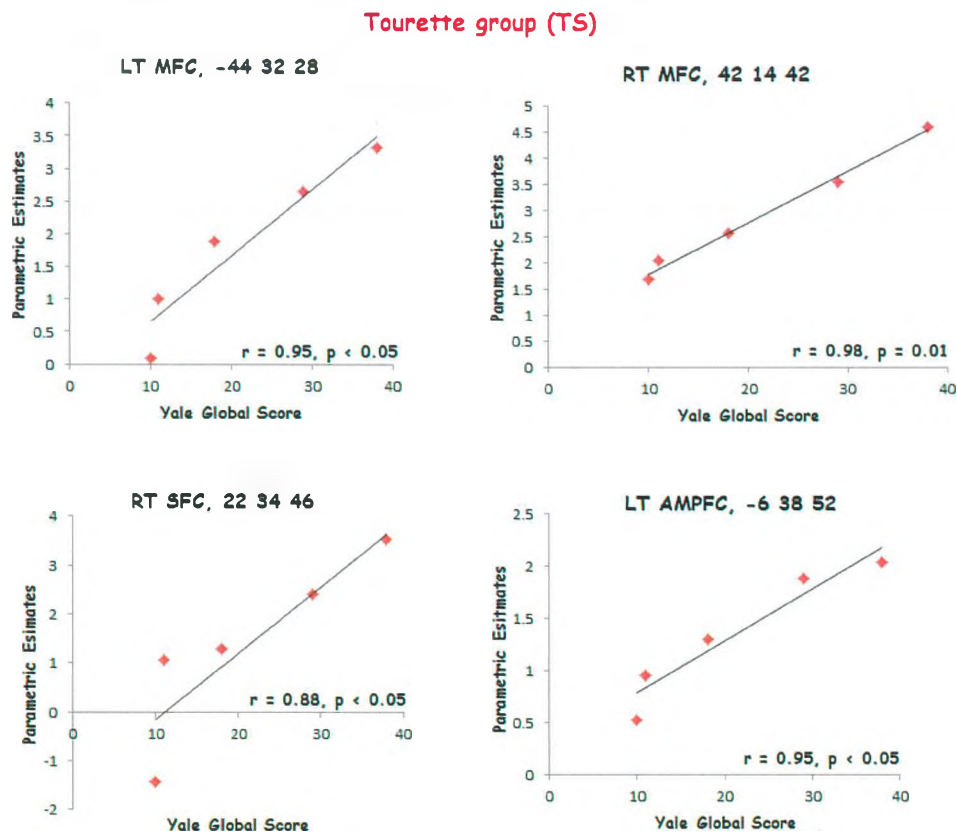


Figure 5.5. Scatter plots to illustrate the correlation between the BOLD (WAIT > GO) parametric estimates and the Yale Global Score for each subject in the TS group in a priori ROIs.

Tourette group (TS)

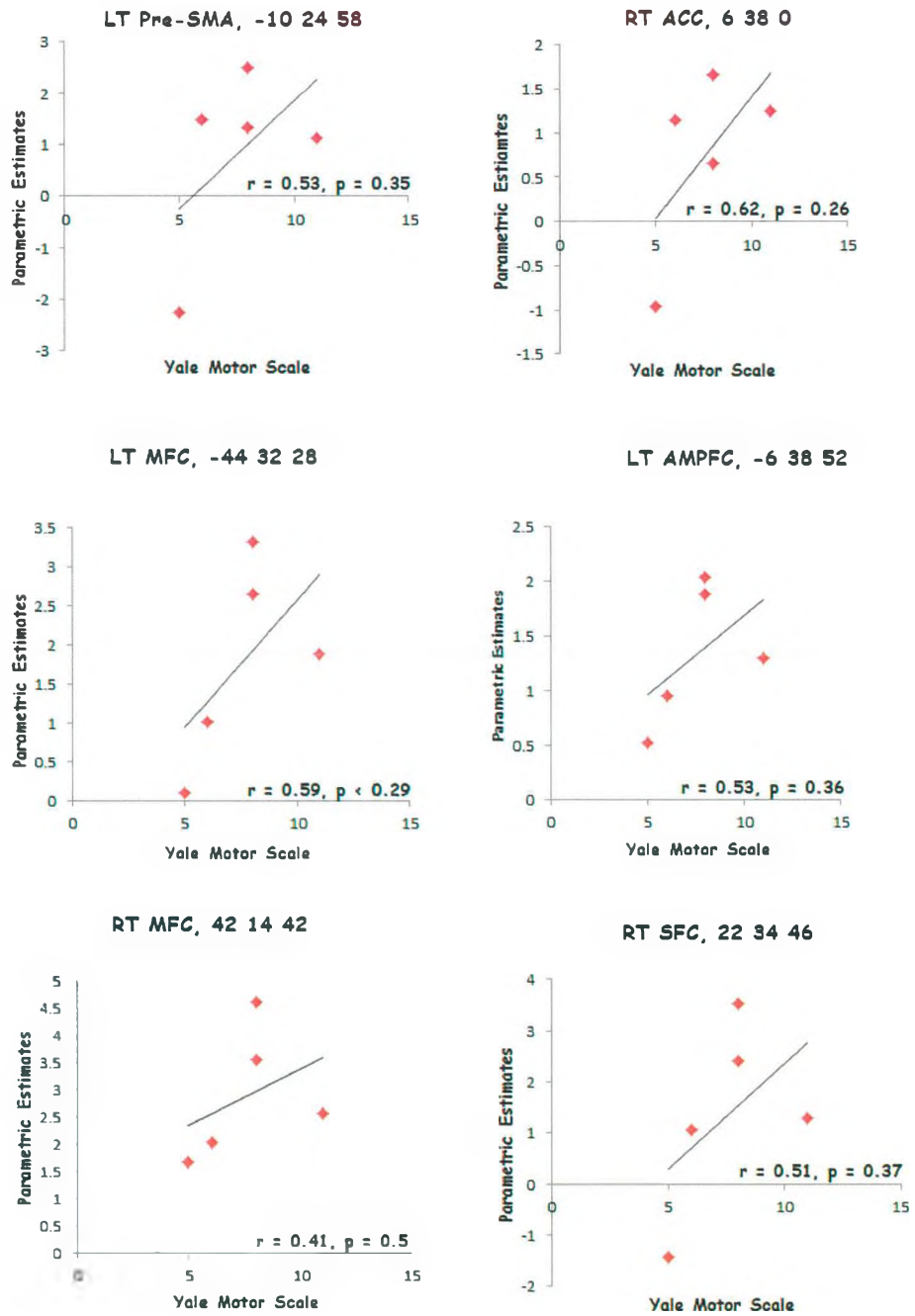


Figure 5.6. Scatter plots to illustrate the correlation between the BOLD (WAIT > GO) parametric estimates and the Yale Motor Scale for each subject in the TS group in a priori ROIs.

Comparison of subject groups to response withholding (WAIT>GO) (Fixed Effects)

Figure 5.7 shows the (WAIT > GO) for the CS and TS groups overlaid. There can be seen to be very little spatial overlap between responses in the CS group and the TS group. Due to this, the *FFX* comparison of response withholding for the CS group greater than the TS group, [(WAIT > GO)_{CS} > (WAIT > GO)_{TS}], showed significant activation in multiple brain regions including left SMA, inferior frontal cortex (IFC), precentral gyrus, right postcentral gyrus (somatosensory cortex), extending to inferior parietal cortex, middle cingulate cortex (MCC), middle temporal cortex, insula cortex and cerebellum, as shown in Figure 5.8 summarized in Table 5.5.

In contrast, when comparing increased activity in the TS group with the CS group [(WAIT > GO)_{TS} > (WAIT > GO)_{CS}], significant activation was found in the right DLPFC, MCC, insula lobe and striatum, as summarized in Table 5.6.

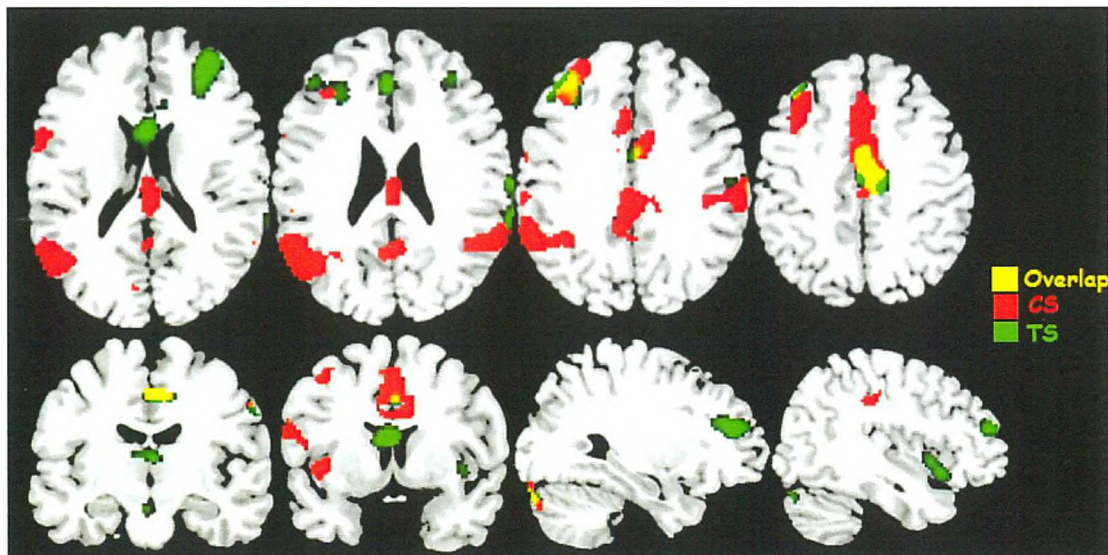


Figure 5.7. FFX within-group analysis showing brain regions associated with response withholding activity (WAIT > GO) in CS (in red) and TS (in green).

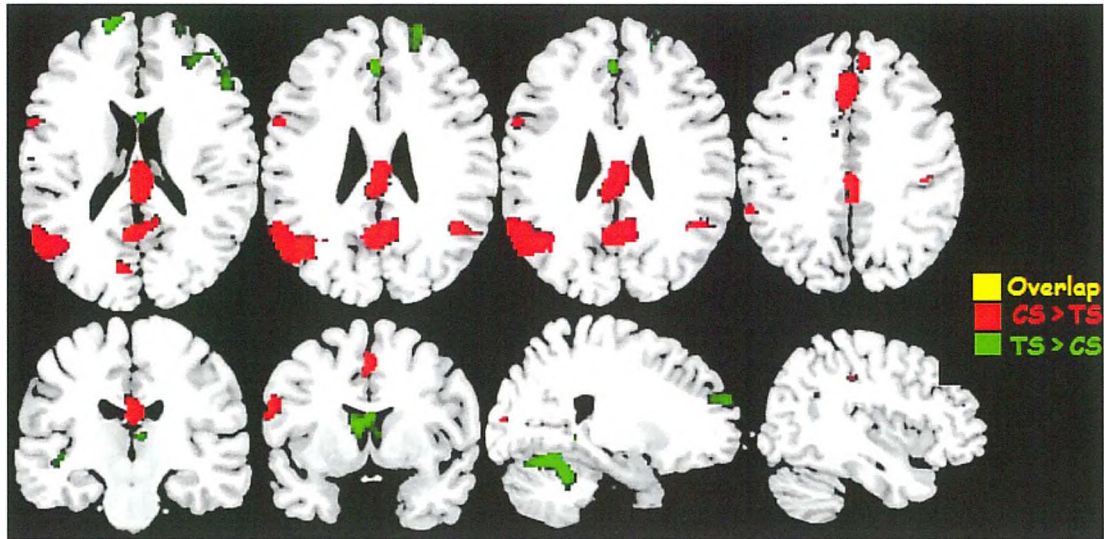


Figure 5.8. FFX between-group showing brain regions associated with response withholding activity in CS greater than TS ($(WAIT > GO)_{CS} > (WAIT > GO)_{TS}$) (in red) and TS greater than CS ($(WAIT > GO)_{TS} > (WAIT > GO)_{CS}$) (in green).

| Brain Region | Side | MNI Coordinates | | | Z-score | T value |
|-----------------------------|------|-----------------|-----|-----|---------|---------|
| | | x | y | z | | |
| Pre-SMA | L | -4 | 20 | 46 | 3.41 | 3.42 |
| IFC (P.Opercularis; BA 44) | L | -62 | 6 | 18 | 3.33 | 3.34 |
| Precentral gyrus | L | -60 | -2 | 32 | 3.98 | 3.98 |
| Postcentral gyrus | R | 40 | -28 | 38 | 3.73 | 3.74 |
| IPL (Supramarginal gyrus) | L | -52 | -50 | 34 | 4.44 | 4.45 |
| IPL (Angular gyrus) | L | -40 | -60 | 30 | 4.26 | 4.27 |
| MCC | L | -2 | -28 | 32 | 3.16 | 3.17 |
| MTC | L | -44 | -62 | 22 | 3.11 | 3.12 |
| Insula Lobe | L | -32 | 26 | 2 | 3.84 | 3.84 |
| Cerebellum (Lob. VIIa Crus) | L | -32 | -88 | -28 | 4.08 | 4.08 |
| BG (Caudate nucleus) | L | -10 | 3 | 12 | 3.3 | 3.31 |

Table 5.5. Significant brain areas associated with response withholding activity within $(WAIT > GO)_{CS} > (WAIT > GO)_{TS}$ contrast for FFX analysis.

| Brain Region | Side | MNI Coordinates | | | Z-score | T value |
|-----------------------------|------|-----------------|-----|-----|---------|---------|
| | | x | y | z | | |
| MFC | R | 31 | 39 | 18 | 3.41 | 3.42 |
| | L | -28 | 35 | 20 | 3.2 | 3.19 |
| MCC | L | -5 | -25 | 30 | 3.16 | 3.17 |
| Insula Lobe | L | -30 | 20 | 4 | 3.84 | 3.84 |
| Cerebellum (Lob. VIIa Crus) | L | -28 | -83 | -28 | 4.08 | 4.08 |
| BG (Caudate nucleus) | L | -10 | 2 | 15 | 3.15 | 3.21 |

Table 5.6. Significant brain areas associated with response withholding activity within $(WAIT > GO)_{TS} > (WAIT > GO)_{CS}$ contrast for FFX analysis.

Comparison of subject groups to response withholding (WAIT>GO) (Random Effects)

Figure 5.9 shows corresponding random effects group maps for the (WAIT > GO) contrast for the CS and TS groups overlaid. A CS within-group random effects analysis yielded significant activation in the bilateral superior frontal cortex, left rostral prefrontal cortex, anterior and posterior cingulate cortex, corpus callosum, temporal cortex and bilateral cerebellum. Importantly, increased activation was found in left striatum, as summarized in Table 5.6. In contrast, the TS group revealed significant activation in the right DLPFC extending to the left ACC, cerebellum and striatum, as summarized in Table 5.7. Again, there can be seen to be very little overlap between responses in the CS group and the TS group.

The more stringent *RFX* comparison of response withholding for the CS group greater than the TS group, [(WAIT > GO)_{CS} > (WAIT > GO)_{TS}], showed significant activation in the inferior frontal cortex and striatum only. In contrast, the [(WAIT > GO)_{TS} > (WAIT > GO)_{CS}] contrast resulted in significant activation being found only in the right DLPFC-particularly the middle frontal cortex and striatum.

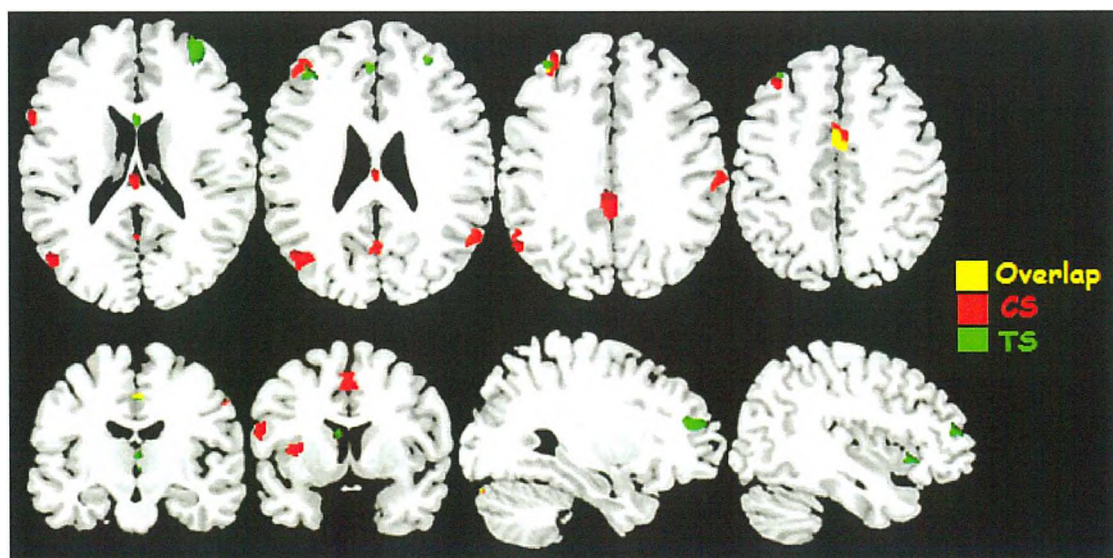


Figure 5.9. RFX within-group analysis showing brain regions associated with response withholding activity (WAIT > GO) in CS (in red) and TS (in green).

| Brain Region | Side | MNI Coordinates | | | Z-score | T value |
|-----------------------------|------|-----------------|-----|-----|---------|---------|
| | | x | y | z | | |
| IFC | R | 35 | 30 | 1 | 3.78 | 3.82 |
| Rostral PFC (BA10) | L | -6 | 52 | 8 | 3.58 | 5.41 |
| Corpus callosum | L | -2 | 28 | 6 | 2.27 | 5.35 |
| ACC (BA 24) | R | 2 | 38 | 4 | 4.8 | 6.2 |
| MTC | R | 44 | -66 | 18 | 2.97 | 4.44 |
| Cerebellum (Lob. VIIa Crus) | L | -12 | -38 | -16 | 3.2 | 5.1 |
| BG (Caudate nucleus) | L | -12 | 2 | 18 | 3.23 | 4.21 |

Table 5.6. Significant brain areas associated with response withholding in the CS for the RFX analysis

| Brain Region | Side | MNI Coordinates | | | Z-score | T value |
|-----------------------|------|-----------------|-----|-----|---------|---------|
| | | x | y | z | | |
| MFC | R | 29 | 56 | 22 | 3.25 | 3.38 |
| ACC | L | -5 | 49 | 5 | 3.16 | 3.21 |
| Insula Lobe | L | -30 | 20 | 4 | 3.84 | 3.84 |
| Cerebellum (Lobule V) | L | -28 | -83 | -28 | 4.08 | 4.08 |
| BG (Caudate nucleus) | L | -10 | 2 | 15 | 3.8 | 5.2 |

Table 5.7. Significant brain areas associated with response withholding in the TS group for the RFX analysis.

5.6.4 Discussion

The current study aimed to investigate cognitive functioning in Tourette syndrome subjects, compared to an age-matched control group (CS), using a GO/WAIT task involving motor response inhibition.

Behavioural results

Behavioural results revealed that reaction times (RT) on switch trials were longer than repeat trials for the GO task in both the TS and CS groups, and results showed a significant ‘switch cost’ in the GO task within the TS group, but not for the CS group. This might reflect the required time that the TS subjects take for the additional effort to suppress the motor tics and simultaneously initiate the appropriate response (Biswal et al., 1998; Fattapposta et al., 2005). These findings lend credence to the hypotheses that the fronto-striatal circuits are disrupted in TS (Singer et al., 2003, 2006; Leckman et al., 2010; Mazzone et al., 2010) and is in concordance with the existence of a dynamic task-set reconfiguration’ (TSR) process, a group of

executive control processes ranging from attention shifting, goal retrieval, facilitation and maintenance of the task-relevant information and inhibition of a prior task set (Monsell, 2003). Two possible theories can explain the existence of this switch cost within the TS group. First, the ‘switch cost’ observed within the TS group might reflect the time consumed by TSR control processes, and their progress (Rogers & Monsell 1995). Alternatively, the switch cost suggests that Tourette syndrome might affect the ability to transfer and switch from one task state to another, with there being competition between the initiation of a task-related set in a given context and the unwanted movements. The Tourette subjects try to initiate the desired task and simultaneously try to inhibit the urge to tic which interferes with the task performance (Allport et al., 2000; Yeung et al., 2003).

fMRI data

Main effect of task within groups

The imaging results revealed that motor preparation and execution activity was elicited in multiple brain regions, including bilateral prefrontal cortex, IFC, primary motor cortex (M1), bilateral supplementary motor area (SMA), posterior parietal cortex, insula cortex, anterior and middle cingulate cortex, striatum, thalamus and cerebellum, consistent with previous studies (as reviewed in Aron, 2010; Chambers et al., 2009; Chikazoe, 2010; Levy and Wagner, 2011). These results suggest that the motor execution process engages fronto-striatal-thalamic and motor cortical nuclei which is consistent with the so-called “direct pathway” of the basal ganglia. However, less activation was observed in the striatum and thalamus in TS compared to the control group. This is striking as it might reflect the dysfunctional connectivity in the direct fronto-striatal pathway in making a GO response. It is

noteworthy that the pattern of activation observed in control subjects in this study is consistent with that found for the GO response, in all experiments in Chapter (4).

Response withholding activity in both TS and CS groups showed significant activation in cortical brain regions including bilateral motor cortex, inferior frontal cortex (IFC), left supplementary motor area (SMA), inferior parietal lobule, anterior and middle cingulate cortex, insula cortex and cerebellum. Moreover, significant activation extended to sub-cortical structures including left striatum, bilateral pallidum, and thalamus. However, in TS subjects, the bilateral DLPFC-particularly the middle frontal cortex, was more engaged compared to the CS group. In addition, less activation in the pallidum structure was observed in the TS group compared to CS group. These results might suggest the TS group recruit the DLPFC as a compensatory mechanism to enhance the cognitive abilities due to the functional disturbances within the fronto-striatal pathways (Marsh et al., 2007; Serrien et al., 2005; Jackson et al., 2011).

Inhibition of an initiated response, the (WAIT > GO) contrast, was associated in the CS group with activation in bilateral supplementary motor area (SMA), left dorsolateral prefrontal cortex (DLPFC), IFC, precentral gyrus, bilateral postcentral gyrus (somatosensory cortex), bilateral inferior parietal cortex, anterior cingulate cortex (ACC), middle temporal cortex, insula and cerebellum. In contrast, the TS subjects showed significant activation in bilateral DLPFC, bilateral somatosensory cortex extending to the inferior parietal cortex, insula cortex and cerebellum. These agree with previous reviewed studies that show similar cortical maps of activation

during the performance of inhibition tasks (as reviewed in Aron, 2010; Chambers et al., 2009; Chikazoe, 2010; Levy and Wagner, 2011).

Comparison of subject groups

The *FFX* comparison of response withholding in the CS group and with that in the TS group, showed significant activation in multiple brain regions including SMA, inferior frontal cortex (IFC), precentral gyrus, postcentral gyrus (somatosensory cortex), extending to inferior parietal cortex, middle cingulate cortex (MCC), middle temporal cortex, insula cortex and cerebellum. Whilst response withholding in the TS group compared to the CS group, revealed significant activation in the right DLPFC-particularly the middle frontal cortex.

The *RFX* analysis supported this finding with comparison of response withholding in the CS group to the TS group, showing significant activation in the IFC and striatum. A finding also consistent with the previous results in Chapter 4 using the same (GO/WAIT) cognitive paradigm. This may reflect that the IFC (in healthy control subjects) is a critical node in mediating response inhibition by biasing the competition between motor programs through the subthalamic nucleus (STN) within the striatum which results in dampening the STN activity that has broad effects upon the striatum and palladium (Mink, 1996).

Whilst the TS group compared to the CS group, revealed significant activation in the right DLPFC-particularly the middle frontal cortex. These findings taken together with those found using the *FFX*-between group analyses, lends credence to the view that the control over motor tics might come through the active suppression of

motor cortex excitability by increasing cognitive control mechanisms and recruiting additional cortical regions to help in the control of motor outputs (Mueller et al., 2006; Jackson et al., 2007; Jackson et al. 2011). For example, the results showed that the DLPFC is engaged during the inhibitory control as a compensatory response to the existence of functional disturbances in the efficiency of fronto-striatal pathways (Marsh et al., 2007, Jackson et al., 2011; Serrien et al., 2005; Church et al., 2009a, 2009b). The dysfunction in the fronto-striatal pathway consequently affects the other sub-neural circuits including the motor cortex areas, DLPFC, rostral/orbital PFC, and ACC. Therefore, this dysfunction could lead to changes in the functioning of these frontal cortex regions, which results in, for example, a reduction in intracortical inhibition and hyperexcitability within motor cortex in TS, leading to cognitive impairments in individuals with TS. This view is further supported by the findings that tic severity (YGTSS) was highly positively associated with the BOLD response in bilateral DLPFC. The correlation between the BOLD signal in DLPFC and the clinical (YGTSS) scores indicates that the increased activation in DLPFC aid in controlling the motor output due to the hyperexcitability of motor cortex in individuals with TS.

Another possibility is that the DLPFC activation may reflect the engagement of the indirect fronto– striatal pathway for a proactive selective inhibition mechanism (Aron et al., 2011). This is an important area to be further investigated, as the Tourette subjects may implement a selective mechanism rather than a global mechanism in order to suppress motor tics.

Reduced engagement of the striatum in TS, as observed, is compelling given its key role in cognitive function, for example the response inhibitory mechanism (Aron, 2010; Chambers et al., 2009; Chikazoe, 2010; Levy and Wagner, 2011). Several lines of evidence have shown that the striatum is a critical node in the pathogenesis of numerous disorders of inhibition including ADHD (Rubia et al., 1999; Castellanos et al., 2002), and obsessive-compulsive disorder OCD (van den Heuvel et al., 2005a, 2005b; Woolley et al., 2008). The striatum is thought to play a crucial role in a wide range of cognitive functions including response inhibition via the fronto-striatal indirect pathway (Alexander 1986; Middleton and Strick, 2000, 2002; Nambu et al., 2000, 2002, Mink, 1996). In healthy subjects, reduced striatal activity has been associated with response inhibition failure (Aron et al., 2006, Vink et al., 2005; Rubia, 2005; Padmala and Pessoa, 2010).

The correlation analysis showed a significant positive linear relationship between the BOLD response (parameter estimate) in the (Pre-SMA and ACC) ROIs and the GO-Switch RT for the CS group. Furthermore, the tic severity was highly positively correlated with BOLD activation in the TS group. Therefore, individuals with high tic scores showed increased BOLD activation. These results lend support to the hypothesis that individuals with TS develop the ability to control the urge to tic by enhancing cognitive control via recruiting other prefrontal cortical region (i.e., DLPFC) (Jackson et al., 2011; Neuner et al., 2011, Baym et al., 2008; Mueller et al., 2006).

In conclusion, Tourette syndrome subjects compared with healthy control subjects demonstrated significantly increased activation in the dorsolateral prefrontal

cortex (DLPFC)-particularly middle frontal cortex, and reduced activity in the striatum during the performance of motor response inhibition task. These findings support the hypothesis that individuals with TS are unable to recruit critical cortical and sub-cortical nodes that are typically involved in mediating behavioural inhibition (as discussed in earlier experiments). Moreover, the results here provide important evidence for increased engagement of the DLPFC as a compensatory response to the existence of the fronto-striatal circuits dysfunction in the TS group (Marsh et al., 2007; Jackson et al., 2011). However, there are some issues that should be considered with these results including, the small sample number of the Tourette subjects included in this study, the wide range of motor and vocal tic severity, and finally the medication status of the Tourette subjects. Further research into fronto-striatal pathways in individuals with TS subjects will provide insight into the neural basis of cognitive and behavioural abnormalities observed in affected individuals, and the clinical implication for therapeutic use.

Chapter 6

6.1 Introduction: Motor learning

Optimal behaviour and skill acquisition require continuous performance monitoring in order to evaluate action outcomes. This monitoring is essential for responding to deviations of action outcomes from intended goals and for detecting situations requiring behavioural adjustment. Therefore, positive outcomes result in reinforcement and negative outcomes call for strategy adjustment. Learning from the consequences of actions is a fundamental characteristic of humans and non-primates. Edward Lee Thorndike (1911/1970) originally described this phenomenon in his ‘law of effect’, in which he explained that the responses to a given stimulus that are accompanied by feelings of satisfaction are highly likely to be connected to that stimulus or situation and therefore will be more likely to reoccur in the future, whilst the responses that are followed by negative results are less likely to reoccur. This is the basis for the principle of *reinforcement learning*.

The reinforcement learning (RL) principle has originally come from mathematical and computational models of psychology. The main concepts of modern reinforcement learning arise from classical and instrumental conditioning theories in psychology (Barto & Sutton, 1997). However, the term reinforcement learning is not widely used in psychology research (Barto, 1995). Reinforcement learning is a paradigm which describes how an agent should take actions in a given environmental context in order to maximize a long term sum or accumulation of future reward outcomes. In the reinforcement learning process the agent learns through its interactions with the environment and not through an explicit supervisor or

supervisory stimuli. This can be achieved by learning how to optimize behaviour and predict the consequences of actions in terms of reward and punishment.

The ability to learn from feedback or reward prediction is critical in everyday life activities in order to adapt behaviour in various environments. Reward prediction is a key function used to make appropriate decisions in different environmental contexts. Humans and animals learn whether the sensory information of upcoming stimuli is rewarding or punishing through stimulus–response reward experiences. However, the reward prediction error (RPE) can be viewed as the difference between the expected reward value and the received reward outcome. This difference occurs when updating reward prediction is correlated with sensory information or a signal that indicates a reward is coming up which leads to a revision of expectations (Sutton and Barto 1998; Schultz and Dickinson 2000; Waelti et al. 2001). A positive reward prediction error (PPE) occurs during unexpected delivery of reward or when the reward occurred earlier than expected. PPE can also occur during the presentation of a reward-predicting event, or perhaps when the reward was larger than predicted. In contrast, a negative reward prediction error (NPE) occurs during the omission of an expected reward.

Converging evidence from rodents, humans, and non-human primates studies indicates that re-entrant connectivity between cortical structures (including the prefrontal and limbic system) and the midbrain dopaminergic system are critical to reward-based learning and the use of expectancies of reinforcers in guiding and developing new motor plan (Calabrese et al., 1996; Wickens et al., 1995, 1996; Graybiel et al., 1994, 1995). Dopamine-dependent mechanisms facilitate reinforcement learning signals in the striatum and strengthen the related information

in the prefrontal cortex that are used to form expectations about receiving rewards which result in reinforcement-based decisions (Schultz and Romo, 1992b; Schultz, 2000; Joel and Wiener, 2000; Takikawa et al., 2004; Graybiel et al., 1994, 1995; Kawagoe et al., 1998).

The basal ganglia, particularly the striatum, are widely thought to be involved in different aspects of the learning, timing, and selection of action (Packard and Knowlton, 2002). The striatum has been recognized as a critical structure in integrating the multi-modalities of information during learning of stimulus-response association, motor and cognitive functions, for the following unique features (Joel and Wiener, 1994; Suzuki et al., 2001). First, it is connected via distinct loop circuits with many cortical areas including prefrontal, medial prefrontal, cingulate, and premotor and primary motor cortices (Alexander et al., 1990; Gerardin et al., 2003; Parthasarathy et al., 1992; Selemon and Goldman-Rakic, 1985; Takada et al., 1998, Mink et al., 2003), thus it has access to multimodal information. Second, the striatum has strong reciprocal connections with the dopaminergic structures including substantia nigra pars compacta (SNc) and the ventral tegmental area (VTA), therefore it can regulate multi-modality afferents by the dopaminergic effect (Hollerman and Schultz, 1998; Schultz, 1992a, 2000; Joel et al., 2000; Takikawa et al., 2004).

The main aim of this experiment is to study basal ganglia function using fMRI at ultra-high magnetic field (7 Tesla) in motor learning, including motor prediction and reward mechanism using a 'Motor Prediction task'.

6.2 Experiment 5

6.2.1 Material and methods

6.2.1.1 Participants

Twelve right-handed healthy participants (9 female, age range: 19–29 years, mean age: 22.1 ± 2.4 years) were enrolled in this study. None had any signs or history of neurological or psychiatric diseases. All participants gave written informed consent to the study after the procedure was fully explained and they were compensated for their time. The protocol was approved by the local Research Ethics Committee (SPMMRC, The University of Nottingham, UK).

6.2.1.2 Experimental Task and Procedure

Stimuli were presented to the participants by a computer controlled projection system that delivered a visual stimulus to a projection screen located at the foot of the magnet bore. The participant viewed this screen using prism glasses through a system of mirrors located inside the magnet room. The scanning room was darkened to allow easy visualization of the task stimuli.

Participants were asked to keep the thumbs of their right hand on a single micro-switch mounted on a (MR-compatible) response box positioned on the lower abdomen in the midline of the body. Stimulus presentation was computer controlled and delivered using MATLAB software by a laptop located outside the scanner. This computer was triggered by a TTL signal from the scanner to record the precise timing of button presses together with the timing of the acquisition of every slice scan in each image volume.

Before each scanning, participants were received training outside of the scanner. They performed a number of practice trials completing a minimum of 5 trials of each type of task blocks (Learn and Test) to ensure they fully understood the task. The scanning session consisted of four event-related experimental runs of approximately 5 minutes each, the first two blocks were *Learning* blocks and the other two were *Test* blocks. The task comprised a square-shaped stimulus that was displayed on the centre of the screen in one of three colours (green, red and blue) which then changed to white. Participants were instructed to respond as fast as possible to each stimulus by pressing a button-box when the colour of the stimulus changed to white. Responses should coincide with the coloured square changing to white. Responses which coincided with the coloured square changing to white or immediately after the change earned 200 points. Points scored then decreased by 20% of points (40 points) for every 50 ms delay after the change, with zero points scored for responses at or after 250ms. Thus, the faster the correct response the higher the participants score.

In learning blocks, each trial started with the presentation of a blank screen for 1000 ms, followed by a coloured square stimulus presented on the centre of the screen for a period of time depending on the colour which then changed to white colour. The order of the three different coloured stimuli was random, with a fixed different timing of 1000 ms for red, 1300ms for green and 1800ms for blue, as shown in Figure 6.1. Feedback was given 1000 ms after each response. All stimuli were presented at a rate of one approximately every 7 s.

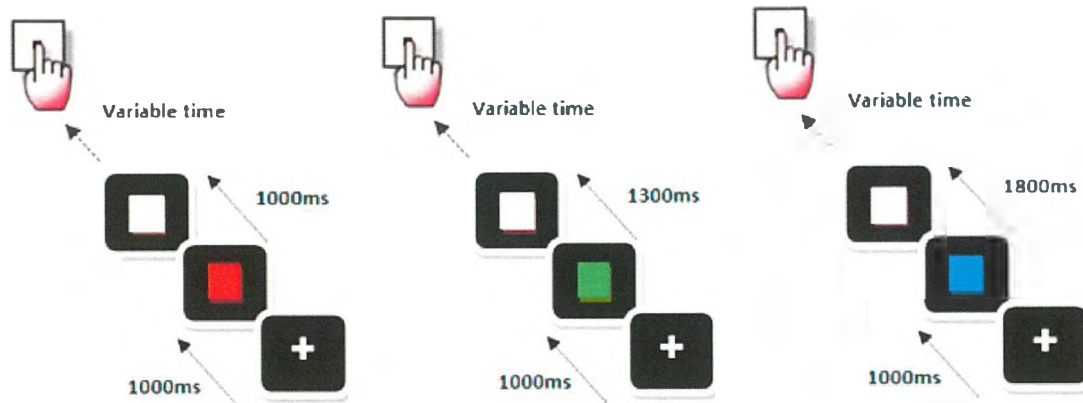


Figure 6.1. Stimuli types and timing in the learning phase; coloured squares were presented for a fixed period of time depending on the colour and participants responded by pressing a key as close as possible to the time when the square changed to white.

In the test blocks once learning had occurred, the same task was used but the coloured square-shaped stimuli did not always change to white, and the coloured stimuli (red, green and blue) were presented randomly with variable interval timings for which they were shown from 1000 ms to 2500 ms, as shown in Figure 6.2a. This kind of variable interval stimuli presentation resulted in three conditions as follows. (C1): coloured square stimulus changes at the predicted time. (C2a): coloured square changes *earlier* than the predicted time. (C2b): coloured square changes *later* than the predicted time, and (C3): colour square doesn't change to white colour, as shown in Figure 6.2b. All stimuli were presented at a rate of one approximately every 9 s. The same number of red, green and blue stimuli (33% of each type) was presented during the event-related functional MRI data acquisition.

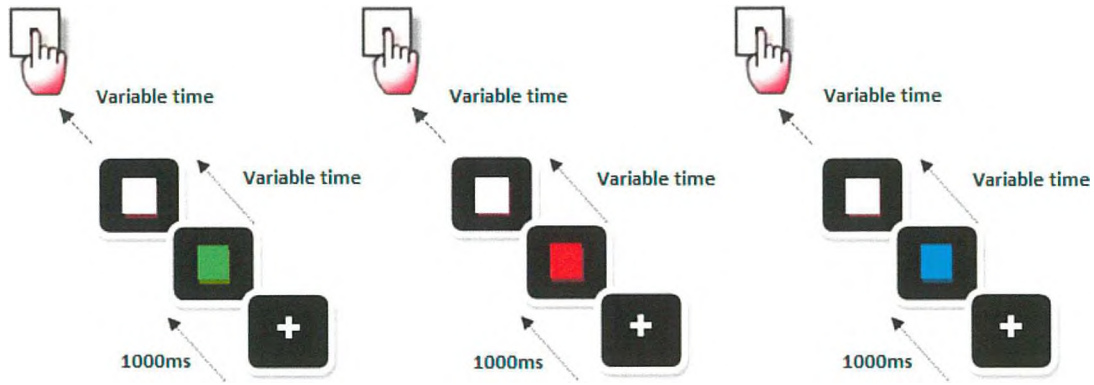


Figure 6.2a. Stimuli types and timing in the test phase; coloured squares were presented for a variable period of time from (1000 – 2500 ms) and participants responded by pressing a key as close as possible to the time when the square changed to white.

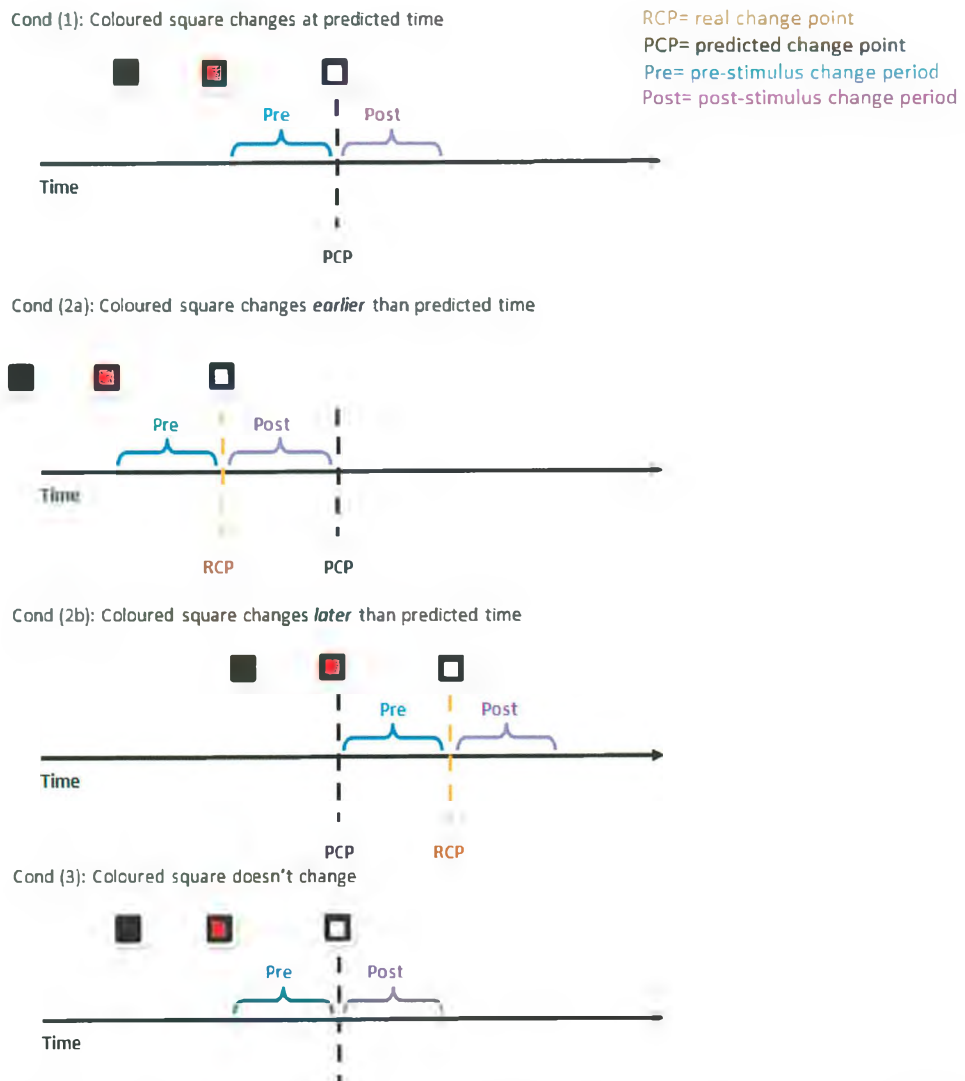


Figure 6.2b. Stimuli types and timing in the test phase; coloured squares were presented for a variable period of time from (1000 – 2500 ms) which resulted in three types of conditions; (C1) coloured square changed at the predicted time, (C2a) coloured square changed earlier than the predicted time, (C1) coloured square changed later than the predicted time, (C1) coloured square does not change to white. Note that the red square here is just for illustration and it can be any of the three mentioned colours.

6.2.1.3 MRI data acquisition

MRI data were acquired on a 7 Tesla Philips Achieva System equipped with a head transmit coil and 16 channel SENSE receive coil. The subject's head was immobilized using foam cushions to reduce head movement.

Changes in blood oxygenation level-dependent (BOLD) fMRI signal were measured using a dual gradient echo-echo-planar imaging (GE-EPI) sequence (echo time: $TE_1/TE_2 = 10.3 / 29.3$ ms, 2 mm isotropic resolution with no slice gap, 32 slices, FOV = $192 \times 160 \times 164$ mm, flip angle = 90° , repetition time TR = 2.5 s). Four runs in total were collected, for each run, a total of 96 EPI volume images were acquired. Anatomical MR images were acquired with a Magnetic Prepared Rapid Acquisition Gradient Echo (MPRAGE) sequence (TR = 16 ms, TE = 4.38, FoV = $192 \times 169 \times 164$ mm, flip angle = 8° , 384×384 matrix, 169 slices per slab, slice thickness = 1 mm, no gap, voxel size = $1.5 \times 1.5 \times 1.5$ mm).

6.2.2 Data Analysis

6.2.2.1 Behavioral data

The correct response reaction times (RT) for all trials for each subject were divided into 7 bins across the duration of the experiment (i.e., first four trials, second four trials, etc) Each bin consisted of four RTs. Median correct RTs were calculated for each bin. The mean of each subjects median RT was then calculated for each bin for each of the two learning runs. The difference between the median RT value of the first bin and the median value of the last bin for each subject across both runs were calculated and entered in one sample T-Test.

6.2.2.2 fMRI data analysis-preprocessing

Before statistical analysis, using SPM5 (Statistical Parametric Mapping, Wellcome Department of Cognitive Neurology, Institute of Neurology, University College London, UK, www.fil.ion.ucl.ac.uk/spm), images for all participants were pre-processed and realigned to the first image of each time series using a six parameter linear transformation (a rigid-body rotation and translation correction) and re-sliced using sinc interpolation. The images for all participants were then spatially normalized into the Montreal Neurological Institute (MNI) space, then smoothed and convolved in space with a three-dimensional isotropic Gaussian kernel of 8 mm (FWHM).

6.2.2.3 fMRI data analysis-model estimation and statistics

fMRI data were analysed at two levels. At the first level analysis, each subject was modelled independently. The imaging data for each subject were analysed on a voxel-by-voxel basis using the principles of the general linear model (Friston et al., 1995) as implemented in SPM5. Prior to model estimation, all images were globally scaled and time series were filtered by using high pass filter to remove low frequency signals (below 160s). fMRI time series were analysed by fitting a convolved canonical hemodynamic response function (HRF) to the onsets of the stimuli types separately. Each session was modelled separately. Therefore, the design matrix consisted of four sessions, the first two blocks were learning blocks and the remaining two were test blocks. In the learning block, each run consisted of only one type of trial, where the coloured stimulus always changed to white, with two conditions; Pre and Post stimulus change.

In test block, each run consisted of four types of trial; ‘Predicted’ (C1): coloured square stimulus changed at the predicted time, ‘Early’ (C2a): coloured square changed earlier than the predicted time, ‘Late’ (C2b): coloured square changed later than the predicted time and ‘Absent’ (C3): colour square did not change to white. Each trial consisted of two conditions; Pre and Post stimulus change. Thus, in total, the design matrix composed of two regressors of interest for each learning session and eight regressors of interest for each test session. Six motion regressors, indicating amount of translation and rotation in the x, y and z dimensions for each 2.5 s TR, were also included in the analysis as covariates of no interest. Eight experimental contrasts of interest were created: for the learning phase; Pre-change > baseline, Post-change > baseline; for the test phase; Pre-change of condition ‘Predicted’ (C1) > Pre-change of condition ‘Early’ (C2a), Pre-change of condition ‘Late’ (C2b) > Pre-change of condition ‘Predicted’ (C1), Pre-change of condition ‘Late’ (C2b) > Pre-change of condition ‘Early’ (C2a), Post-change of condition ‘Early’ (C2a) > Post-change of condition ‘Predicted’ (1), Post-change of condition ‘Late’ (C2b) > Post-change of condition ‘Predicted’ (C1), Post-change of condition ‘Absent’ (3) > Post-change of condition ‘Predicted’ (C1).

Second level analysis (group analysis) consisted of a random effects analysis across subjects. Contrast maps from all participants were created and submitted to one sample t-tests. All group maps were thresholded using whole brain statistics, with a height threshold of $T = 3.16$, extent threshold of 10 voxels and the threshold of $P_{FDR} < 0.05$ for multiple comparisons.

6.2.2.4 Parametric analysis

A new model was created for each subject including time as a parametric regressor for each trial for the Pre and Post stimulus change in learning blocks. Contrast images were generated for Pre and Post stimuli, reflecting the relationship between BOLD activity and time, and these were used in a second-level random effects analysis. Another model was created for each subject with separate regressors specifying the absolute temporal deviation in time from the expected time of the stimulus change in test blocks along with the following conditions:

- (I) The Pre-stimulus change of condition 'Early' (C2a).
- (II) The Post-stimulus change of condition 'Early' (C2a).
- (III) The Pre-stimulus change of the condition 'Late' (C2b).
- (IV) The Post-stimulus change of condition 'Late' (C2b).

These contrasts were assessed in a random effects analysis using a one-sample t-test.

6.2.2.5 Region of interest (ROI) analysis

In order to further explore activity in the regions identified in the foregoing whole-brain analyses, a region of interest (ROI) analysis approach was used. ROI analyses were performed on a number of brain regions that were identified anatomically and functionally and derived from voxel-wise statistical map of the Pre (C2b > C1) contrast based on their role in mediating learning and reward processes. The following brain areas were identified anatomically using (WFU_PickAtlas) (Tzourio-Mazoyer et al., 2002); bilateral globus pallidus (GP) and bilateral ventral striatum. Bilateral habenular nuclei were identified functionally by growing a sphere (10 mm radius) centred at the peak of the activation of MNI coordinates (-4/4, -26, 1) as found in previous studies (Ullsperger and von Cramon, 2003). Bilateral ventral

medial prefrontal cortex (VMPFC) were also identified functional by growing a sphere (10 mm radius) centred at the peak of the activation of MNI coordinates (-10/10, 44, -8) as found in previous studies (Ullsperger and von Cramon, 2003).

6.2.3 Results

6.2.3.1 Behavioral Data

Figure 6.3 shows the mean of the median RT for each bin across subjects for each learning blocks for A) the first run and B) the second run.

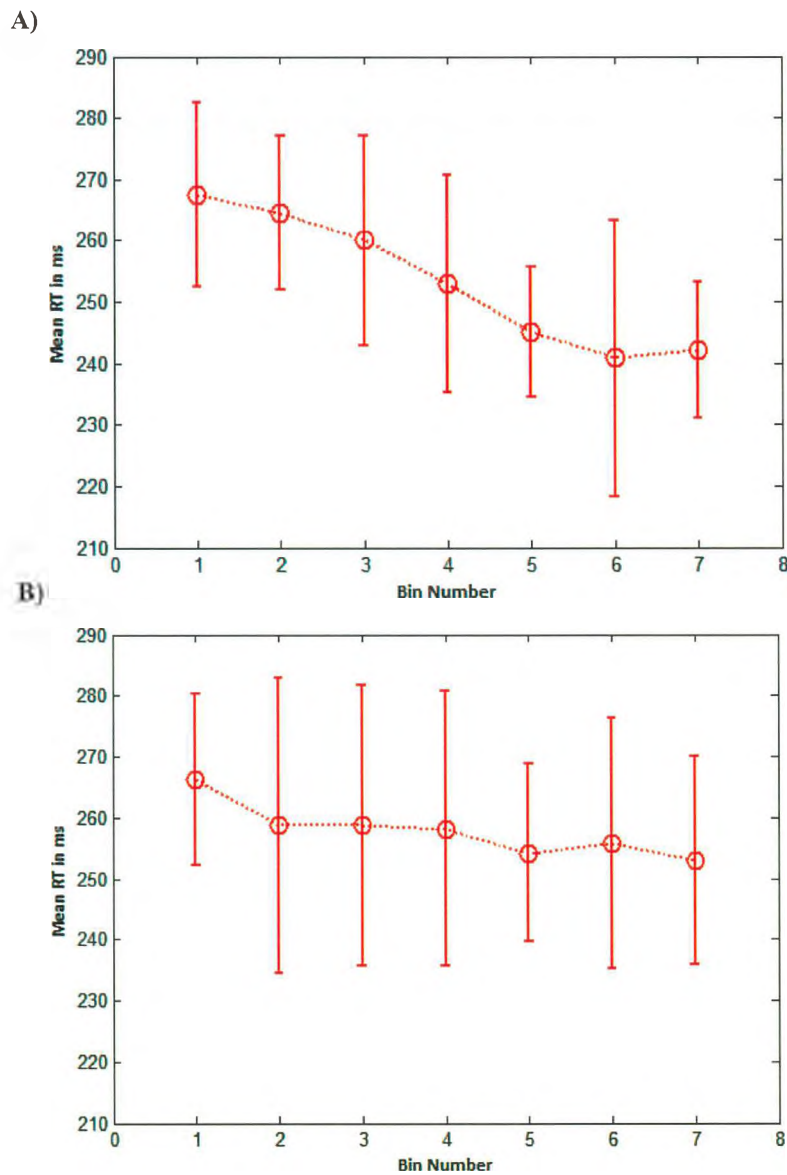


Figure 6.3. The mean of the median RT for each bin across subjects for each learning blocks for A) run 1 and B) run 2.

One-sample t-tests were conducted to compare the mean of the difference between (the 1st and last bins) for each run separately and for both runs together across subjects compared to zero as test value. There was a significant difference in the scores for first run (25 ± 5 ms; $M \pm SEM$); ($t = 3.12$, $p < 0.05$). In contrast, no significant difference in the scores for second run was found (13 ± 3 ms; $M \pm SEM$); ($t = 0.3$, $p = 0.6$). Finally, there was a significant difference in the scores for both runs together (53 ± 17 ms; $M \pm SEM$); ($t = 3.07$, $p < 0.05$).

6.2.3.2 fMRI data

1) Learning blocks

Reward expectancy-related activity; Pre-change > baseline

Reward anticipatory processes in learning modulate neural activity in several brain areas, including the lateral prefrontal cortex (LPFC), medial prefrontal cortex MPFC, premotor area, inferior parietal lobule, olfactory cortex, ACC, MCC. Moreover, significant activations were observed in the sub-cortical structures including striatum, thalamus and midbrain regions, as shown in Figure 6.4 and summarized in Table 6.1.

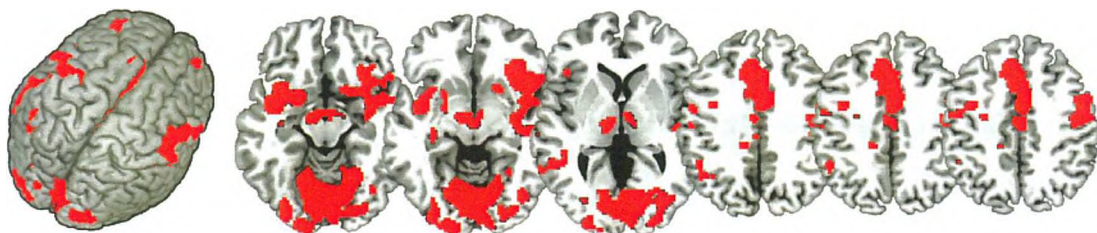


Figure 6.4. Brain regions associated with pre-change learning period. $P_{FDR} < 0.001$, corrected for multiple comparisons.

| Brain Region | Side | MNI Coordinates | | | Z-score | T value |
|----------------------------|------|-----------------|-----|-----|---------|---------|
| | | x | y | z | | |
| Pre-SMA | R | 2 | 14 | 46 | 5.5 | 13.34 |
| AMPFC | L | -6 | 30 | 42 | 4.99 | 10.23 |
| SFC | R | 28 | 60 | 10 | 3.96 | 6.12 |
| MFC | L | -36 | 44 | 14 | 4.95 | 10 |
| IFC (P.Opercularis) | R | 60 | 18 | 2 | 4.88 | 9.63 |
| (P.Triangularis; BA 45) | L | -52 | 18 | 16 | 4.29 | 7.17 |
| Precentral gyrus | L | -46 | -4 | 32 | 5.56 | 13.83 |
| Postcentral gyrus | L | -62 | 0 | 24 | 4.64 | 8.52 |
| Olfactory cortex | L | -20 | 4 | -16 | 4.31 | 7.24 |
| IPL (Angular gyrus) | L | -42 | -54 | 34 | 4.28 | 7.15 |
| IPL (Supramarginal gyrus) | L | -44 | -46 | 32 | 4.16 | 6.73 |
| ACC | R | 4 | 28 | 16 | 4.89 | 10.13 |
| | L | -10 | 26 | 30 | 5.2 | 13.07 |
| MCC (BA 24) | R | 4 | 2 | 42 | 4.74 | 9.33 |
| | L | -6 | -24 | 32 | 5.25 | 11.68 |
| STC | L | -64 | -44 | 16 | 4.84 | 9.45 |
| MTC | L | -52 | -46 | 2 | 4.71 | 8.84 |
| Insula lobe (BA 13) | R | 42 | 4 | -12 | 4.92 | 9.84 |
| | L | -36 | 12 | -12 | 4.29 | 6.87 |
| Rolandic operculum (BA 43) | R | 54 | -10 | 12 | 5.04 | 10.49 |
| | L | -44 | 0 | 16 | 4.48 | 7.9 |
| Lingual gyrus (BA 19) | R | 22 | -70 | -2 | 5.42 | 11.9 |
| | L | 0 | -80 | -8 | 6.54 | 24.37 |
| SOC (BA 31) | L | -16 | -76 | 24 | 4.13 | 6.66 |
| Middle occipital cortex | L | -26 | -76 | 28 | 4.65 | 8.58 |
| Hippocampus | L | -36 | -16 | -16 | 4.6 | 8.37 |
| Cerebellum | R | 20 | -50 | -20 | 5.6 | 13.55 |
| | L | -14 | -82 | -16 | 5.78 | 15.6 |
| BG (Putamen) | R | 32 | -12 | -6 | 5.11 | 10.89 |
| Thalamus | L | -10 | -16 | 2 | 4.78 | 9.18 |
| Midbrain | L | -6 | -8 | -10 | 4.99 | 10.24 |

Table 6.1. Abbreviation: L, Left; R, right; BA, Brodmann area; DM, dorsomedial; VL, ventrolateral; SMFC, anterior medial prefrontal cortex; SMA, supplementary motor area; SFC, superior frontal cortex; MFC, middle frontal cortex; IFC, inferior frontal cortex; IPL, inferior parietal lobule; ACC, anterior cingulate cortex; MCC, middle cingulate cortex; PCC, posterior cingulate cortex; MTC, middle temporal cortex; ITC, inferior temporal cortex; SOC, superior occipital cortex; BG, basal ganglia; GP, globus pallidus.

2) (i) Test blocks: Pre contrasts

Reward expectancy-related activity; Pre-change 'Predicted' (C1) > Pre-change 'Early' (C2a)

Holding expectation in an unpredictable context was analysed by comparing the pre-stimulus change of condition 'Predicted' (C1) to the pre-stimulus change of condition 'Early' (C2a). This revealed significant activation in the DLPFC, superior

orbitofrontal cortex, ACC, MCC, insula lobe, parahippocampus. Interestingly, striatum, and midbrain region were strongly activated, as shown in Figure 6.5 and summarized in Table 6.2.

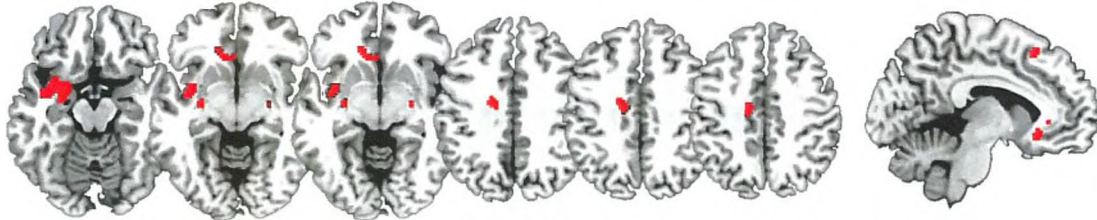


Figure 6.5. Brain regions associated with expectation of an event. $P_{FDR} < 0.05$, corrected for multiple comparisons.

| Brain Region | Side | MNI Coordinates | | | Z-score | T value |
|-------------------------|------|-----------------|-----|-----|---------|---------|
| | | X | y | z | | |
| AMPFC | L | -6 | 26 | 54 | 3.29 | 4.44 |
| MFC | R | 48 | 28 | 34 | 2.69 | 3.29 |
| | L | -32 | 52 | 6 | 3.31 | 4.48 |
| IFC (P.Opercularis) | R | 38 | 16 | 30 | 3.32 | 4.49 |
| Superior orbital cortex | R | 22 | 56 | -4 | 2.8 | 3.49 |
| ACC | L | -10 | 28 | -8 | 3.23 | 4.31 |
| MCC | L | -16 | -10 | 40 | 3.68 | 5.36 |
| Insula Lobe | L | -36 | 0 | -12 | 3.55 | 5.02 |
| Parahippocampus (BA 34) | L | -22 | 2 | -14 | 3.2 | 4.25 |
| BG (Putamen) | L | -28 | -18 | -8 | 2.82 | 3.55 |
| BG (External GP) | R | 24 | -10 | -4 | 2.95 | 3.76 |
| Brainstem (Midbrain) | R | 6 | -12 | -16 | 7.67 | 4.42 |

Table 6.2. Significant brain areas associated with an expected event.

Surprise-related activity; Pre-change 'Late' (C2b) > Pre-change 'Predicted' (C1)

Surprise-related activity showed widespread brain regions where the BOLD signal increased when the expected event was absent compared to holding expectation. For example, subjects were surprised when the expected event did not occur at the expected time. These regions involve DLPFC, MPFC, anterior and posterior cingulate cortex, inferior temporal cortex, rolandic operculum. Sub-

cortically, putamen, MD nucleus of thalamus, habenula and midbrain regions was found significantly active, as shown in Figure 6.6 and summarized in Table 6.3.

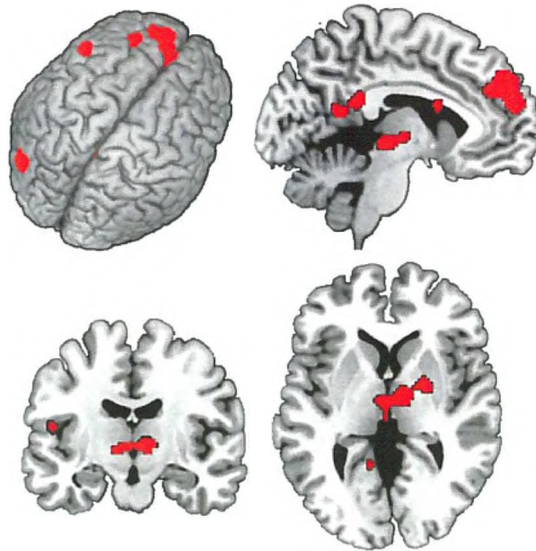


Figure 6.6. Brain regions associated with holding expectation. $P_{FDR} < 0.05$, corrected for multiple comparisons.

| Brain Region | Side | MNI Coordinates | | | Z-score | T value |
|----------------------------|------|-----------------|-----|-----|---------|---------|
| | | x | y | z | | |
| AMPFC (BA 9) | L | -6 | 48 | 32 | 5.27 | 11.82 |
| SFC (BA 9) | L | -16 | 54 | 36 | 4.14 | 6.68 |
| MFC | L | -28 | 44 | 32 | 3.91 | 5.96 |
| IFC (BA 9) | L | -54 | 18 | 30 | 3.9 | 5.95 |
| IFC (P.Orbitalis) | L | 46 | 32 | -10 | 3.34 | 4.54 |
| ACC (BA 32) | L | -2 | 40 | -4 | 2.85 | 3.58 |
| MCC (BA 31) | R | 4 | -42 | 32 | 4.21 | 6.91 |
| PCC (BA 31) | R | 4 | -52 | 30 | 3.97 | 6.16 |
| | L | 0 | -48 | 24 | 3.97 | 6.14 |
| ITC | R | 48 | -64 | -12 | 3.01 | 3.86 |
| Temporal pole (BA 38) | L | -50 | 16 | -10 | 3.14 | 4.12 |
| Rolandic operculum (BA 43) | L | -50 | -10 | 14 | 3.33 | 4.52 |
| Lingual gyrus | R | 10 | -50 | -2 | 4.06 | 6.44 |
| Superior occipital cortex | L | -20 | -62 | 26 | 3.19 | 4.23 |
| Middle occipital cortex | L | -40 | -78 | 26 | 3.78 | 5.6 |
| IOC (BA 19) | L | -46 | -76 | -8 | 2.99 | 3.82 |
| BG (Putamen) | R | 24 | 2 | 8 | 3.57 | 5.05 |
| Thalamus | R | 10 | -12 | 2 | 3.68 | 5.35 |
| Habenula | R | 4 | -24 | 1 | 3.71 | 5.39 |
| | L | -4 | -26 | 1 | 3.65 | 5.31 |
| MD nucleus of thalamus | L | -2 | -14 | 2 | 3.05 | 3.88 |
| Brainstem (Midbrain) | R | 6 | -24 | -4 | 3.78 | 5.62 |

Table 6.3. Significant brain areas associated with the non-occurrence of an expected event (surprise mechanism).

Surprise-related activity; Pre-change 'Late' (C2b) > Pre-change 'Early' (C2a)

This contrast revealed significant activity in brain regions that were associated with the absence of an expected event compared to when there was no anticipation, including DLPFC, ACC and insula lobe. In addition, a significant activation was observed in the sub-cortical structures including the striatum and thalamus, as shown in Figure 6.7 and summarised in Table 6.4.

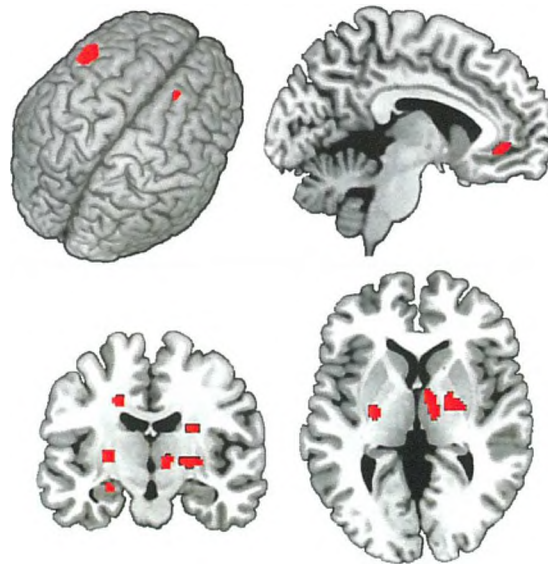


Figure 6.7. Brain regions associated with the absence of an expected event. $P_{FDR} < 0.05$, corrected for multiple comparisons.

| Brain Region | Side | MNI Coordinates | | | Z-score | T value |
|---------------------|------|-----------------|-----|-----|---------|---------|
| | | x | y | z | | |
| SFC | R | 14 | 24 | 48 | 3 | 3.85 |
| IFC (BA 9) | L | -54 | 10 | 38 | 3.86 | 5.82 |
| ACC | R | 2 | 30 | -8 | 4.93 | 9.87 |
| | L | -2 | 40 | -4 | 3.96 | 6.13 |
| Insula lobe (BA 13) | L | -40 | 4 | -12 | 2.79 | 3.47 |
| Hippocampus | L | -24 | -10 | -16 | 3 | 3.86 |
| BG (Putamen) | L | -26 | -12 | 4 | 2.8 | 3.48 |
| BG (External GP) | R | 22 | -8 | 0 | 2.94 | 3.73 |
| Thalamus | R | 10 | -14 | 0 | 3.12 | 4.1 |

Table 6.4. Significant brain areas associated the absence of an expected event.

(ii) Test blocks: Post contrasts

Earlier (unpredicted) event-related activity; Post-change 'Early' (C2a) > Post-change 'Predicted' (C1)

Several brain areas showed an increase in neural activity when the event (unexpected event) occurred earlier than expected compared to when expected event occurred at the predicted time. These areas involve DLPFC, VMPFC, superior orbital frontal cortex, anterior and middle cingulate cortex, insula lobe, parahippocampus and putamen, in Figure 6.8 and summarised in Table 6.5.

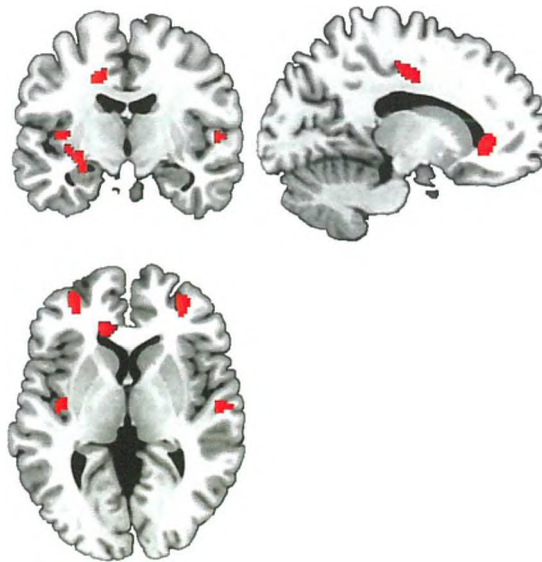


Figure 6.8. Brain regions associated with earlier (unpredicted) event occurrence. $P_{FDR} < 0.05$, corrected for multiple comparisons.

| Brain Region | Side | MNI Coordinates | | | Z-score | T value |
|-------------------------|------|-----------------|-----|-----|---------|---------|
| | | x | y | z | | |
| MFC | R | 32 | 50 | 2 | 3.12 | 4.09 |
| | L | -30 | 52 | 6 | 3.04 | 3.92 |
| IFC | R | 38 | 18 | 30 | 3.06 | 3.96 |
| | L | -32 | 6 | -16 | 3.56 | 5.05 |
| Superior orbital cortex | R | 22 | 56 | -4 | 2.59 | 3.13 |
| ACC | L | -10 | 28 | -8 | 3.28 | 4.47 |
| MCC | L | -14 | -14 | 44 | 3.67 | 5.18 |
| STC | R | 56 | -12 | 4 | 3.16 | 4.15 |
| Insula lobe | L | -36 | 0 | -12 | 3.56 | 5.05 |
| Parahippocampus (BA 34) | L | -22 | 2 | -14 | 3.18 | 4.2 |
| BG (Putamen) | L | -28 | -10 | -8 | 2.75 | 3.43 |

Table 6.5. Significant brain areas associated with earlier (unpredicted) event occurrence.

Later event-related activity; Post-change 'Late' (C2b) > Post-change 'Predicted'(C1)

A significant activation was also observed in the pre-SMA, IFC, IPL, ACC, STC and cerebellum regions when the event occurred after the expected time compared to when the event occurred exactly at the expected time, as shown in Figure 6.9 and summarised in Table 6.6.

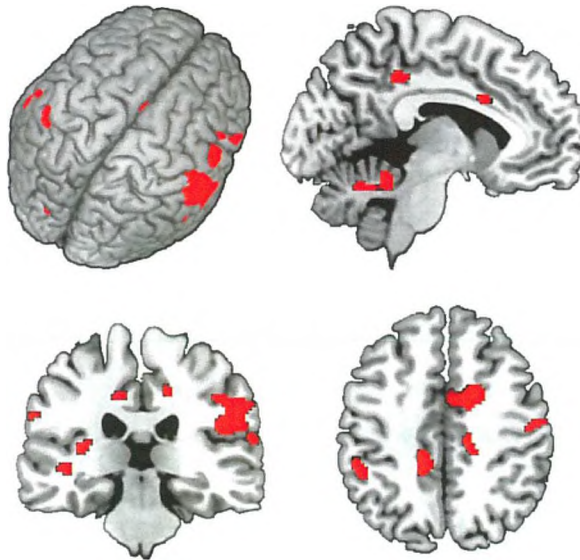


Figure 6.9. Brain regions associated with later (unpredicted) event occurrence. $P_{FDR} < 0.05$, corrected for multiple comparisons.

| Brain Region | Side | MNI Coordinates | | | Z-score | T value |
|-----------------------------|------|-----------------|-----|-----|---------|---------|
| | | x | y | z | | |
| (Pre)-SMA | R | 6 | 0 | 48 | 4.02 | 6.13 |
| IFC (P.Triangularis; BA 45) | R | 60 | 24 | 18 | 3.24 | 4.34 |
| Precentral gyrus | R | 48 | 2 | 30 | 3.55 | 5.04 |
| Postcentral gyrus | R | 62 | -18 | 38 | 4.54 | 8.13 |
| IPL | L | -48 | -42 | 44 | 3.18 | 4.21 |
| Supramarginal gyrus (BA 2) | R | 58 | -26 | 38 | 5.49 | 13.29 |
| | L | -64 | -28 | 30 | 3 | 3.85 |
| ACC (BA 32) | R | 18 | 44 | 8 | 3.34 | 4.55 |
| MCC | R | 16 | -28 | 44 | 3.13 | 4.1 |
| | L | -12 | -34 | 40 | 4.39 | 7.54 |
| STC | R | 50 | -8 | -2 | 4.14 | 6.66 |
| | L | -48 | -4 | -2 | 3.14 | 4.13 |
| Fusiform gyrus (BA 37) | L | -22 | -48 | -14 | 3.9 | 5.96 |
| Cerebellum (Lob. V,VI) | R | 10 | -44 | -18 | 3.68 | 5.35 |
| Cerebellar vermis | - | 0 | -50 | -22 | 3.59 | 5.13 |

Table 6.6. Significant brain areas associated with later (unpredicted) event occurrence.

Omitted event-related activity; Post-change 'Absent' (C3) > Post-change 'Predicted' (C1)

The non-occurrence of expected event was associated with increase in BOLD activity in multiple cortical brain regions including, LPFC, pre-SMA, VMPFC, MCC, PCC and insula cortex, as shown in Figure 6.10 and summarised in Table 6.7.



Figure 6.10. Brain regions associated with omitted event. $P_{\text{FDR}} < 0.005$, corrected for multiple comparisons.

| Brain Region | Side | MNI Coordinates | | | Z-score | T value |
|----------------------------|------|-----------------|-----|-----|---------|---------|
| | | x | y | z | | |
| (Pre)-SMA | R | 8 | 24 | 54 | 3.52 | 4.95 |
| | L | -2 | 2 | 46 | 3.23 | 4.31 |
| SMF cortex (BA 8) | L | -4 | 26 | 54 | 3.77 | 5.59 |
| SFC | L | -14 | 18 | 54 | 3.41 | 4.71 |
| MFC | R | 38 | 26 | 32 | 5.01 | 10.32 |
| IFC (BA 9) | R | 56 | 20 | 26 | 5.02 | 10.37 |
| | L | -36 | 32 | 4 | 3.64 | 5.25 |
| Middle orbital cortex | R | 12 | 40 | -6 | 3.73 | 5.48 |
| IPL | L | -58 | -36 | 38 | 5.36 | 12.38 |
| Supramarginal gyrus (BA 3) | R | 64 | -20 | 38 | 4.99 | 9.95 |
| ACC (BA 24) | L | -2 | 14 | 26 | 3.7 | 5.39 |
| MCC (BA 24) | R | 8 | -20 | 44 | 4.49 | 7.95 |
| | L | -12 | -32 | 46 | 5.04 | 10.47 |
| PCC | L | -8 | -44 | 8 | 3.52 | 4.95 |
| STC (BA 21) | L | -40 | -10 | -10 | 4.93 | 9.89 |
| Insula Lobe (BA 13) | L | -32 | 14 | -12 | 3.28 | 4.41 |
| Precunes (BA 31) | R | 4 | -50 | 40 | 4.08 | 6.5 |
| Lingual gyrus (BA 18) | L | -2 | -80 | -4 | 4.61 | 8.4 |
| Fusiform gyrus | R | 28 | -56 | -10 | 5.13 | 11 |

Table 6.7. Significant brain areas associated with with omitted event.

6.2.3.3 Parametric modulation

Modelling trial-by-trial learning by time using a parametric contrast (post-learning) showed prefrontal, medial prefrontal cortex, posterior parietal cortex, insula cortex, ventral striatum, thalamus and midbrain activity correlated positively with forming expectations about receiving rewards which results in reinforcement, as shown in Figure 6.11 and summarised in Table 6.8.

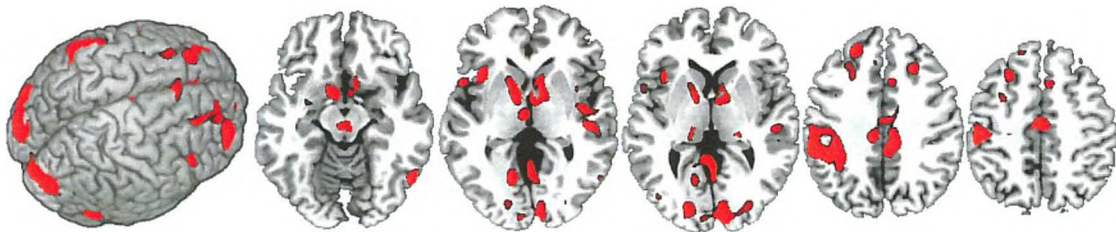


Figure 6.11. Brain regions associated with omitted event. $P_{FDR} < 0.005$, corrected for multiple comparisons.

| Brain Region | Side | MNI Coordinates | | | Z-score | T value |
|----------------------------|------|-----------------|-----|-----|---------|---------|
| | | x | y | z | | |
| (Pre)-SMA | R | 8 | 20 | 54 | 3.22 | 4.28 |
| SMF cortex | L | -10 | 32 | 40 | 4.51 | 8.01 |
| MFC | R | 22 | 24 | 38 | 4.91 | 9.8 |
| | L | -34 | 6 | 50 | 3.77 | 5.58 |
| IFC (P.Opercularis; BA 44) | L | -46 | 16 | 12 | 3.6 | 5.16 |
| Precentral gyrus | R | 46 | -12 | 46 | 3.73 | 5.48 |
| IPL (Supramarginal gyrus) | L | -54 | -20 | 36 | 3.77 | 5.59 |
| ACC | L | -6 | 16 | 22 | 3.88 | 5.89 |
| MCC | R | 12 | -32 | 40 | 3.23 | 4.3 |
| | L | -12 | -28 | 42 | 3.79 | 5.63 |
| STC | R | 62 | -14 | 2 | 3.46 | 4.82 |
| MTC (BA 37) | R | 54 | -64 | -2 | 5.2 | 11.38 |
| | L | -42 | -54 | 14 | 3.78 | 5.61 |
| ITC (BA 20) | R | 54 | -58 | -16 | 4.16 | 6.76 |
| | L | -48 | -54 | -8 | 2.81 | 3.51 |
| Insula lobe (BA 13) | R | 42 | -4 | -4 | 4.18 | 6.8 |
| Rolandic operculum | L | -54 | 4 | 8 | 4.29 | 7.18 |
| Lingual gyrus | L | -20 | -72 | -4 | 3.7 | 5.39 |
| Calcarine gyrus | R | 16 | -88 | 10 | 4.47 | 7.84 |
| | L | -8 | -92 | 8 | 3.28 | 4.41 |
| Cuneus | R | 14 | -94 | 16 | 4.64 | 8.56 |
| | L | -12 | -58 | 226 | 3.4 | 4.69 |
| Superior occipital gyrus | R | 28 | -82 | 20 | 4.14 | 6.69 |
| | L | -20 | -90 | 22 | 4.17 | 6.79 |
| Middle occipital gyrus | L | -42 | -78 | 22 | 3.88 | 5.89 |
| Inferior occipital gyrus | L | -52 | -66 | -16 | 3.92 | 6.02 |
| Parahippocampus | R | 28 | -34 | -8 | 3.23 | 4.3 |
| BG (Putamen) | L | -18 | 10 | 2 | 3.2 | 4.29 |
| BG (Pallidum) | L | -14 | 8 | -2 | 3.4 | 4.67 |
| Thalamus | L | -8 | -8 | -4 | 3.82 | 5.73 |
| Midbrain | L | -2 | -14 | -2 | 3.05 | 3.95 |

Table 6.8. Significant brain areas correlated positively with forming expectation and using these expectancies reinforcers to guide goal-oriented behavior.

Positive prediction error (PPE)

The correlation between the BOLD response and the absolute magnitude of positive prediction error was found within the VLPFC, VMPFC, Amygdala, insula lobe, and bilateral striatum, as shown in Figure 6.12 and summarised in Table 6.9.

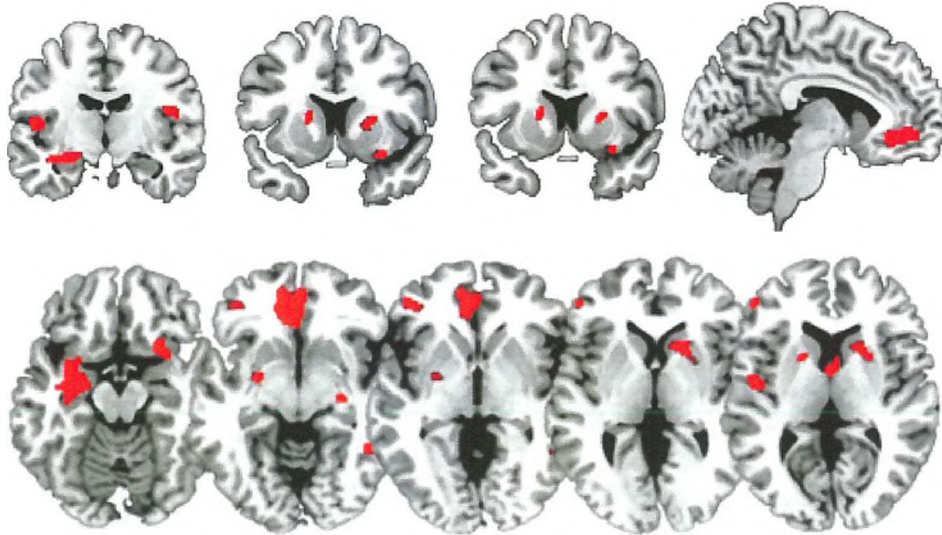


Figure 6.12. Brain regions where the BOLD signal was correlated with the absolute magnitude of positive prediction error $P_{FDR} < 0.05$, corrected for multiple comparisons.

| Brain Region | Side | MNI Coordinates | | | Z-score | T value |
|----------------------|------|-----------------|-----|-----|---------|---------|
| | | x | y | z | | |
| SFC | L | -16 | 46 | 22 | 3.42 | 4.71 |
| IFC (P.Triangularis) | L | -50 | 44 | 6 | 3.41 | 4.71 |
| (P.orbitalis) | L | -38 | 42 | -4 | 3.2 | 4.24 |
| VMPFC (BA 10) | L | -10 | 50 | -4 | 3.81 | 5.69 |
| ACC (BA 32) | L | -4 | 36 | -8 | 3.89 | 5.91 |
| ITC | R | 46 | -50 | -8 | 2.8 | 3.48 |
| Insula lobe | R | 26 | 14 | -16 | 4.5 | 7.97 |
| | L | -26 | 8 | -16 | 3.35 | 4.57 |
| Rolandic operculum | L | -50 | -6 | 10 | 3.48 | 4.85 |
| Amygdala | L | -24 | -6 | -14 | 4.37 | 7.48 |
| Hippocampus | L | -32 | -12 | -14 | 3.06 | 3.96 |
| BG (Putamen) | R | 26 | 10 | 8 | 2.98 | 3.81 |
| | L | -18 | 10 | 10 | 3.29 | 4.43 |
| BG (Caudate nucleus) | R | 18 | 16 | 4 | 3.81 | 5.69 |

Table 6.9. Significant brain areas associated with positive prediction error.

Negative prediction error (NPE)

Activation within the superior and middle temporal cortex, amygdala, and bilateral striatum increased in a linear fashion with the absolute magnitude of negative prediction error as shown in Figure 6.13 and summarised in Table 6.10.

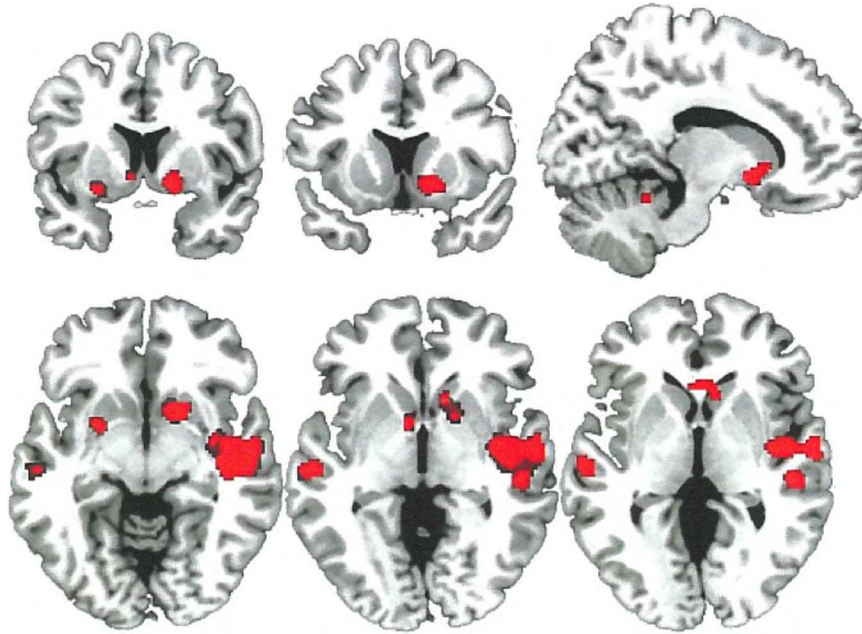


Figure 6.13. Brain regions where the BOLD signal was correlated with the absolute magnitude of negative prediction error $P_{FDR} < 0.05$, corrected for multiple comparisons.

| Brain Region | Side | MNI Coordinates | | | Z-score | T value |
|-------------------|------|-----------------|-----|-----|---------|---------|
| | | x | y | z | | |
| STC | R | 62 | -10 | 0 | 4.4 | 7.6 |
| MTC | L | -56 | -64 | 16 | 3.72 | 5.45 |
| Calcarine gyrus | L | -16 | -72 | 12 | 2.94 | 3.73 |
| Amygdala | L | -20 | 0 | -14 | 3.43 | 4.75 |
| BG (Putamen) | R | 16 | 10 | -8 | 4.09 | 6.53 |
| | L | -24 | 4 | -10 | 3.2 | 4.38 |
| Cerebellar vermis | R | 6 | -46 | -20 | 3.24 | 4.32 |

Table 6.10. Significant brain areas associated with negative prediction error.

6.2.3.4 ROI results

The mean BOLD fMRI response in each ROI including habenula, globus pallidus, striatum, VMPFC for each 'Pre' condition including 'Predicted' (C1), 'Early' (C2a), 'Late' (C2b), 'Absent' (C3) is illustrated in Figure 6.14a. One sample t-tests showed significant increases in BOLD signal in the habenula ROI under pre-change 'Late' (C2b) condition ($F(1, 11) = 19.75$; $p < 0.01$), globus pallidus (GP) ($F(1, 11) = 26.5$; $p < 0.01$), and caudate nucleus ($F(1, 11) = 15.5$; $p < 0.01$). A significant increase in BOLD activation was also found in ventromedial prefrontal cortex (VMPFC) ROI under pre-change 'Predicted' (C1) condition ($F(1, 11) = 9.5$; $p < 0.01$).

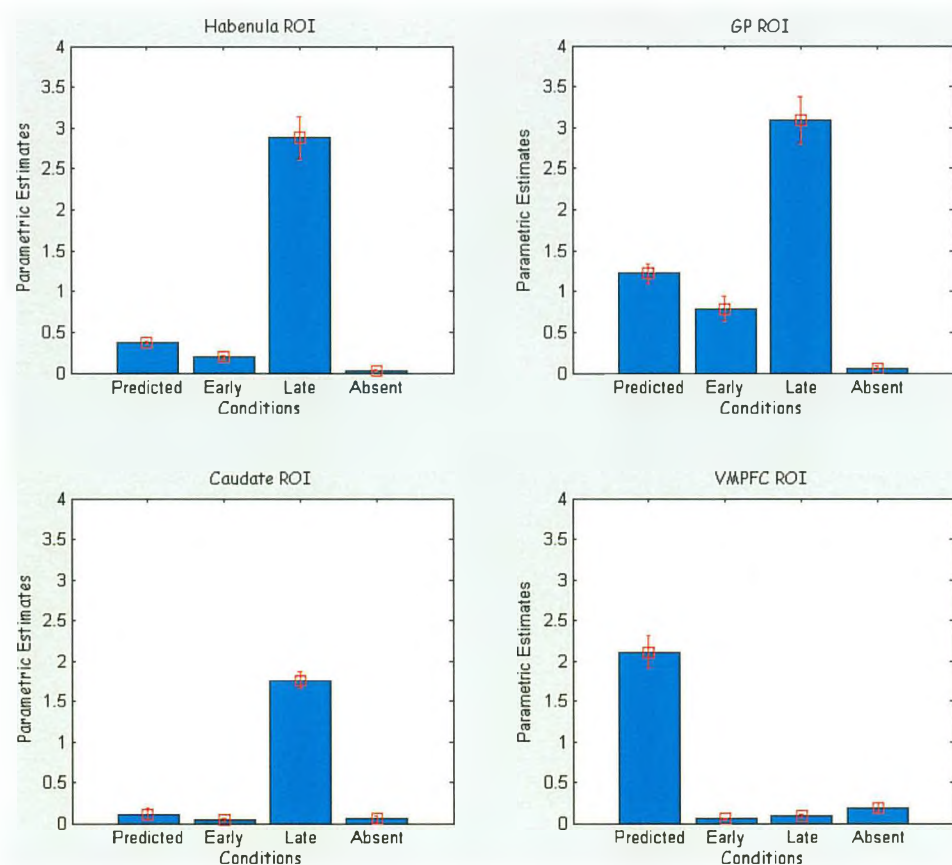


Figure 6.14a. BOLD response in predefined ROI in different conditions of Pre stimulus change.

The mean BOLD fMRI response in each ROI including habenula, globus pallidus, striatum, VMPFC for each ‘Post’ condition including ‘Predicted’ (C1), ‘Early’ (C2a), ‘Late’ (C2b), ‘Absent’ (C3) is illustrated in Figure 6.14b. One sample t-tests showed significant increases in BOLD signal in the habenula ROI under post-change ‘Absent’ (C3) condition ($F(1, 11) = 25; p < 0.01$), globus pallidus (GP) ($F(1, 11) = 19.1; p < 0.01$), and caudate nucleus ($F(1, 11) = 19.5; p < 0.01$). A significant increase in BOLD activation was also found in ventromedial prefrontal cortex (VMPFC) ROI under post-change ‘Early’ (C2a) condition ($F(1, 11) = 24; p < 0.01$).

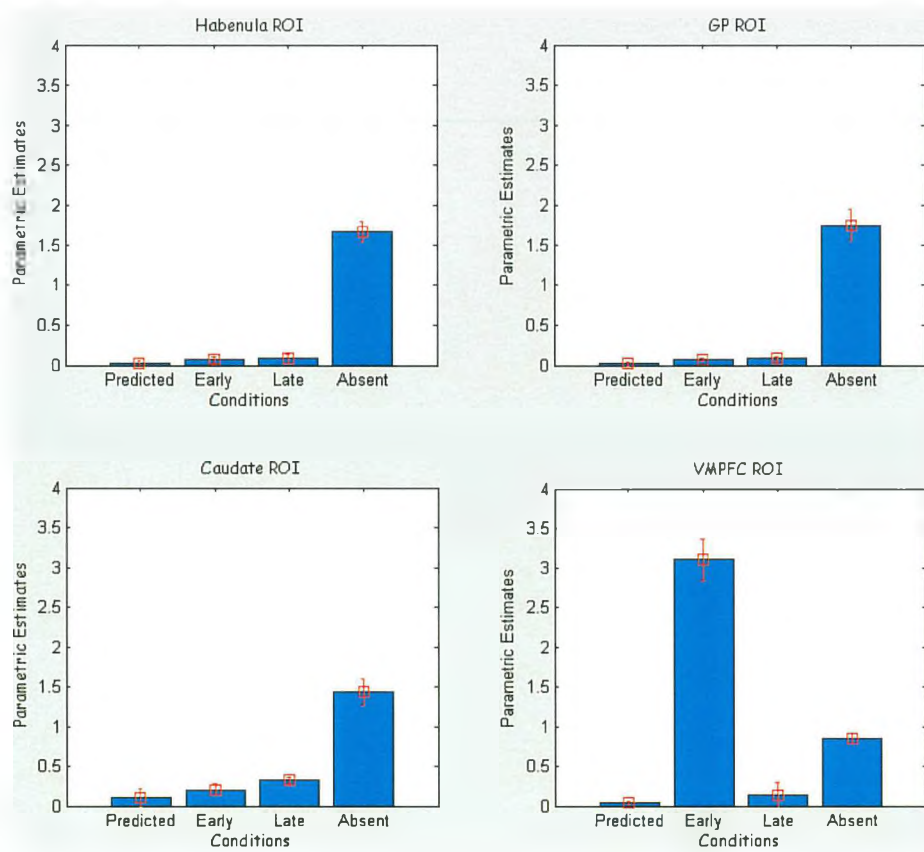


Figure 6.14b. BOLD response in predefined ROI in different conditions of Post stimulus change.

The BOLD fMRI response in each ROI (habenula, globus pallidus, striatum, VMPFC) for a priori theoretical conditions: ‘Neutral’ (pre: C2a); ‘Expect’ (pre: C1 and pre: C3); ‘Confirm’ (post: C1); ‘PPE’ [positive prediction error] (post: C2a);

'NPE' [negative prediction error] (pre: C2b and post: C3) are shown in Figure 6.14c. These data show that the effects of positive and negative prediction error are clearly dissociable between conditions and from each other across the predefined brain regions.

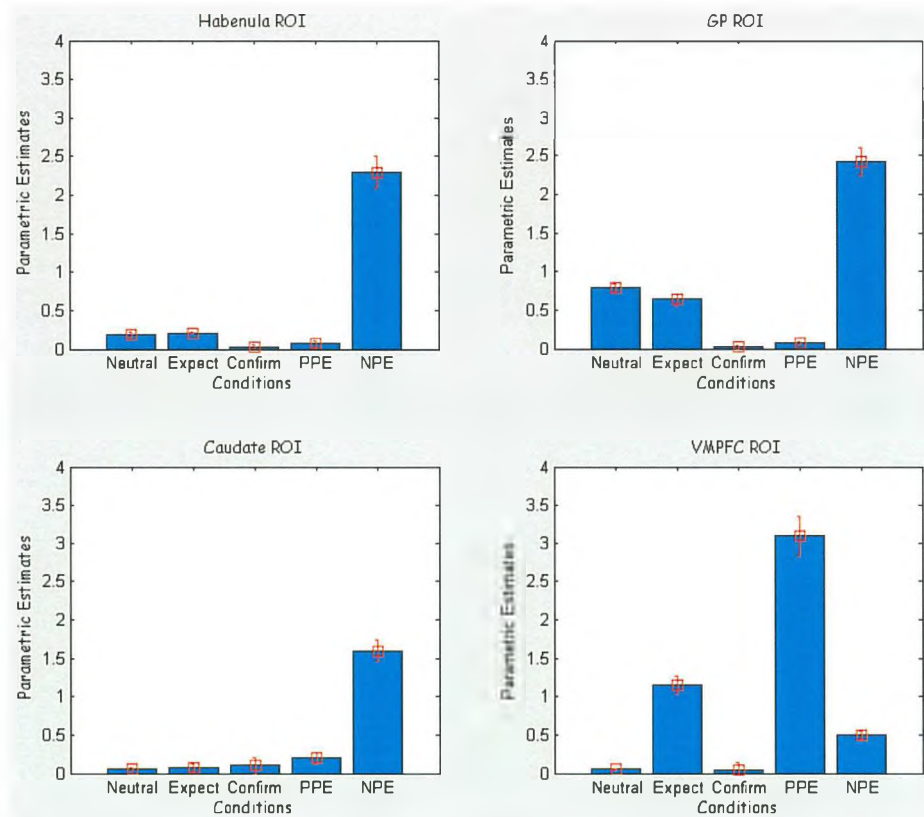


Figure 6.14c. BOLD response in predefined ROI in different conditions for a priori theoretical conditions.

6.2.4 Discussion

The present study aimed to investigate the role of the sub-cortical structures in mediating reward-learning process and how the human brain behaves during a reward-related learning paradigm, specifically the prediction of rewards and progression of reward learning.

The analysis of the behavioural data in learning blocks suggested that reaction times (RT) were influenced by the motivational feedback or rewards. Reaction times were adjusted after the incentive outcomes (scores), and RT was more likely to decrease in subsequent trials. This can be shown clearly by looking at the mean RT of the first bin compare to the RT of the subsequent bin in the same run or block (Figure 6.3). Moreover, RT was more likely to decrease from one run to another. This can be shown clearly by looking at the mean RT of the first bin (in the first learning session compare to that of the first bin in the second learning session or block (Figure 6.3). Therefore, this suggests that feedback about the current performance was critical to the subjects and was used to regulate and adjust behaviour in a trial-by-trial fashion.

Several findings related to different aspects of reward-associated learning including the prediction and acquisition of reward associations and their modulation as learning progresses were observed in the results. First, reward prediction process in learning context, in which the subject always received feedback or rewards, modulates neural activity in multiple brain regions, including the DLPFC, MPFC, posterior parietal cortex, olfactory cortex, ACC, MCC, in addition to the sub-cortical structures including striatum, thalamus and midbrain regions. These regions may be involved in reward prediction based on immediate outcome, as the learning phase in this experiment involves rewards at fixed (predictable) interval timing. This is in accordance with previous studies in mediating reward prediction (Tanaka et al., 2004; Berns et al., 2001; McClure et al., 2003; Aharon et al., 2001; Marco-Pallarés et al., 2007).

Second, brain activations associated with prediction of an event in unpredictable context were observed in the DLPFC, superior orbitofrontal cortex, ACC, MCC, insula cortex, parahippocampus. In addition, striatum, and midbrain region were also found strongly activated. This is an interesting finding as the striatum-particularly the caudate nucleus was found active in the learning associations that varied in their predictability (Delgado et al. 2000, 2005; Marco-Pallarés et al., 2007). Moreover, the findings here are in compliance with the physiological (Fiorillo et al., 2003) and neuroimaging studies (Aron et al., 2004b) showing that dopaminergic neurons in the midbrain are sensitive to predictability by varying their firing rates according to uncertainty. It was also found that this midbrain activity correlated with striatum activity as a target of such dopaminergic projections (Aron et al. 2004b).

Third, different brain regions were found to be active when an expected event-related reward is omitted. These regions involve DLPFC, MPFC, anterior and posterior cingulate cortex, in addition to, putamen, MD nucleus of thalamus, habenula and midbrain regions. The results here suggest that subjects are surprised when an expected event didn't occur at the expected time. This omission of an expected outcome results in a negative reward prediction error (NPE) (in simple words, when outcomes are worse or less than expected) (McClure et al., 2003; O'Doherty et al., 2003). The findings here are in agreement with prediction learning studies in humans (Berns et al., 2001; McClure et al., 2003; Aharon et al., 2001; Breiter et al., 2001; Delgado et al., 2005; Elliott et al., 2004; Kirsch et al., 2003; O'Doherty et al., 2002, 2004; Pagnoni et al., 2002). Some studies have shown that these regions are involved in negative prediction error signaling during fear conditioning (Burgos-Robles et al., 2007; Kalisch et al., 2006; Lebrón et al., 2004; Milad and Rauch, 2007; Spoormaker

et al., 2011). In monkeys, neurophysiological studies have shown that dopaminergic neurons in the midbrain terminate firing in response to the predicted but omitted reward deliverance which indicates that the monkey experiences a negative prediction error (NPE) (Schultz et al., 1997, 1998). To further assess the relationship of the observed brain activation with the negative prediction error, the a priori ROI including (habenula, striatum, globus pallidus) were identified for each 'Pre' and 'Post' conditions including 'Predicted' (C1), 'Early' (C2a), 'Late' (C2b), 'Absent' (C3) (as will be discussed later).

A fourth finding was that the positive prediction error (PPE) was associated with increased activation in the SMA, VMPFC, IFC, IPL, ACC, MCC, insula cortex, superior orbital frontal cortex, parahippocampus, putamen and cerebellum. This comes in line with previous studies that show a similar pattern of activation in the processing of positive prediction error in learning paradigms (Roesch and Olson, 2003; Tobler et al., 2006; McClure et al., 2003; O'Doherty et al., 2003, 2006; Tremblay and Schultz, 2000; Critchley et al., 2001, Tanka et al., 2004; Marco-Pallares et al., 2007). Interestingly, among these regions the VMPFC was observed significantly active when the event occurred earlier or later than an expected time. This might suggest that VMPFC is involved in the estimate of an event's value in order to be adjusted in an upwards manner from trial-to-trial (Plassmann et al., 2007). To determine the relationship between the BOLD signal and the conditions of the paradigm, the VMPFC ROI was identified for each 'Pre' and 'Post' condition including 'Predicted' (C1), 'Early' (C2a), 'Late' (C2b), 'Absent' (C3) (as will be discussed later).

In the parametric modulation, trial-by-trial learning in time modulated the activity in the fronto-parietal network and mesencephalic (midbrain) dopamine system. The activity of the fronto-parietal network might reflect the processing of positive feedback information at the beginning of the learning process, which induced working memory functions for the pre-requisite processes to adjust the responses upwards (Koch et al., 2008). The mesencephalic dopaminergic system enhances the reinforcement learning mechanism in the basal ganglia and sharpens the representations of associative values in the prefrontal cortex that are used to guide reinforcement-based decisions.

Interestingly, the correlation between the BOLD response and the absolute magnitude of positive prediction error was found within the VLPFC, VMPFC, amygdala, insula lobe, and bilateral striatum. On the other hand, activation within the superior and middle temporal cortex, amygdala, and bilateral striatum increased in a linear fashion with the absolute magnitude of negative prediction error.

The ROI analysis revealed that the BOLD fMRI response in habenula and globus pallidus (GP) were significantly increased and associated with the omission of an expected event. This is striking as the habenular neurons are excited by the omission of reward. In contrast, the habenula was observed inhibited in a situation of positive prediction. These findings are in accordance with previous studies showed that rewarding stimulation suppresses the habenular activity (Gallistel and Tretiak, 1985; Matsumoto and Hikosaka, 2007) and recent studies showed that activation in habenula was associated with negative reward prediction errors (Salas et al., 2010;

Ide and Li, 2011). Moreover, it was also observed that the activity of the globus pallidus is significantly increased when the habenula activity increased.

However, in this ROI analysis, it is important to acknowledge that-in humans-the habenula's size is very small, around 30 mm³ in volume and the habenula ROI that was identified in this study by growing a sphere of (10 mm radius) centred at the peak of the activation was much larger than the actual size of the habenula which means that the surrounding nuclei were included in that ROI.

The habenula (Hb) is a small nucleus located above the thalamus at its posterior end close to the midline. It is divided into two segments; a medial (MHb) and lateral (LHb) nucleus (Lecourtier and Kelly, 2007). The unique position of habenular complex raises the importance of this structure in contributing in a wide range of cognitive functions including motivation behavior and reward-based learning (Lecourtier and Kelly, 2007; Hikosaka et al., 2008). The anatomical connections of the habenular nuclear complex indicate that it is a link between prefrontal brain areas and midbrain nuclei (Sutherland, 1982). It receives excitatory inputs from both the cerebral cortex (prefrontal areas) and GPi and exerts influence on the dopaminergic midbrain regions including the ventral tegmental area and the substantia nigra pars compacta (SNc), as shown in Figure 6.15 (Herkenham and Nauta, 1979; Sutherland, 1982; Ellison, 2002; Bianco and Wilson, 2009). The GPi excitatory projections to the habenula (lateral part, LHb) might explain the relationship between the habenula and the globus pallidus observed in the current results. This suggests that the GPi may initiate reward-associated signals via its excitatory effects on the habenula, which then influences the dopaminergic midbrain system through inhibitory projections (Hong

and Hikosaka, 2008). These connections, from the GPi to the habenula, might be critical in linking the sub-cortical structures to the limbic system in order to mediate the reward-based learning mechanism (Hong and Hikosaka, 2008; Matsumoto and Hikosaka, 2009; Hikosaka et al., 2008). This is further supported by electrophysiological studies, for example, Christoph (1986) demonstrated that electrical stimulation of the lateral habenula induces inhibitions in the midbrain dopamine neurons. In addition, it was also observed that even weak electrical stimulation of the habenula, particularly the lateral part, elicited strong inhibitions in dopamine neurons (Matsumoto and Hikosaka, 2007, 2009).

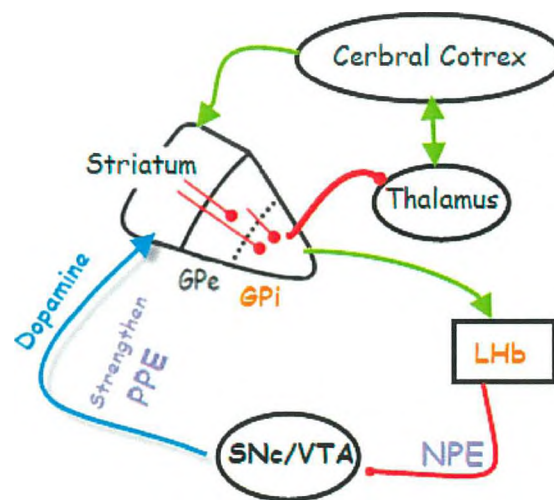


Figure 6.15. Circuit diagram showing the relationship between the habenula (lateral part, LHb) and the basal ganglia. Excitatory, inhibitory and modulatory projections are illustrated with green arrow, red filled circles and blue arrow, respectively. SNc, substantia nigra compacta; VTA, ventral tegmental area. Negative prediction error (NPE) signals are transmitted from the GPi, through excitatory connections, to the LHb and then to the SNc/VTA. The SNc/VTA sends signals to strengthen the positive prediction error (PPE) to the striatum.

Furthermore, lesion studies showed that habenula lesions lead to increased activation of dopaminergic neurons (Lisoprawski et al., 1980). Similar studies in human showed that the negative feedback indicating task failure activates the

habenula during the performance of a Motor Prediction task (Ullsperger and von Cramon, 2003). Taken together with the present results, these findings suggest that the GPi activity leads to increased excitatory effect on habenula which then leads to inhibition of dopamine neurons resulting in suppression of behaviour associated with the omission of an expected event (Hong and Hikosaka, 2008; Matsumoto and Hikosaka, 2007, 2009).

Another important finding was that the ROI analysis revealed that the BOLD fMRI response in the striatum was significantly increased and correlated more with negative prediction errors when an expected event was withdrawn. This finding might reflect the neural responses that are typically elicited by the surprise mechanism. This is consistent with previous studies that showed that the activation in the striatum was related to the NPE (i.e., during the absence of expected reward)(Rodriguez et al., 2006; Knutson et al., 2001; O'Doherty et al., 2003; Morris et al., 2012), however, other studies showed that striatal activity was associated with positive prediction error (i.e., when an expected reward obtained) (Berns et al., 2001; McClure et al., 2003; Pagnoni et al., 2002), others found it associated with positive outcomes (Ullsperger and von Cramon, 2003). This discrepancy, between the neuroimaging findings of striatal activation, might be due to distinct features of the behavioural paradigms used.

Moreover, another interesting finding was that the activity of the VMPFC increased and was associated with positive prediction error when the event occurred earlier or later than an expected time. It was also observed that VMPFC activity decreases when the event becomes more predictable. This might reflect that the VMPFC is involved in the reward-based expectation prior to decision making and

after receiving rewards (Sescousse et al., 2010; Smith et al., 2010). The findings here suggest that this region may be involved in assessing or estimating the (reward or event) value before taking action. This interpretation is in accordance with previous studies demonstrating the role of VMPFC in immediate prediction of rewards (Tremblay and Schultz, 2000; Critchley et al., 2001), action selection based on reward prediction (Rogers et al., 1999; Rolls et al., 2000; O'Doherty, et al., 2003) and assessing of subjects' valuations that comes from reinforcement learning models (Tanaka et al., 2004; Behrens et al., 2008; Gläscher et al., 2009; Wunderlich et al., 2010). This was further supported from lesion studies where patients with lesion in the VMPFC tend to have impaired decision-making and autonomic responses deficits (Barrash et al., 2000). These ROI data show that the effects of positive and negative prediction error are clearly dissociable between conditions and from each other across the predefined brain regions.

In conclusion, the findings here show that the feedback is crucial for learning and in adjusting future motor behaviour. As a novel finding, the BOLD response in the habenula and GPi was observed to be increased by the absence of an expected event or no reward-predicting event, and inhibited or decreased by the occurrence of expected event or reward-predicting event. However, this should be taken with caution as the BOLD fMRI is obviously blind to the neurotransmitter changes. Given that the haemodynamic responses measured by fMRI may reflect mainly inputs (synaptic input and local interneuron processing) to an activated region rather than the spiking activity of projection neurons (Logothetis, 2001, 2003). Therefore, it is difficult to interpret whether the observation of increased fMRI signal in the habenula or GPi is excitation or inhibition as both processes are active. In the

neurophysiological studies, it is well documented that the GPi sends excitatory neural projections to the habenula which leads to increased inhibitory projections from the habenula to the dopaminergic midbrain neurons, thus resulting in suppression of motor behaviour associated with the omission of an expected event or rewards (Hong and Hikosaka, 2008; Matsumoto and Hikosaka, 2007, 2009).

The current results echo the previous mentioned studies, demonstrating that the dopamine-dependent mechanisms enhance reinforcement learning signals, and extend them to involve some sub-cortical structures and midbrain regions (i.e., habenula). It is challenging to speculate the role of these region in mediating reward-based learning and decision making processes. Future work, could build on the current experiment by zooming into the sub-cortical structures with high spatial resolution fMRI using the advantages of the ultra-high magnetic field. This would allow the habenular parts (medial and lateral) to be specified and the relationship with other basal ganglia nuclei investigated.

Chapter 7

7.1 General discussion

The experiments in this thesis have explored aspects of cognitive function and motor learning-based prediction mechanisms using ultra-high magnetic field (UHF) as it provides high signal-to-noise ratio (SNR) and high BOLD contrast-to-noise ratio (CNR) for fMRI, allowing high spatial resolution data to be collected (Olman et al., 2003). A dual-echo image acquisition was used to acquire a gradient-echo images at two echo times to optimize the detection of neural activity across sub-cortical and cortical brain regions which have different T_2^* values, with a weighted summation of the data being shown to be the optimal analysis method to enhance BOLD sensitivity across cortical and sub-cortical areas.

The functional results of inhibiting an initiated response (Chapter 4, Experiment 1), the (WAIT > GO) contrast as a measure of response inhibition, was associated with activation in striatum and thalamus regions, in addition to activation of the SMA and right IFC. These results are similar to prior studies (i.e., Aron and Poldrack, 2006; Chikazoe et al., 2009; Cai et al., 2011) in which the same brain regions were found to be significantly active during successful stopping trials in the stop signal and GO/NO-GO paradigms. This neural network is concordant with a “hyperdirect” pathway, in which the prefrontal cortex sends fast and direct activity to the STN. Furthermore, the STN receives direct input from two main foci the pre-SMA and the rIFC (Inase et al., 1999; Aron et al., 2007b). These findings implicate that these regions are key nodes of this putative neural network.

In Experiment 2, the results of response suppression in the context of cancelling an ongoing action, the NO-GO > GO contrast as a marker of response inhibition, was associated with activation in relatively similar brain regions to those found in Experiment 1. However, it was observed that the dorsolateral prefrontal cortex (DLPFC) and anterior cingulate cortex (ACC) were more involved and engaged in cancelling an initiated motor action compared to the response withholding process in Experiment 1. This may be attributed to the role of the DLPFC in the on-line maintenance and manipulation of information which reflects the working memory function (Mostofsky et al., 2003; Simmonds et al., 2008). On the other hand, the involvement of ACC might reflect its role in conflict monitoring (Carter et al., 1998, 2000; MacDonald et al., 2000; Paus, 2001). The ACC was found most active in the GO/NO-GO paradigm rather than the GO/WAIT paradigm and this may be a result of the different task-demands, with the subject needing to withhold the motor response under (WAIT condition) in GO/WAIT version whilst the subjects need to cancel the initiated motor action or switching off the motor program under (NO-GO) condition in the GO/NO-GO paradigm. Therefore, the DLPFC and ACC regions seem to have distinct, complementary roles in a neural network serving inhibitory control.

The results of inhibiting an initiated response in an unpredicted context (Experiment 3) recruited a similar pattern of activation as was observed in Experiment 1. This includes activation in the DLPFC, M1, bilateral inferior parietal lobules, MCC and IFC, in addition to activation in the striatum and midbrain regions. However, it is important to note that this neural network might be also involved in mediating prediction uncertainty as it is in agreement with previous studies (i.e., Huettel et al., 2005; Grinband et al., 2006).

Direct comparison between studies (Chapter 4) points to the critical involvement of a putative neural network (including SMA, IFC, and thalamus) in implementing *withholding* strong response tendency. It was also found that the response *cancelling* process is associated with increased activation in bilateral DLPFC and ACC regions. In addition, the response withholding process in an unpredicted context-was compared to the same process in a predicted manner which revealed sub-cortical activation increases in bilateral striatum and bilateral thalamic nuclei. Moreover, the results of the conjunction analysis in order to examine commonalities between the neural basis of different forms of inhibition, withholding of pre-potent response in Experiment 1 and cancelling an initiated motor response in Experiment 2, demonstrated that the rIFC is the only region that shows the significant common activation across both tasks. These findings were further supported by the results of the ROI analyses using predefined ROI across all experiments in Chapter 4, which revealed significant correlations with the behavioural RT measure. Considering these studies, it is clear that both distinct and common brain regions are associated with inhibition mechanisms across different paradigms.

A common behavioural finding over Experiments 1, 2 and 3 was the ‘switch cost’, with reaction times (RT) on switch trials being longer than on repeat trials in the GO task across all experiments. This result is in accordance with the existence of an endogenous ‘task-set reconfiguration’ (TSR) process which includes shifting attention between the different aspects of the task, retrieving goals, maintaining the state of readiness (activating working memory), activation of relevant task-representations and inhibition of irrelevant task-representations (Monsell, 2003). This dynamic process is a pre-requisite of the task-specific processes in order to achieve flexible

goal-directed behaviour and improve performance. Another possible interpretation is that the switch cost is attributable to conflict arising from working memory due to the recent performance of two different tasks (Allport et al., 2000; Gilbert et al., 2002; Yeung et al., 2003).

In Chapter 5, the GO/WAIT paradigm was used to compare cognitive function in Tourette subjects (TS) to healthy control subjects (CS) (Experiment 4). Results showed significantly increased activation in the dorsolateral prefrontal cortex (DLPFC)-particularly middle frontal cortex, and less activity in the striatum during the performance of motor response inhibition in the TS group. This result might indicate that increased engagement of the DLPFC reflects a compensatory mechanism to the dysfunction of the fronto-striatal circuits in the TS group (Marsh et al., 2007; Jackson et al., 2011). The increased BOLD response in DLPFC region most likely associated with increasing control over tics due to the altered patterns of control over motor outputs in TS that can arise as a result of changed intracortical connectivity (Makki et al., 2009; Neuner et al., 2010; Plessen et al., 2004; Jackson et al., 2011, 2012). The fronto-striatal dysfunction extended to involve reduced engagement of the striatum in the TS group. However, there are some issues that should be considered when discussing these results including, the small sample number of the subjects included in this experiment, the wide range of motor and vocal tic severity and finally, the medication status of the Tourette subjects.

In Experiment 4, the results of the correlation analysis demonstrated a significant positive linear relationship between the BOLD response in the pre-SMA and ACC predefined ROIs and the RT behavioural measures in the healthy control

group. Furthermore, for the TS group, tic severity was highly positively correlated with BOLD signal in the DLPFC. The increased BOLD response is associated with increased tics, reflecting that the control over motor tics might come through the inhibition of motor cortex excitability by involving prefrontal cortex during movement preparation and execution (Jackson et al., 2012). These findings support the view that individuals with TS develop the ability to control the urge to tic by enhancing cognitive control (Jackson et al., 2011; Neuner et al., 2011). In general, these results support the hypothesis that individuals with TS are unable to recruit critical cortical and sub-cortical nodes that are typically involved in mediating behavioural inhibition.

In Chapter 6, the results of Experiment 5 showed that feedback is critical for learning and adjusting target-orientated behaviour in advance. It was found that reward prediction-based learning, in which the subject always received feedback or rewards, modulates neural activity in the fronto-parietal network and mesencephalic (midbrain) dopamine system. This fronto-parietal network activity may reflect the involvement of working memory functions in order to process the positive feedback information at the beginning phase of the learning process (Koch et al., 2008). The mesencephalic dopaminergic system enhances the reinforcement learning mechanism in the basal ganglia and sharpen the representation of task-elements in the prefrontal cortex that are used to guide reinforcement-based decisions.

The results of the parametric in time and ROI analysis in Experiment 5 showed that BOLD response in the habenula and GPi increased by the omission of an expected event and decreased by the occurrence of an expected event or reward-

predicting event. This novel finding suggests that the habenula might be a source of negative prediction error as it was inhibited by positive hedonic stimuli (Matsumoto and Hikosaka, 2007). It was also observed that the BOLD fMRI response in the striatum was significantly correlated with negative prediction errors when an expected event was omitted. This finding might reflect the neural responses that are typically elicited by surprise mechanism. This is consistent with previous studies which have shown that activation in striatum is associated to the NPE (Rodriguez et al., 2006; O'Doherty et al., 2003; Morris et al., 2011). Another important finding was that activity of the VMPFC is associated with positive prediction error when the event occurred earlier or later than an expected time. It was also observed that VMPFC activity decreased when events became more predictable. This might reflect that the VMPFC is involved in reward-based prediction prior to decision making and after receiving rewards (Sescousse et al., 2010; Smith et al., 2010). The findings here suggest that this region may be involved in assessing or estimating the (reward or event) value before taking action.

The analysis of the behavioural data in learning runs suggested that reaction times were influenced by the motivational feedback and the RTs were adjusted after the incentive outcomes (scores). RT decreased in subsequent trials as was observed clearly by comparing the mean RT across bins, and furthermore, RT was more likely to decrease from one run to another. Therefore, the findings showed that the feedback about the current performance was critical to the subjects and was used to regulate and adjust behaviour in a trial-by-trial manner. In general, the results of Experiment 5 support the view that dopamine-dependent mechanisms enhance reinforcement learning in the basal ganglia-particularly striatum and strengthen the associated task-

information in the prefrontal cortex that are used to form expectations about receiving rewards which results in reinforcement (Schultz et al., 1992, 2000).

This thesis aims to investigate the basal ganglia function in cognitive and motor tasks using ultra-high field MRI (7 Tesla). The basal ganglia activation (BG) was consistently observed in all functional imaging studies in this thesis, challenging the traditional view that the BG have been regarded as motor structures that regulate the initiation of movements. The BG was found activated in the cognitive (GO/WAIT) tasks and Motor Prediction task, supporting the notion that the BG mediates not only motor function but also non-motor (cognitive) functions. Importantly, the parallel loops originate in broad regions of the cortex, engage particular subdivisions of the basal ganglia and thalamic nuclei, and ultimately projects in the prefrontal cortex can explain the similar pattern of activation in cortical and related basal ganglia subdivisions that was demonstrated in the results (Alexander and Crutcher, 1990; Schultz et al., 2000). fMRI at ultra-high fields (7 Tesla) has shown to provide better spatial resolution and higher sensitivity for BOLD signal contrast, suggesting its suitability for investigating basal ganglia and midbrain nuclei functions in humans. For example, a reward-related task that was used in Experiment 5 probed both reward prediction and reward outcome behavioural constructs that mediated by the midbrain nuclei (i.e., Habenula). Although high resolution fMRI revealed significant BOLD-related activity in the midbrain regions it was difficult to identify these structures as they are fine and nearby nuclei with high iron content. In addition to that, the lack of the midbrain atlas for neuroimaging data is another limitation. It is promising that high resolution fMRI will help investigating dysfunction of the direct and indirect circuits in basal ganglia disorder such as Parkinson's disease (PD), and Tourette syndrome (TS).

7.2 Using fMRI to measure neural inhibition

Functional magnetic resonance imaging (fMRI) is used to detect the localized haemodynamic changes in a brain region in response to neural activity (Ogawa et al., 1992). Logothetis and colleagues (2001) have shown that the haemodynamic responses measured by fMRI may reflect mainly inputs (synaptic input and local interneuron processing) to an activated region, rather than the spiking activity of projection neurons from that region. Thus, the BOLD signal might only reflect a fraction of the changes in neural activity in response to a neurocognitive process or task.

Another important consideration about the interpretation of the fMRI BOLD signal is whether the observation of increased fMRI BOLD signal in a particular brain region is due to facilitation (when glutamate, the primary excitatory neurotransmitter in the brain is released into synapses) or inhibition (when GABA, the primary inhibitory neurotransmitter in the brain is released into synapses) (Poldrack, 2006). When glutamate is released into synapses, it leads to increased glucose uptake from the blood vessels which results in increased BOLD signal (Shulman et al., 1998). However, it remains possible that the inhibitory signals can result in decreased neural firing, but an increase in fMRI signal (Lauritzen 2001). For example, in Experiment 5, the increased signal in the habenula nucleus in a condition of negative prediction error may reflect the activity of GABAergic signals arising from the habenula which could result in decreased firing of midbrain dopaminergic neurons when an expected reward does not occur. Moreover, increased signal in the GPi was associated with increased signal in habenula when the predicted event omitted. It is important to note that in neurophysiological studies, it is shown that the GPi sends excitatory neural projections to the habenula, which leads to increased inhibitory signals becoming

projected from the habenula to the dopaminergic midbrain neurons, thus resulting in suppression of motor behaviours associated with the omission of an expected event or reward (Hong et al., 2008; Matsumoto and Hikosaka, 2007, 2009). Therefore, the interpretation of fMRI BOLD signal changes must take into account the fact that the BOLD fMRI is blind to the neurotransmitter changes.

7.3 Future directions

The balance between excitation and inhibition modulates the circuits in the brain which results in adjusting behaviour and flexible interaction with the environmental changes. An alternative MR approach for assessing brain function, which allows the direct detection of endogenous metabolic pathways involved in excitatory (glutamate) and inhibitory (GABA) neurotransmission, is *in vivo* magnetic resonance spectroscopy (MRS). MRS is used to quantify the neurotransmitter concentration in particular regions of the brain. For example, this technique can be used to quantify changes in the concentration of GABA (the primary inhibitory neurotransmitter) in a specific region during task performance. This technique can give a unique insight into the relationship between physiology and behaviour. It can also elucidate whether the effect of projections from one brain region to another is inhibitory or excitatory. For example, MRS can provide further understanding of the relationship between the habenula and the GPi that was described in Experiment 5.

Given the strong connectivity between the putative stopping nodes including the pre-SMA, IFG, and the STN, the use of transcranial magnetic stimulation (TMS) allows the measurement of different parameters (e.g timing) of excitatory and inhibitory process within this neural network. TMS can be used in a paired-pulse

(ppTMS) protocol to study aspects of cortical excitability and inhibition with high degree of specificity. Moreover, the combination of TMS with fMRI might shed light on the functional connectivity and specificity of cognitive function in the human brain. This combined technique can be used to predict the changes in sub-cortical structures by modulating the connectivity between cortical and sub-cortical structures. For example, it might be possible to differentiate between the involvement of “hyperdirect” and “indirect” pathways of the basal ganglia in inhibitory control. Moreover, ppTMS combined with fMRI can give insights into the neural basis of cognitive and behavioural abnormalities observed in individuals with Tourette syndrome and provide clinical implications for therapeutic use.

7.4 Conclusion

Ultra-high magnetic field (UHF) provides high signal-to-noise ratio (SNR) and high BOLD contrast sensitivity and the dual-echo approach provides increased data acquisition efficiency when both sub-cortical and cortical regions are of interest. The sensitivity of fMRI BOLD signal can be significantly increased by combining data from dual-echo sequences compared to conventional single-echo time acquisition method. Moreover, combining a weighted summation (ws) is the ideal approach to optimize the BOLD.

The functional imaging results demonstrate that making GO response engages the fronto-striatal pathway, consistent with the so-called “direct pathway” of the basal ganglia. Inhibiting an initiated response recruits the “hyperdirect” pathway of the basal ganglia. In Tourette subjects, the increased engagement of the DLPFC may reflect a compensatory mechanism to the existence of the fronto-striatal circuits

dysfunction in TS group. Moreover, in the Motor Prediction task, the dopamine-dependent mechanisms enhance reinforcement learning in the basal ganglia. It was also observed that the PPE and NPE are signalled in different brain regions. These findings motivate new behavioural paradigms for investigating the control of response tendencies in healthy subjects and individuals with neurological syndromes. This thesis has highlighted that further work needs to be conducted on elucidating the role of the basal ganglia in cognitive function and motor learning using complementary techniques.

References

- Aguirre, G. K. and D'Esposito, M. (2000). Experimental design for brain fMRI. In C. Moonen and T.W. Bandettini (Eds.), *Functional MRI* (pp. 369-380). Heidelberg: Springer-Verlag Berlin.
- Aharon, I., Etcoff, N., Ariely, D., Chabris, C. F., O'Connor, E., and Breiter, H. C. (2001). Beautiful faces have variable reward value: fMRI and behavioural evidence. *Neuron*, *32*, 537-551.
- Albin, R. L., and Mink, J. W. (2006). Recent advances in Tourette syndrome research. *Trends in Neuroscience*, *29*, 175-82.
- Albin, R. L., Young, A. B., and Penney, J. B. (1989). The functional anatomy of basal ganglia disorders. *Trends in Neuroscience*, *12*, 366-375.
- Alexander, G. E. (1994). Basal ganglia-thalamocortical circuits: their role in control of movement. *Journal of Clinical Neurophysiology*, *11*, 420-431.
- Alexander, G. E., and Crutcher, M. D. (1990). Functional architecture of basal ganglia circuits: neural substrates of parallel processing. *Trends Neuroscience*, *13*, 266-271.
- Alexander, G. E., DeLong, M. R., and Strick, P. L. (1986). Parallel organization of functionally segregated circuits linking basal ganglia and cortex. *Annual Review of Neuroscience*, *9*, 357-381.
- Allen, G., Buxton, R. B., Wong, E. C. and Courchesne, E. (1997). Attentional activation of the cerebellum independent of motor involvement. *Science*, *275*, 1940-1943.
- Allport, A. and Wylie, G. (2000). 'Task-switching', stimulus-response bindings, and negative priming. In S. Monsell, and J. Driver (Eds.), *Control of Cognitive Processes: Attention and Performance* (pp. 35-70). Cambridge, MA: MIT.
- American Psychiatric Association (2000). *Diagnostic and Statistical Manual of Mental Disorders*, (4th ed.). Washington, DC: American Psychiatric Association.

- Andres, P. (2003). Frontal cortex as the central executive of working memory: time to revise our view. *Cerebral Cortex*, 39, 871-895.
- Arnold, S. E. and Trojanowski, J. Q (1996). Recent advances in defining the neuropathology of schizophrenia. *Acta Neuropathologica*, 92, 217-231.
- Aron, A. R. (2007a). The neural basis of inhibition in cognitive control. *The Neuroscientist*, 13, 1-15.
- Aron, A. R. (2009). Introducing a special issue on stopping action and cognition. *Neuroscience and Biobehavioral Reviews*, 33, 611-612.
- Aron, A. R. (2011). From reactive to proactive and selective control: developing a Richer model for stopping inappropriate responses. *Biological Psychiatry*, 69, 55-68.
- Aron, A. R., Behrens, T. E., Frank, M. J., Smith, S. and Poldrack, R. A. (2007b). Triangulating a cognitive control network using diffusion-weighted MRI and functional MRI. *Journal of Neuroscience*, 27, 3743-3752.
- Aron, A. R., Fletcher, P. C., Bullmore, E. T., Sahakian, B. J., and Robbins, T. W. (2003). Stop-signal inhibition disrupted by damage to right inferior frontal gyrus in humans. *Nature Neuroscience*, 6, 115–116.
- Aron A. R. and Poldrack, R. A. (2005). The cognitive neuroscience of response inhibition: relevance for genetic research in ADHD. *Biological Psychiatry*, 57, 1285-1292.
- Aron, A. R. and Poldrack, R. A. (2006) .Cortical and sub-cortical contributions to stop signal response inhibition: role of the subthalamic nucleus. *Journal of Neuroscience*, 26, 2424–2433.
- Aron, A. R., Robbins, T. W., and Poldrack, R. A. (2004a). Inhibition and the right inferior frontal cortex. *Trends in Cognitive Sciences*, 8, 170-177.
- Aron, A. R., Shohamy, D., Clark, J., Myers, C., Gluck, M.A. and Poldrack, R.A. (2004b). Human midbrain sensitivity to cognitive feedback and uncertainty during classification learning. *Journal of Neurophysiology*, 92, 1144-1152.

- Aron, A. R, and Verbruggen, F. (2008). Stop the presses: Dissociating a selective from a global mechanism for stopping. *Psychological Science*, *19*, 1146 -1153.
- Ashburner, J. and Friston, K. J. (2000). Image registration. In C.T.W. Moonen and P.A. Bandettini (Eds.), *Functional MRI* (pp. 285-299). Heidelberg: Springer-Verlag Berlin.
- Ashburner, J. and Friston, K. J. (2003a). Rigid body registration. In R.S.J. Frackowiak, K.J. Friston, C. Frith, R. Dolan, C.J. Price, S. Zeki, J. Ashburner, and W.D. Penny (Eds.), *Human brain function* (2nd ed.), San Diego, CA: Elsevier Academic Press.
- Ashburner, J. and Friston, K. J. (2003b). Spatial normalization using basis functions. In R.S.J. Frackowiak, K.J. Friston, C. Frith, R. Dolan, C.J. Price, S. Zeki, J. Ashburner, and W.D. Penny (Eds.), *Human brain function* (2nd ed.). San Diego, CA: Elsevier Academic Press.
- Balthasar, K. (1957). Über das anatomische Substrat de generalisierten Tic-Krankheit (maladie des tics, Gilles de la Tourette): Entwicklungshemmung des corpus striatum. *Archiv für Psychiatrie und Nervenkrankheiten*, *195*, 531-549.
- Band, G. P. and van Boxtel, G. J. (1999). Inhibitory motor control in stop paradigms: review and reinterpretation of neural mechanisms. *Acta Psychologica (Amsterdam)*, *101*, 179-211.
- Barnes, D. E., Yaffe, K., Satariano, W. A., and Tager, I. B. (2003). A longitudinal study of cardiorespiratory fitness and cognitive function in healthy older adults. *Journal of American Geriatrics Society*, *51*, 459-465.
- Barrash, J., Tranel, D., Anderson, S. W. (2000). Acquired personality disturbances associated with bilateral damage to the ventromedial prefrontal region. *Developmental Neuropsychology*, *18*, 355-381.
- Barto, A. G. (1995). Adaptive critics and the basal ganglia. In J.C. Houk, J.L. Davis and D.G. Beiser (Eds.), *Models of Information Processing in the Basal Ganglia* pp. (215-232). Boston, MA: MIT Press.

- Barto, A. G. and Sutton, R. S. (1997). Reinforcement learning in artificial intelligence. In J.W. Donahoe, and V.P. Dorsel (Eds.), *Neural Network Models of Cognition* (pp. 358-386). USA: Elsevier.
- Baumgardner, T. L., Singer, H. S., Denckla, M. B., Rubin, M. A., Abrams, M. T., Colli, M. J., and Reiss, A. L. (1996). Corpus callosum morphology in children with Tourette syndrome and attention deficit hyperactivity disorder. *Neurology*, *47*, 477-482.
- Baym, C. L., Corbett, B. A., Wright, S. B., and Bunge, S. A. (2008). Neural correlates of tic severity and cognitive control in children with Tourette syndrome. *Brain*, *131*, 165-179.
- Baxter, L. R., Schwartz, J. M., Guze, B. H., Bergman, K., and Szuba, M. P. (1990). PET imaging in obsessive compulsive disorder with and without depression. *Journal of Clinical Psychiatry*, *51*, 61-69.
- Beal, M. F. (1998). Excitatory and nitric oxide in Parkinson's disease pathogenesis. *Annals of Neurology*, *44*, 110-114.
- Beckmann, C., Noble, J., and Smith, S. (2001). Investigating the intrinsic dimensionality of fMRI data for ICA. In *Seventh International Conference on Functional Mapping of the Human Brain*.
- Beckmann, C., Jenkinson, M., and Smith, S. M. (2003). General multi-level linear modeling for group analysis in fMRI. *NeuroImage*, *20*, 1052-1063.
- Beckmann, C., Tracey, I., Noble, J., and Smith, S. (2000). Combining ICA and GLM: A hybrid approach to fMRI analysis. In *Sixth International Conference on Functional Mapping of the Human Brain*.
- Behrens, T. E., Hunt, L. T., Woolrich, M. W., and Rushworth, M. F. (2008). Associative learning of social value. *Nature*, *456*, 245-249.
- Beiser, D. G. and Houk, J. C. (1998). Model of cortical-basal ganglionic processing: Encoding the serial order of sensory events. *Journal of Neurophysiology*, *79*, 3168-3188.

- Berns, G. S., McClure, S. M., Pagnoni, G., and Montague, P. R. (2001). Predictability modulates human brain response to reward. *Journal of Neuroscience*, *21*, 2793-2798.
- Bevan, M. D., Atherton, J. F., Baufreton, J. (2006). Cellular principles underlying normal and pathological activity in the subthalamic nucleus. *Current Opinion in Neurobiology*, *16*, 621-628.
- Bianco, I. H., Wilson, S. W. (2009). The habenular nuclei: a conserved asymmetric relay station in the vertebrate brain. *Philosophical Transactions of the Royal Society B: Biological Sciences*, *364*, 1005-1020.
- Bigler, E., Lowry, C. M., Kerr, B., Tate, D. F., Hessel, C. D., and Earl, H. D., Miller, M. J., Rice, S. A., Smith, K. H., Tschanz, J. T., Welsh-Bohmer, K., Plassman, B., and Victoroff, J. (2003). Role of white matter lesions, cerebral atrophy, and APOE on cognition in older persons with and without dementia: The Cache County, Utah, study of memory and aging. *Neuropsychology*, *17*, 339-352.
- Biswal, B. B. and Ulmer, J. L. (1999). Blind source separation of multiple signal sources of fMRI data sets using independent component analysis. *Journal of Computer Assisted Tomography*, *23*, 265-271.
- Biswal, B., Ulmer, J. L., Krippendorfer, R. L., Harsch, H. H., Daniels, D. L., Hyde, J. S., and Haughton, V. M. (1998). Abnormal cerebral activation associated with a motor task in Tourette syndrome. *American Journal of Neuroradiology*, *19*, 1509-1512.
- Blamire, A. M., Ogawa, S., Ugurbil, K., Rothman, D., McCarthy, G., Ellermann, J. M., Hyder, F., Rattner, Z., and Shulman, R. G. (1992). Dynamic mapping of the human visual cortex by high-speed magnetic resonance imaging. *Proceedings of the National Academy of Sciences of the United States of America*, *89*, 11069-11073.

- Bloch, M. H., Leckman, J. F., Zhu, H., and Peterson, B. S. (2005). Caudate volumes in childhood predict symptom severity in adults with Tourette syndrome. *Neurology*, *65*, 1253-1258.
- Bodurka, J., Ye, F., Petridou, N., Murphy, K., and Bandettini, P. A. (2007). Mapping the MRI voxel volume in which thermal noise matches physiological noise-implications for fMRI. *NeuroImage*, *34*, 542-549.
- Boecker, H., Jankowski, J., Ditter, P., and Scheef, L. (2008). A role of the basal ganglia and midbrain nuclei for initiation of motor sequences. *NeuroImage*, *39*, 1356-1369.
- Bogacz, R., Wagenmakers, E.-J., Forstmann, B. U., and Nieuwenhuis, S. (2010). The neural basis of the speed-accuracy tradeoff. *Trends in Neuroscience*, *33*, 10-16.
- Bohlhalter, S., Goldfine, A., Matteson, S., Garraux, G., Hanakawa, T., and Kansaku, K., Wurzman, R., and Hallett, M. (2006). Neural correlates of tic generation in Tourette syndrome: an event-related functional MRI study. *Brain*, *129*, 2029-2037.
- Bornstein, R. A. and Baker, G. B. (1991). Neuropsychological performance and urinary phenylethylamine in Tourette syndrome. *The Journal of neuropsychiatry and clinical neurosciences*, *3*, 417-421.
- Boucher, L., Palmeri, T. J., Logan, G. D, and Schall, J. D. (2007). Inhibitory control in mind and brain: An interactive race model of countermanding saccades. *Psychological Review*, *114*, 376-397.
- Boxerman, J. L., Bandettini, P. A., Kwong, K. K., Baker, J. R., Davis, T. L., Rosen, B. R., and Weisskoff, R. M. (1995). The intravascular contribution to fMRI signal change: Monte Carlo modelling and diffusion-weighted studies in vivo. *Magnetic Resonance in Medicine*, *34*, 4-10.
- Brammer, M. J. (2001). Head motion and its correction. In P. Jezzard, P.M. Matthews, and S.M. Smith (Eds.), *Functional MRI: An introduction to methods* (pp. 243-250). New York, NY: Oxford University Press.

- Braun, A. R. Randolph, C., Stoetter, B., Mohr, E., Cox, C., Vladar, K., Sexton, R., Carson, R. E., Herscovitch, P., and Chase, T. N. (1995). The functional anatomy of Tourette syndrome: an FDG-PET study. II: Relationships between regional cerebral metabolism and associated behavioural and cognitive features of the illness. *Neuropsychopharmacology*, *13*, 151-168.
- Braver, T. S., Barch, D. M., Gray, J. R., Molfese, D. L., and Snyder, A. (2001). Anterior cingulate cortex and response conflict: effects of frequency, inhibition and errors. *Cerebral Cortex*, *11*, 825-836.
- Braver, T. S., Cohen, J. D., Nystrom, L. E., Jonides, J., Smith, E. E., Noll, D. C. (1997). A parametric study of prefrontal cortex involvement in human working memory. *NeuroImage*, *5*, 49-62.
- Breiter, H. C., Aharon, I., Kahneman, D., Dale, A., and Shizgal, P. (2001). Functional imaging of neural responses to expectancy and experience of monetary gains and losses. *Neuron*, *30*, 619-639.
- Breiter, H. C., Rauch, S. L., Kwong, K. K., Baker, J. R., Weisskoff, R. M., Kennedy, D. N., Kendrick, A. D., Davis, T. L., Jiang, A., Cohen, M. S., Stern, C. E., Belliveau, J. W., Baer, L., O'Sullivan, R. L., Savage, C. R., Jenike, M. A., and Rosen, B. R. (1996). Functional magnetic resonance imaging of symptom provocation in obsessive-compulsive disorder. *Archives of General Psychiatry*, *53*, 595-606.
- Brett, M., Anton, J. L., Valabregue, R., Poline, J. B. (2002). Region of interest analysis using an SPM toolbox. In *Eighth International Conference on Functional Mapping of the Human Brain*.
- Buckner, R. L., Bandettini, P. A., O'Craven, K. M., Savoy, R. L., Petersen, S. E., Raichle, M. E., and Rosen, B. R. (1996). Detection of cortical activation during averaged single trials of a cognitive task using functional magnetic imaging. *Proceeding of the National Academy of Sciences of the United States of America*, *93*, 14878-14883.

- Bunge, S. A., Dudukovic, N. M., Thomason, M. E., Vaidya, C. J., and Gabrieli, J.D. (2002). Immature frontal lobe contributions to cognitive control in children: evidence from fMRI. *Neuron*, 33, 301-311.
- Bunge, S. A., Ochsner, K. N., Desmond, J. E., Glover, G. H., and Gabrieli, J. D. (2001). Prefrontal regions involved in keeping information in and out of mind. *Brain*, 124, 2074-2086.
- Burgos-Robles, A., Vidal-Gonzalez, I., Santini, E., and Quirk, G. J. (2007). Consolidation of fear extinction requires NMDA receptor-dependent bursting in the ventromedial prefrontal cortex. *Neuron*, 53, 871-880.
- Bush, G., Whalen, P. J., Rosen, B. R., Jenike, M. A., McInerney, S. C., and Rauch, S. L. (1998). The counting Stroop: an interference task specialized for functional neuroimaging-validation study with functional MRI. *Human Brain Mapping*, 6, 270-282.
- Buxton, R. B. (2002). *Introduction to functional magnetic resonance imaging: Principles and techniques*. Cambridge: Cambridge University Press.
- Cai, W. and Leung, H. (2009). Cortical activation during manual response inhibition guided by colour and orientation cues. *Brain Research*, 1261, 20-28.
- Cai, W., Oldenkamp, C., and Aron, A. R. (2011). A proactive mechanism for selective suppression of response tendencies. *Journal of Neuroscience*, 31, 5965-5969.
- Calabrese, P., Markowitsch, H. J., Durwen, H. F., Widlitzek, B., Haupts, M., Holinka, B., and Gehlen, W. (1996). Right temporofrontal cortex as critical locus for the ephory of old episodic memories. *Journal of Neurology, Neurosurgery, and Psychiatry*, 61, 304-310.
- Carlson, S. M. and Moses, L. J. (2001). Individual differences in inhibitory control and children's theory of mind. *Child Development*, 72, 1032-1053.

- Carter, C. S., Braver, T. S., Barch, D. M., Botvinick, M. M., Noll, D., and Cohen, J. D. (1998). Anterior cingulate cortex, error detection and the online monitoring of performance. *Science*, *280*, 747-749.
- Carter, C. S., Macdonald, A. M., Botvinick, M. M., Ross, L. L., Stenger, V. A., Noll, D., and Cohen, J. D. (2000). Parsing executive processes: Strategic vs. evaluative functions of the anterior cingulate cortex. *Proceedings of the National Academy of Sciences of the United States of America*, *97*, 1944-1948.
- Castellanos, F. X., Lee, P. P., Sharp, W., Jeffries, N. O., Greenstein, D. K., and Clasen, L. S. (2002). Developmental trajectories of brain volume abnormalities in children and adolescents with attention-deficit hyperactivity disorder. *Journal of the American Medical Association*, *288*, 1740-1748.
- Cavanna, A. E., Servo, S., Monaco, F., Robertson, M. M. (2009). The behavioral spectrum of Gilles de la Tourette syndrome. *The Journal of Neuropsychiatry and Clinical Neurosciences*, *21*, 13-23.
- Chambers, C. D., Bellgrove, M.A., Stokes, M. G., Henderson, T. R., Garavan, H., Robertson, I. H., Morris, A. P., and Mattingley, J. B. (2006). Executive 'brake failure' following deactivation of human frontal lobe. *Journal of Cognitive Neuroscience*, *18*, 444-455.
- Chambers, C. D., Garavan, H., and Bellgrove, M. A. (2009). Insights into the neural basis of response inhibition from cognitive and clinical neuroscience. *Neuroscience and Biobehavioural Reviews*, *33*, 636-646.
- Channon, S., Flynn, D., and Robertson, M. M. (1992). Attentional deficits in Gilles de la Tourette syndrome. *Neuropsychiatry, Neuropsychology and Behavioural Neurology*, *5*, 170-177.
- Channon, S., Gunning, A., Frankl, J., and Robertson, M. M. (2006). Tourette syndrome (TS): Cognitive performance in adults with uncomplicated TS. *Neuropsychology*, *20*, 58-65.

- Chevrier, A., Noseworthy, M. D., and Schachar, R. (2004). Neural activity associated with failed inhibition: An event related fMRI study of performance monitoring. *Brain and Cognition*, *54*, 163-165.
- Chevrier, A. D., Noseworthy, M. D., and Schachar, R. (2007). Dissociation of response inhibition and performance monitoring in the stop-signal task using event-related fMRI. *Human Brain Mapping*, *28*, 1347-1358.
- Chikazoe, J. (2010). Localizing performance of go/no-go tasks to prefrontal cortical subregions. *Current Opinion in Psychiatry*, *23*, 267-272.
- Chikazoe, J., Konishi, S., Asari, T., Jimura, K., and Miyashita, Y. (2007). Activation of right inferior frontal gyrus during response inhibition across response modalities. *Journal of Cognitive Neuroscience*, *19*, 69-80.
- Chikazoe, J., Jimura, K., Asari, T., Yamashita, K., Morimoto, H., and Hirose, S., Miyashita, Y., and Konishi, S. (2009). Functional dissociation in right inferior frontal cortex during performance of go/no-go task. *Cerebral Cortex* *19*, 146-152.
- Christoph, G. R., Leonzio, R. J., and Wilcox, K. S. (1986). Stimulation of the lateral habenula inhibits dopamine-containing neurons in the substantia nigra and ventral tegmental area of the rat. *Journal of Neuroscience*, *6*, 613-619.
- Church, J. A., Fair, D. A., Dosenbach, N. U., Cohen, A. L., Miezin, F. M., Petersen, S. E., and Schlaggar, B. L. (2009b). Control networks in paediatric Tourette syndrome show immature and anomalous patterns of functional connectivity. *Brain*, *132*, 225-238.
- Church, J. A., Wenger, K. K., Dosenbach, N. U., Miezin, F. M., Petersen, S. E., and Schlaggar, B. L. (2009a). Task control signals in pediatric Tourette syndrome show evidence of immature and anomalous functional activity. *Frontiers in Human Neuroscience*, *3*, 38.
- Clark, V. P., Fannon, S., Lai, S., and Benson, R. (2001). Paradigm-dependent modulation of event-related fMRI activity evoked by the oddball task. *Human Brain Mapping*, *14*, 116-127.

- Clark, V. P., Fannon, S., Lai, S., Benson, R., and Bauer, L. (2000). Responses to rare visual target and distractor stimuli using event-related fMRI. *Journal of Neurophysiology*, *83*, 3133-3139.
- Cools, R., Clark, L., Owen, A. M., Robbins, T. W. (2002). Defining the neural mechanisms of probabilistic reversal learning using event-related functional magnetic resonance imaging. *Journal of Neuroscience*, *22*, 4563-4567.
- Cools, R., Clark, L., and Robbins, T. W. (2004). Differential responses in human striatum and prefrontal cortex to changes in object and rule relevance. *Journal of Neuroscience*, *24*, 1129-1135.
- Cornish, K. M, Sudhalter, V., Turk, J. (2004). Attention and language in fragile X. *Mental Retardation and Developmental Disabilities Research Reviews*, *10*, 11-16.
- Cover, T. M. and Thomas, J. A. (1991). *Elements of Information Theory* (99th Ed.). New York, NY: Wiley-Interscience.
- Coxon, J. P., Stinear, C. M., and Byblow, W. D. (2009). Stop and go: the neural basis of selective movement prevention. *Journal of Cognitive Neuroscience*, *21*, 1193-1203.
- Critchley, H. D., Mathias, C. J., and Dolan, R. J. (2001). Neural activity in the human brain relating to uncertainty and arousal during anticipation. *Neuron*, *29*, 537-545.
- Cromwell, H. C. and Schultz, W. (2003). Effects of expectations for different reward magnitudes on neuronal activity in primate striatum. *Journal of Neurophysiology*, *89*, 2823-2838.
- Curtis, D., Brett, P., Dearlove, A. M., McQuillin, A., Kalsi, G., and Robertson, M. M., Gurling, H. M. (2004). Genome scan of Tourette syndrome in a single large pedigree shows some support for linkage to regions of chromosomes 5, 10 and 13. *Psychiatric Genetics*, *14*, 83-87.

- Dagenbach, D., and Carr, T.H. (1994). *Inhibitory processes in attention, memory, and language*. San Diego, CA: Elsevier Academic Press.
- Dale, A. M. and Buckner, R. L. (1997). Selective averaging of individual trials using fMRI. *Human Brain Mapping, 5*, 329-340.
- Davidson P. S. R. and Glisky, E. L. (2002). Neuropsychological correlates of recollection and familiarity in normal aging. *Cognitive, Affective, and Behavioural Neuroscience, 2*, 174-186.
- Delgado, M. R., Miller, M. M., Inati, S., and Phelps, E. A., (2005). An fMRI study of reward-related probability learning. *NeuroImage, 24*, 862-873.
- Delgado, M. R., Nystrom, L. E., Fissell, C., Noll, D. C., and Fiez, J. A. (2000). Tracking the hemodynamic responses to reward and punishment in the striatum. *Journal of Neurophysiology, 84*, 3072-3077.
- DeLong, M. R. (1990). Primate models of movement disorders of basal ganglia origin. *Trends in Neuroscience, 13*, 281-285.
- DeLong M. R. (2000). The basal ganglia. In E.R. Kandel, J.H. Schwartz and T.M. Jessell (Eds.), *Principles of Neural Science* (pp. 853-867). New York, N.Y: McGraw-Hill.
- DeLong, M. R. and Wichmann, T. (2007). Circuits and circuit disorders of the Basal Ganglia. *Archives of Neurology, 64*, 20-24.
- Dempster, F. (1993). Resistance to interference: Developmental changes in basic processing mechanisms. In R.P.M. Howe (Ed.), *Emerging themes in cognitive development: Vol. 1. Foundations* (pp. 3-27). New York, NY: Springer-Verlag.
- Dempster, F. and Brainerd, C. (1995). *Interference and inhibition in cognition*. San Diego, CA: Elsevier Academic Press.
- D'Esposito, M., Ballard, D., Zarahn, E., and Aguirre, G. K. (2000). The role of prefrontal cortex in sensory memory and motor preparation: an event-related fMRI study. *NeuroImage, 11*, 400-408.

- Detre, J. A. and Wang, J. (2002). Technical aspects and utility of fMRI using BOLD and ASL. *Clinical Neurophysiology*, 113, 621-634.
- Diler, S. D., Reyhanli, M., Toros, F., Kibar, M., and Avci, A. (2002). Tc-99m-ECD SPECT brain imaging in children with Tourette syndrome. *Yonsei Medical Journal*, 43, 403-310.
- Donaldson, D. I. and Buckner, R. L. (2001). Effective Paradigm Design. In P.M. Matthews, P. Jezzard and A.C. Evans (Eds.), *Functional Magnetic Resonance Imaging of the Brain: Methods for Neuroscience*. Oxford: Oxford University Press.
- Donders, F. C. (1868/1969). On the speed of mental processes. In W.G. Koster (Ed.), *Attention and performance II* (pp. 412-431). Amsterdam: North-Holland.
- Doya, K. (1999). What are the computations of the cerebellum, the basal ganglia and the cerebral cortex? *Neural Networks*, 12, 961-974.
- Doya, K. (2000). Complementary roles of basal ganglia and cerebellum in learning and motor control. *Current Opinion in Neurobiology*, 10, 732-739.
- Duann, J. R., Ide, J. S., Luo, X., and Li, C. S. (2009): Functional connectivity delineates distinct roles of the inferior frontal cortex and presupplementary motor area in stop signal inhibition. *Journal of Neuroscience*, 29, 10171-10179.
- Duong, T. Q., Yacoub, E., Adriany, G., Hu, X., Ugurbil, K., Kim, S. G. (2003). Microvascular BOLD contribution at 4 and 7 T in the human brain: gradient-echo and spin-echo fMRI with suppression of blood effects. *Magnetic Resonance in Medicine*, 49, 1019-1027.
- Eickhoff, S. B., Stephan, K. E., Mohlberg, H., Grefkes, C., Fink, G. R., Amunts, K., and Zilles, K., (2005). A new SPM toolbox for combining probabilistic cytoarchitectonic maps and functional imaging data. *NeuroImage*, 25, 1325-1335.

- Eidelberg, D., Moeller, J. R., Antonini, A., Kazumata, K., Dhawan, V., Budman, C., and Feigin, A. (1997). The metabolic anatomy of Tourette syndrome. *Neurology*, *48*, 927-934.
- Elliott, R., Newman, J. L., Longe, O. A., William D., J. F., (2004). Instrumental responding for rewards is associated with enhanced neuronal response in sub-cortical reward systems. *NeuroImage*, *21*, 984-990.
- Ellison, G. (2002). Neural degeneration following chronic stimulant abuse reveals a weak link in brain, fasciculus retroflexus, implying the loss of forebrain control circuitry. *European Neuropsychopharmacology*, *12*, 287-297.
- Elsinger, C. L, Harrington, D. L, and Rao, S. M. (2006). From preparation to online control: reappraisal of neural circuitry mediating internally generated and externally guided actions. *NeuroImage*, *31*, 1177-1187.
- Fabiani, M., Gratton, G., and Federmeier, K. D. (2007). Event-related brain potentials: Methods, theory, and application. In J.T. Cacioppo, L. Tassinary, and G. Berntson (Eds.), *Handbook of Psychophysiology* (pp. 85-119). Cambridge: Cambridge University Press.
- Fattapposta, F., Restuccia, R., Colonnese, C., Labruna, L., Garreffa, G., Bianco, F. (2005). Gilles de la Tourette syndrome and voluntary movement: a functional MRI study. *Psychiatry Research*, *138*, 269-272.
- Felling, R. J. and Singer, H. S. (2011). Neurobiology of Tourette Syndrome: Current Status and Need for Further Investigation. *Journal of Neuroscience*, *31*, 12387-12395.
- Fernandez-Ruiz, J., Diaz, R., Hall-Haro, C., Vergara, P., Mischner, J., Nuñez, L., Drucker-Colin, R., Ochoa, A., and Alonso, M. E. (2003). Normal prism adaptation but reduced after-effect in basal ganglia disorders using a throwing task. *European Journal of Neuroscience*, *18*, 689-694.
- Fiorillo, C. D., Tobler, P. N., and Schultz, W. (2003). Discrete coding of reward probability and uncertainty by dopamine neurons. *Science*, *299*, 1898-1902.

- Foster, J. K., Black, S. E., Buck, B. H., and Bronskill, M. J. (1997). Ageing and executive functions: A neuroimaging perspective. In P. Rabbitt (Ed.), *Methodology of frontal and executive function* (pp. 117–134). East Sussex: Psychology Press.
- Fredericksen, K. A., Cutting, L. E., Kates, W. R., Mostofsky, S. H., Singer, H. S., Cooper, K. L., Lanham, D. C., Denckla, M. B., and Kaufmann, W. E. (2002). Disproportionate increases of white matter in right frontal lobe in Tourette syndrome. *Neurology*, *58*, 85-89.
- Fried, I., Katz, A., McCarthy, G., Sass, K. J., Williamson, P., Spencer, S. S., and Spencer, D. D. (1991). Functional organization of human supplementary motor cortex studied by electrical stimulation. *Journal of Neuroscience*, *11*, 3656-3666.
- Friedman, N. P. and Miyake, A. (2004). The relations among inhibition and interference control functions: A latent variable analysis. *Journal of Experimental Psychology: General*, *133*, 101-135.
- Frison, L. and Pocock, S. J. (1992). Repeated measures in clinical trials: An analysis using mean summary statistics and its implications for design. *Statistics in medicine*, *11*, 1685-1704.
- Friston, K. J., Holmes, A., Poline, J. B., Price, C. J., and Frith, C. D. (1996a). Detecting activations in PET and fMRI: levels of inference and power. *NeuroImage*, *4*, 223-235.
- Friston, K. J., Holmes, A. P., Worsley, K. J., Poline, J. P., Frith, C. D., and Frackowiak, R. S. J. (1995). Statistical parametric maps in functional imaging: A general linear approach. *Human Brain Mapping*, *2*, 189-210.
- Friston, K. J., Josephs, O., Rees, G. and Turner, R. (1998). Nonlinear event-related responses in fMRI. *Magnetic Research in Medicine*, *39*, 41-52.
- Friston, K. J., Penny, W. D., and Glaser, D. E. (2005). Conjunction revisited. *NeuroImage*, *25*, 661-667.

- Friston, K., Price, C., Fletcher, P., Moore, C., Frackowiak, R., and Dolan, R. (1996b). The trouble with cognitive subtraction. *NeuroImage*, 4, 97-104.
- Friston, K. J., Zarahn, E., Josephs, O., Henson, R. N. A., and Dale, A. M. (1999). Stochastic designs in event-related fMRI. *NeuroImage*, 10, 607-619.
- Fuster, J. M. (1997). *The prefrontal cortex: anatomy, physiology and neuropsychology of the frontal lobe*. Philadelphia, PA: Lippincott-Raven.
- Gallistel, C. R. and Tretiak, O. (1985) Microcomputer systems for analyzing 2-deoxyglucose autoradiographs. In R. R. Mize, (Ed.), *The Microcomputer in Cell and Neurobiology Research*. New York, NY: Elsevier-North Holland Publishing.
- Garavan, H., Hester, R., Murphy, K., Fassbender, C., Kelly, C., (2006). Individual differences in the functional neuroanatomy of inhibitory control. *Brain Research*, 1105, 130–142.
- Garavan, H., Ross, T.J., and Stein, E.A. (1999). Right hemispheric dominance of inhibitory control: An event-related functional MRI study. *Proceedings of the National Academy of Sciences of the United States of America*, 96, 8301-8306.
- Gati, J.S., Menon, R.S., Ugurbil, K., and Rutt, B.K. (1997). Experimental determination of the BOLD field strength dependence in vessels and tissue. *Magnetic Resonance in Medicine*, 38, 296-302.
- Gates, L., Clarke, J., Stokes, A., Somorjai, R., Jarmasz, M., Vandorpe, R., and Dursun, S. M. (2004). Neuroanatomy of coprolalia in Tourette syndrome using functional magnetic resonance imaging. *Progress in Neuropsychopharmacology Biological Psychiatry*, 28, 397-400.
- Gauggel, S., Rieger, M., Fegho, V. T. A. (2004). Inhibition of ongoing responses in patients with Parkinson's disease. *Journal of Neurology, Neurosurgery and Psychiatry*, 75, 539-544

- Gerardin, E., Lehericy, S., Pochon, J. B., Tezenas du Montcel, S., Mangin, J. F., Poupon, F., Agid, Y., Le Bihan, D., and Marsault, C. (2003). Foot, hand, face and eye representation in the human striatum. *Cerebral Cortex*, *13*, 162-169.
- Gilbert, D. L., Bansal, A. S., Sethuraman, G., Sallee, F. R., Zhang, J., and Lipps, T., and Wassermann, E. M. (2004). Association of cortical disinhibition with tic, ADHD, and OCD severity in Tourette syndrome. *Movement Disorders*, *19*, 416-425.
- Gilbert, D. L., Sallee, F. R., Zhang, J., Lipps, T. D., and Wassermann, E. M. (2005). Transcranialmagnetic stimulation-evoked cortical inhibition: a consistent marker of attention-deficit/hyperactivity disorder scores in Tourette syndrome. *Biological Psychiatry*, *57*, 1597-600.
- Gilbert, S. J. and Shallice, T. (2002). Task switching: a PDP model. *Cognitive Psychology*, *44*, 297-337.
- Gilles de la Tourette, G. (1885). Étude sur une affection nerveuse caractérisée par de l'incoordination motrice accompagnée d'écholalie et de coprolalie [French]. *Achieves of Neurology*, *9*, 158-200.
- Gläscher, J., Hampton, A. N., and O'Doherty, J. P. (2009). Determining a role for ventromedial prefrontal cortex in encoding action-based value signals during reward-related decision making. *Cerebral Cortex*, *19*, 483-495.
- Goudriaan, A. E., Oosterlaan, J., de Beurs, E., and van den Brink, W. (2006). Neurocognitive functions in pathological gambling: a comparison with alcohol dependence, Tourette syndrome and normal controls. *Addiction*, *101*, 534-547.
- Gowland, P.A. and Bowtell, R. (2007). Theoretical optimization of multi-echo fMRI data acquisition. *Physics in Medicine and Biology*, *52*, 1801-1813.
- Graybiel, A. M., Aosaki, T., Flaherty, A. W., and Kimura, M. (1994). The basal ganglia and adaptive motor control. *Science*, *265*, 1826-1831.

- Graybiel, A. M. and Kimura, M. (1995). Adaptive neural networks in the basal ganglia. In J.C. Houk, J.L. Davis, and D.G. Beiser (Eds.), *Models of information processing in the basal ganglia* (p. 103-116). Cambridge, MA: MIT Press.
- Grinband, J., Hirsch, J., and Ferrera, V. P. (2006). A neural representation of categorization uncertainty in the human brain. *Neuron*, *49*, 767-783.
- Gurney, K. N., Prescott, T. J., and Redgrave, P. (1998). The Basal Ganglia viewed as an Action Selection Device. *In the Proceedings of the Eighth International Conference on Artificial Neural Networks*.
- Haber, S. N. (1986). Neurotransmitters in the human and nonhuman primate basal ganglia. *Human Neurobiology*, *5*, 159-168.
- Hagberg, G. E., Indovina, I., Sanes, J. N., and Posse, S. (2002). Real-time quantification of T₂* changes using multiecho planar imaging and numerical methods. *Magnetic Resonance in Medicine*, *48*, 877-882
- Hamalainen, M. S., Hari, R., Ilmoniemi, R. J., Knuutila, J., and Lounasmaa, O. V. (1993). Magnetoencephalography—theory, instrumentation, and applications to noninvasive studies of the working human brain. *Reviews of Modern Physics*, *65*, 413-498.
- Hampshire, A., Chamberlain, S. R., Monti, M. M., Duncan, J., and Owen, A. M. (2010). The role of the right inferior frontal gyrus: Inhibition and attentional control. *NeuroImage*, *50*, 1313-1319.
- Harlow, J. M. (1848). "Passage of an iron rod through the head". *Boston Medical and Surgical Journal*, *39*, 389-393.
- Harnishfeger, K. K. (1995). The Development of Cognitive Inhibition: Theories, Definitions, and Research Evidence. In F. Dempster (Ed.), *Interference and inhibition in cognition* (pp. 175-192). San Diego, CA: Elsevier Academic Press.

- Harrington, D. L., Boyd, L. A., Mayer, A.R., Sheltraw, D. M., Lee, R. R., Huang, M., and Rao, S. M. (2004). Neural representation of interval encoding and decision making. *Cognitive Brain Research*, 21, 193-205.
- Hasegawa, R. P., Peterson, B. W., and Goldberg, M. E. (2004). Prefrontal neurons coding suppression of specific saccades. *Neuron*, 43, 415-25.
- Hashemi, R. H., Bradley, W. G., and Lisanti, C. J. (2004). *MRI the basics* (2nd ed.). Philadelphia, PA: Lippincott Williams and Wilkins.
- Heeger, D. J. and Ress, D. (2002). What does fMRI tell us about neuronal activity? *Nature Reviews Neuroscience*, 3, 142-151.
- Heise, K. F., Steven, B., Liuzzi, G., Thomalla, G., Jonas, M., Müller-Vahl, K., Sauseng, P., Münchau, A., Gerloff, C., and Hummel, F. C. (2010). Altered modulation of intracortical excitability during movement preparation in Gilles de la Tourette syndrome. *Brain*, 133, 580-590.
- Herkenham, M. and Nauta, W. J. (1979). Efferent connections of the habenular nuclei in the rat. *The Journal of Comparative Neurology*, 187, 19-47.
- Herrnstein, R. J. (1970). On the law of effect. *Journal of the Experimental Analysis of Behavior*, 13, 243-266
- Hikosaka, O., Sesack, S. R., Lecourtier, L., and Shepard, P. D. (2008). Habenula: crossroad between the basal ganglia and the limbic system. *Journal of Neuroscience*, 28, 11825-11829.
- Hollerman, J. R. and Schultz, W. (1998). Dopamine neurons report an error in the temporal prediction of reward during learning. *Nature Neuroscience*, 1, 304-309.
- Hong, S. and Hikosaka, O. (2008). The globus pallidus sends reward-related signals to the lateral habenula. *Neuron*, 60, 720 -729.
- Horowitz, A. L. (1995). *MRI physics for radiologists*. (3rd ed.) New York, NY: Springer-Verlag.

- Huettel, S. A., Song, A. W., and McCarthy, G. (2005). Decisions under uncertainty: probabilistic context influences activation of prefrontal and parietal cortices. *Journal of Neuroscience*, *25*, 3304-3311.
- Hutto, D. (2008). *Folk Psychological Narratives: The Sociocultural Basis of Understanding Reasons*. Cambridge, MA: MIT Press.
- Hyde, T. M., Stacey, M. E., Coppola, R., Handel, S. F., Rickler, K. C., and Weinberger, D. R. (1995). Cerebral morphometric abnormalities in Tourette syndrome: a quantitative MRI study of monozygotic twins. *Neurology*, *45*, 1176-1182.
- Ide, J. S. and Li, C. R. (2011). Error-related functional connectivity of the habenula in humans. *Frontiers in Human Neuroscience*, *5*, 1-13.
- Isoda, M. and Hikosaka, O. (2007). Switching from automatic to controlled action by monkey medial frontal cortex. *Nature Neuroscience*, *10*, 240-248.
- Iversen, S. D. and Mishkin, M. (1970). Perseverative interference in monkeys following selective lesions of the inferior prefrontal convexity. *Experimental Brain Research*, *11*, 376-86.
- Ivry, R. B. (1996). The representation of temporal information in perception and motor control. *Current Opinion in Neurobiology*, *6*, 851-857.
- Jackson, G. M., Mueller, S. C., Hambleton, and K., Hollis, C. P. (2007). Enhanced cognitive control in Tourette Syndrome during task uncertainty. *Experimental Brain Research*, *182*, 357-364.
- Jackson, G. M., Swainson, R., Cunnington, R., and Jackson, S. R. (2001). ERP correlates of executive control during repeated language switching. *Bilingualism: Language and Cognition*, *4*, 169-178.
- Jackson, S. R., Parkinson, A., Manfredi, V., Millon, G., Hollis, C., and Jackson, G. M. (in press). Motor excitability is reduced prior to voluntary movement in children and adolescents with Tourette syndrome.

- Jackson, S. R., Parkinson, A., Jung, J., Ryan, S. E., Morgan, P. S., Hollis, C., and Jackson, G. M. (2011). Compensatory neural reorganization in Tourette syndrome. *Current Biology*, *21*, 580-585.
- Jahanshahi, M., Jones, C. R. G., Dirnberger, G. and Frith C. D. (2006). The Substantia Nigra Pars Compacta and Temporal Processing. *The Journal of Neuroscience*, *26*, 12266-12273.
- Jahfari, S., Stinear, C. M., Claffey, M., Verbruggen, F., and Aron, A. R. (2009). Responding with restraint: What are the neurocognitive mechanisms? *Journal of Cognitive Neuroscience*, *22*, 1479-1492.
- Janavs, J. L. and Aminoff, M. J. (1998). Dystonia and chorea in acquired systemic disorders. *Journal of Neurology, Neurosurgery and Psychiatry*, *65*, 436-45.
- Jeffries, K. J., Schooler, C., Schoenbach, C., Herscovitch, P., Chase, T. N., and Braun, A. R. (2002). The functional neuroanatomy of Tourette syndrome: an FDG PET study III: functional coupling of regional cerebral metabolic rates. *Neuropsychopharmacology*, *27*, 92-104.
- Jenkinson, M., Bannister, P., and Smith, S. (2002). Improved optimisation for the robust and accurate linear registration and motion correction of brain images. *NeuroImage*, *17*, 825-841.
- Jenkinson, M. and Smith, S. M. (2001). A Global Optimisation Method for Robust Affine Registration of Brain Images. *Medical Image Analysis*, *5*, 143-156.
- Jezzard, P. and Clare, S. (2001). Principles of nuclear magnetic resonance and MRI. In P. Jezzard, P.M. Matthews, and S.M. Smith (Eds.), *Functional MRI: an introduction to methods* (pp. 67-92). New York, NY: Oxford University Press.
- Jezzard, P., Matthews, P., and Smith, S. (2001). *Functional MRI: An Introduction to Methods*. Oxford: Oxford University Press.
- Joel, D. and Wiener, I. (1994). The organization of the basal ganglia-thalamocortical circuits: open interconnected rather than closed segregated. *Neuroscience*, *63*, 363-379.

- Joel, D. and Wiener, I. (2000). The connections of the dopaminergic system with the striatum in rats and primates: An analysis with respect to the functional and compartmental organization of the striatum. *Neuroscience*, 96, 451-474.
- Jog, M. S., Kubota, Y., Connolly, C. I., Hillegaart V., and Graybiel, A. M. (1999). Building neural representations of habits. *Science*, 286, 1745-1749.
- Johannes, S., Wieringa, B. M., Mantey, M., Nager, W., Rada, D., and Muller-Vahl, K. R., Emrich, H. M., Dengler, R., Münte, T. F., and Dietrich, D. (2001). Altered inhibition of motor responses in Tourette Syndrome and Obsessive-Compulsive Disorder. *Acta Neurologica Scandinavica*, 104, 36-43.
- Jones, R. M., Somerville, L. H., Li, J., Ruberry, E. J., Libby, V., Glover, G., Voss, H. U., Ballon, D. J. and Casey, B. J. (2011). Behavioural and neural properties of social reinforcement learning. *The Journal of Neuroscience*, 31, 13039-13045.
- Kalisch, R., Korenfeld, E., Stephan, K.E., Weiskopf, N., Seymour, B., and Dolan, R.J., (2006). Context-dependent human extinction memory is mediated by a ventromedial prefrontal and hippocampal network. *Journal of Neuroscience*, 26, 9503-9511.
- Karayanidis, F., Coltheart, M., Michie, P. T., and Murphy, K. (2003). Electrophysiological correlates of anticipatory and post-stimulus components of task-switching. *Psychophysiology*, 40, 329–348.
- Kates, W. R., Frederikse, M., Mostofsky, S. H., Folley, B. S., Cooper, K., Mazur-Hopkins, P., Kofman, O., Singer, H. S., Denckla, M. B., Pearlson, G. D., and Kaufmann, W. E. (2002). MRI parcellation of the frontal lobe in boys with attention deficit hyperactivity disorder or Tourette syndrome. *Psychiatry Research*, 116, 63-81.
- Kawagoe, R., Takikawa, Y., and Hikosaka, O. (1998). Expectation of reward modulates cognitive signals in the basal ganglia. *Nature Neuroscience*, 1, 411-416.

- Kawohl, W., Brühl, A., Krowatschek, G., Ketteler, D., and Herwig, U. (2009). Functional magnetic resonance imaging of tics and tic suppression in Gilles de la Tourette syndrome. *World Journal of Biological Psychiatry, 10*, 567-570.
- Kelly, A. M. C., Hester, R., Foxe, J. J., Shpaner, M., and Garavan, H. (2006). Flexible cognitive control: Effects of individual differences and brief practice on a complex cognitive task. *NeuroImage, 31*, 866-886.
- Kiebel, S. J. and Holmes, A. P. (2003). The general linear model. In R.S.J. Frackowiak, K. J. Friston, C. Frith, R. Dolan, C. J. Price, S. Zeki, J. Ashburner, and W. D. Penny (Eds.), *Human brain function* (2nd ed.). San Diego, CA: Elsevier Academic Press.
- Kim, S-G., Ugurbil, K., and Strick, P.L. (1994). Activation of a cerebellar output nucleus during cognitive processing. *Science, 265*, 949-951.
- Kirsch, P., Schienle, A., Stark, R., Sammer, G., Blecker, C., Walter, B., Ott, U., Burkart, J., and Vaitl, D. (2003). Anticipation of reward in a nonaversive differential conditioning paradigm and the brain reward system: an event-related fMRI study. *Neuroimage, 20*, 1086-1095.
- Fett, K. A., Dimitropoulos, T., and Karlan, R. (1997). Asymmetry of basal ganglia perfusion in Tourette syndrome shown by technetium-99m-HMPAO SPECT. *Journal of Nuclear Medicine, 38*, 188-191.
- Knight, J. A. and Kaplan, E. (2003). *The handbook of Rey-Osterrieth Complex Figure usage: Clinical and research applications*. Lutz, FL: Psychological Assessment Resources.
- Knutson, B., Fong, G. W., Adams, C. M., Varner, J. L., and Hommer, D. (2001). Dissociation of reward anticipation and outcome with event-related fMRI. *NeuroReport, 12*, 3683-3687.

- Koch, K., Schachtzabel, C., Wagner, G., Reichenbach, J. R., Sauer, H., and Schlösser, R. (2008). The neural correlates of reward-related trial-and-error learning: An fMRI study with a probabilistic learning task. *Learning and Memory*, *15*, 728-732
- Konishi, S., Nakajima, K., Uchida, I., Kikyo, H., Kameyama, M., and Miyashita, Y. (1999). Common inhibitory mechanism in human inferior prefrontal cortex revealed by event-related functional MRI. *Brain*, *122*, 981-991.
- Konishi, S., Nakajima, K., Uchida, I., Sekihara, K., and Miyashita, Y. (1998). No-go dominant brain activity in human inferior prefrontal cortex revealed by functional magnetic resonance imaging. *European Journal of Neuroscience*, *10*, 1209-1213.
- Krack, P., Hariz, M. I., Baunez, C., Guridi, J., and Obeso J. A. (2010). Deep brain stimulation: from neurology to psychiatry? *Trends in Neurosciences*, *33*, 474-484.
- Kruger, G. and Glover, G.H. (2001). Physiological noise in oxygenation-sensitive magnetic resonance imaging. *Magnetic Resonance in Medicine*, *46*, 631-637.
- Lange, N., Strother, S., Anderson, J., Nielsen, F., Holmes, A., Kolenda, T., Savoy, R., and Hansen, L. (1999). Plurality and resemblance in fMRI data analysis. *NeuroImage*, *10*, 282-303.
- Lappin, J. S. and Eriksen, C. W. (1966). Use of a delayed signal to stop a visual reaction-time response. *Journal of Experimental Psychology*, *72*, 805-811.
- Lawrence, A.D., Sahakian, B.J., and Robbins, T.W. (1998). Cognitive functions and corticostriatal circuits: Insights from Huntington's disease. *Trends in Cognitive Sciences*, *2*, 379-388.
- Leber, A. B., Turk-Browne, N. B., Chun, M. M. (2008). Neural predictors of moment-to-moment fluctuations in cognitive flexibility. *Proceeding of the National Academy of Sciences of the United States of America*, *105*, 1359-13597.

- Lebrón, K., Milad, M. R., and Quirk, G. J., (2004). Delayed recall of fear extinction in rats with lesions of ventral medial prefrontal cortex. *Learning and Memory*, *11*, 544-548.
- Leckman, J. F., Denyss, D., Mataix-Cols, D., Hollander, E., Rauch, S. L., Saxena, S., Miguel, E. C., Phillips, K. A., and Stein, D. J. (2010). Obsessive-Compulsive Disorder: A review of the diagnostic criteria and subtype and dimensional and specifiers for DSM-V. *Depression and Anxiety*, *27*, 507-527.
- Leckman, J. F., Riddle, M. A., Hardin, M. T., Ort, S. I., Swartz, K. L., Stevenson, j., and Cohen, D. J. (1989). The Yale Global Tic Severity Scale (YGTSS): Initial testing of a clinical rated scale of tic severity. *Journal of the American Academy of Child and Adolescent Psychiatry*, *28*, 566-573.
- Lecourtier, L. and Kelly, P. H. (2007). A conductor hidden in the orchestra? Role of the habenular complex in monoamine transmission and cognition. *Neuroscience and Biobehavioural Reviews*, *31*, 658-672.
- Lee, J. S., Yoo, S. S., Cho, S. Y., Ock, S. M., Lim, M. K., and Panych, L. P. (2006). Abnormal thalamic volume in treatment-naive boys with Tourette syndrome. *Acta Psychiatrica Scandinavica*, *113*, 64-67.
- Lehericy, S., Ducros, M., Van de Moortele, P. F., Francois, C., Thivard, L., Poupon, C., Swindale, N., Ugurbil, K., Kim, D. S. (2004): Diffusion tensor fiber tracking shows distinct corticostriatal circuits in humans. *Annals of Neurology*, *55*, 522-529.
- Leung, H. and Cai, W. (2007). Common and differential ventrolateral prefrontal activity during inhibition of hand and eye movements. *Neuroscience and Biobehavioral Reviews*, *27*, 9893-9900.
- Levy, R., Friedman, H. R., Davachi, L., and Goldman-Rakic, P. S. (1997). Differential activation of the caudate nucleus in primates performing spatial and nonspatial working memory tasks. *Journal of Neuroscience*, *17*, 3870-3882.

- Levy, B. J. and Wagner, A. D. (2011). Cognitive control and right ventrolateral prefrontal cortex: reflexive reorienting, motor inhibition, and action updating. *Annals of the New York Academy of Sciences*, 1224, 40-62.
- Lewis, P. A. and Miall, R. C. (2006). A right hemispheric prefrontal system for cognitive time measurement. *Behavioural Processes*, 71, 226 -234.
- Lezak, M. (1995). Neuropsychological assessment. New York, NY: Oxford University Press.
- Li, Z., Wu, G. H., Zhao, X. L., Luo, F., and Li, S. J. (2002). Multiecho segmented EPI with Z-shimmed background gradient compensation (MESBAC) pulse sequence for fMRI. *Magnetic Resonance in Medicine*, 48, 312-321.
- Lisoprawski, A., Herve, D., Blanc, G., Glowinski, J., and Tassin, J. P. (1980). Selective activation of the mesocortico-frontal dopaminergic neurons induced by lesion of the habenula in the rat. *Brain Research*, 183, 229-234.
- Logan, G. D. (1985). Executive control of thought and action. *Acta Psychologica*, 60, 193-210.
- Logan, G. D. (1994). On the Ability to Inhibit Thought and Action: A User's guide to the Stop Signal Paradigm. In D. Dagenbach, T.H. Carr, (Eds.), *Inhibitory Processes in Attention, Memory, and Language* (pp. 189-239). San Diego, CA: Elsevier Academic Press.
- Logan, G. D. and Cowan, W. B. (1984). On the ability to inhibit thought and action: a theory of an act of control. *Psychological Review*, 91, 295-327.
- Logothetis, N. (2003). The underpinnings of the BOLD functional magnetic resonance imaging signal. *Journal of Neuroscience*, 23, 3963-3971.
- Logothetis, N. K., Pauls, J., Augath, M., Trinath, T. and Oeltermann, A. (2001). Neurophysiological investigation of the basis of the fMRI signal. *Nature*, 412, 150-157.

- Luders, H., Lesser, R. P., Dinner, D. S., Morris, H. H., Wyllie, E., and Godoy, J. (1988). Localization of cortical function: new information from extraoperative monitoring of patients with epilepsy. *Epilepsia*, *29*, 56-65.
- MacDonald, P. A. and Joordens, S. (2000). Investigation a memory-based account of negative priming: support for selection-feature mismatch. *Journal of Experimental Psychology: Human Perception and Performance*, *26*, 1478-96.
- MacLeod, C., Dodd, M., Sheard, E., Wilson, D., and Bibi, U. (2003). In opposition to inhibition. In B. Ross (Ed.), *The psychology of learning and motivation* (pp. 163-214). San Diego, CA: Elsevier Academic Press.
- MacMillan, L. B., Hein, L., Smith, M. S., Piascik, M. T., and Limbird, L. E. (1996). Central hypotensive effects of the K2A-adrenergic receptor subtype. *Science*, *273*, 801-803.
- Maldjian, J. A., Laurienti, P. J., Burdette, J. B., Kraft, R. A. (2003). An Automated Method for Neuroanatomic and Cytoarchitectonic Atlas-based Interrogation of fMRI Data Sets. *NeuroImage*, *19*, 1233-1239.
- Maldjian J. A., Laurienti P. J., Burdette, J. H. (2004). Precentral Gyrus Discrepancy in Electronic Versions of the Talairach Atlas. *NeuroImage*, *21*, 450-455.
- Malloy, P. F., Cohen, R. A., and Jenkins, M. A. (1998). Frontal lobe function and dysfunction. In P.J. Snyder and P.D. Nussbaum (Eds.), *Clinical neuropsychology: A pocket handbook for assessment* (pp. 573-590). Washington, DC: American Psychological Association.
- Makki, M. I., Behen, M., Bhatt, A., Wilson, B., and Chugani, H. T. (2008). Microstructural abnormalities of striatum and thalamus in children with Gilles de la Tourette syndrome. *Movement Disorders*, *23*, 2349-2356.
- Malapani, C., Rakitin, B., Levy, R., Meck, W. H., Deweer, B., Dubois, B., and Gibbon, J. (1998). Coupled temporal memories in Parkinson's disease: a dopamine-related dysfunction. *Journal of Cognitive Neuroscience*, *10*, 316-331.

- Marco-Pallares, J., Müller, S. V., and Münte, T. F. (2007). Learning by doing: an fMRI study of feedback-related brain activations. *NeuroReport*, *18*, 1423-1426.
- Marsh, R., Zhu, H., Wang, Z., Skudlarski, P., and Peterson, B. S. (2007). A Developmental fMRI Study of Self-Regulatory Control in Tourette Syndrome. *The American Journal of Psychiatry*, *164*, 955-966.
- Matsumoto, M. and Hikosaka, O. (2007). Lateral habenula as a source of negative reward signals in dopamine neurons. *Nature*, *447*, 1111-1115.
- Matsumoto, M. and Hikosaka, O. (2009). Representation of negative motivational value in the primate lateral habenula. *Nature Neuroscience*, *12*, 77-84.
- Mazzone, L., Yu, S., Blair, C., Gunter, B. C., Wang, Z., Marsh, R., and Peterson, B. S. (2010). An FMRI study of frontostriatal circuits during the inhibition of eye blinking in persons with Tourette syndrome. *The American Journal of Psychiatry*, *167*, 341-349.
- McClure, S. M., Berns, G. S., and Montague, P. R. (2003). Temporal prediction errors in a passive learning task activate human striatum. *Neuron*, *38*, 339-346.
- McNab, F., Leroux, G., Strand, F., Thorell, L., Bergman, S., Klingberg, T. (2008). Common and unique components of inhibition and working memory: An fMRI, within-subjects investigation. *Neuropsychologia*, *46*, 2668-2682.
- McNaught, K. St. P. and Mink, J. W. (2011). Advances in understanding and treatment of Tourette syndrome. *Nature Reviews Neurology*, *7*, 667-676.
- Meck, W. H. Penney, T. B., and Pouthas, V. (2008). Cortico-striatal representation of time in animals and humans. *Current Opinion in Neurobiology*, *18*, 145-152.
- Meiran, N. (1996). Reconfiguration of processing mode prior to task performance. *Journal of Experimental Psychology: Learning, Memory, and Cognition*, *22*, 1423-1442.
- Mesulam, M. M. (1985). *Principles of behavioural neurology*. Philadelphia, PA: F. A. Davis.

- Mesulam, M. M., Mufson, E. J., and Wainer, B. H. (1986). Three-dimensional representation and cortical projection topography of the nucleus basalis (Ch4) in the macaque: Concurrent demonstration of choline acetyltransferase and retrograde transport with a stabilized tetramethylbenzidine method for horseradish peroxidase. *Brain Research*, 367, 301-308.
- Middleton, F. A. and Strick, P.L. (1997). Cerebellar output channels. In: J. Schmahmann (Ed.), *The Cerebellum in Cognition* (pp. 61–107). San Diego, CA: Elsevier Academic Press.
- Middleton, F. A. and Strick, P. (2000). Basal ganglia output and cognition: evidence from anatomical, behavioral, and clinical studies. *Brain and Cognition*, 42, 183-200.
- Middleton, F. A. and Strick, P. L. (2002). Basal ganglia "projections" to the prefrontal cortex of the primate. *Cerebral Cortex*, 12, 926-935
- Milad, M. R. and Rauch, S. L. (2007). The role of the orbitofrontal cortex in anxiety disorders. *Annals of the New York Academy of Sciences*, 1121, 546-561.
- Milham, M. P., Banich, M. T., Webb, A., Barad, V., Cohen, N. J., Wszalek, T., and Kramer, A. F. (2001). The relative involvement of anterior cingulate and prefrontal cortex in attentional control depends on nature of conflict. *Cognitive Brain Research*, 12, 467-473.
- Milham, M. P., Erickson, K. I., Banich, M. T., Kramer, A. F., Webb, A., Wszalek, T., and Cohen, N. J. (2002). Attentional control in the aging brain: insights from an fMRI study of the Stroop task. *Brain and Cognition*, 49, 277-296.
- Miller, E.K. (2000). The prefrontal cortex and cognitive control. *Nature Reviews Neuroscience*, 1, 59-65.
- Miller, E. K. and Cohen, J. D. (2001). An integrative theory of prefrontal cortex function. *Annual Review of Neuroscience*, 24, 167–202.
- Mink, J.W. and Thach, W.T. (1993). Basal ganglia intrinsic circuits and their role in behavior. *Current Opinion in Neurobiology*, 3, 950-957.

- Mink, J. W. (1996). The basal ganglia: focused selection and inhibition of competing motor programs. *Progress in Neurobiology*, 50, 381-425.
- Mink, J.W. (2001). Basal ganglia dysfunction in Tourette syndrome: a new hypothesis. *Paediatric Neurology*, 25, 190-198.
- Mink, J. W. (2003). The basal ganglia and involuntary movements. *Achieves of Neurology*, 60, 1365-1368.
- Mishkin, M. (1964). Perseveration of central sets after frontal lesions in monkey. In J.M. Warren and K. Akert (Eds.), *The frontal granular cortex and behaviour* (pp. 219-241). New York, NY: McGraw-Hill.
- Miyake, A., Friedman, N. P., Emerson, M. J., Witzki, A.H., Howerter, A., Wager, T. D., (2000). The unity and diversity of executive functions and their contributions to complex “Frontal Lobe” tasks: a latent variable analysis. *Cognitive Psychology*, 41, 49–100.
- Moll, G.H., Heinrich, H., Wischer, S., Tergau, F., Paulus, W., and Rothenberger, A. (1999). Motor system excitability in healthy children: developmental aspects from transcranial magnetic stimulation. *Electroencephalography and Clinical Neurophysiology*, 51, 243-249.
- Monakow, K.H., Akert, K., and Künzle, H. (1978) Projections of the precentral motor cortex and other cortical areas of the frontal lobe to the subthalamic nucleus in the monkey. *Experimental Brain Research*, 33, 395-403.
- Moriarty, J., Campos Costa, D., and Schmitz, B., Trimble, M. R., Ell, P. J., Robertson, M. M. (1995). Brain perfusion abnormalities in Gilles de la Tourette syndrome. *The British Journal of Psychiatry*, 16, 249-254.
- Moriarty, J., Varma, A. R., and Stevens, J., Fish, M., Trimble, M. R., and Robertson, M. M. (1997). A volumetric MRI study of Gilles de la Tourette syndrome. *Neurology*, 49, 410-415.

- Morris, R. W., Vercammen, A., Lenroot, R., Moore, L., Langton, J. M., Short, B., Kulkarni, J., Curtis, J., O'Donnell, M., Weickert, C. S., and Weickert, T. W. (2012). Disambiguating ventral striatum fMRI-related bold signal during reward prediction in schizophrenia. *Molecular Psychiatry*, *17*, 280-289
- Mostofsky, S. H., Schafer, J. G., Abrams, M. T., Goldberg, M. C., Flower, A. A., Boyce, A., Courtney, S. M., Calhoun, V. D., Kraut, M. A., Denckla, M. B., and Pekar, J. J. (2003). fMRI evidence that the neural basis of response inhibition is task-dependent. *Cognitive Brain Research*, *17*, 419-430.
- Mostofsky, S. H. and Simmonds, D. J. (2008). Response inhibition and response selection: Two sides of the same coin. *Journal of Cognitive Neuroscience*, *20*, 1-11.
- Mostofsky, S. H., Wendlandt, J., Cutting, L., Denckla, M. B, and Singer, H. S. (1999). Corpus callosum measurements in girls with Tourette syndrome. *Neurology*, *53*, 1345-1347.
- Mueller, S. C., Jackson, G. M., Dhalla, R., Datsopoulos, S., and Hollis, C. P. (2006). Enhanced cognitive control in young people with Tourette's syndrome. *Current Biology*, *16*, 570-573.
- Muller, N. G. and Knight, R. T. (2006). The functional neuroanatomy of working memory: contributions of human brain lesion studies. *Neuroscience*, *139*, 51-58.
- Nambu, A. (2005). A new approach to understand the pathophysiology of Parkinson's disease. *Journal of Neurology*, *252*, 1-4.
- Nambu, A. (2008). Seven problems on the basal ganglia. *Current Opinion in Neurobiology*, *18*, 595-604.
- Nambu, A. (2009). Functions of direct, indirect and hyperdirect pathways. *Brain Nerve*, *61*, 360-372.
- Nambu, A. (2011). Somatotopic organization of the primate basal ganglia. *Frontiers in Neuroanatomy*, *5*, 1-9.

- Nambu, A., Kaneda, K., Tokuno, H., and Takada, M. (2000). Abnormal pallidal activity evoked by cortical stimulation in the parkinsonian monkey. *Society for Neuroscience Abstract*, 26, 960.
- Nambu, A., Kaneda, K., Tokuno, H., and Takada, M. (2002). Organization of corticostriatal motor inputs in monkey putamen. *Journal of Neurophysiology*, 88, 1830-1842.
- Nambu, A., Shigemi Mori, D. G. S., and Mario, W. (2004). A new dynamic model of the cortico-basal ganglia loop. *Progress in Brain Research*, 143, 461-466.
- Nambu, A., Takada, M., Inase, M., and Tokuno, H. (1996). Dual somatotopical representations in the primate subthalamic nucleus: evidence for ordered but reversed body-map transformations from the primary motor cortex and the supplementary motor area. *Journal of Neuroscience*, 16, 2671-2683.
- Neubert, F., Mars, R. B., Buch, E. R., Olivier, E., and Rushworth, M. F. (2010). Cortical and sub-cortical interactions during action reprogramming and their related white matter pathways. *Proceedings of the National Academy of Sciences of the United States of America*, 107, 13240-13245.
- Neuner, I., Kupriyanova, Y., Stöcker, T., Huang, R., Posnansky, O., Schneider, F., and Shah, N. J. (2011). Microstructure assessment of grey matter nuclei in adult Tourette patients by diffusion tensor imaging. *Neuroscience Letters*, 487, 22-26.
- Nichols, T., Brett, M., Andersson, J., Wager, T., and Poline, J. P. (2005). Valid conjunction inference with the minimum statistic. *NeuroImage*, 25, 653-660.
- Nieuwenhuis, S., Yeung, N., Van den Wildenberg, W., and Ridderinkhof, K. R. (2003). Electrophysiological correlates of anterior cingulate function in a go/no-go task: Effects of response conflict and trial type frequency. *Cognitive, Affective, and Behavioural Neuroscience*, 3, 17-26.
- Nigg, J. (2000). On inhibition/disinhibition in developmental psychopathology: views from cognitive and personality psychology and a working inhibition taxonomy. *Psychological Bulletin*, 126, 220-246.

- Nigg, J. T. (2001). Is ADHD a Disinhibitory Disorder? *Psychological Bulletin*, *127*, 571-598.
- Nigg, J. T. (2005). Neuropsychologic theory and findings in attention-deficit/hyperactivity disorder: The state of the field and salient challenges for the coming decade. *Biological Psychiatry*, *57*, 1424-1435.
- Nigg, J. T., Stavro, G., Ettenhofer, M., Hambrick, D. Z., Miller, T., and Henderson, J. M. (2005). Executive functions and ADHD in adults: Evidence for selective effects on ADHD symptom domains. *Journal of Abnormal Psychology*, *114*, 706-717.
- Obeso, J. A., Marin C., Rodriguez-Oroz, C., Blesa, J., Benitez-Temiño, B., Mena-Segovia, J., Rodríguez, M., and Olanow, C. W. (2008). The basal ganglia in Parkinson's disease: current concepts and unexplained observations. *Annals of Neurology*, *64*, 30-46.
- O'Doherty, J.P., Buchanan, T. W., Seymour, B., and Dolan, R. J. (2006). Predictive neural coding of reward preference involves dissociable responses in human ventral midbrain and ventral striatum. *Neuron*, *49*, 157-166.
- O'Doherty, J. P., Dayan, P., Friston, K., Critchley, H., and Dolan, R. J. (2003). Temporal difference models and reward-related learning in the human brain. *Neuron*, *38*, 329-337.
- O'Doherty, J. P., Dayan, P., Schultz, J., Deichmann, R., Friston, K., and Dolan, R. J. (2004). Dissociable roles of ventral and dorsal striatum in instrumental conditioning. *Science*, *304*, 452-454.
- O'Doherty, J. P., Deichmann, R., Critchley, H. D., and Dolan, R. J. (2002). Neural responses during anticipation of a primary taste reward. *Neuron*, *33*, 815-826.
- Ogawa, S., Lee, T. M., Kay, A. R., and Tank, D. W. (1990a). Brain magnetic resonance imaging with contrast dependent on blood oxygenation. *Proceedings of the National Academy of Sciences of the United States of America*, *87*, 9868-9872.

- Ogawa, S., Lee, T. M., Nayak, A. S. and Glynn, P. (1990b). Oxygenation-sensitive contrast in magnetic resonance imaging of rodent brain at high magnetic fields. *Magnetic Resonance in Medicine*, 14, 68-78.
- Ogawa, S., Tank, D. W., Menon, R., Ellermann, J. M., Kim, S.-G., Merkle, H. and Ugurbil, K. (1992). Intrinsic signal changes accompanying sensory stimulation: Functional brain mapping with magnetic resonance imaging. *Proceedings of the National Academy of Sciences of the United States of America*, 89, 5951-5955.
- Olman, C., Ronen, I., Ugurbil, K., and Kim, D. S. (2003). Retinotopic mapping in cat visual cortex using high-field functional magnetic resonance imaging. *Journal of Neuroscience Methods*, 131, 161-170.
- Orth, M., Munchau, A., and Rothwell, J. C. (2008). Corticospinal system excitability at rest is associated with tic severity in Tourette syndrome. *Biological Psychiatry*, 64, 248-251.
- Orth, M. and Rothwell, J. C. (2009). Motor cortex excitability and comorbidity in Gilles de la Tourette syndrome. *Journal of Neurology Neurosurgery and Psychiatry*, 80, 29-34.
- Owen, A. M., Doyon, J., Petrides, M., and Evans, A. C. (1996). Planning and spatial working memory: a positron emission tomography study in humans. *European Journal of Neuroscience*, 8, 353-364.
- Owen, A. M., Doyon, J., Dagher, A., Sadikot, A., and Evans, A. C., (1998). Abnormal basal ganglia outflow in Parkinson's disease identified with PET. Implications for higher cortical functions. *Brain*, 121, 949-965.
- Packard, M. G. and Knowlton, B. J. (2002). Learning and memory functions of the basal ganglia. *Annual Review of Neuroscience*, 25, 563-593.
- Padmala, S. and Pessoa, L. (2010). Interactions between cognition and motivation during response inhibition. *Neuropsychologia*, 48, 558-565.

- Pagnoni, G., Zink, C. F., Montague, P. R., and Berns, G. S. (2002). Activity in human ventral striatum locked to errors of reward prediction. *Nature Neuroscience*, *5*, 97-98.
- Parent, A. and De Bellefeuille, L. (1982). Organization of efferent projections from the internal segment of globus pallidus in primate as revealed by fluorescence retrograde labelling method. *Brain Research*, *245*, 201-213.
- Parent, A. and Hazrati, L. N. (1993). Anatomical aspects of information processing in primate basal ganglia. *Trends in Neuroscience*, *16*, 111-116
- Parthasarathy, H. B., Schall, J. D., and Graybiel, A. M. (1992). Distributed but convergent ordering of corticostriatal projections: Analysis of the frontal eye field and the supplementary eye field in the macaque monkey. *Journal of Neuroscience*, *12*, 4468-4488.
- Pastor, M. A., Artieda, J., Jahanshahi, M., Obeso, J. A. (1992). Time estimation and reproduction is abnormal in Parkinson's disease. *Brain*, *115*, 211-225.
- Pasupathy, A. and Miller, E. K. (2005). Different time courses of learning-related activity in the prefrontal cortex and striatum. *Nature*, *433*, 873-876.
- Paulus, M. P., Hozack, N., Frank, L., and Brown, G. C. (2002). Error rate and outcome predictability affect neural activation in prefrontal cortex and anterior cingulate during decision-making. *NeuroImage*, *15*, 836-846.
- Paus, T. (2001). Primate anterior cingulate cortex, where motor control, drive and cognition interface. *Nature Reviews Neuroscience*, *2*, 417-424.
- Paus, T., Petrides, M., Evans, C., and Meyer, E. (1993). Role of the human anterior cingulate cortex in the control of oculomotor, manual, and speech responses: a positron emission tomography study. *Journal of Neurophysiology*, *70*, 453-469.
- Penadés, R., Catalán, R., Rubia, K., Andrés, S., Salamero, M., and Gastó, C. (2006). Impaired response inhibition in obsessive compulsive disorder. *European Psychiatry*, *22*, 404-410.

- Penney, J. B. and Young, A. B. (1981). GABA as the pallidothalamic neurotransmitter: Implications for basal ganglia function. *Brain Research*, 207, 195-199.
- Peters, A. M., Brookes, M. J., Hoogenraad, F.G., Gowland, P. A., Francis, S. T., Morris, P. G., and Bowtell, R. (2007). T₂* measurements in human brain at 1.5, 3 and 7 T. *Magnetic Resonance Imaging*, 25, 748-753.
- Peterson, B., Leckman, J. F., Duncan, J. S., Wetzles, R., Riddle, M. A., Hardin, M. T., and Cohen, D. J. (1994). Corpus callosum morphology from magnetic resonance images in Tourette syndrome. *Psychiatry Research*, 55, 85-89.
- Peterson, B. S., Pine, D. S., Cohen, P., and Brook, J. S. (2001). Prospective, longitudinal study of tic, obsessive-compulsive, and attention-deficit/hyperactivity disorders in an epidemiological sample. *Journal of the American Academy of Child and Adolescent Psychiatry*, 40, 685-695.
- Peterson, B., Riddle, M. A., Cohen, D. J., Katz, L. D., Smith, J. C., Hardin, M. T., Leckman, J. F. (1993). Reduced basal ganglia volumes in Tourette syndrome using three-dimensional reconstruction techniques from magnetic resonance images. *Neurology*, 43, 941-949.
- Peterson, B. S., Skudlarski, P., Anderson, A. W., Zhang, H., Gatenby, J. C., Lacadie, C. M., Leckman, J. F., and Gore, J. C. (1998). A functional magnetic resonance imaging study of tic suppression in Tourette syndrome. *Archives of General Psychiatry*, 55, 326-333.
- Peterson, B.S., Skudlarski, P., Gatenby, J. C., Zhang, H., Anderson, A. W., and Gore, J. C. (1999). Multiple distributed attentional systems. *Biological Psychiatry*, 45, 1237-258.
- Peterson, B. S., Thomas, P., Kane, M. J., Scahill, L., Zhang, H., and Bronen, R. King, R. A., Leckman, J. F., Staib, L. (2003). Basal Ganglia volumes in patients with Gilles de la Tourette syndrome. *Archives of General Psychiatry*, 60, 415-424.
- Petrides, M. (2000). The role of the mid-dorsolateral prefrontal cortex in working memory. *Experimental Brain Research*, 133, 44-54.

- Petrides, M. (1994). Frontal lobes and working memory: Evidence from investigations of the effects of cortical excisions in nonhuman primates. In F. Boller, J. Grafman (Eds.), *Handbook of neuropsychology* (pp. 59-84). Amsterdam: Elsevier.
- Pizzagalli, D. A. (2007). Electroencephalography and high-density electrophysiological source localization, In J.T. Cacioppo, L.G. Tassinary, G.G. Berntson, (Eds.), *Handbook of Psychophysiology* (pp. 56–84). Cambridge: Cambridge University Press.
- Plassmann, H., O’Doherty, J., and Rangel, A. (2007). Orbitofrontal cortex encodes willingness to pay in everyday economic transactions. *Journal of Neuroscience*, *27*, 9984-9988.
- Plessen, K. J., Wentzel-Larsen, T., Hugdahl, K., Feineigle, P., Klein, J., Staib, L. H., Leckman, J. F., Bansal, R, and Peterson, B. S. (2004). Altered interhemispheric connectivity in individuals with Tourette’s disorder. *American Journal of Psychiatry*, *161*, 2028-2037.
- Poldrack, R. A. (2006). Can cognitive processes be inferred from neuroimaging data? *Trends in Cognitive Science*, *10*, 59-63.
- Poldrack, R. A., Clark, J., Pare-Blagoev, E. J., Shohamy, D., Creso Moyano, J., Myers, C., and Gluck, M. A. (2001). Interactive memory systems in the human brain. *Nature*, *414*, 546–550.
- Poldrack, R. A., Fletcher, P. C., Henson, R. N., Worsley, K. J., Brett, M., and Nichols T. E. (2008). Guidelines for reporting an fMRI study. *NeuroImage*, *2*, 409-414.
- Poldrack, R. A., Prabhakaran, V., Seger, C. A., and Gabrieli, J. D. E. (1999). Striatal activation during cognitive skill learning. *Neuropsychology*, *13*, 564-574.
- Poline, J. B., Kherif, F., and Penny, W. D. (2007). Contrasts and Classical Inference. In, R. S. Frackowiak, K.J. Friston, C.D. Frith, R.J. Dolan, C.J. Price, S. Zeki, J. Ashburner, and W.D. Penny (Eds.), *Human Brain Function* (pp. 126-140). San Diego, CA: Elsevier Academic Press.

- Poole, M. and Bowtell, R. (2008). Volume parcellation for improved dynamic shimming. *Magnetic Resonance Materials in Physics, Biology and Medicine*, 21, 31-40.
- Poser, B.A., Versluis, M.J., Hoogduin, J.M., and Norris, D.G. (2006). BOLD contrast sensitivity enhancement and artifact reduction with multiecho EPI: parallel-acquired inhomogeneity-desensitized fMRI. *Magnetic Resonance in Medicine*, 55, 1227-1235.
- Posner, M. I. and Dehaene, S. (1994). Attentional networks. *Trends in Neuroscience*, 17, 75-79.
- Posner, M. and DiGirolamo, G. (1998). Executive attention: conflict, target detection, and cognitive control. In R. Parasuraman, (Ed.), *The Attentive Brain* (pp. 401-423). Cambridge, MA: MIT Press.
- Posse, S., Fitzgerald, D., Gao, K. X., Habel, U., Rosenberg, D., Moore, G. J., and Schneider, F. (2003). Real-time fMRI of temporolimbic regions detects amygdala activation during single-trial self-induced sadness. *NeuroImage*, 18, 760-768.
- Posse, S., Wiese, S., Gembris, D., Mathiak, K., Kessler, C., Grosse-Ruyken, M.L., Elghahwagi, B., Richards, T., Dager, S.R., and Kiselev, V.G. (1999). Enhancement of BOLD-contrast sensitivity by single-shot multi-echo functional MR imaging. *Magnetic Resonance in Medicine*, 42, 87-97.
- Rao, S. M., Bobholz, J. A., Hammeke, T. A., Rosen, A. C., Woodley, S. J., Cunningham, J. M., Cox, R. W., Stein, E. A., and Binder, J. R. (1997). Functional MRI evidence for sub-cortical participation in conceptual reasoning skills. *Neuroreport*, 8, 1987-1993.
- Rao, S. M., Mayer, A. R., Harrington, D. L. (2001). The evolution of brain activation during temporal processing. *Nature Neuroscience*, 4, 317-323.
- Richards, J. E. (2003). The development of visual attention and the brain. In M. de Haan, M.H. Johnson (Eds.), *The cognitive neuroscience of development* (pp. 73-98). Hove: Psychology Press.

- Ridderinkhof, K. R., Scheres, A., Oosterlaan, J., and Sergeant, J. A. (2005). Delta plots in the study of individual differences: New tools reveal response inhibition deficits in AD/HD that are eliminated by methylphenidate treatment. *Journal of Abnormal Psychology, 114*, 197-215.
- Ridderinkhof, K. R., Ullsperger, M., Crone, E. A., and Nieuwenhuis, S. (2004). The role of the medial frontal cortex in cognitive control. *Science, 306*, 443-447.
- Riddle, M. A., Rasmussen, A. M., Woods, S. W. and Hoffer, P. B. (1992). SPECT imaging of cerebral blood flow in Tourette syndrome. *Advances in Neurology, 58*, 207-211.
- Rieger, M., Gauggel, S., and Burmeister, K. (2003). Inhibition of ongoing responses following frontal, nonfrontal, and basal ganglia lesions. *Neuropsychology, 17*, 272-282.
- Robbins, T. W. and Everitt, B. J. (1999). Motivation and reward. In M. J. Zigmond, F. E. Bloom, S. C. Landis, J. L. Roberts, and L. R. Squire (Eds.), *Fundamental neuroscience* (pp. 1245-1260). San Diego, CA: Elsevier Academic Press.
- Rodriguez, P. F., Aron, A. R., and Poldrack, R. A. (2006). Ventral striatal/nucleus accumbens sensitivity to prediction errors during classification learning. *Human Brain Mapping, 27*, 306-313.
- Roesch, M. R. and Olson, C. R. (2003). Impact of expected reward on neuronal activity in prefrontal cortex, frontal and supplementary eye fields and premotor cortex. *Journal of Neurophysiology, 90*, 1766-1789.
- Roessner, V., Banaschewski, T., Fillmer-Otte, A., Becker, A., Albrecht, B., Sergeant, J., Tannock, R., Rothenberger, A. (2008). Color perception deficits in co-existing attention-deficit=hyperactivity disorder and chronic tic disorders. *Journal of Neural Transmission, 115*, 235-239.

- Roessner, V., Overlack, S., Schmidt-Samoa, C., Baudewig, J., Dechent, P., Rothenberger, A., and Helms, G. (2011). Increased putamen and callosal motor subregion in treatment-naïve boys with Tourette syndrome indicates changes in the bihemispheric motor network. *The Journal of Child Psychology and Psychiatry*, 52, 306-314.
- Rofé, Y. (2008). "Does Repression Exist? Memory, Pathogenic, Unconscious and Clinical Evidence". *Review of General Psychology*, 12, 63-85.
- Rogers, R. D., Andrews, T. C., and Grasby, P. M., Brooks, D. J. and Robbins, T. W. (2000). Contrasting cortical and sub-cortical activations produced by attentional-set shifting and reversal learning in humans. *Journal of Cognitive Neuroscience*, 12, 142-162.
- Rogers, R. D. and Monsell, S. (1995). Costs of a predictable switch between simple cognitive tasks. *Journal of Experimental Psychology: General*, 124, 207-231.
- Rogers, R. D., Owen, A. M., Middleton, H. C., Williams, E. J., Pickard, J. D., Sahakian, B. J., and Robbins, T. W. (1999). Choosing between small, likely rewards and large, unlikely rewards activates inferior and orbital prefrontal cortex. *Journal of Neuroscience*, 20, 9029-9038.
- Rolls, E. T. (2000). The orbitofrontal cortex and reward. *Cerebral Cortex*, 10, 284-294.
- Royall, D. R., Lauterbach, E. C., Cummings, J. L., Reeve, A., Rummans, T. A., and Kaufer, D. I. LaFrance, W. C., and Coffey, C. E. (2002). Executive control function: A review of its promises and challenges for clinical research. *Journal of Neuropsychiatry and Clinical Neurosciences*, 14, 377-405.
- Rowe J. B. and Passingham, R. E. (2001). Working memory for location and time: Activity in prefrontal area 46 relates to selection rather than maintenance in memory. *NeuroImage*, 14, 77-86.
- Rowe, J. B., Toni, I., Josephs, O., Frackowiak, R. S., and Passingham, R. E. (2000). The prefrontal cortex: Response selection or maintenance within working memory? *Science*, 288, 1656-1660.

- Rubia, K. (2005). Studies of neuro-developmental psychiatric disorders using MRI. *Psychiatry*, 4, 6-10.
- Rubia, K., Overmeyer, S., Taylor, E., Brammer, M., Williams, S., Simmons, A., Andrew, C., and Bullmore, E. (1998). Prefrontal involvement in “temporal bridging” and timing movement. *Neuropsychologia*, 36, 1283-1293.
- Rubia, K., Overmeyer, S., Taylor, E., Brammer, M., Williams, S. C., Simmons, A., Andrew, C., and Bullmore, E.T. (1999). Hypofrontality in Attention Deficit Hyperactivity Disorder during higher order motor control: a study with fMRI. *American Journal of Psychiatry*, 156, 891-896.
- Rubia, K., Russell, T., Overmeyer, S., Brammer, M. J., Bullmore, E. T., Sharma, T., Simmons, A., Williams, S. C., Giampietro, V., Andrew, C. M., and Taylor, E. (2001). Mapping motor inhibition: conjunctive brain activations across different versions of go/no-go and stop tasks. *NeuroImage*, 13, 250-261.
- Rubia, K., Smith, A. B., Brammer, M. J., and Taylor, E. (2003). Right inferior prefrontal cortex mediates response inhibition while mesial prefrontal cortex is responsible for error detection. *NeuroImage*, 20, 351-358.
- Rushworth, M. F., Walton, M. E., Kennerley, S. W., and Bannerman, D. M. (2004). Action sets and decisions in the medial frontal cortex. *Trends in Cognitive Science*, 8, 410-417.
- Sakagami, M., Tsutsui, K., Lauwereyns, J., Koizumi, M., Kobayashi, S., and Hikosaka, O. (2001). A code for behavioral inhibition on the basis of color, but not motion, in ventrolateral prefrontal cortex of macaque monkey. *Journal of Neuroscience*, 21, 4801-4808.
- Saint-Cyr, J. A., Taylor, A. E., and Nicholson, K. (1995). Behaviour and the basal ganglia. *Advances in Neurology*, 65, 1-28.
- Salas, R., Baldwin, P., de Biasi, M., and Montague, P. R. (2010). BOLD responses to negative reward prediction errors in human habenula. *Frontiers in Human Neuroscience*, 4, 1-7.

- Sasaki, K., Gemba, H., and Tsujimoto, T. (1989). Suppression of visually initiated hand movement by stimulation of the prefrontal cortex in the monkey. *Brain Research*, 495, 100-107.
- Scangos, K. W and Stuphorn, V. (2010). Medial frontal cortex motivates but does not control movement initiation in the countermanding task. *Journal of Neuroscience*, 30, 1968-1982.
- Schenck J. F. (1996). The role of magnetic susceptibility in magnetic resonance imaging: MRI magnetic compatibility of the first and second kinds. *Medical Physics*, 6, 815-850.
- Schultz, W. (1992a). Activity of dopamine neurons in the behaving primate. *Seminars in Neuroscience*, 4, 129-138
- Schultz, W. (1998). Predictive reward signal of dopamine neurons. *Journal of Neurophysiology*, 80, 1-27.
- Schultz, W. (2000). Multiple reward signals in the brain. *Nature Reviews Neuroscience*, 1, 199-207.
- Schultz, W. (2007). Multiple dopamine functions at different time courses. *Annual Review of Neuroscience*, 30, 259-288.
- Schultz, W., Dayan, P., and Montague, P. R. (1997). A neural substrate of prediction and reward. *Science*, 275, 1593-1599.
- Schultz, W. and Dickinson, A. (2000). Neuronal coding of prediction errors. *Annual Review of Neuroscience*, 23, 473-500,
- Suzuki, T., Miura, M., Mishimura, K., and Aosaki, T. (2001). Dopamine-dependent synaptic plasticity in the striatal cholinergic interneurons. *The Journal of Neuroscience*, 21, 6492-6501.
- Schultz, W. and Romo, R. (1992b). Role of primate basal ganglia and frontal cortex in the internal generation of movements. I. Preparatory activity in the anterior striatum. *Experimental Brain Research*, 91, 363-84.

- Seger, C. A. and Cincotta, C. M. (2005). The roles of the caudate nucleus in human classification learning. *Journal of Neuroscience* 25, 2941-51.
- Selemon, L. D. and Goldman-Rakic, P. S. (1985). Longitudinal topography and interdigitation of cortico-striatal projections in the rhesus monkey. *Journal of Neuroscience*, 5, 776-794.
- Serrien, D. J., Nirkko, A. C., Loher, T. J., Lövlblad, K-O., Buirgunder, J-M., and Wiesendanger, M., (2002). Movement control of manipulative tasks in patients with Gilles de la Tourette syndrome. *Brain*, 125, 290-300.
- Serrien, D. J., Orth, M., Evans, A. H., Lees, A. J., and Brown, P. (2005). Motor inhibition in patients with Gilles de la Tourette syndrome: Functional activation patterns as revealed by EEG coherence. *Brain*, 128, 116-125.
- Sescousse, G., Redouté, J., and Dreher, J. C. (2010). The architecture of reward value coding in the human orbitofrontal cortex. *Journal of Neuroscience*, 30, 13095-13104.
- Shohamy, D., Myers, C. E., Grossman, S., Sage, J., Gluck, M. A., Poldrack, R. A. (2004). Cortico-striatal contributions to feedback-based learning: converging data from neuroimaging and neuropsychology. *Brain*, 127, 851-859.
- Sharp, D. J., Bonnelle, V., De Boissezon, X., Beckmann, C. F., James, S. G., Patel, M. C., and Mehta, M. A. (2010). Distinct frontal systems for response inhibition, attentional capture, and error processing. *Proceeding of the National Academy of Sciences of the United States of America*, 107, 6106-6111.
- Sowell, E. R., Kan, E., Yoshii, J., Thompson, P. M., Bansal, R., Xu, D., Toga, A. W., and Peterson, B. S. (2008). Thinning of sensorimotor cortices in children with Tourette syndrome. *Nature Neuroscience*, 11, 637-639.
- Simmonds, D. J., Pekar, J. J., and Mostofsky, S. H. (2008). Meta-analysis of Go/No-go tasks demonstrating that fMRI activation associated with response inhibition is task-dependent. *Neuropsychologia*, 46, 224-232.

- Singer, H. S., Harris, K. (2006). Circuits to synapses: The pathophysiology of Tourette syndrome. In S. Gilman (Ed.), *Neurobiology of disease*. Burlington, MA: Elsevier Academic Press.
- Singer, H. S. and Minzer, K. (2003). Neurobiology of Tourette syndrome: concepts of neuroanatomical localization and neurochemical abnormalities. *Brain and Development*, 25, 70-84.
- Singer, H. S., Reiss, A. L., Brown, J. E., Aylward, E. H., Shih, B., Chee, E., Harris, E. L., Reader, M. J., Chase, G. A., Bryan, R. N., and Denckla, M. B. (1993). Volumetric MRI changes in basal ganglia of children with Tourette syndrome. *Neurology*, 43, 950-956.
- Smith, D. V., Hayden, B. Y., Truong, T. K., Song, A. W., Platt, M. L., and Huettel, S. A. (2010). Distinct value signals in anterior and posterior ventromedial prefrontal cortex. *Journal of Neuroscience*, 30, 2490-2495.
- Smith, E. E. and Jonides, J. (1999). Storage and executive processes in the frontal lobes. *Science*, 283, 1657-1661.
- Smith, R. (1992). *Inhibition: history and meaning in the sciences of mind and brain*. Berkeley, CA: University of California Press.
- Smith, S., Bannister, P., Beckmann, C., Brady, M., Clare, S., Flitney, D., Hansen, P., Jenkinson, M., Leibovici, D., Ripley, B., Woolrich, M., and Zhang, Y. (2001). FSL: New tools for functional and structural brain image analysis. In *Seventh International Conference on Functional Mapping of the Human Brain*.
- Spoormaker, V. I., Andrade, K. C., Schröter, M. S., Sturm, A., Goya-Maldonado, R., Sämann, P. G., and Czisch, M. (2011). The neural correlates of negative prediction error signalling in human fear conditioning. *NeuroImage*, 54, 2250-2256.
- Stern, E., Silbersweig, D. A., Chee, K-Y., Holmes, A., Robertson, M. M., Trimble, M., Frith, C. D., Frackowiak, R. S., and Dolan, R. J. (2000). A functional neuroanatomy of tics in Tourette syndrome. *Archives of General Psychiatry*, 57, 741-748.

- Stocker., A. A. and Simoncelli., E. P. (2006). Noise characteristics and prior expectations in human visual speed perception. *Nature Neuroscience*, 4, 578-585.
- Stoetter, B., Braun, A. R., Randolph, C., Gernert, J., Carson, R. E., Herscovitch, P., Chase, T. N. (1992). Functional neuroanatomy of Tourette syndrome. Limbic-motor interactions studied with FDG PET. *Advances in neurology*, 58, 213-226.
- Stuphorn, V. and Schall, J. D. (2006). Executive control of countermanding saccades by the supplementary eye field. *Nature Neuroscience*, 9, 925-931.
- Sutherland, R. J. (1982). The dorsal diencephalic conduction system: a review of the anatomy and functions of the habenular complex. *Neuroscience and Biobehavioural Reviews*, 6, 1-13.
- Sutton, R. S. and Barto, A. G. (1998). *Reinforcement Learning: An Introduction*. Cambridge, MA: MIT Press.
- Swainson, R., Cunnington, G., Rorden, C., Peters, A., Morris, P., and Jackson, S. (2003). Cognitive control mechanisms revealed by ERP and fMRI: Evidence from repeated task-switching. *Journal of Cognitive Neuroscience*, 15, 785-799.
- Swann, N. C., Cai, W., Conner, C. R., Pieters, T. A., Claffey, M. P., George, J. S., Aron, A. R., and Tandon, N. (2012). Roles for the pre-supplementary motor area and the right inferior frontal gyrus in stopping action: Electrophysiological responses and functional and structural connectivity. *NeuroImage*, 59, 2860-2870.
- Swann, N., Tandon, N., Canolty, R., Ellmore, T. M., McEvoy, L. K., and Dreyer, S., DiSano, M., and Aron, A. R. (2009). Intracranial EEG reveals a time- and frequency-specific role for the right inferior frontal gyrus and primary motor cortex in stopping initiated responses. *Journal of Neuroscience*, 29, 12675-12685.

- Troyer, A. K., Graves, R. E., and Cullum, C. M. (1994). Executive functioning as a mediator of the relationship between age and episodic memory in healthy aging. *Aging and Cognition, 1*, 45-53.
- Turner, R., Jezzard, P., Wen, H., Kwong, K.K., Le Bihan, D., Zeffiro, T., and Balaban, R.S. (1993). Functional mapping of the human visual cortex at 4 and 1.5 Tesla using deoxygenation contrast EPI. *Magnetic Resonance in Medicine, 29*, 277-279.
- Tzourio-Mazoyer, N., Landeau, B., Papathanassiou, D., Crivello, F., Etard, O., Delcroix, N., Mazoyer, B., and Joliot, M. (2002). Automated anatomical labeling of activations in SPM using a macroscopic anatomical parcellation of the MNI MRI single-subject brain. *NeuroImage, 15*, 273-289.
- Ullsperger, M. and von Cramon, D. Y. (2003). Error monitoring using external feedback: specific roles of the habenular complex, the reward system, and the cingulate motor area revealed by functional magnetic resonance imaging. *Journal of Neuroscience, 23*, 4308-4314.
- Utter, A. A. and Basso, M. A. (2008). The basal ganglia: an overview of circuits and function. *Neuroscience and Biobehavioural Reviews, 32*, 333-342.
- van den Heuvel, O. A., Veltman, D. J., Groenewegen, H. J., Cath, D. C., van Balkom, A. J., and van Hartskamp, J., Barkhof, F., and van Dyck, R. (2005a). Frontal-striatal dysfunction during planning in obsessive-compulsive disorder. *Archives of General Psychiatry, 62*, 301-309.
- van den Heuvel, O. A., Veltman, D. J., Groenewegen, H. J., Witter, M. P., Merkelbach, J., Cath, D. C. van Balkom, A. J., van Oppen, P., and van Dyck, R. (2005b). Disorder-specific neuroanatomical correlates of attentional bias in obsessive-compulsive disorder, panic disorder, and hypochondriasis. *Archives of General Psychiatry, 62*, 922-933.
- van der Zwaag, W., Francis, S., Head, K., Peters, A., Gowland, P., Morris, P., and Bowtell, R. (2009). fMRI at 1.5, 3 and 7 T: characterising BOLD signal changes. *NeuroImage, 47*, 1425-1434.

- van Schouwenburg, M. R., den Ouden, H. E., Cools, R. (2010). The human basal ganglia modulate frontal-posterior connectivity during attention shifting. *Journal of Neuroscience*, *30*, 9910-9918.
- Verbruggen, F., Aron, A. R, Stevens, M. A, and Chambers, C. D. (2010). Theta burst stimulation dissociates attention and action updating in human inferior frontal cortex. *Proceeding of the National Academy of Sciences of the United States of America*, *107*, 13966-13971.
- Verbruggen, F., Liefoghe, B., and Vandierendonck, A. (2004). The interaction between stop signal inhibition and distractor interference in the flanker and Stroop task. *Acta Psychologica* *116*, 21-37.
- Verbruggen, F. and Logan, G. (2009). Models of response inhibition in the stop-signal and stop-change paradigms. *Neuroscience and Biobehavioural Reviews*, *33*, 647-661.
- Vergheze, J., Lipton, R. B., Katz, M. J., Hall, C. B., Derby, C. A., Kuslansky, G., Ambrose, A. F., Sliwinski, M., and Buschke, H. (2003). Leisure activities and the risk of dementia in the elderly. *The New England Journal of Medicine*, *348*, 2508-2516.
- Vince, M. A. (1948). The intermittency of control movements and the psychological refractory period. *British Journal of Psychology*, *38*, 149-157.
- Vink, M., Ramsey, N. F., Raemaekers, M., Kahn, R. S. (2006). Striatal dysfunction in schizophrenia and unaffected relatives. *Biological Psychiatry*, *60*, 32-39.
- Vitek, J. L., Chockkank V., Zhang, J. Y., Kaneoke, Y., Evatt, M., DeLong, M. R., Triche, S., Mewes, K., Hashimoto, T., Bakay, R. A. (1999). Neuronal activity in the basal ganglia in patients with generalized dystonia and hemiballismus. *Annals of Neurology*, *46*, 22-35.
- Volz, K. G., Schubotz, R. I., and von Cramon, D. Y. (2003). Predicting events of varying probability: uncertainty investigated by fMRI. *NeuroImage*, *19*, 271-280.

- Volz, K.G., Schubotz, R.I., and von Cramon, D.Y. (2004). Why am I unsure? Internal and external attributions of uncertainty dissociated by fMRI. *NeuroImage*, 21, 848-857.
- Waelti, P., Dickinson, A., and Schultz, W. (2001). Dopamine responses comply with basic assumptions of formal learning theory. *Nature*, 412, 43-48.
- Wager, T. D. and Smith, E. E. (2003). Neuroimaging studies of working memory: A meta-analysis. *Cognitive, Affective, and Behavioural Neuroscience*, 3, 255-274.
- Wager, T. D., Sylvester, C. Y., Lacey, S. C., Nee, D. E., Franklin, M., and Jonides, J. (2005). Common and unique components of response inhibition revealed by fMRI. *NeuroImage*, 27, 323-340.
- Wagner, A. D., Schacter, D. L., Rotte, M., Koustaal, W., Maril, A., Dale, A., Rosen, B., and Buckner, R. L. (1998). Building memories: remembering and forgetting of verbal experiences as predicted by brain activity. *Science*, 21, 188-191.
- Watkins, L. H., Sahakian, B. J., Robertson, M. M., Veale, D. M., Rogers, R. D., Pickard, K. M. Aitken, M. R., and Robbins, T. W. (2005). Executive function in Tourette syndrome and obsessive-compulsive disorder. *Psychological Medicine*, 35, 571-582.
- Weder, B. J., Leenders, K. L., Vontobel, P., Nienhusmeier, M., Keel, A., Zaunbauer, W., Vonesch, T., and Ludin, H. P. (1999). Impaired somatosensory discrimination of shape in Parkinson's disease: association with caudate nucleus dopaminergic function. *Human Brain Mapping*, 8, 1-12.
- Weiskopf, N., Klose, U., Birbaumer, N., and Mathiak, K. (2005). Single-shot compensation of image distortions and BOLD contrast optimization using multi-echo EPI for real-time fMRI. *NeuroImage*, 22, 1068-1079.

- Wichmann, T., Bergman, H., Starr, P. A., Subramanian, T., Watts, R. L., and DeLong, M. R. (1999) Comparison of MPTP-induced changes in spontaneous neuronal discharge in the internal pallidal segment and the substantia nigra pars reticulata in primate. *Experimental Brain Research*, 125, 397-409.
- Wichmann, T. and DeLong, M. R. (1996). Functional and pathophysiological models of the basal ganglia. *Current Opinion in Neurobiology*, 241, 981-983
- Wickens, J. R. and Kötter, R. (1995). Cellular models of reinforcement. In J.C. Houk, J.L Davis, and D.G. Beiser, (Eds.), *Models of information processing in the Basal Ganglia* (pp. 187-214). Cambridge, MA: MIT Press.
- Wickens, J. R., Begg, A. J., and Arbuthnott, G. W. (1996). Dopamine reverses the depression of rat corticostriatal synapses which normally follows high-frequency stimulation of cortex in vitro. *Neuroscience*, 70, 1-5.
- Winstanley, C. A., Baunez, C., Theobald, D. E. and Robbins, T. W. (2005) Lesions to the subthalamic nucleus decrease impulsive choice but impair autoshaping in rats: the importance of the basal ganglia in Pavlovian conditioning and impulse control. *European Journal of Neuroscience*, 21, 3107-3116.
- Wolf, S. S., Jones, D. W., Knable, M. B., Gorey, J. G., Lee, K. S., Hyde, T. M., Coppola, R., Weinberger, D. R. (1996). Tourette syndrome: Prediction of phenotypic variation in monozygotic twins by caudate nucleus D2 receptor binding. *Science*, 273, 1225-1227.
- Woolley, J., Heyman, I., Brammer, M., Frampton, I., McGuire, P. K., Rubia, K. (2008). Brain activation in paediatric obsessive compulsive disorder during tasks of inhibitory control. *British Journal of Psychiatry*, 192, 25-31
- Worbe, Y., Gerardin, E., Hartmann, A., Valabre'gue, R., Chupin, M., Tremblay, L., Vidailhet, M., Colliot, O., and Lehe'ricy, S. (2010). Distinct structural changes underpin clinical phenotypes in patients with Gilles de la Tourette syndrome. *Brain*, 133, 3649-3660.

- Worsley, K. J. (2001). Statistical analysis of activation images. In P. Jezzard, P.M. Matthews, and S. M. Smith (Eds.), *Functional MRI: An introduction to methods* (pp. 251-270). New York, NY: Oxford University Press.
- Wunderlich, K., Rangel, A., O'Doherty, J. P. (2010). Economic choices can be made using only stimulus values. *Proceedings of the National Academy of Sciences of the United States of America*, *107*, 15005-15010.
- Wylie, S. A., van den Wildenberg, W. P., Ridderinkhof, K. R., Bashore, T. R., Powell, V. D., Manning, C. A., and Wooten, G. F. (2009). The effect of Parkinson's disease on interference control during action selection. *Neuropsychologia*, *47*, 145-157.
- Yacoub, E., Duong, T.Q., Van de Moortele, P.F., Lindquist, M., Adriany, G., Kim, S.G., Ugurbil, K., and Hu, X.P. (2003). Spin-echo fMRI in humans using high spatial resolutions and high magnetic fields. *Magnetic Resonance in Medicine*, *49*, 655-664.
- Yacoub, E., Shmuel, A., Logothetis, N., and Ugurbil, K. (2007). Robust detection of ocular dominance columns in humans using Hahn Spin Echo BOLD functional MRI at 7 Tesla. *NeuroImage*, *37*, 1161-1177.
- Yacoub, E., Shmuel, A., Pfeuffer, J., Van De Moortele, P.F., Adriany, G., Andersen, P., Vaughan, J.T., Merkle, H., Ugurbil, K., and Hu, X. (2001). Imaging brain function in humans at 7 Tesla. *Magnetic Resonance in Medicine*, *45*, 588-594.
- Yacoub, E., Van De Moortele, P.F., Shmuel, A., and Ugurbil, K. (2005). Signal and noise characteristics of Hahn SE and GE BOLD fMRI at 7 T in humans. *NeuroImage*, *24*, 738-750.
- Yeung, N., & Monsell, S. (2003). The effects of recent practice on task switching. *Journal of Experimental Psychology: Human Perception and Performance*, *29*, 919-936.
- Yoon, D. Y., Gause, C. D., Leckman, J. F., and Singer, H. S. (2007). Frontal dopaminergic abnormality in Tourette syndrome: a postmortem analysis. *Journal of the Neurological Sciences*, *255*, 50-56.

- Zandbelt, B. B. and Vink, M. (2010). On the role of the striatum in response inhibition. *Public Library of Science One*, 5, e13848.
- Zheng, D., Oka, T., Bokura, H., and Yamaguchi, S. (2008). The key locus of common response inhibition network for no-go and stop signals. *Journal of Cognitive Neuroscience*, 20, 1434-1442.
- Ziemann, U., Paulus, W., and Rothenberger, A. (1997). Decreased motor inhibition in Tourette disorder: evidence from transcranial magnetic stimulation. *The American Journal of Psychiatry* 154, 1277-1284.
- Zimmerman, A. M., Abrams, M. T., Giuliano, J. D., Denckla, M. B., and Singer, H. S. (2000). Sub-cortical volumes in girls with Tourette syndrome: support for a gender effect. *Neurology*, 54, 2224-2229.